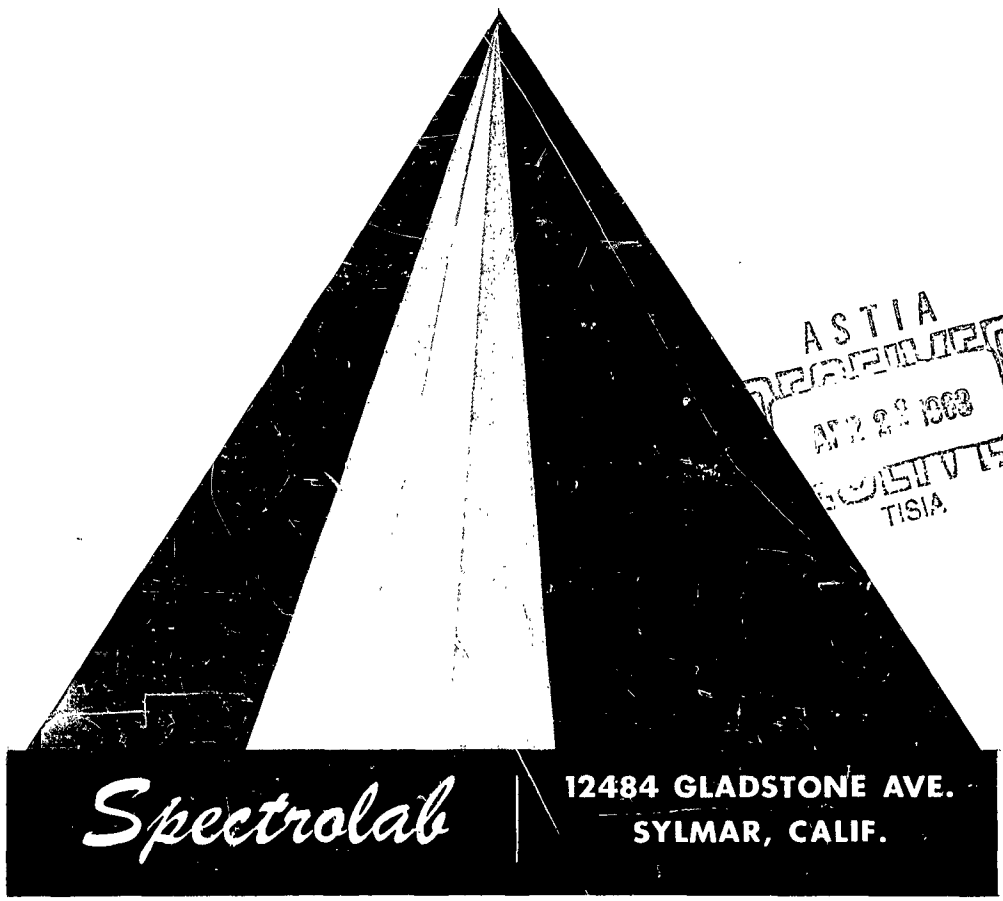
401872

CATALOGED BY ASTIA
AS AD No. 401872



ASTIA
RECEIVED
APR 28 1963
TISIA

COPY NO. 73

Best
Available
Copy

INVESTIGATION OF OPTICAL COATINGS

FOR SOLAR CELLS

FINAL REPORT

1 June 1961 through 10 September 1962
Contract No. DA 36-039 SC-87449
Order No. 40647-PM-61-93-93
ARPA Order No. 80-61

U. S. Army Signal Research and Development
Laboratory, Fort Monmouth, New Jersey

Prepared by

Dr. R. J. Romagnoli
Senior Physicist

SPECTROLAB
11921 Sherman Way
North Hollywood, California

The work performed under this contract was made possible by the support of the Advanced Research Projects Agency under Order No. 80-61, through the United States Army Signal Research and Development Laboratory.

OBJECT: Study of thermal equilibrium coatings for use with concentrator type solar photovoltaic converters with particular emphasis on spectrally selective reflective coatings of the multilayer interference type.

TABLE OF CONTENTS

		PAGE
LIST OF ILLUSTRATIONS		i
LIST OF TABLES		
SECTION 1.	PURPOSE	1-1
SECTION 2.	ABSTRACT	2-1
SECTION 3.	PUBLICATIONS, REPORTS AND CONFERENCES	3-1
SECTION 4.	FACTUAL DATA	4-1
Task A.	Performance Studies of Solar Power System	4-1
Task B.	Silicon Solar Cell Performance Characteristics	4-29
Task C.	Filter Performance Characteristics	4-35
Task D.	Experimental Mirror Filters	4-37
SECTION 5.	OVERALL CONCLUSIONS	5-1
SECTION 6.	RECOMMENDATIONS	6-1
ILLUSTRATIONS		
APPENDIX A	REFLECTION FILTER SPECIFICATIONS	
APPENDIX B	SPECTRAL TRANSMITTANCE CURVES FOR EXPERIMENTAL REFLECTION FILTERS	

LIST OF ILLUSTRATIONS

Figure No.	Title
1	Typical Silicon Cell Relative Spectral Response, Relative Solar Spectral Irradiance and Their Product.
2	Spectral Emissivity of Typical 1960 Non-Gridded "Red" Cell with Solakote "A" Filter.
3	Relative Thermal Effects on Open Circuit Voltage, Short Circuit Current, Maximum Power, and Power Into a Matched Load for Typical Silicon Solar Cell.
4	Equilibrium Temperature vs. Solar Irradiance for 1960 Non-Gridded "Red" Cells.
5	Equilibrium Temperature, Thermal Degradation Factor, and Relative Output of Cell Array vs. Illumination.
6	Effect of Illumination Level on Open Circuit Voltage, Short Circuit Current, Voltage and Current at Maximum Power, and Relative Conversion Efficiency for Typical Silicon Solar Cell.
7	Output per Cell Relative to Coated (Solakote "A") Cell without Concentration vs. Area Concentration.
8	Solar Concentrator Configuration.
9	Solar Cell Temperature as a Function of Illumination on the Cell for C_R = 1.0.
10	Solar Cell Temperature as a Function of Illumination on the Cell for C_R = 4.
11	Solar Cell Temperature as a Function of Illumination on the Cell for C_R = 6.25.
12	Solar Cell Temperature as a Function of Illumination on the Cell for C_R = 9.
13	Solar Cell Temperature as a Function of Illumination on the Cell for C_R = 16.
14	Typical Temperature Characteristic of an Experimental Gridded "Red" Silicon Solar Cell.
15	Typical Temperature Characteristic of a Heliotek Gridded "Blue" Cell.
16	Concentrator Filter of "Red" Cells Type SL 120/83.
17	Concentrator Filter for "Red" Cells Type Sl 200/82.
18	Concentrator Filter for "Red" Cells Type Sl 350/80.

Figure No.	Title
19	Power Output of Array for Varying Concentration Ratios and Ideal Filter Band-Pass Widths in the Cassegrainian Collector Configuration with Experimental Gridded "Red" Cell with Red Cell Temperature Power Degradation Coefficient = .0061/°C.
20a	Power Output of Array for Varying Concentration Ratios and Ideal Filter Band-Pass Widths in the Cassegrainian Collector Configuration with Hypothetical Gridded "Blue" Cell with "Red" Cell Temperature - Power Degradation Coefficient = .0060/°C.
20b	Power Output of Array for Varying Concentration Ratios and Ideal Filters Band-Pass Widths in the Cassegrainian Collector Configuration with Heliotek Gridded "Blue" Cell with "Blue" Cell Temperature Power Degradation Coefficient = .0041/°C.
21	Fraction of the Solar Energy and Cell Power Output Occurring in Region Found by Choosing Filter Band-Pass Limits at Equal Height on the Response Curve of the Experimental Gridded "Red" Silicon Solar Cell. Also, $(\beta_m - 1)$, where β_m is the Multiplier of the Average Absolute Efficiency (at the Reference Temperature) Between λ_A and λ_B to give the Average Efficiency Within the R_λ Limits.
22	Fraction of the Solar Energy and Cell Power Output Occurring in Region Found by Choosing Filter Band-Pass Limits at Equal Height on the Response Curve of the Heliotek Gridded "Blue" Silicon Solar Cell. Also, $(\beta_m - 1)$, where β_m is the Multiplier of the Average Absolute Efficiency (at the Reference Temperature) Between λ_A and λ_B to give the Average Efficiency Within the R_λ Limits.
23	Normalized Response and Cumulative Solar Energy and Power Output of Experimental Gridded "Red" Silicon Solar Cell as a Fraction of the Total Between λ_A and λ_B.
24	Normalized Response and Cumulative Solar Energy and Power Output of Heliotek Gridded "Blue" Silicon Solar Cell as a Fraction of the Total Between λ_A and λ_B.
25	Spectral Distribution of Solar Cell Response and Filter Transmission.
26	Solar Cell Power Output vs. Temperature and Incident Energy for Heliotek Gridded "Blue" Cell (Sunlight at Table Mountain).
27	Solar Cell Maximum Power Voltage and Open Circuit Voltage vs. Temperature (Sunlight on Table Mountain) for Heliotek Gridded "Blue" Cell.
28	Solar Cell Current vs. Temperature for Heliotek Gridded "Blue" Cell.
29	Hemispherical Total Emittance of Heliotek Gridded "Blue" Cell with Solakote "B" Filter.

Figure No.	Title
30	Effect of Cell Series Resistance on Current versus Illumination.
31	Spectral Transmittance of Typical SL-120 Reflecting Filter.
32	Spectral Transmittance of Typical SL-200(I) Reflecting Filter.
33	Spectral Transmittance of Typical SL-200(II) Reflecting Filter.
34	Spectral Transmittance of Typical SL-350 Reflecting Filter.
35	Variation in Cut-off Wavelengths, λ_2 and λ_3, with Angle of Incidence.
36	SL 350 Reflecting Filters.
37	Reflecting Filter Test Apparatus.
38	Reflecting Filter Test Apparatus with Collimator.
39	Close-Up of Reflecting Filter Test Apparatus.
40 to 113 (incl)	Reflection Filter I-V Curves - Table Mountain (see Table 4-IX).

LIST OF APPENDIX ILLUSTRATIONS

Figure No.	Title
APPENDIX A	
I	Filter SL 120/83 Characteristics (Specification).
II	Filter SL 200/82 Characteristics (Specification).
III	Filter SL 350/80 Characteristics (Specification).
IV	Substrate Dimensions and Specifications.
APPENDIX B	
B-1 to B-24	Spectral Transmittance Curves for Reflection Filters at 0° Angle of Incidence.
B-25 to B-29	Variation in Spectral Transmittance with Angle of Incidence for Representative SL 350 Filter.
B-30 to B-34	Variation in Spectral Transmittance with Angle of Incidence for Representative SL 200-II Filter.
B-35 to B-39	Variation in Spectral Transmittance with Angle of Incidence for Representative SL 200-I Filter.
B-40 to B-44	Variation in Spectral Transmittance with Angle of Incidence for Representative SL 120 Filter.

LIST OF TABLES

TABLE NO.		PAGE NO.
4-I	Elementary Study of Solar-Cell Output with Radiation Filtering and Concentration.	4-22
4-II	Summary of Results for Solar Cell Outputs with Radiation Filtering and Concentration.	4-23
4-III	Cell Power Outputs without Concentration or Filters.	4-24
4-IV	Computation of Solar Cell Output with Ideal Filters on one Concentrator Mirror.	4-25
4-V	Computation of Solar Cell Output with Realizable Filter on one Concentrator Mirror.	4-26
4-VI	Comparison of Liberty Mirror Filter Data with Specification Values.	4-38
4-VII	Typical Experimental Configurations Investigated in Filter Fabrication.	4-40
4-VIII	Mean Transmittance of Spectrolab Mirror Filters.	4-43
4-IX	Figure Numbering System for Reflection Filter I-V Curves.	4-46
4-X	Short-Circuit Current Data for SL 350 Mirror Filters.	4-47

Section 1
PURPOSE

Photovoltaic conversion of solar energy for auxiliary power in space vehicles is, at present, the most practical source of auxiliary power of this type and is, essentially, the only proven method. Current space programs rely almost exclusively on photovoltaic conversion by silicon solar cells for all but the shortest of space flights. Similarly, silicon cells can also be employed for the conversion of solar energy to electrical energy in earth-bound applications.

In general, our purpose is to improve the design of silicon cell power systems by improving the dependability and performance and by reducing the cost. The following three factors contribute to the efficiency of conversion of solar radiant energy to electrical energy by silicon solar cells:

1. the performance characteristics of the silicon solar cell,
2. the radiation incident on the solar cell, and
3. the heat transfer environment of the silicon solar cell.

The photovoltaic cell performance "characteristics" refer to curves showing electrical power , current, and voltage output data as functions of:

1. the total intensity of the incident radiation,
2. the spectral distribution of the incident radiation, and
3. the cell temperature.

The incident radiation can be described in terms of the total intensity, the spectral distribution, and the angle of incidence upon the photovoltaic cell assembly. The heat transfer environment of the photovoltaic cell is important since there is considerable reduction of solar cell conversion efficiency with increasing cell temperature.

This particular program is concerned with the use of concentrated and filtered solar radiation on silicon photovoltaic cells in solar power systems. The application of concentrating mirrors can, under certain conditions, contribute significantly to the reduction of weight and cost for photovoltaic solar energy conversion systems. Since the major problem encountered with the application of concentrating mirrors in photovoltaic conversion devices is that of temperature control, optical coatings can be of great importance in a unified design of a concentrating photovoltaic conversion system. It is anticipated that the filtering produced by such coatings will afford important increases of power output per cell by rejecting radiations which mostly heat the cells and by accepting only the radiations which most advantageously yield power output. Thus, the investigation and development of spectrally selective multilayer interference filters to provide optimum-reflection bandwidth coatings for concentrator surfaces is of primary importance.

Optimum coatings for concentrator systems will, to a large extent, depend upon the system configuration and the properties of cells. Therefore, in addition to the development of coatings for concentrators, this effort will include cell and system studies directed towards the integration of the coatings into actual concentrating systems, including investigations of thermal and insolation effects on silicon cell conversion efficiency and consideration of design parameters for an optimum concentrating photovoltaic solar energy conversion system.

In order to arrive at the optimum spectral characteristics for coatings to be used for solar concentrating systems, it is necessary to accurately determine thermal and current degradation of solar cells. Recent data indicates that the latest cells may be improved in these respects as compared to early cells and moreover that at high insolation the thermal effects may be different from those at lower levels of illumination.

The results of these investigations will be used to determine the optimum temperatures and concentration ratios for silicon solar cells. The spectral responses of the latest cells at this elevated temperature will be used to determine the ideal system spectral characteristics. Experimental mirror filters approaching these idealized characteristics will then be fabricated and tests will be made to evaluate the results, within the limits of test capabilities in the laboratory and on Table Mountain.

As previously stated, application of concentrators to photovoltaic solar energy conversion systems can, when properly designed, result in savings in two important system parameters, cost and weight. Since the efficiency of presently available photovoltaic energy-converting devices is decreased by highly concentrated insolance,* a reduction in the subtended area of the system will not be simultaneously achieved. However, further development effecting changes in the efficiency characteristics of such devices may permit the achievement of subtended-area reduction in the future.

The power output from a solar auxiliary power system is determined by the overall converter efficiency and the intercepted radiative flux. For the same insolance (near Earth), the area of the concentrator photovoltaic system will be greater than for the conventional arrangement, both because of collection and reflection losses in the concentrating optics and the greater thermal and series resistance degradation in the conversion devices. A reduction in cost can, however, be realized if an essential decrease in the number of solar cells applied can be achieved, so that the savings in solar cell costs will outweigh a potential additional cost of the reflecting surfaces. A reduction in the weight of this system may also be ob tained, since the reflecting surfaces can be of lightweight materials and design. This advantage is particularly important for systems

---

* A. Herchakowski and E. Kittl, "Design Considerations for a Photovoltaic Conversion System Using Concentration" (Proc. 15th Ann. Power Sources Conf., May 9-11, 1961), pp 120-124.

operating in strong radiation fields, where heavy quartz or glass must be used for shielding. On the other hand, a concentrator system requires orientation, although such orientation need not be close because of the relatively low concentration ratios. Thus, in order to design the solar cells, filters and concentrators in a photovoltaic cell solar power system and to evaluate the cost and performance of the system, it is necessary to consider the entire power system.

The performance studies of the entire solar power system of the first six months of the contract work period will lead to the formulation of specifications for reflecting, or mirror, filters; such filters can be fabricated by depositing spectrally selective optical coatings on glass substrates. In accordance with the contract statement of work, samples of such filters will be fabricated and evaluated.

SECTION 2

ABSTRACT

The use of concentrated and filtered solar radiation on silicon photovoltaic cells in solar power systems was investigated as a method of improving the performance and of reducing the weight and cost of such systems. In connection with this study, the development of spectrally selective multilayer interference filters was undertaken. Since optimum coatings for concentrator systems will depend upon the system configuration and the properties of the silicon solar cells, in order to conduct a performance analysis of a system with concentration and filtering, it was first necessary to study the performance of the entire system as well as the performance characteristics of solar cells and filters. The investigation indicated that the efficiency of concentration obtainable with a reflection filter depends strongly upon the spectral properties of the filter. On the basis of these studies, elementary conditions of system design for optimum performance were established. Also a basic plan was outlined for fabrication of a prototype solar system with concentration and filtering.

Following these analyses, filter performance characteristics were evaluated and specifications were formulated for suitable experimental mirror filters which might be fabricated to provide the desired concentration and filtering. Experimental mirror filters were then fabricated and data was obtained on the effect of such mirror filters on solar power system performance.

It can be concluded from this investigation that the use of concentration and filtering can afford valuable improvements in the cost and weight of solar power systems by increasing the power per cell.

SECTION 3

PUBLICATIONS, REPORTS AND CONFERENCES

The following publications, reports and conferences have resulted directly from research and development by Spectrolab under Contract No. DA 36-039 SC-87449 during the report period 1 June 1961 through 10 September, 1962. (There were no lectures resulting from this work.)

Publications and Conferences.

A paper "Photovoltaic System Using Concentrators" was presented by J.G. Beisenring at the Sixteenth Annual Power Sources Conference at Atlantic City, N.J. This conference was held 22-24 May 1962 under the sponsorship of the Power Sources Division, U.S. Army Signal Research and Development Laboratory of Fort Monmouth, N.J. The paper will also appear in the "Proceedings of the Sixteenth Annual Power Sources Conference" scheduled for publication in October, 1962.

Reports.

Monthly Letter of Progress reports for the report period have been submitted as follows:

Reports No. 1 - 7 for June, 1961 through December 1961, respectively;
Reports No. 8 - 15 for January, 1962 through August, 1962, respectively.

Also, two semi-annual reports were submitted, i.e. Technical Summary Report No.1, 1 June 1961 through 30 June 1961 and Technical Summary Report No.2, 1 July 1961 through 31 December 1961.

Section 4

FACTUAL DATA

Task A. Performance Studies of Solar Power System Using Silicon Cells

Phase 1. An Elementary Study of Solar Cell Performance with Radiation Concentration and Filtering.

The analysis of this section is based upon cells which are typical of those in production during 1960. The particular cell which is the subject of this study will be designated "1960 non-gridded red cell". The spectral sensitivity of this cell is shown in Fig. 1. The cell was covered with a Solakote "A" filter for the improvement of its emissivity and absorptivity. The spectral emissivity of the "1960 non-gridded red cell" with Solakote "A" filter is shown in Figure 2. The performance of the "1960 non-gridded red cell" for conditions of deep space under air-mass-zero insolation (see Fig.1) was determined using the following simple approximations of the radiative heat transfer properties of the cell and panel surfaces:

Cell surface-area utilization	0.90
Coated-cell emissivity	0.87
Coated-cell solar absorptivity	0.91
Effective emissivity of non-active front panel surface	0.65
Effective absorptivity of non-active front panel surface	0.20
Rear panel surface emissivity	0.90
Thermal conductance from front panel surface to rear panel surface	∞

The relative performance of this cell as a function of temperature is shown in Figure 3.

Under the above-described conditions, the equilibrium

temperature would be 317°K at unity concentration ratio for cells having an efficiency of ten percent. Fig. 4 compares the curve of equilibrium temperature as a function of incident energy for ten-percent efficient bare cells with the same data for Solakote "A" coated cells of ten-percent efficiency Also, using the aforementioned approximations, curves of the equilibrium temperature, the thermal degradation (i.e., the relative efficiency) and the relative output of 1960 non-gridded red cells having Solakote "A" filters were obtained as functions of the incident energy and are shown in Figure 5. The saturation effect of high irradiation on the performance of silicon cells was neglected in computing these curves The relative output curve indicates that the cell output rises rather slowly with incident energy and reaches a broad peak at approximately 310 mw/cm^2 incident energy, at which point the equilibrium temperature of the cell is 387°K. At incident energies exceeding 310 mw/cm^2, the output decreases with increasing irradiation.

The performance curves shown in Fig. 6 as functions of incident energy, but at constant cell temperature, indicate that output efficiency will be further degraded at high illumination levels. As will be indicated later, this is due to cell series-resistance.

In Fig. 5 it is shown that for an achromatic concentrator, a maximum output gain of only about 28 percent is achieved at an energy concentration ratio of 310/140 = 2.2, and an area concentration ratio of 2.2/rs, where "r" is the concentrator reflectance and "s" is the area utilization factor. Since the solar cell has varying spectral sensitivity and an approximately constant absorptivity over the spectral range of the incident radiation, an additional gain can be achieved by concentrating only the part of the spectrum which is most active in producing

electrical power and by eliminating the regions for which the thermal degradation predominates.

It is clear from basic considerations that under the conditions described, the maximum output for such a cell array (using 1960 non-gridded "red" cells) would result from monochromatic irradiation at a wavelength of about 820 mμ and an intensity of about 310 mw/cm^2 (ignoring saturation effects). For truly monochromatic light, this would require an infinite concentration ratio. Fortunately, suitably reducing the concentration ratio does not great affect the output.

An analysis of cell output as a function of area concentration ratio, assuming 310 mw/cm^2 incident energy on the cell, was made by varying the bandwidth transmitted to the solar cell. The results of this analysis presented in Fig. 7 show that by spectral selection and concentration it is possible, in an ideal sense, to increase the cell output from 1.28 to 3.04 times that of a coated, oriented, non-concentrated and, substantially, non-filtering system. Thus, the relative output is reduced by only 4 percent for a reduction in concentration ratio from infinity to 10. Therefore, the physical factors with respect to size, weight, tracking accuracy, and mechanical and optical design (to provide uniformity) which are associated with large concentration ratios, and which contribute to some of the major advantages of photovoltaic solar conversion as compared to other solar energy power sources, are still valid for a photovoltaic system with filtering and concentration which is associated with a low concentration ratio.

There are negligible gains, and in fact, disadvantages for area concentration ratios greater than 10. However, the relative output falls

off rapidly as the area concentration ratio is reduced below 10. For an area concentration ratio of 7, the relative output is down to 2.64, 13 percent below the maximum. The desirable concentration ratio for a given problem would be the result of a compromise obtained by evaluating numerous factors, e.g., complexity, reliability, orientation requirements. For the particular cells and heat transfer environment used in the analysis, the optimum concentration ratio will lie between 2.2 and 10. The results of this preliminary and elementary analysis are summarized in Table 4-I. An important conclusion from these results is that the maximum silicon solar cell output obtained with radiation filtering and concentration, in the deep thermal environment, is about three times the output obtained without filtering and concentration. This maximum of power output under these conditions is due to the opposite effects of the increase of power due to illumination and the degradation of power by cell heating. Of course, if by some means this cell heating is limited as the cell illumination is increased, the maximum silicon solar cell output is much higher and will be limited most probably by cell series-resistance.

It should be emphasized that the foregoing conclusions apply to the "1960 non-gridded red cell", for which the cell series-resistance has been neglected. In addition, these conclusions are based on the heat transfer environment of deep space. In ground applications of solar power systems it is necessary to also consider radiative heat transfer from the sky and terrain as well as heat transfer by convection to the atmosphere, in determining photovoltaic cell temperatures.

Phase 2. Further Studies of Solar Cell Performance with Radiation Concentration and Filtering.

(a) System Configuration.

For these studies, the solar power system is a Cassegrainian configuration of primary and secondary mirrors with an array of silicon solar cells as shown in Figure 8A. The system is assumed to be operating in deep space. The performance of this system has been investigated for various silicon cells and reflection filter designs. (The heat transfer environment is the same in all cases and such that the cell temperatures are determined by the data in Figures 9 through 13).

(b) Solar Cell Array Equilibrium Temperature Analysis.

The following analysis relates steady-state cell temperature to: (a) the incident energy to the cell, (b) the cell conversion efficiency, and (c) the reflector-array geometry for a Cassegrainian reflector system.

The following assumptions were made:

(1) All radiant flux incident on the cell is either absorbed as thermal energy or converted into electrical energy. (Present day cells have high absorptivity characteristics. This characteristic is particularly valid for reflector-filtering concentrator systems since reflection of filtered energy by the cell degrades system overall efficiency.)

(2) All solar energy reflected by the primary reflector is uniformly distributed upon the secondary reflector of the Cassegrainian system.

(3) Emissivity of non-reflective surface (back surface) of primary reflector is 0.95, attainable with coatings.

(4) Emissivity of reflective surfaces is 1.0. (Present reflective coatings have emissivities of approximately 0.95.)

(5) Emissivity of shaded surface of Cassegrainian array is 0.95, attainable with coatings.

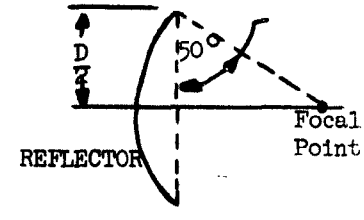
(6) The surface properties of the directly sun-lighted surface of the Cassegrainian secondary reflector are:

$\alpha = 0.09$, $\epsilon = 0.90$ (coating properties anticipated in the near future).

(7) Uniform distribution of reflected flux upon the array. (Departure from this assumption is small for the D/d values considered.)

(8) Absorptivity of the reflective surface of the secondary reflector is 0.05 for the Cassegrainian system. (This is presently attainable for selective wavelengths.)

(9) The paraboloidal reflector rim-focal point angle (illulstrated below) is 50°.



(10) Thermal gradients within the array as well as within the primary and secondary reflectors were neglected. (These gradients are minimal due to weight and thermal distortion considerations.)

(11) Planetary effects such as albedo and surface radiation were neglected.

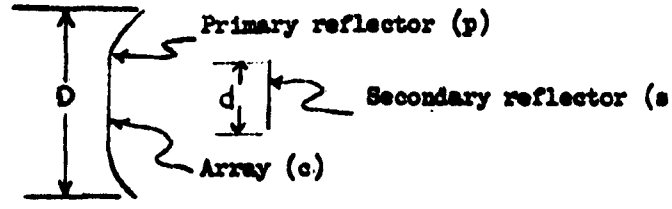
The following nomenclature was used to define the heat transfer environment of the Cassegrainian solar power system:

A_{proj}	Projected area
A	Surface area
α	Surface solar absorptivity
S	Solar flux
d	Array and secondary reflector diameter
D	Primary reflector diameter
F_e	Emissivity factor
F_A	Configuration factor
σ	Stefan-Boltzmann constant
T	Temperature (°K)
S_c	Flux incident to cell
β	Percent cell conversion of incident energy into electrical energy

Subscripts:

p1	Reflective surface of primary reflector
p2	Non-reflective surface of primary reflector
s1	Surface of secondary reflector
s2	Other reflector surface (relative to s1)
c1	Photovoltaic cell side of array
c2	Other surface of array (relative to c1)
sp	Space

(c) Analysis:



CASSEGRAINIAN FLUX CONCENTRATION REFLECTOR SYSTEM

A heat balance for a Cassegrainian flux concentration reflector system can be expressed, in terms of flux incident to the cell, by the following three equations:

I $$\frac{A_{Proj}}{A_p}\left[\alpha_{p_1} S - \left(\frac{S_s}{1-\alpha_{s1}}\right)\left(\frac{A_s}{D^2-d^2}\right)\right] = \left[F_{\varepsilon_{p_1-sp}} F_{A_{p2-sp}} + F_{\varepsilon_{p_1-sp}} F_{A_{p_1-sp}} + F_{\varepsilon_{p_1-s1}} F_{A_{p_1-s1}} + F_{\varepsilon_{p_1-c1}} F_{A_{p_1-c1}}\right]\sigma T_p^4 - F_{\varepsilon_{p_1-s1}} F_{A_{p_1-s1}} \sigma T_s^4 - F_{\varepsilon_{p_1-c1}} F_{A_{p_1-c1}} \sigma T_c^4.$$

II $$\frac{A_{Sproj}}{A_s}\left[S\alpha_{s2} + \frac{S_s \alpha_{s1}}{1-\alpha_{s1}}\right] = \left[F_{\varepsilon_{s2-sp}} F_{A_{s2-sp}} + F_{\varepsilon_{s1-sp}} F_{A_{s1-sp}} + F_{\varepsilon_{s1-c1}} F_{A_{s1-c1}} + F_{\varepsilon_{s2-p1}} F_{A_{s2-p1}}\right]\sigma T_s^4 - F_{\varepsilon_{s1-c1}} F_{A_{s1-c1}} \sigma T_c^4 - F_{\varepsilon_{s1-p1}} F_{A_{s1-p1}} \sigma T_p^4.$$

III $$(1-\rho) S_c = \left[F_{\varepsilon_{c1-sp}} F_{A_{c1-sp}} + F_{\varepsilon_{c1-sp}} F_{A_{c1-sp}} + F_{\varepsilon_{c1-s1}} F_{A_{c1-s1}} + F_{\varepsilon_{c1-p1}} F_{A_{c1-p1}}\right]\sigma T_c^4 - F_{\varepsilon_{c1-s1}} F_{A_{c1-s1}} \sigma T_s^4 - F_{\varepsilon_{c1-p1}} F_{A_{c1-p1}} \sigma T_p^4.$$

The resulting cell temperatures (to the fourth power) are shown as Figures 9 to 13 for various concentration ratios, C_R, as functions of flux incident to cell and percent cell conversion of incident energy. The results in these figures are based on complete absorptivity of flux incident to the cells. Thus, for systems incorporating flux filtering by the cell, or for systems incorporating low-absorptivity cells, the results will have to be modified.

(d) Performance Analyses.

The power output of a solar cell may be increased by increasing the intensity of the light impinging on it with a solar concentrating-mirror system. However, as previously demonstrated, a point is reached at which an increase in light intensity produces more thermal degradation of the cell than increase in power output. Figure 14 contains a curve of a typical temperature characteristic of an experimental gridded "red" silicon solar cell. A similar curve for a "blue" cell is shown in Figure 15. Also, the response of the cell varies with wavelength and does not best match the solar spectrum in space. If spectrally selective filters are used on the surface of the mirror, the wavelengths of the solar spectrum that contribute more to the heating of the cells than to the power output may not be reflected by the mirror but may instead be transmitted by it, and thus be removed from the working beam finally reaching the solar cells. With this control over the spectrum and temperature of the cells, we may choose our operating

conditions to maximize the power output for each physical concentration ratio, that is, $C_R = \left(\frac{D}{d}\right)^2 - 1$.

In the study of this design and performance problem the following cases are considered:

(1) Experimental 1960 gridded "red" cell with its maximum power-temperature characteristic used with ideal concentrator filters.

(2) Heliotek gridded "blue" cell with the "red" cell maximum power-temperature characteristic used with ideal concentrator filters.

(3) Experimental gridded "red" cell with its maximum power-temperature characteristic used with realizable * concentrator filters.

(4) Heliotek gridded "blue" cell with the "red" cell maximum power-temperature characteristic used with realizable * concentrator filters.

(5) Heliotek gridded "blue" cell with its maximum power-temperature characteristic used with ideal filters.

(6) Heliotek gridded "blue" cell with its maximum power-temperature characteristic used with realizable * filters.

The assumptions of the performance analyses are:

(1) The ideal filters used have 100-percent reflectivity in the band-pass region and zero-percent reflectivity in the band-stop region.

---

* "Realizable" is used in the sense that, given sufficient time and effort, it should be possible according to previous experience to produce such a filter, although such filters are not within the present production capability.

(2) The spectral reflection and transmission characteristics of the realizable* concentrator filters are shown in Figures 16, 17 and 18.

(3) The response of the solar cell to each wavelength of solar energy is degraded by temperature in the same ratio so that the shape of the response curve remains constant and only its amplitude changes.

(4) The power output of the cell at constant temperature is a linear function of illumination. (For relatively low concentrations, this statement is true.)

(5) The load impedance matches that of the array for any operating condition.

Nomenclature with respect to the spectral characteristics of the solar radiation, relative cell response, and concentration filter reflectance:

β — Percent conversion of energy incident on the solar cell to electrical power.

β_m — The number by which the average response between λ_A and λ_B is multiplied to give the average response between a narrower band-pass region chosen between limits at an equal height on the R_λ curve,

$$\beta_m = \frac{\int_{\lambda_1}^{\lambda_2} R_\lambda S_\lambda d\lambda \Big/ \int_{\lambda_1}^{\lambda_2} S_\lambda d\lambda}{\int_{\lambda_A}^{\lambda_B} R_\lambda S_\lambda d\lambda \Big/ \int_{\lambda_A}^{\lambda_B} S_\lambda d\lambda}$$

*See footnote on Page 4 - 10.

R_λ The relative response of the solar cell to a wavelength of light, λ.

S_λ The intensity of the solar energy at a wavelength, λ.

λ Wavelength.

λ_A, λ_B The lower and upper cut-off wavelengths of the solar cell, respectively.

λ_1, λ_2 The lower and upper cut-off wavelengths of the filter, respectively.

M_T Coefficient of temperature degradation of the solar cell.

The following calculations have been performed for two types of silicon solar cells: one, called the "experimental 'red' cell", has a spectral response curve which peaks at 0.82 micron; the other, commonly called the "Heliotek 'blue' cell", has a spectral response curve which peaks at 0.85 micron. Graphs of both are presented in Figures 23 and 24. In addition, Figures 23 and 24 include, for the red and blue cells, respectively, the cumulative solar energy and power output as a fraction of the total between λ_A and λ_B. The data for "S" is just the Johnson Curve, the air-mass-zero solar spectrum in space near the earth, where the total flux is 140 mw/cm^2. Of this, the red cell, having cut-off wavelengths of 0.405 micron and 1.165 microns, responds to 95.8 mw/cm^2, while the blue cell, having cut-off wavelengths of 0.36 micron and 1.20 microns responds to 103.5 mw/cm^2.

Subject to the previously stated assumptions, a necessary condition for filter optimization is that the "cut-on" and cut-off wavelengths fall at equal values of the relative cell response curve. This "R_λ" designates the bandwidth used by specifying the region located between equal response heights on the response curve of the cell. The fraction of the solar energy and cell power output occurring in the region found by choosing filter band-pass limits at equal height on the response curve of the cell, is shown in Figures 21 and 22 for red and blue cells, respectively. In addition, $(\beta_m - 1)$ is also plotted, where β_m is the multiplier of the average absolute efficiency, at the reference temperature, between λ_A and λ_B, necessary to obtain the average efficiency within the R_λ limits, as defined in the nomenclature. The power output of the array for varying concentration ratios and ideal filter band-pass widths is shown in Figures 19, 20a and 20b for the red and the blue cells, respectively.

For both the red and the blue cells, it was assumed in the calculations that the average absolute value of the response between λ_A and λ_B at 303°K is 13.3 percent. This assumes an absolute peak response of the red cell at 25 percent and of the blue cell at only 21.4 percent. The following analysis and specific example will indicate how the curves in Figures 19, 20a and 20b were constructed.

(c) Optimization Procedure for Ideal Filters.

The first step in the optimization procedure is to determine the method for selecting the bandwidth and the centerline of the filter passband. A preliminary check shows that even for the relatively low concentration ratio of four

it is not desirable to use the total broad-band energy since narrowing the band-pass limits a small amount, in any arbitrary manner, has the effect of increasing the power output.

Since all of the broad-band energy will not be used, the portion that is used should be chosen in a manner such that with any given amount of solar energy input, the average efficiency of converting solar energy to electrical energy will be the highest. This is done by choosing the filter band-pass limits at equal heights on the response curve of the cell. This choice has a twofold effect on increasing the power output for any energy input. First, with the highest conversion efficiency at a constant temperature, the output is highest. Second, with more of the input energy being converted to electrical energy, there is less that is being converted only into heating, and therefore less thermal degradation.

Now, it remains to use the curves herein presented to find the actual operating point of the cell. This is done in the following example for the experimental "red" cell:

(1) Choose a concentration ratio and R_λ value. In this case, select $C_R = 4$ and $R_\lambda = 0.5$.

(2) The broad-band energy which, without filtering, would be concentrated on the solar-cell array is:

$$S_{conc.} = (C_R) \int_{\lambda_A}^{\lambda_B} S_\lambda \, d\lambda = (4)(95.8) \approx 383.5 \ mw/cm^2$$

(3) The energy in the R_λ limit of 0.5 is found with the help of Figure 21. From the abscissa of $R_\lambda = 0.5$, we find the corresponding ordinate of the fraction of: $\int_{\lambda_A}^{\lambda_B} S_\lambda \, d\lambda$ that is in that limit, or (0.534). Thus, $S_{\text{scene. and filter}} = 383.5 \times 0.534 = 204.5$ mw/cm^2.

(4) $\beta_{303°K}$ can now be found. From Figure 21, $\beta_m - 1 = 0.46$, or $\beta_m = 1.46$. Hence, if the average absolute value of the response of the cell between λ_A and λ_B is 13.3 percent, then

$$\beta_{303°K} = 1.46 \times 13.3 = 19.42 \text{ percent},$$

the average absolute response in the wavelength limits dictated by $R_\lambda = 0.5$, and at the temperature 303° K.

(5) The β chosen above will be thermally degraded. Therefore, the actual β of the cell will be less. For the first approximation, choose: $\beta = 14$ percent. Then, from Figure 10 above the 204.5 mw/cm^2 abscissa, we find the (temperature)^4 for $\beta = 14$ by interpolating between the $\beta = 10$ and $\beta = 15$ lines:

$$T^4_{(\beta = 14)} = 166 \times 10^8 \text{ °K}^4, \text{ or } T = 358.5° \text{ K}.$$

From Figure 14 we find the thermal degradation coefficient to be:

$$R_T = 0.666$$

$$\beta_T = 19.42 \ (0.666) = 12.9 \text{ percent}$$

Hence, we see that our estimate of β was too high, so we make a new lower estimate:

$$\beta = 12.6; \quad T^4 = 169 \times 10^8; \quad T = 360.6;$$

$$\beta = 19.42\ (0.653) = 12.65 \text{ percent.}$$

The two β's now agree as closely as can be expected with the graphical accuracies involved. The power output is then:

$$P = 0.1265\ (204.5) = 24.8 \text{ mw/cm}^2.$$

This procedure is repeated for a number of R_λ values for each concentration ratio until the curves in Figures 19, 20a and 20b are generated. We see that for each concentration ratio, the power output peaks at higher R values for higher concentration ratios. Obviously, neglecting size and weight considerations, the greatest power output will be for $R_\lambda = 1.00$, $C_R = \infty$.

(f) Results of Performance Analyses.

Using the methods and the thermal environment data previously discussed, the performance of three "ideal" and three "realizable"* filters for use with the "red" and "blue" silicon cells was estimated. Curves for realizable filters are shown in Figures 16, 17 and 18, in the "dotted-line" curves. The "solid-line" curves are convenient approximations used in the computation. The realizable filter characteristics were determined for use with a "red" cell with peak spectral response

---

*See footnote, Page 4 - 10.

at wavelength λ = 0.82 micron. These filters will require from nine to sixteen or more layers. As the bandwidth narrows, the number of layers required increases. Each ideal filter has the same cut-off wavelength as the corresponding realizable filter and also has zero transmittance in the passband and perfect transmittance outside the passband, as previously defined. For both the red and blue cells, the solar insolation was assumed to be 140 mw/cm^2 and the broad-band efficiency (between λ_A and λ_B) of both cells was assumed to be 13.3 percent at 303° K. This gives the red cell a peak efficiency of 25 percent, and the blue cell a peak of 21.4 percent. Thus, it is seen immediately that for equal broad-band efficiencies, and at high concentration ratio, C_R, the red cell performs better than the blue. However, for equal peak efficiencies, the opposite is true.

The computations and results for the ideal filters are shown in Table 4 - IV. From Figures 23 and 24, the R_λ values corresponding to the filter cutoffs were found and tabulated. In those few cases where the "left" and "right" values of R_λ differ by a small amount, the average is given. The concentration ratios may be checked against Figures 19 and 20 by noting which curves peak at the specified values of R_λ. Finally, the output power was read from the peak values of these curves, and tabulated in Table 4 - IV.

Table 4 - V shows computations made for the performance of the realizable filters.

It is especially important to note here that the "experimental silicon gridded 'red' cell" (with temperature coefficient of 0.0060/°C) and the "Heliotek silicon gridded 'blue' cell" are actual existing cell types. The hypothetical silicon gridded blue cell, on the other hand, is a purely hypothetical cell with the same characteristics as the existing Heliotek "blue" cell, except for the temperature power coefficient which is the same as that for the "red" cell. This hypothetical cell is included in order to demonstrate the critical importance of the temperature-power coefficient. For comparison with the results in Table 4-II, the cell power outputs at a concentration ratio of one and with no filters, except as used on the cell in all cases, are as shown in Table 4-III.

For the higher concentration ratios the cell power outputs are much greater with the ideal filters than with the realizable filters; however, for the lowest concentration ratios the power outputs per cell are only slightly higher for the ideal filter. The reduction of power output with the realizable filters is due almost entirely to the excessive heating effect of the radiation transmitted to the solar cells by the realizable filters outside their passbands. This effect is relatively less at the lowest concentration ratio since in this case the heat transmitted to the cell outside the passband is small in comparison to that transmitted in the wide passband. With the ideal filter the maximum power output per cell occurs at the highest concentration ratio; however, with the realizable filters the maximum power output per cell occurs at an optimum concentration ratio between 9 and 4. The curves on Figure 25 are presented for better understanding of

on Figure 25 differ. For these corresponding cases, the power output of the "red" cells exceeds the power output for the "blue" cells only as the area under the solar spectral response curves within the filter passband in Figure 25 for the "red" exceeds that for the "blue" cell. The increase of power of the blue cell with its proper temperature-power coefficient, 0.0041/°C, is due to both its lower temperature-power coefficient and to the filters which are optimum for the "blue" cells.

(g) A Summary Statement of the Elementary Design Conditions for Optimum Performance of a Silicon-Cell Solar Power System Using Radiation Filtering and Concentration.

The elementary design conditions for optimum performance of a silicon-cell solar power system which employs both filtering and concentration have been previously discussed and analyzed in this report.

Consider first the case where the greatest maximum power per cell is sought. For ideal filters, the filter passbandwidth should be small and at the wavelength of cell maximum spectral response and with the small bandwidth, the illumination concentration ratio should be so high that the combined conditions of illumination intensity and cell temperature yield the maximum power output. For realizable filters, the illumination concentration ratio will be in the range 6 to 12, depending on the filter performance, and the corresponding filter passband limits will intersect the solar-cell relative response curve at equal values on the high and low wavelength sides of the curve. As the filter performance improves, the illumination concentration ratio will become higher and the filter passbandwidth will be narrower for the greatest maximum power

performance. For the case of the maximum power per unit area of system solar beam aperture, the radiation concentration ratio is only slightly greater than unity, even with ideal filters. With realizable filters, the greatest power per unit solar beam aperture occurs at radiation concentration ratio of unity and a concentrator filter yields little, if any, advantage. Thus, it is not to be expected that radiation concentration and filtering will yield more power per unit area of solar beam.

(h) Major Conclusions of the System Performance Analyses.

For silicon cell solar power systems operating in deep space heat transfer environment:

(1) The greatest possible power output per cell with radiation concentration and filtering is three to four times as great as the power output without concentration and filtering, depending on the cell performance characteristics.

(2) The feasible power output per cell, with presently available silicon cells and presently feasible filters, is three times greater with radiation concentration and filtering than without concentration and filtering. This power output per cell will occur at a concentration ratio in the range 6 to 12.

(3) The maximum power output per cell is critically dependent on the silicon cell and filter performance characteristics.

TABLE 4 - I

Elementary Study of Solar-Cell Output with Radiation Filtering and Concentration

Concentration Ratio, C_R	Temperature °K	Filters	Power Output (percent)
1	317°	None	100
2.2	-	Solakote "A"	128
10	-	Perfect narrow band	282
∞	387°	Perfect narrow band	304

TABLE 4 - II

SUMMARY OF RESULTS FOR SOLAR CELL OUTPUTS WITH RADIATION FILTERING AND CONCENTRATION

Solar Cell	Experimental Silicon Gridded "red"			Heliotek Silicon Gridded "blue"			Heliotek Silicon Gridded "blue"		
Temperature Power Coefficient	"red" cell .0060/° C Figure 5-14			"red" cell .0060/° C Figure 5-14			"blue" cell .0041/°C Figure 5-15		
Concentration ratio, C_R	16	9	4	16	9	4	16	9	4
Filters Cutoff Wavelength (microns)	.77 .89	.72 .92	.625 .975	.77 .89	.72 .92	.625 .975	.695 .925	.630 .950	.500 1.020
Ideal Filter: Power Output (mw/cm^2)	35.25	32.25	26.90	29.60	28.50	25.30	41.40	38.40	30.70
Realizable Filters:	SL120/83	SL200/82	SL350/80	SL120/83	SL200/82	SL350/80	SL230/81	SL320/79	SL520/76
Power Output (mw/cm^2)	15.10	24.80	24.80	14.0	22.6	23.7	31.2	35.3	29.5

TABLE 4-III

CELL POWER OUTPUTS WITHOUT CONCENTRATION OR FILTERS

CELL	EXPERIMENTAL SILICON GRIDDED "RED"	HELIOTEK SILICON GRIDDED "BLUE"	HELIOTEK SILICON GRIDDED "BLUE"
Temperature-Power Characteristic	"Red" cell .0060/°C Figure 5-14	"Red" cell .0060/°C Figure 5-14	"Blue" cell .0041/°C Figure 5-15
Output Power (mw/cm^2)	10.5	11.4	12.2

TABLE 4 - IV

COMPUTATION OF SOLAR CELL OUTPUT WITH IDEAL FILTERS ON ONE CONCENTRATOR MIRROR

Solar Cell	Experimental Silicon Gridded "red"			Hypothetical Silicon Gridded "blue"			Heliotek Silicon Gridded "blue"		
Temperature-Power Characteristic	"Red" Cell .0060/° C Figure 5-14			"Red" Cell .0060/°C Figure 5-14			"Blue" Cell .0041/° C Figure 5-15		
Concentrator ratio, C_R	16	9	4	16	9	4	16	9	4
Ideal Filters									
Bandwidth Microns	.120	.200	.350	.120	.200	.350	.230	.320	.520
Cutoff Wavelength (microns)	.77 .89	.72 .92	.625 .975	.77 .89	.72 .92	.625 .975	.695 .925	.630 .950	.500 1.020
R_λ	.91	.82	.60	.97	.91	.74	.89	.79	.51
Output Power mw/cm^2	35.25	32.55	26.90	29.60	28.50	25.30	41.40	38.50	30.70

TABLE 4 - V

COMPUTATION OF SOLAR CELL OUTPUT WITH REALIZABLE FILTER ON ONE CONCENTRATOR MIRROR

1. Solar Cell	Experimental Silicon Gridded "red"			Heliotek Silicon Gridded "blue"			Heliotek Silicon Gridded "blue"		
2. Temperature Power Characteristic	"red" cell .0060/° C Figure 5-14			"red" cell .0060/°C Figure 5-14			"blue" cell .0041/°C Figure 5-15		
3. Concentration Ratio, C_R	16	9	4	16	9	4	16	9	4
Filters:									
4. Bandwidth Microns	.120	.200	.350	.120	.200	.350	.230	.320	.520
5. Cutoff Wavelengths, Microns	.77 .89	.72 .92	.625 .975	.77 .89	.72 .92	.625 .975	.695 .925	.630 .950	.500 1.020
6. Filter Number	SL120/83 SL200/82 SL350/80			SL120/83 SL200/82 SL350/80			SL230/81 SL320/79 SL520/76		
7. R_λ	.91	.82	.61	.98	.92	.75	.89	.79	.51
Fraction of Solar Energy between λ_1 and λ_2									
8. $\dfrac{\int_{\lambda_1}^{\lambda_2} S(\lambda)\,d\lambda}{\int_{\lambda_A}^{\lambda_B} S(\lambda)\,d\lambda}$	.19	.23	.44	.17	.21	.40	.25	.37	.65

TABLE I - V (Cont'd)

9. Reflectance x fraction of solar energy in two bands: λ_A to λ_1 and λ_2 to λ_B	.08	.08	.06	.08	.08	.06	.07	.06	.03
10. Reflectance x fraction of solar energy outside range of λ_A to λ_B	.02	.02	.02	.02	.02	.02	.02	.02	.02
11. Sum: (8) + (9) + (10)*	.29	.33	.52	.27	.31	.48	.34	.45	.70
12. Incident flux, ideal filter, $(C_R)\cdot(8)\times\int_{\lambda_A}^{\lambda_B} S_\lambda\, d\lambda$ (mw/cm^2)	291	198	169	291	198	169	414	344	269
13. Flux incident to cells with realizable filters $(C_R)\cdot(11)\times\int_{\lambda_A}^{\lambda_B} S_\lambda\, d\lambda$ (mw/cm^2)	445	284	199	445	284	199	564	420	290
14. Cell temperature, ideal filter °K	390	355	342	391	356	343	424	406	386
15. Cell temperature realizable filter °K	443	394	358	444	396	359	472	430	395

*Numbers in parentheses refer to corresponding item numbers on this page.

TABLE 4 - V (Cont'd)

16. Temperature degradation factor, ideal filter	.47	.68	.76	.46	.67	.74	.51	.58	.66
17. Temperature degradation factor, realizable filter	.16	.45	.67	.15	.44	.66	.31	.48	.62
18. Fraction of cell response between λ_1 and λ_2 $\dfrac{\int_{\lambda_1}^{\lambda_2} S(\lambda) R_\lambda \, d\lambda}{\int_{\lambda_A}^{\lambda_B} S(\lambda) R_\lambda \, d\lambda}$	.26	.40	.68	.20	.35	.62	.29	.45	.77
19. Reflectance x fraction of solar radiation outside range λ_1 to λ_2 $R \propto [(8)-(18)]^*$	.07	.06	.03	.08	.06	.04	.07	.05	.02
20. Sum: (18)+ (19)*	.33	.46	.71	.28	.41	.66	.36	.50	.79
Output of cells with ideal filters mw/cm^2	35.25	32.55	26.90	29.60	28.50	25.30	41.40	38.50	30.70
21. Ratio: $\dfrac{(17)\times(20)}{(16)\times(18)}$*	.43	.71	.92	.46	.79	.95	.75	.92	.96
Output of cells with realizable filters mw/cm^2	15.1	24.8	24.8	14.0	22.6	23.7	31.2	35.3	29.5

*See footnote on preceding page.

TASK 5. Silicon Solar Cell Performance Characteristics

The development of filters and concentrators to be used in systems for the conversion of solar radiation to electrical power by means of silicon photovoltaic cells requires wide and accurate knowledge of the silicon cell performance characteristics.

Phase 1. The principal characteristic curves for silicon solar cells are:

(1) Curves of cell current vs. cell voltage for various illumination intensities and temperatures.

This data is for a constant, usually a standard, temperature and for the same spectral distribution of energy in the incident radiation. A typical silicon cell I-V curve is shown in Figure 26.

(2) Cell maximum-power output.

At a particular point of each I-V curve the cell output power determined by the product, $P = VI$, is a maximum. The maximum power points are located in Figure 26. The maximum power outputs for a cell are to be identified with the same conditions as the I-V curves from which they were determined, i.e., the angle of incidence, the temperature, and the intensity and spectral energy distribution of radiation. At maximum power,

$$P = P_{max}, \; V = V_{mp}, \; I = I_{mp}.$$

(3) Temperature effects on P_{max}, V_{max} and I_{max}.

Figure 26 shows a typical set of I-V curves for various temperatures. In Figures 27 and 28 maximum power, P_{max}; voltage at maximum power, V_{mp}, and current at

$I = I_{mp}$ (all for the I-V curves of Figure 26) are plotted as functions of temperature. The effect of temperature on cell maximum power is usually presented as relative efficiency at maximum power, as, for example, in Figures 14 and 15 which consist of the curves for an experimental gridded "red" cell and for a typical Heliotek gridded "blue" cell.

(4) Effect of illumination intensity on cell maximum power output, maximum-power-point voltage, and efficiency.

This data is plotted in Figure A-4 for experimental cells A-N-12 and A-N-16. The I-V curves for these cells are shown in Figure A - 2. Also shown in Figure A - 4 is the effect of increased insolation for three hypothetical cells of similar characteristics to the aforementioned experimental cells, except that the three hypothetical cells have series resistances of 0, 0.5 and 1.0 ohms, respectively.

(5) Relative spectral response.

The relative spectral response curves of an experimental gridded "red" cell and of a typical Heliotek gridded "blue" cell are shown in Figures 23 and 24. The relative spectral response is denoted by $R(\lambda)$ and is defined as the following ratio:

$$R(\lambda) = \frac{\text{Short circuit current per unit incident ratiation intensity per unit of spectral bandwidth, at the wavelength, } \lambda.}{\text{Peak value of the short-circuit current per unit incident radiation intensity per unit of spectral bandwidth.}}$$

It is assumed in the performance analyses in this report that silicon-cell maximum power response to a broad spectral band of high intensity radiation is

$$P_{max} = p_{\lambda max} \int R(\lambda)S(\lambda)d\lambda \qquad (1)$$

where $p_{\lambda max}$ = solar cell maximum power per unit of spectral bandwidth and per unit of illumination intensity at $\lambda = \lambda_{max}$, and

λ_{max} = λ at which $R(\lambda) = 1$.

The exact extent to which Equation (1) is valid remains to be investigated and determined. In support of the supposition represented by Equation (1), it is well known that the maximum power output to broad-band illumination is, except for small effects due to cell series resistance, proportional to the total illumination, as indicated in Figure A - 3 (revised). As indicated in Figure A - 4, the maximum power voltage changes very little with illumination but, as is well known, the cell short circuit current, I_{sc}, and the cell maximum power current, I_{mp}, are both for cells with acceptably small series resistance proportional to illumination intensity.

The effect of cell series resistance on I_{max} and I_{sc}, as functions of cell illumination, is presented in Figure A - 3 (revised). (The series resistances of Heliotek gridded "blue" cells are in the range 0.38 to 0.48 ohm.)

(6) Silicon cell assembly spectral normal absorptive characteristics.

The spectral normal absorptance is the ratio of the energy absorbed by the surface to the energy incident upon it

for normally incident radiation at any particular wavelength. The spectral absorptance of the cell assembly is important with respect to: (a) radiations for which the cells yield power, (b) radiations which merely heat the cells, and (c) ultraviolet radiations which may damage the cell cover adhesive. Since the silicon cells are opaque in the spectral range of interest, normal absorptance may be determined from measurements of reflectance. The absorptance and reflectance, as well as the relative spectral response, are important for angles of incidence less than 90° in some applications. The spectral absorptance of the solar cells is closely related, physically, to their spectral emittance.

(7) Silicon-cell assembly hemispherical total emittance.

Hemispherical total emittance is defined as the ratio of: (a) the total energy radiated at all wavelengths from a surface to the hemisphere of space surrounding the surface, to (b) the total energy radiated at all wavelengths by a black body at the same temperature. This emittance is critically important with respect to the operating temperature of the silicon cells. For solar cells with spectrally selective absorptance, the spectral emittance is also selective, and thus, the hemispherical total emittance may vary somewhat with temperature. The hemispherical total emittance of silicon cell assemblies is measured by existing techniques. An example of emittance measurements for a Heliotek gridded silicon cell covered with a Solakote "B" filter is presented in Figure 29.

In addition to the discussion of the serious effects of cell series resistance on maximum power output, the report by M. Wolf and Hans Rauschenbach, "Series

Resistance Effects on Solar Cell Measurements;"* also includes a careful discussion of the relation of illumination intensity to the I-V curve and hence to maximum power output. This relationship is such that at constant cell temperature the I-V curves for various intensities of illumination all fit upon each other (to a good approximation) when shifted, both (a) vertically, by an increment of current due to the increment of illumination, and (b) horizontally, by a voltage drop due to the increment of current flowing in the series resistance of the cell. An example of I-V curve shifting is shown in Figure 30; the I-V curves for the solar irradiances 100, 200, and 300 mw/cm^2, which all fit the curve for 400 mw/cm^2 quite well. This method of I-V curve shifting can be used to determine the "light current" and to estimate cell series resistance.

Phase 2. Summary of Silicon Solar Cell Characteristics Relative to the Performance of Solar Power Systems with Radiation Filtering and Concentration.

The following characteristics of silicon photovoltaic cells are critically important to the attainment of high performance of solar power systems using concentrated and filtered radiation on such cells:

(1) Short circuit current spectral response.
(2) Temperature degradation of maximum power and voltage.
(3) Spectral normal absorptance.
(4) Hemispherical total emittance.

Of course, high maximum spectral response occurring in the spectral region of high solar irradiance and small temperature degradation of maximum power will each contribute

*Paper No. CP 61-1006 presented at the American Institute of Electrical Engineers meeting, 23-25 August, 1961 at Salt Lake City Utah. (Included in revised form as appendix of Spectrolab Technical Summary Report No. 2, June 1961, this contract.)

to high system performance. Also, it is highly important that the series resistance of the cells be suitably small so that at high illumination intensities the response remains proportional to illumination intensity. As the power system analyses in this report show, the temperature degradation effect is a major one, especially at the high temperatures which occur at high radiation intensities. The spectral normal absorptance is of importance since it is desirable that the radiation which is converted to power be absorbed and the radiation which would merely heat the cell be reflected. Also, the hemispherical total emittance of the solar cells should be high in order that heat may be rejected by the cell at favorably low temperatures.

As a result of the foregoing solar power system analyses, more specific criteria have evolved with respect to solar-cell performance characteristics.

Task C. Filter Performance Characteristics.

The system performance analyses of this report consider the "idealized" filter as well as filters which are physically attainable. Ideally, the filters should permit all radiation within a particular spectral band to reach the cell faces and should prevent all radiation outside this passband from reaching the cells. Under actual physical conditions, less than this ideal will be attained. It should be possible to produce filters having characteristic curves corresponding to those in Figures 16, 17 and 18. As indicated in the performance analyses, the performance of the solar power system is critically dependent on filter performance.

Elementary considerations indicate that the best system performance will be attained in systems using both filtering and concentration by accomplishing a major part of the radiation filtering at the concentrator surfaces. Additional improvement can then be attained by means of covers on the solar cells. These covers should be designed for optimum performance specifically with respect to:

(1) The protection of the solar cells from damage by contact with other materials and the atmosphere.

(2) The protection of the solar cells from damage by electron bombardment in space.

(3) Hemispherical total emittance.

(4) Additional filtering of radiation.

All of the aforementioned must be attained without serious impairment of the transmission of the radiation effective in yielding power output.

The cell cover filters should reflect strongly in the spectral ranges where the concentrator reflector filters transmit strongly. On the long wavelength side, this range is approximately from 1 to 4 microns. Beyond 4 microns the cell covers must emit strongly, as 9% of the black body radiation is of wavelengths greater than 4 microns for a 150° C surface. For higher temperatures, as may result if concentrator filters are not employed, the cell cover filters would have to emit strongly at shorter wavelengths; such filters would be difficult to produce.

Since excellent cell filters already exist which take into account the aforementioned requirements, the studies discussed in this report were primarily concerned with the use of filters on the concentrator surfaces. Moreover, reflection filters were considered, exclusively, since this type of filter has better performance characteristics and is more suitable, physically, to the optical arrangement of the system.

Task D. Experimental Mirror Filters

Phase 1. Fabrication of Experimental Mirror Filters

a) Mirror Filter Specifications

Appendix A of this report consists of specifications which were formulated, on the basis of the performance analysis, for three types of mirror filters. Figures I, II, and III are idealized filter performance curves for filter types SL 120/83, SL 200/82, and SL 350/80, respectively. (These curves correspond to the idealized "step function" type curves which are shown with engineering approximation curves in Figures 16, 17, and 18). The glass substrate dimensions for the mirror filter are shown in Figure IV.

b) Liberty Mirror Filters

The Liberty Mirror Division of Libby-Owens-Ford fabricated 18 filters, six samples of each filter type, which were to meet the established specifications. Spectral transmittance data was obtained on these filters at Spectrolab using a Cary Model 14 Spectrophotometer. Table 4-VI compares the Liberty mirror filter performance data with the specification requirements. As the filters did not meet the specifications it was necessary to reject them.

TABLE 4-VI

COMPARISON OF LIBERTY MIRROR FILTER
DATA WITH SPECIFICATION VALUES

Filter Type	Passband Center Tolerance		Passband Width Tolerance		Slope			
					Spec.		Actual	
	Spec. mμ	Actual mμ	Spec. mμ	Actual mμ	Short	Long	Short	Long
SL120/83	± 10	+ 80	± 10	+ 240	> -.0003	<.0003	-.0006	.04
SL200/82	± 20	+ 100	± 20	+ 200	> -.0003	<.0003	-.0017	.003
SL350/80	± 30	+ 80	± 30	+ 150	> -.0003	<.0003	-.003	.0045

c) Spectrolab Mirror Filters

Since the Liberty Mirror filters did not meet the specifications which had been formulated for the three types of reflecting filters (see Appendix A) they were rejected and Spectrolab undertook the fabrication of the required filters. Initially 18 filters were fabricated, consisting of six filters of each of the three types, i.e., SL 120/83, SL 200/82, and SL 350/80. However, since the data obtained on the first group of SL 200 type filters did not fully meet expectations, a second group of this filter type was fabricated. This second group was prepared in thinner glass, and later its thickness was built up with plain glass to facilitate handling in the mirror test apparatus.

The mirror filters fabricated for this program were based on standard configurations. Once the specifications had been determined the Vacuum Laboratory undertook a survey of available configurations to determine which were adaptable to achieving the design goals. Generally speaking, there is available a file of thin film configurations to provide reflection bands with various characteristics. These can be modified, within limits, to produce certain desirable shifts or changes of the optical characteristics. Each configuration has been determined theoretically and the sequence of layers and their optical thicknesses computed on the basis of the optical properties of the dielectric materials chosen as the optimum compatible compounds.

The configurations found most adaptable for approaching the required specifications were computed for zinc sulphide (ZnS), lead fluoride (PbF_2), and cryolite ($NaAlF_6$) as the dielectric compounds.

A reflection band centered at a specified wavelength can readily be established by the appropriate choice of materials having indices of refraction sufficiently disparate to provide constructive reinforcement when the materials are deposited in alternate layers of the required optical thicknesses. The other optical properties, particularly transmission and absorption, must be such as to provide the overall final optical characteristics. The intensity of the reflection is determined by the number of alternate layers deposited.

The width of the band is determined by the disparity of the indices and/or the choice of $\frac{\lambda}{4}$ multiples. Thus, in the case of the SL 350/80 specification, it was desired to fabricate a reflector with a bandpass of 350 mμ centered at 800 mμ. An indicated configuration was established as being achievable by depositing alternate single quarter-wave layers of ZnS and $NaAlF_6$. In the case of the SL 200/82 mirror filter specification, the choice was a quarter-wave layer of $NaAlF_6$ alternated with three quarter-wave layers of ZnS; for SL 120/83, the choice was single quarter-wave layers of PbF_2 alternated with single quarter-wave layers of $NaAlF_6$.

In order to arrive at the best possible approximation to the desired specifications, numerous variations of the general theoretical approach were run. The following is a summary of certain typical variations:

TABLE 4-VII

Typical Experimental Configurations
Investigated in Filter Fabrication

Filter Type (Spec. No.)	Experimental Configuration	
	No. of Layers	Materials (alternating)
SL 120/83	9	3/4 λ ZnS 3/4 λ $NaAlF_6$
	11	3/4 λ $NaAlF_6$ 3/4 λ ZnS
SL 200/82*	11	λ/4 ZnS λ/4 PbF_2
	15	λ/4 ZnS λ/4 $NaAlF_6$
	9	3/4 λ ZnS 3/4 λ $NaAlF_6$
	15	λ/4 PbF_2 λ/4 $NaAlF_6$
SL 350/80	13	λ/4 ZnS λ/4 $NaAlF_6$

* Typical configurations used in both SL 200/82 I and SL 200/82 II.

It is apparent that if materials are deposited to achieve constructive interference for a specified wavelength, then at points in the spectrum corresponding to other odd multiples of quarter-wavelengths there will occur other reflection bands. For intermediate points there will occur bands of partial reflection, so that a range curve of the reflection filter will show characteristic dips and peaks on either side of the desired band. In order to reduce these dips and make the transmission outside the passband reasonably smooth, it is necessary to adjust the thicknesses of the alternating layers in a systematic way. This is effectively a method of compensating to adjust the thickness at the points where the dips occur. There is an obvious limit to the practical use of this technique. However, it was used in this program to the extent that predictable sequences were available. Numerous runs were made using both glass and mylar as substrates.

From a mechanical viewpoint, mylar was not too successful. It sags and bends in the tank, and afterward the coating flakes off. In general it is difficult to work with.

Extensive refinement of present configurations, or possibly the computation of an entirely new configuration, would be the minimum requirement to establish a configuration which would achieve the practical optimum. Either choice would entail extensive use of an automatic computer and fabrication of experimental filters to check the validity of the computations.

It is felt that the reflection filters prepared and submitted under this program represent a good approximation to the established design goals within the limits determined by available configurations.

Some mention should be made of the fact that in addition to the theoretical limitations set by the nature of light itself and the physical properties of the materials chosen, there are also instrumental and other factors which have a direct bearing on the practical achievement of a desired configuration. Such factors are the precision to which the thickness of a dielectric layer can be measured, the reliability and reproducibility of the electronic measuring devices, etc.

The reflection filters submitted under this contract are experimental in nature and fabrication. They were prepared for laboratory and limited field evaluation. Therefore, certain precautions should be noted as regards use and handling. The film surfaces should not be handled or touched. Removal of dust will be best accomplished by gentle brushing with a soft camel-hair brush or by means of a soft paper tissue saturated with xylene drawn gently across the surface. The use of other chemicals, including water, should be prohibited.

Phase 2. Spectral Transmittance of Spectrolab Mirror Filters

Spectral transmittance data was obtained on the filters at angles of incidence in the range of 0° to 50° using a Cary Model 14 Spectrophotometer* Figures 31, 32, 33 and 34 are typical spectral transmittance curves at 0° incidence for the four sets of filters. Since the mirror filters are fabricated using 1/4-in. glass substrates, the resulting displacement of the beam at angles of incidence other than zero introduced certain errors. These have been corrected by dividing the transmission curves of the filters by that of clear 1/4-in. glass in the wavelength intervals of interest.

* The spectrophotometer transmittance data obtained on the four sets of mirror filters is included in Appendix B of this report as Figures B-1 through B-44.

An examination of the various transmission curves shows that the most far-reaching effect on the efficiency of the filters caused by varying the angle of incidence is the variation in the cut-off wavelengths, λ_2 and λ_3. The curves of cut-off wavelength as a function of angle of incidence for the four groups of filters are shown in Figure 35. As indicated in the figure, the cut-off wavelengths decrease in value as the angle of incidence is increased from 0° to 50° for all three filter types. The mean transmittance of the filter types and energy fraction reflected is summarized in the following table:

TABLE 4-VIII

Mean Transmittance and Energy Fraction Reflected in Each Spectral Region of Spectrolab Mirror Filters

Filter Type	SPECTRAL REGION					
	$\lambda < \lambda_2$		$\lambda_2 < \lambda < \lambda_3$		$\lambda > \lambda_3$	
	Transmittance	Energy Fraction Reflected	Transmittance	Energy Fraction Reflected	Transmittance	Energy Fraction Reflected
SL-120	75%	35%	5%	30%	65%	35%
SL-200-I	65%	40%	5%	40%	75%	20%
SL-200-II	80%	20%	5%	45%	55%	35%
SL-350	75%	20%	2%	50%	55%	30%

The variation of cut-off with angle of incidence can be minimized. However, significant improvement can be achieved only through much time spent in experimentation. The optical path difference in interference films varies as the cosine of the angle the rays make with the normal to the surface of the film. Hence the thicknesses of the film could be graded to take into account the expected angles, or in the case of a curved surface, to take into account the continuous variation in angles. The easiest way to achieve such a gradation is to produce a reflector by mechanically joining segments or zones, each of which were coated for a specific average angle. The same result may be achieved on a one-piece reflector by masking off zones and coating each one separately. This would be hazardous, however, as one stands the risk of spoiling a carefully performed, tedious task by a misapplication near the finish. Even more desirable would be to insert deflecting masks in the vacuum deposition tank to achieve the desired result. However, this would be the most difficult method to develop and would require much time and effort spent in experimentation.

Without such modifications, one could seek a reflector design which would have only a small variation in angle, as this would minimize the variation of cut-off wavelengths.

Phase 3. Effect of Experimental Mirror Filters on Solar Power System Performance.

Data was obtained on the 24 experimental mirror filters fabricated at Spectrolab to determine the combined effect of the filtering and radiation concentration on solar cell performance for concentration ratios in the range from one to six. The filters were tested in four 6-sample groups: one group consisted of Type SL 120, two groups consisted of Type SL 200 (designated as SL 200-I and SL 200-II), and one group consisted of Type SL 350.

a) Experimental Procedure.

The mirror filters were tested in collimated sunlight at Table Mountain using the apparatus shown in Figures 36 through 39. Data was obtained using a four-cell module consisting of a series connection of two pairs of cells, each pair connected in parallel. The cells used were Heliotek gridded blue P/N silicon solar cells whose relative spectral response curve is given in Figure 24. As a control to evaluate the effects of the mirror filters, two I-V curves were obtained for the solar cell module for direct sunlight, i.e., without the filters. Data was then obtained on current versus voltage, light intensity, and cell temperature for each filter-type group, with the solar cells facing the filters to receive reflected light: first, a single mirror filter was used; then two, three, four, five, and the total of six. The data was taken for three values of i (the angle of incidence) i.e., for $i = 5^{\circ}$, 10°, and 15°. The 18 data runs described were repeated for each filter group, so that I-V curves were obtained using one to six mirror filters for each of the three angles for each 6-filter group.

b) Data Reduction.

A total of 74 I-V curves were run, 18 for each of the four sets of six mirrors: SL 350, SL 200-II, SL 200-I, and SL 120; and two with the panel facing the sun. The data for each set of four runs was reduced to standard conditions of 100 mw/cm^2 (intensity of incident sunlight) and a standard temperature of 28° C for the SL 200-II, SL 200-I, and SL 120 filters. In the case of the SL 350 filters, a standard temperature of 45° C was selected in order to avoid the error introduced by making too great a temperature correction. Figure 40 shows the I-V curve obtained using direct sunlight on the bare cells and corrected to 45° for comparison with the curves obtained for the SL 350 filters. Figure 59 shows a similar curve, corrected to 28° C for comparison with the other three sets of filters, i.e., the SL 200-II, SL 200-I, and SL 120 filters.

Figures 41 through 58 are the I-V curves obtained for the SL 350 reflecting filters: Figures 41 through 46 for a 5° angle of incidence and concentration ratios from one to six, respectively; Figures 47 through 52 for a 10° angle of incidence, and Figures 53 through 58 for a 15° angle of incidence. The other sets of curves are similarly grouped and numbered, as summarized in Table 4-IX.

TABLE 4-IX

Figure Numbering System* for Reflection Filter I-V Curves

Filter type	Figure Numbers*		
	$i = 5^\circ$	$i = 10^\circ$	$i = 15^\circ$
SL 350	41 - 46	47 - 52	53 - 58
SL 200-II	60 - 65	66 - 71	72 - 77
SL 200-I	78 - 83	84 - 89	90 - 95
SL 120	96 - 101	102 - 107	108 - 113

* The six curves of each set were obtained by varying the concentration ratio from one to six, respectively.

c) Discussion of Results.

All of the curves obtained follow the pattern generally expected, with three exceptions. Figures 65, 82, and 83 are slightly inconsistent with the general pattern, probably due to misalignment of one mirror which would have the effect of slightly reducing the concentration ratio. Since sufficient data is presented in the remainder of the curves, reruns of these three sets of data appeared unnecessary.

A short summary of the pertinent data from the curves of a typical set (SL 350) is as follows:

TABLE 4-X

Short Circuit Current Data for SL 350 Mirror Filters
(100 mw/cm^2, 45° C)

Angle of Incidence	Concentration Ratio (CR)	Short-Circuit Current, I_{sc} (ma)
0°	bare cells to sun	107
i = 5°	CR = 1	68
5°	2	139
5°	3	209
5°	4	277
5°	5	334
5°	6	393
10°	6	389
15°	6	374

It is interesting to note that each SL 350 mirror produces a short-circuit current of about 65 percent of that produced by direct sunlight on bare cells. The effect of angle of incidence is noted in the last three items in the table, where, for CR = 6, the short-circuit current drops slightly. This is due to two effects. First, the angle of incidence of reflected light on the cell increases, and cell response is proportional to the cosine of the angle of incidence for angles up to about 40° and falls off more rapidly for greater angles. Since the angle of incidence of reflected light on the cell is double the angle of incidence of sunlight on the mirrors, the cell angle of incidence varied up to 30° in these

tests. The second effect, due to the shift of the passband of the filters toward the lower wavelengths for greater angles of incidence, pushes the reflection band slightly toward the region where the product curve of relative cell response and spectral solar intensity has a higher value, thus cancelling part of the expected reduction of short-circuit current due to increased angle of incidence. However, out in space, after equilibrium temperatures have been established, the lowered efficiency due to increased temperature will have the opposite effect, and the shift toward a greater value on the product curve will produce a lessening of the maximum power.

Section 5

OVERALL CONCLUSIONS

The employment of concentration and filtering of the radiation incident on the photovoltaic cells of solar power systems will afford valuable improvements in cost and weight of solar power systems. These improvements will result from increased power per cell, but not from increased power per unit solar beam area. The available increase of power per cell will significantly reduce system cost and weight, however.

The efficiencies of concentration depend strongly on the spectral properties of the filters. The desired properties are not yet within the present production capability of the art of filter fabrication. According to previous experience, it should be possible, given enough time and effort, to improve the presently attainable filters to the extent that their spectral properties match those herein identified as "realizable".

Section 6

RECOMMENDATIONS

1. Improve filter properties and fabricate reflection filters on concentrator surfaces.

2. Develop adequate methods of performance analysis:

   (a) Use test results to define and determine a valid relative spectral response of solar cells including temperature effects.

   (b) Develop methods and obtain data for computing cell temperatures in solar power systems in deep space, in earth orbit, and, in particular, on the surface of the earth.

   (c) Establish complete, detailed mathematical methods for designing photovoltaic solar power systems which are optimum for specified performance, cost, size and weight.

3. Design and evaluate prototype solar power systems for particular applications.

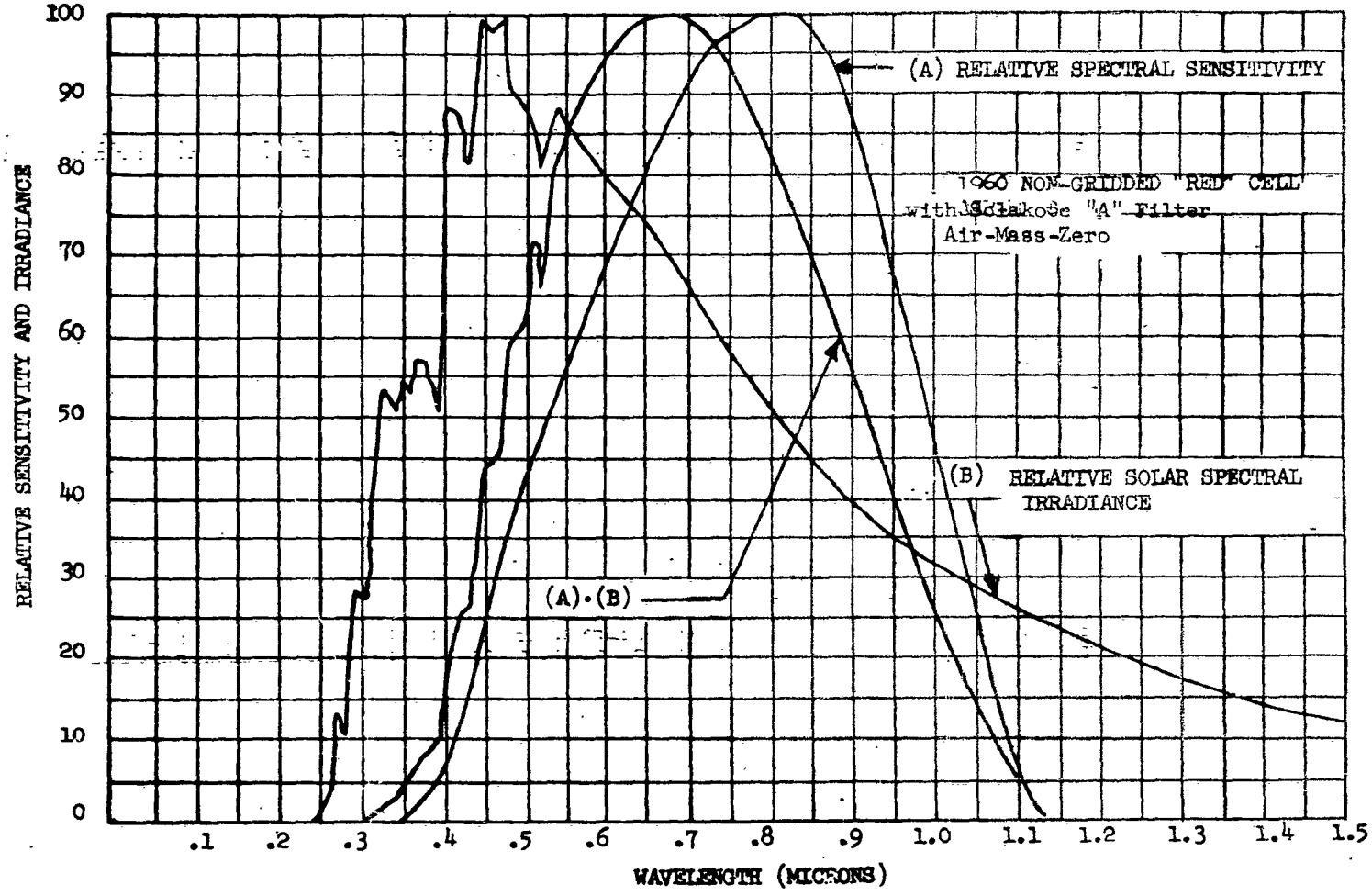


FIGURE 1. TYPICAL SILICON CELL RELATIVE SPECTRAL RESPONSE RELATIVE SOLAR SPECTRAL IRRADIANCE, AND THEIR PRODUCT.

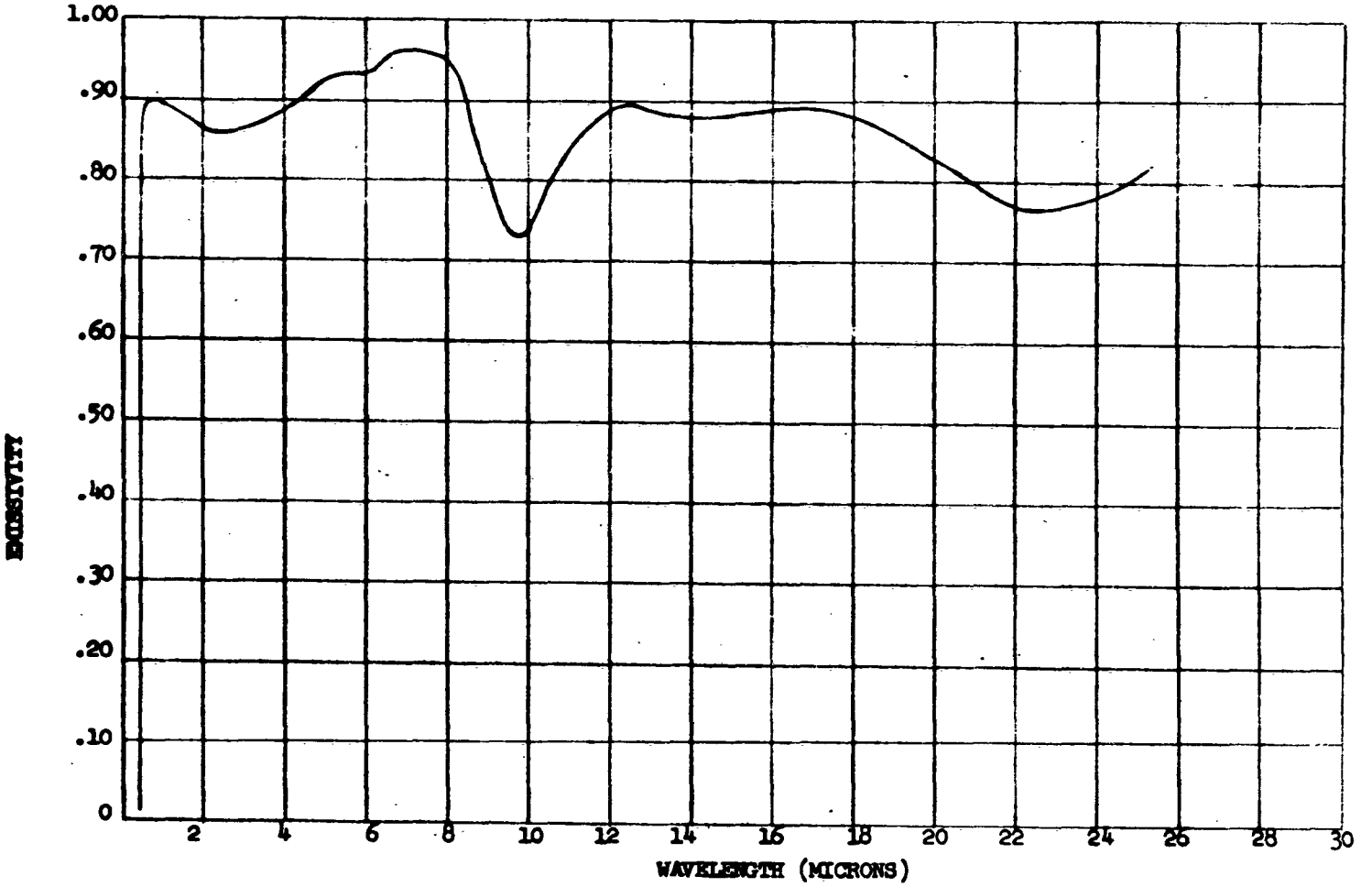


FIGURE 2. SPECTRAL EMISSIVITY OF TYPICAL 1960 NON-GRIDDED "RED" CELL WITH SOLAKOTE "A" FILTER.

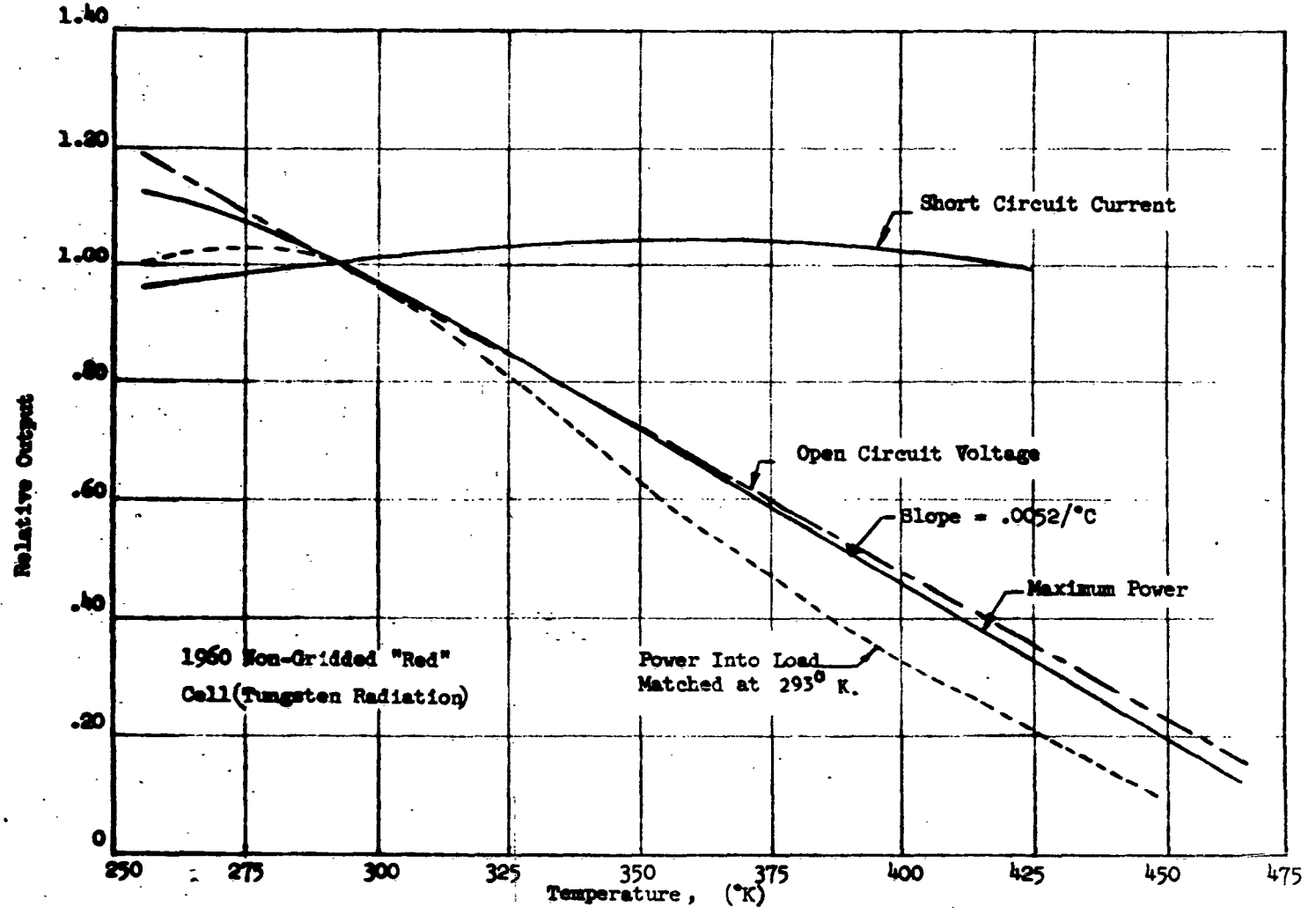


Figure 3. Relative Thermal Effects on Open Circuit Voltage, Short Circuit Current, Maximum Power, and Power Into a Matched Load* for Typical Silicon Solar Cell.

* Room Temperature

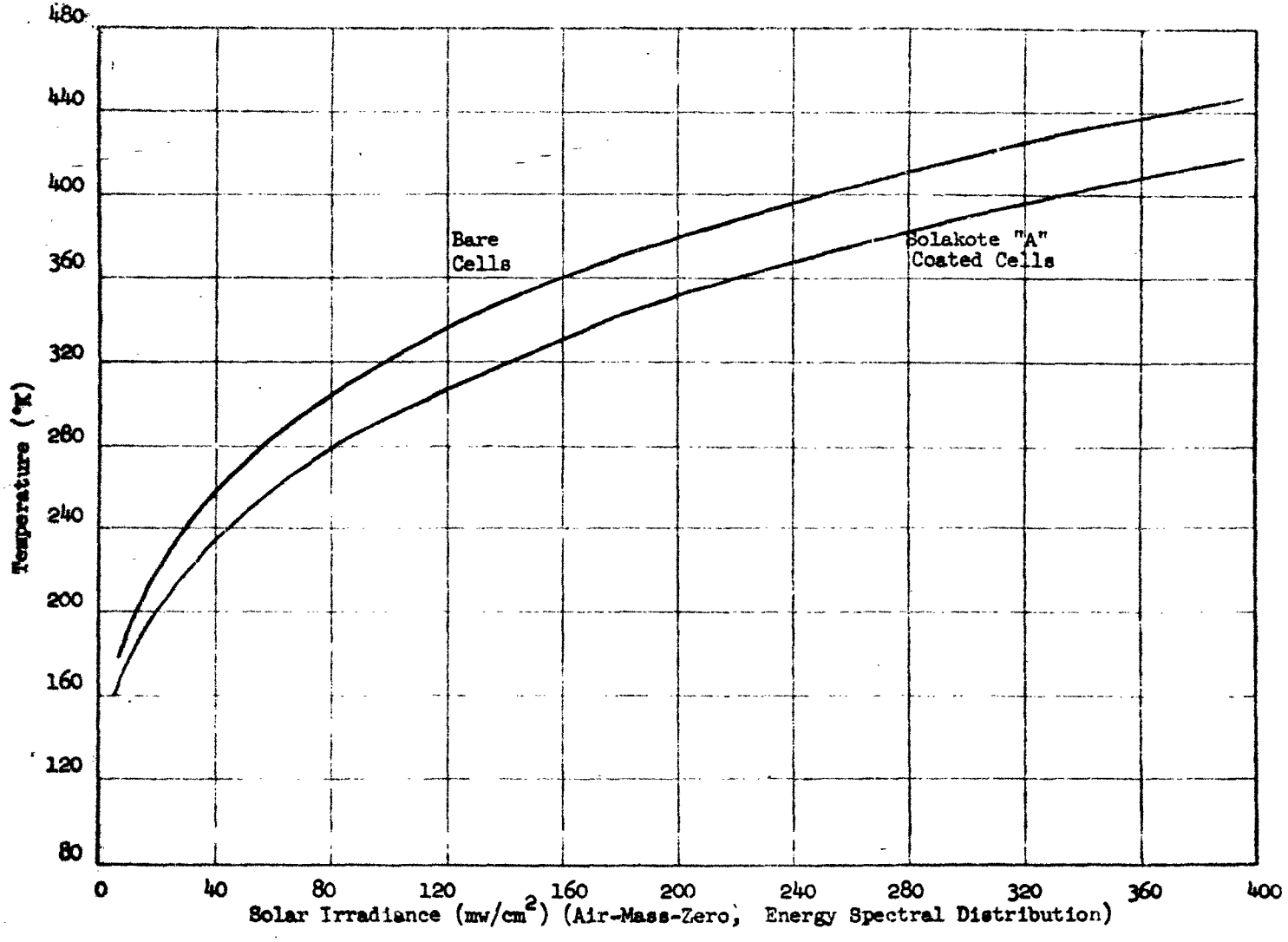


Figure 4. Equilibrium Temperature vs Solar Irradiance for 1960 Non-Gridded "Red" Cells.

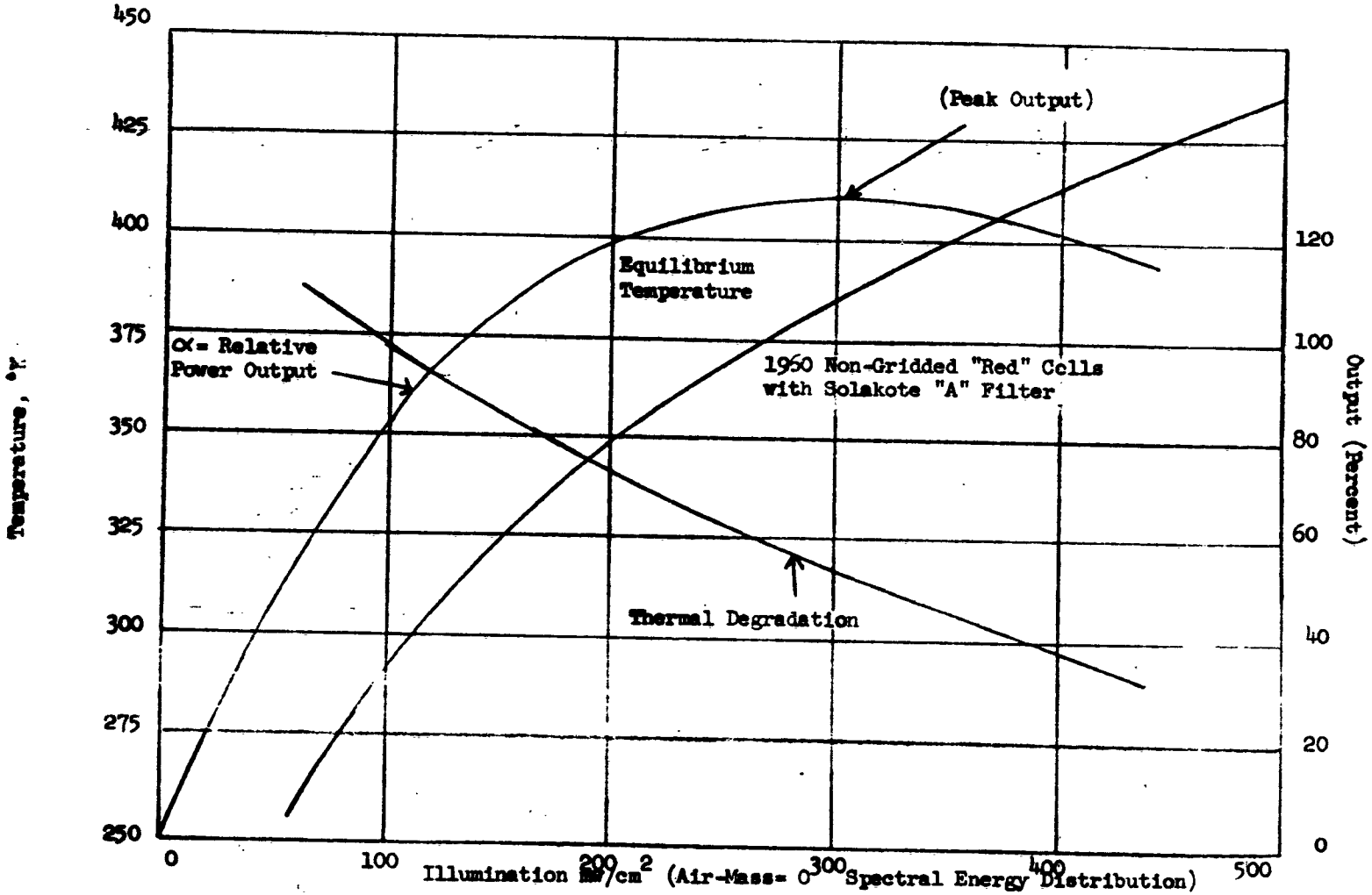


Figure 5. Equilibrium Temperature, Thermal Degradation Factor and Relative Output of Cell Array vs. Illumination.

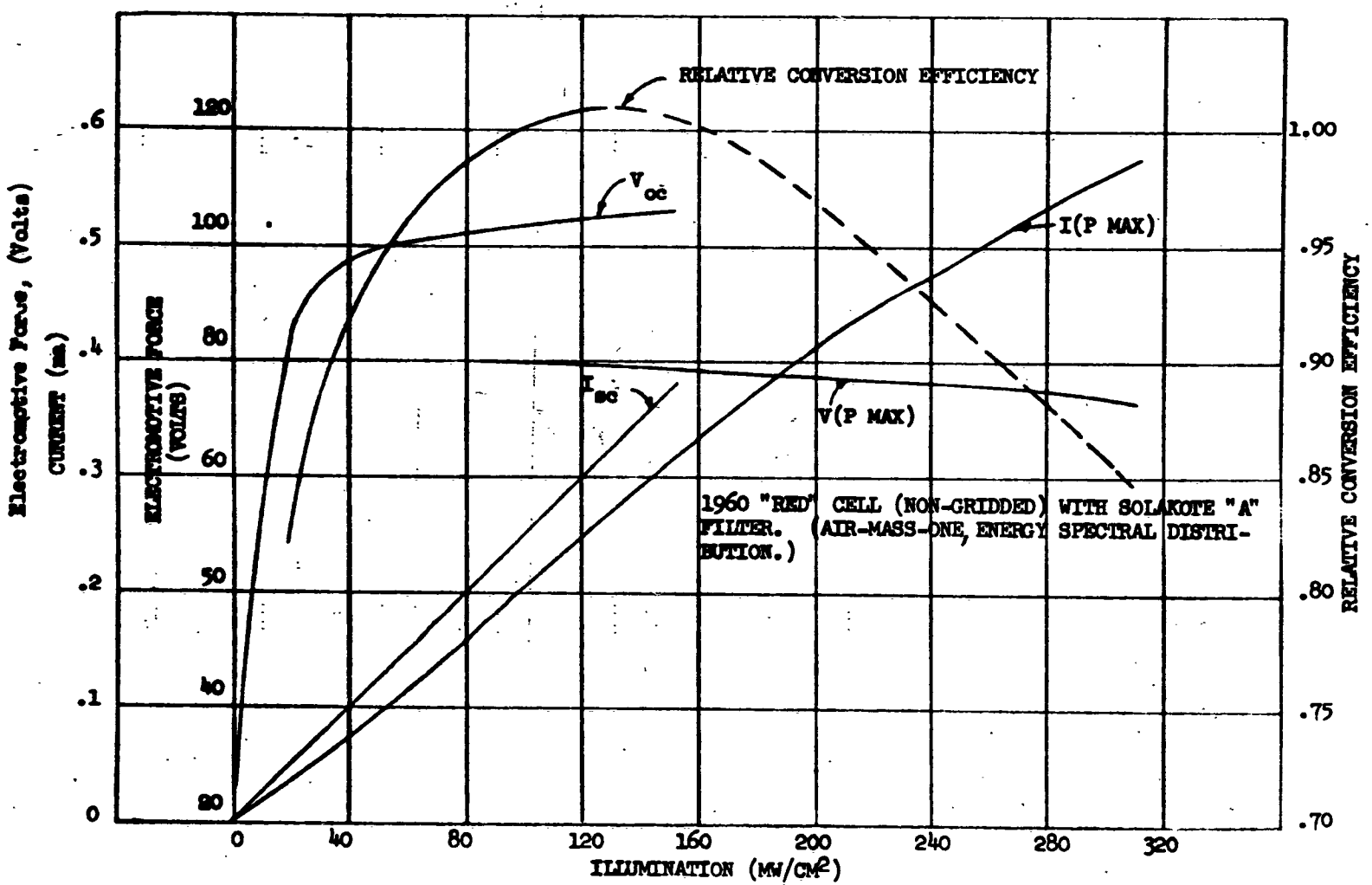


FIGURE 6. EFFECT OF ILLUMINATION LEVEL ON OPEN CIRCUIT VOLTAGE, SHORT CIRCUIT CURRENT, VOLTAGE AND CURRENT AT MAXIMUM POWER, AND RELATIVE CONVERSION EFFICIENCY FOR TYPICAL SILICON SOLAR CELL.

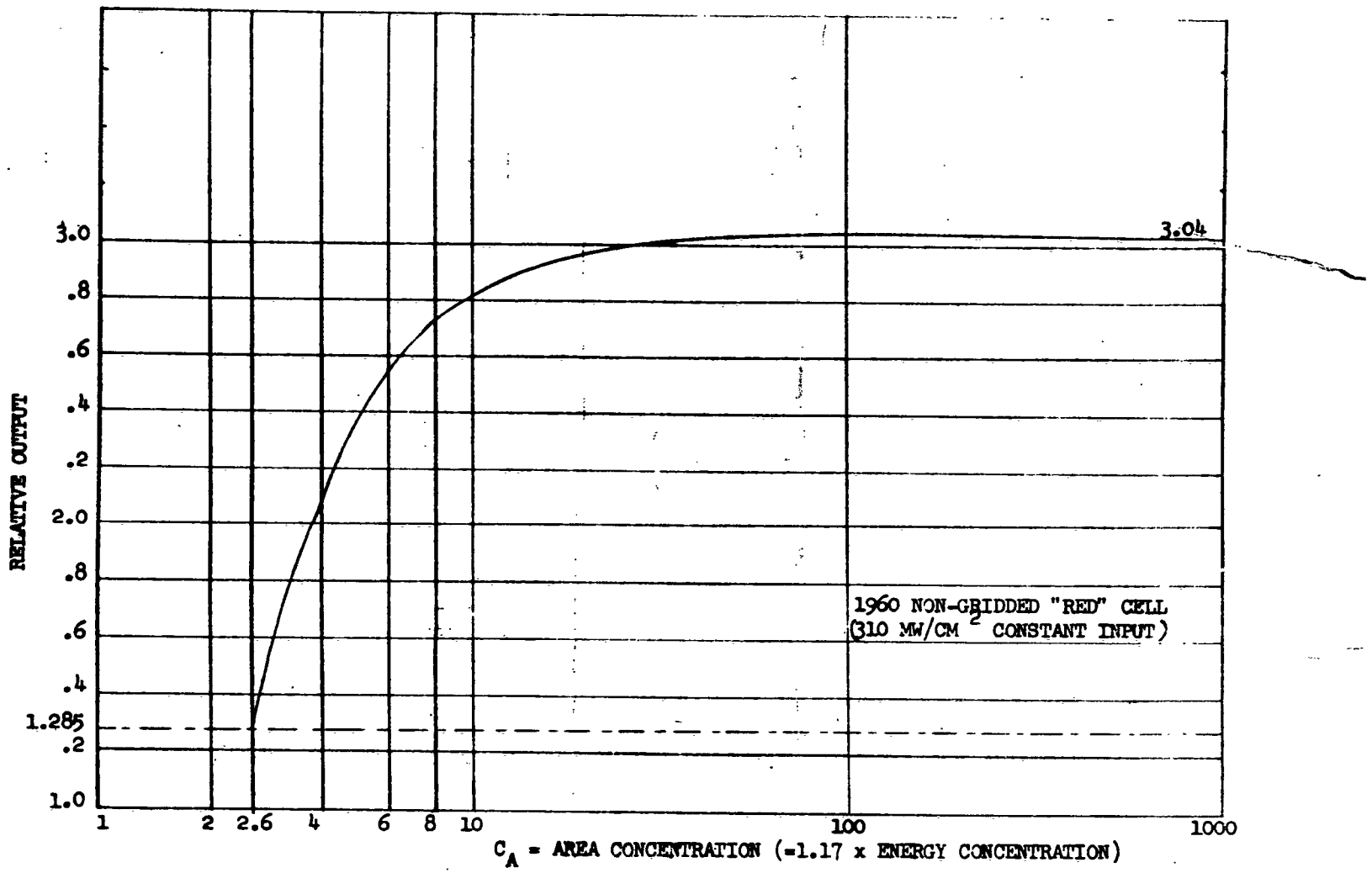
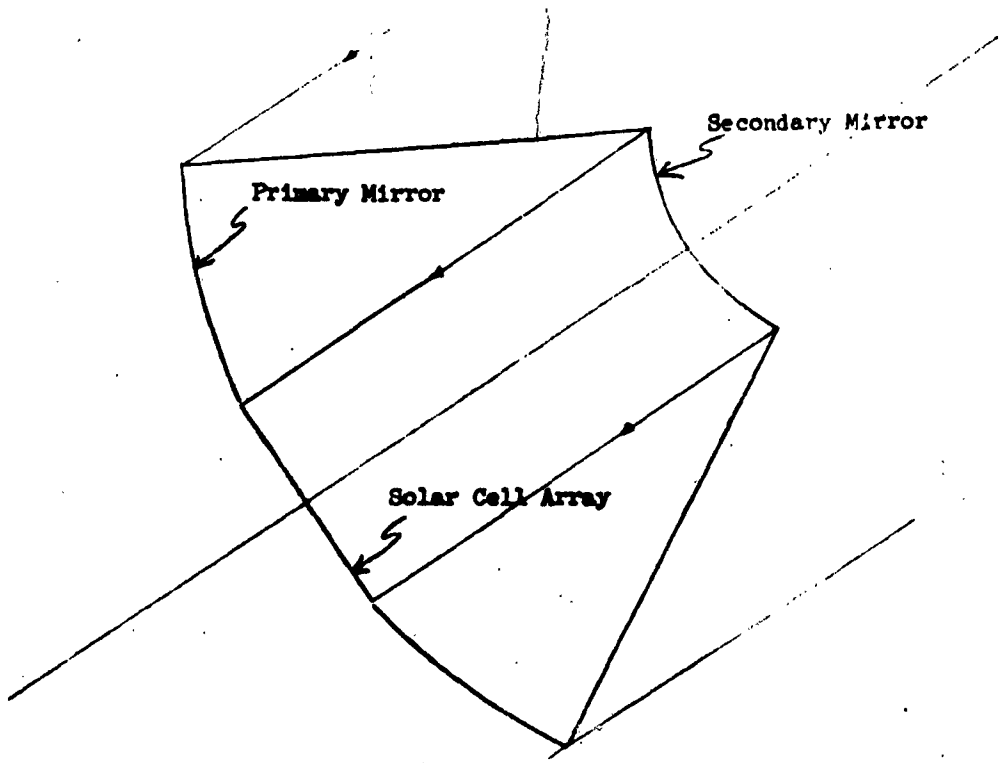
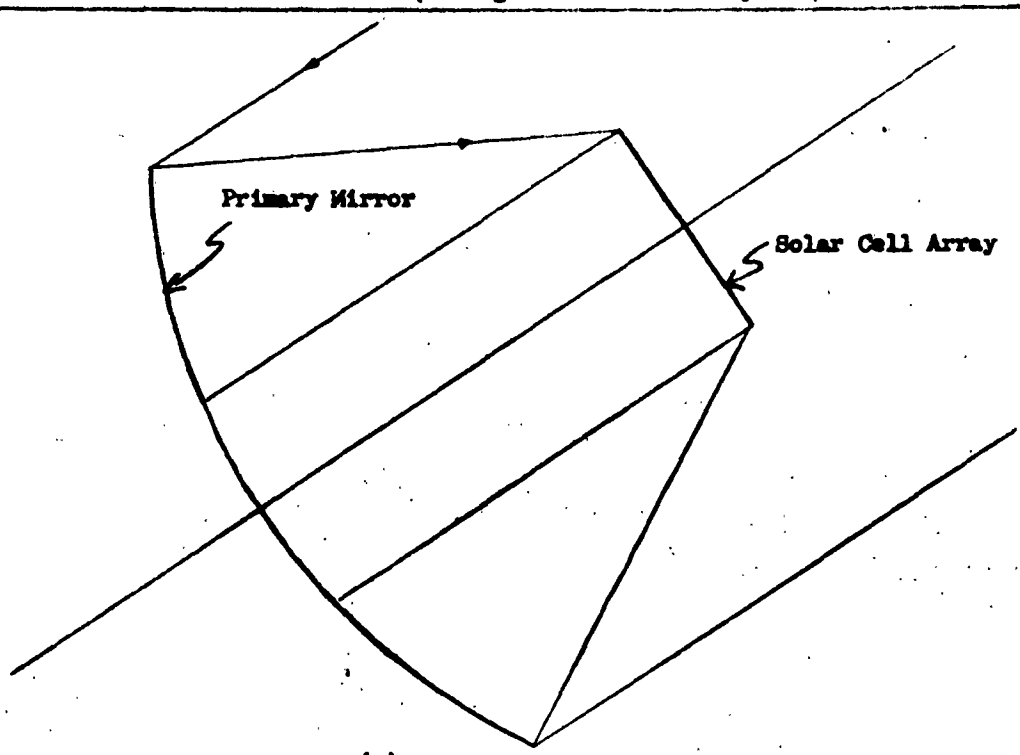


FIGURE 7. OUTPUT PER CELL RELATIVE TO COATED (SOLAKOTE "A") CELL WITHOUT CONCENTRATION VS. AREA CONCENTRATION



(A) Solar Power System I
(Cassegrainian Mirror System)



(B) Solar Power System II

Figure 8. Solar Concentrator Configuration.

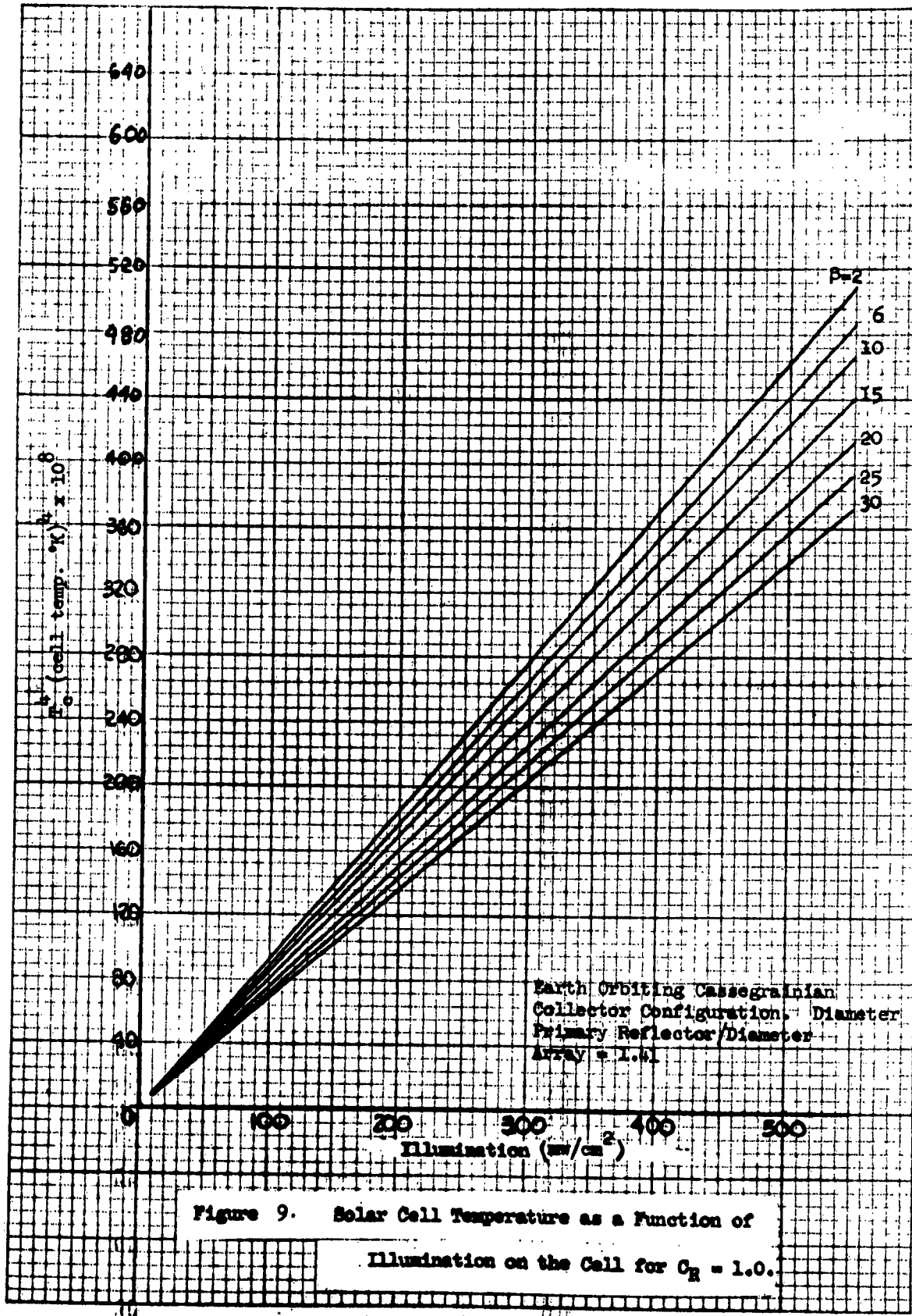


Figure 9. Solar Cell Temperature as a Function of Illumination on the Cell for $C_R = 1.0$.

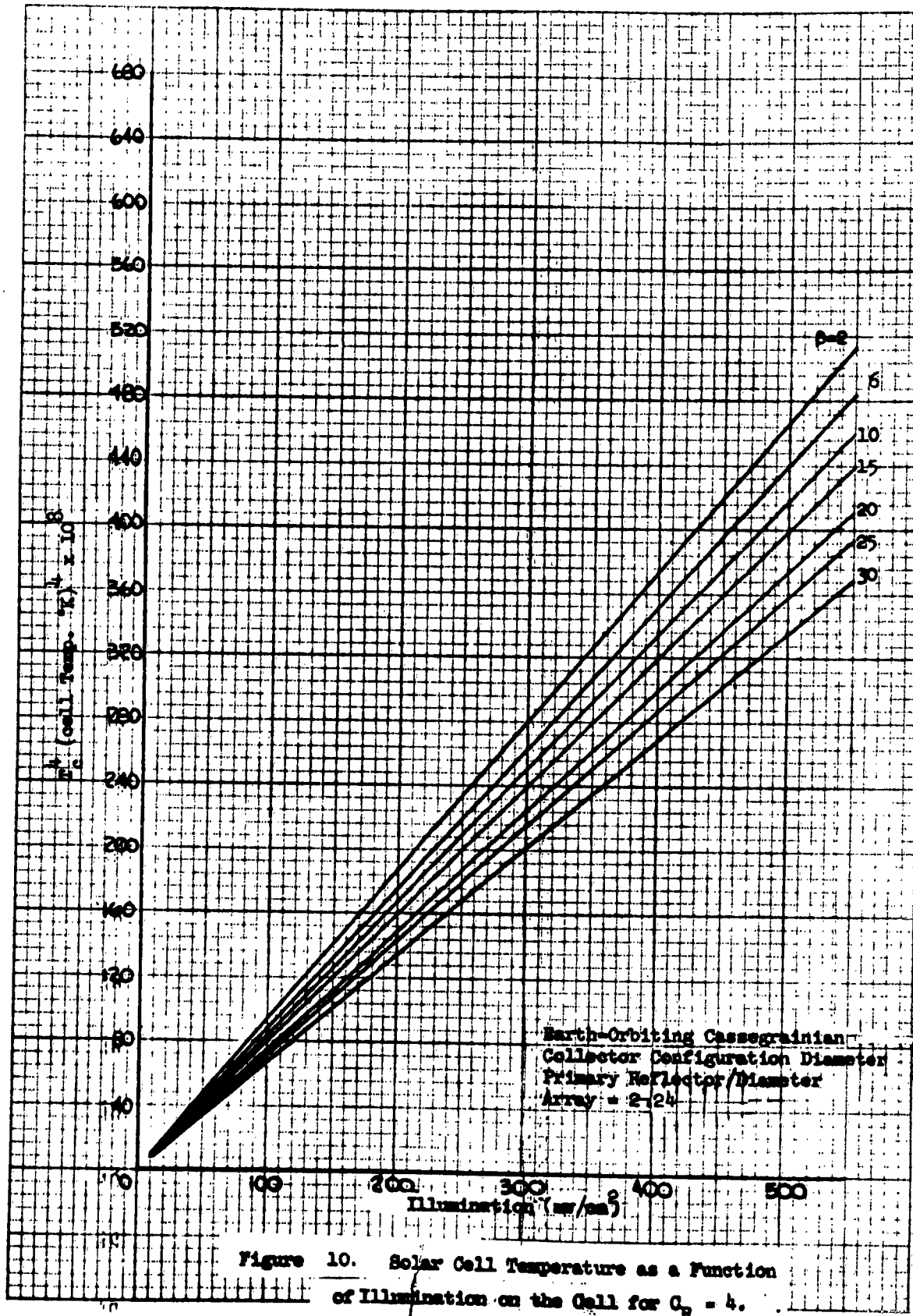


Figure 10. Solar Cell Temperature as a Function of Illumination on the Cell for $C_R = 4$.

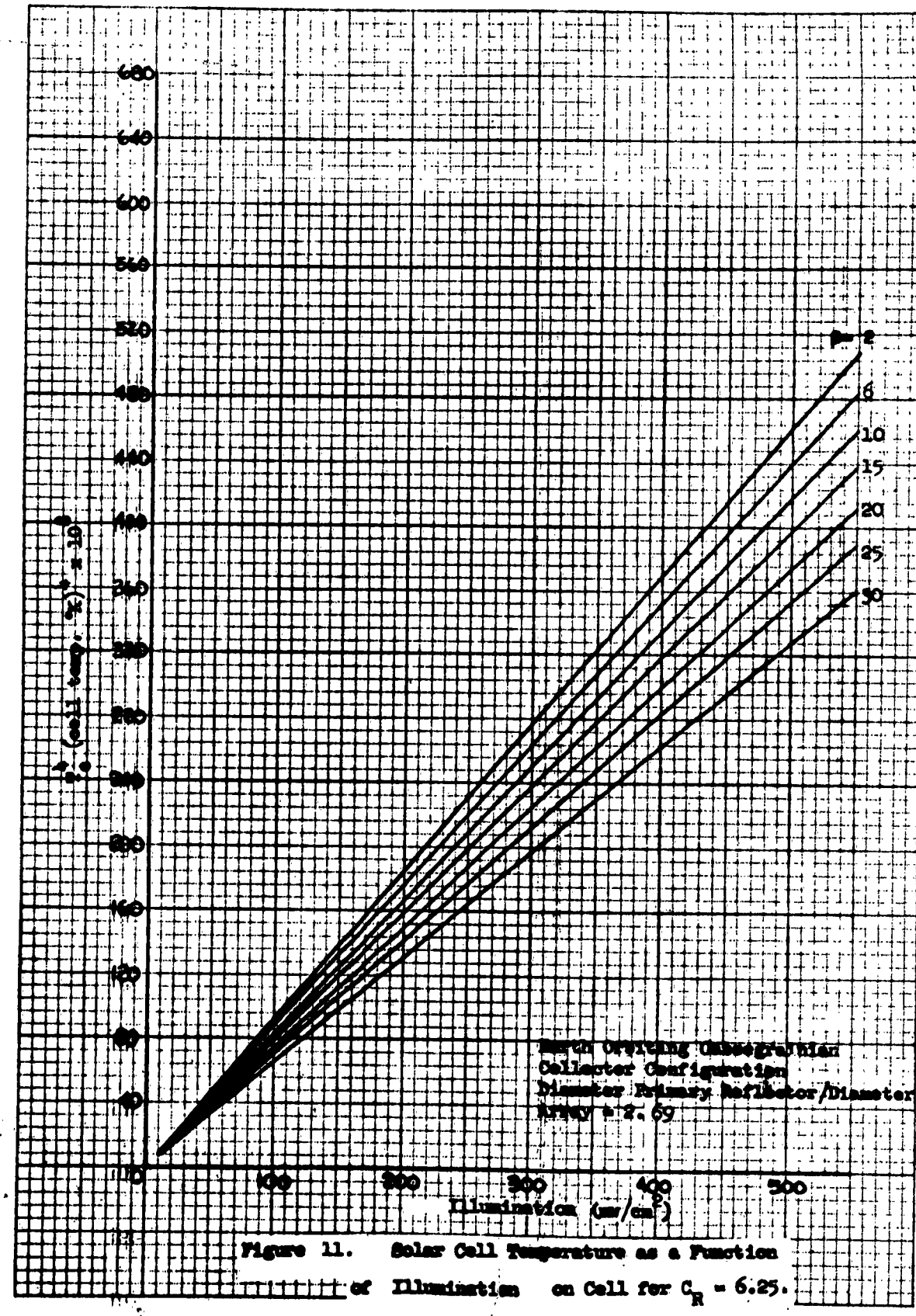


Figure 11. Solar Cell Temperature as a Function of Illumination on Cell for C_R = 6.25.

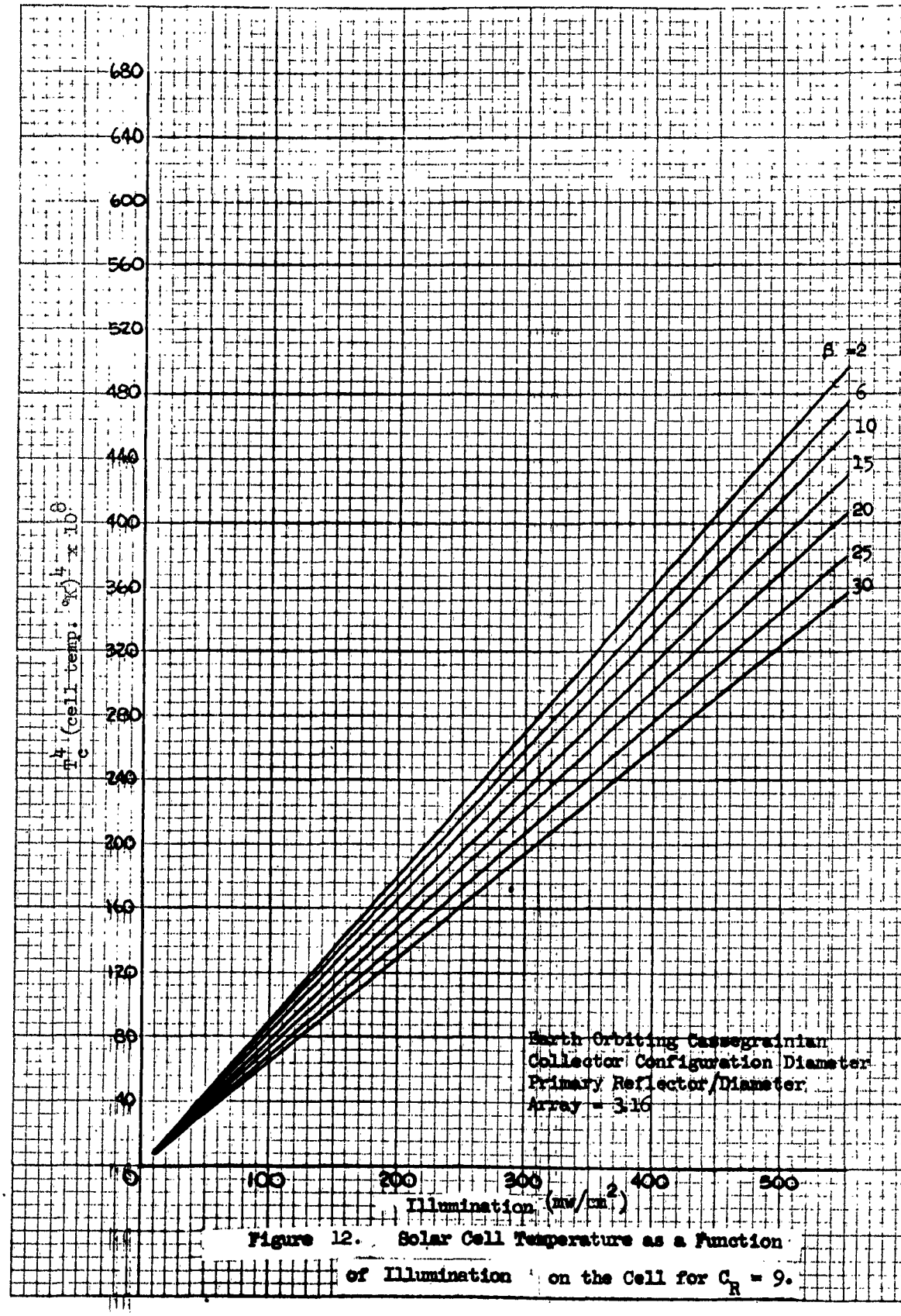


Figure 12. Solar Cell Temperature as a Function of Illumination on the Cell for C_R = 9.

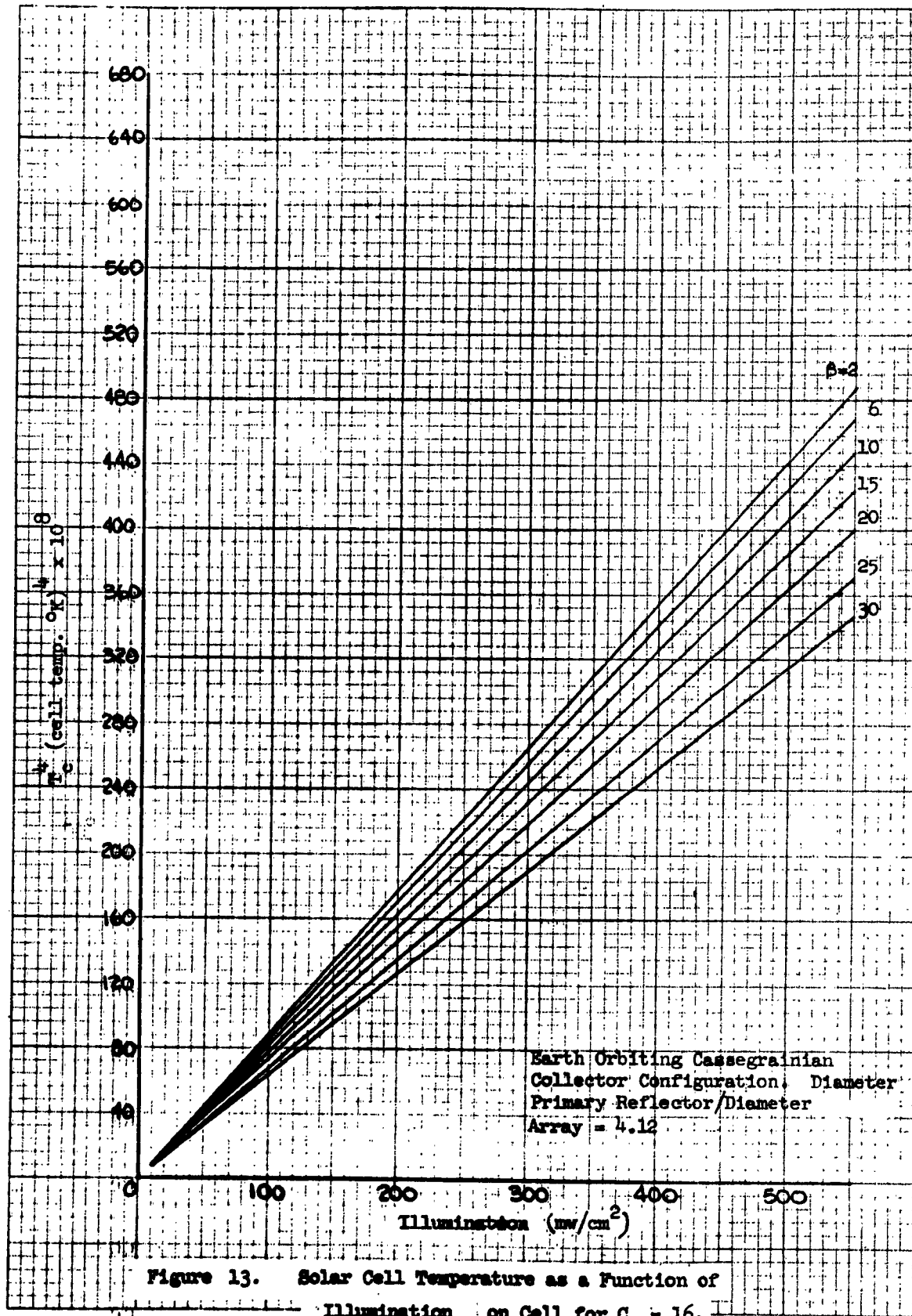


Figure 13. Solar Cell Temperature as a Function of Illumination on Cell for $C_R = 16$.

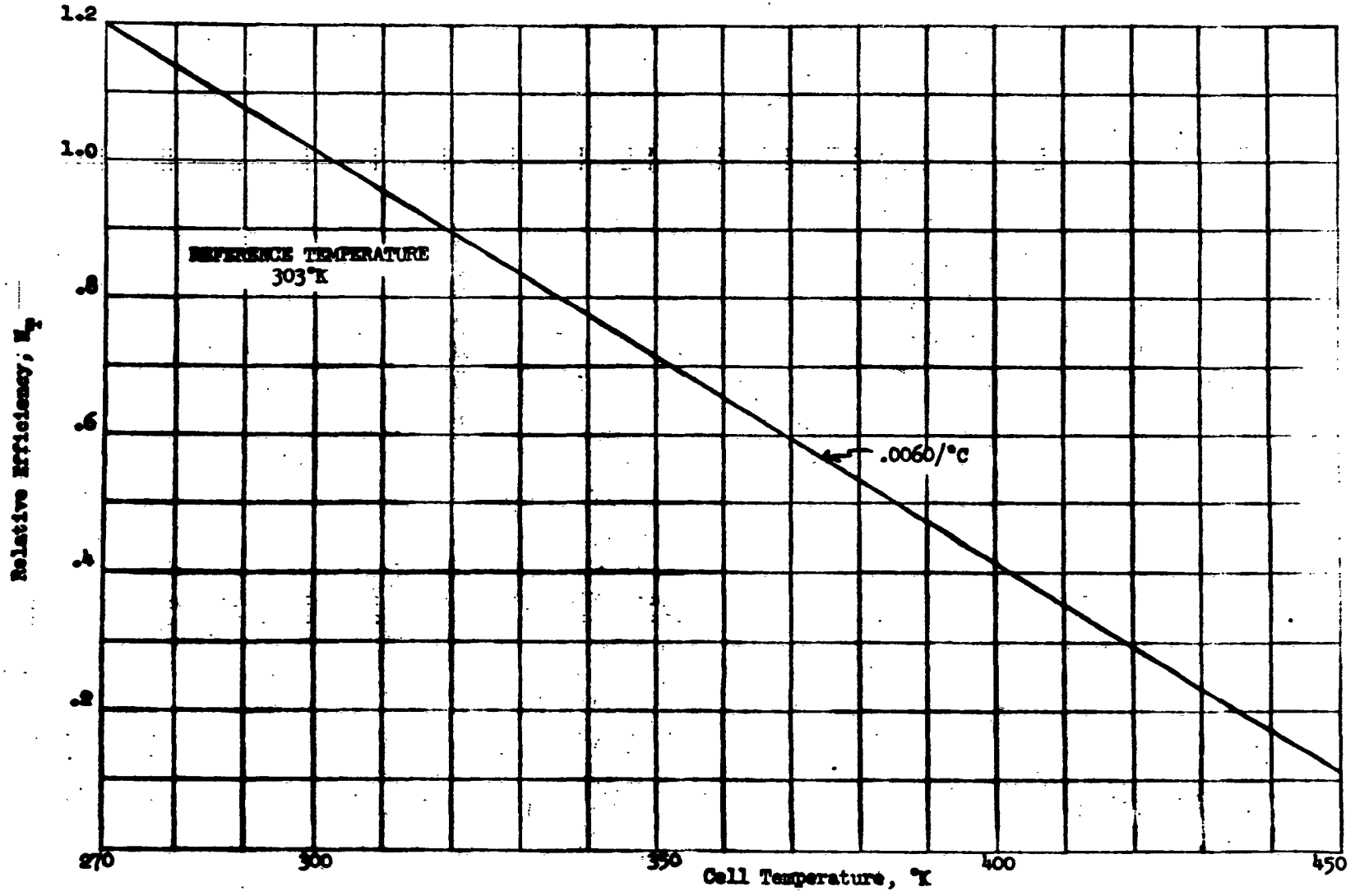


Figure 14. Typical Temperature Characteristic of An Experimental Gridded "Red" Silicon Solar Cell.

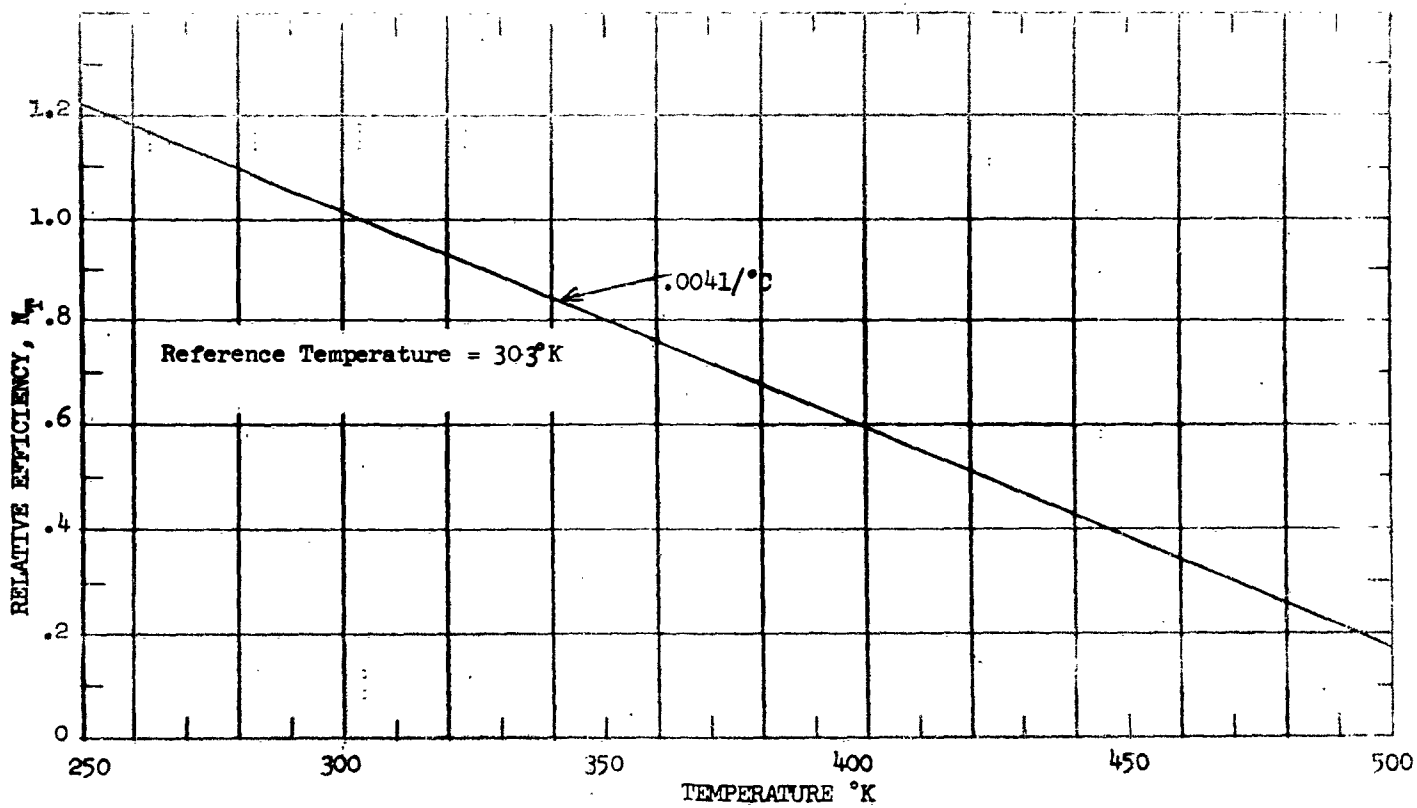


FIGURE 15. TYPICAL TEMPERATURE CHARACTERISTIC OF A HELIOTEK GRIDDED "BLUE" CELL.

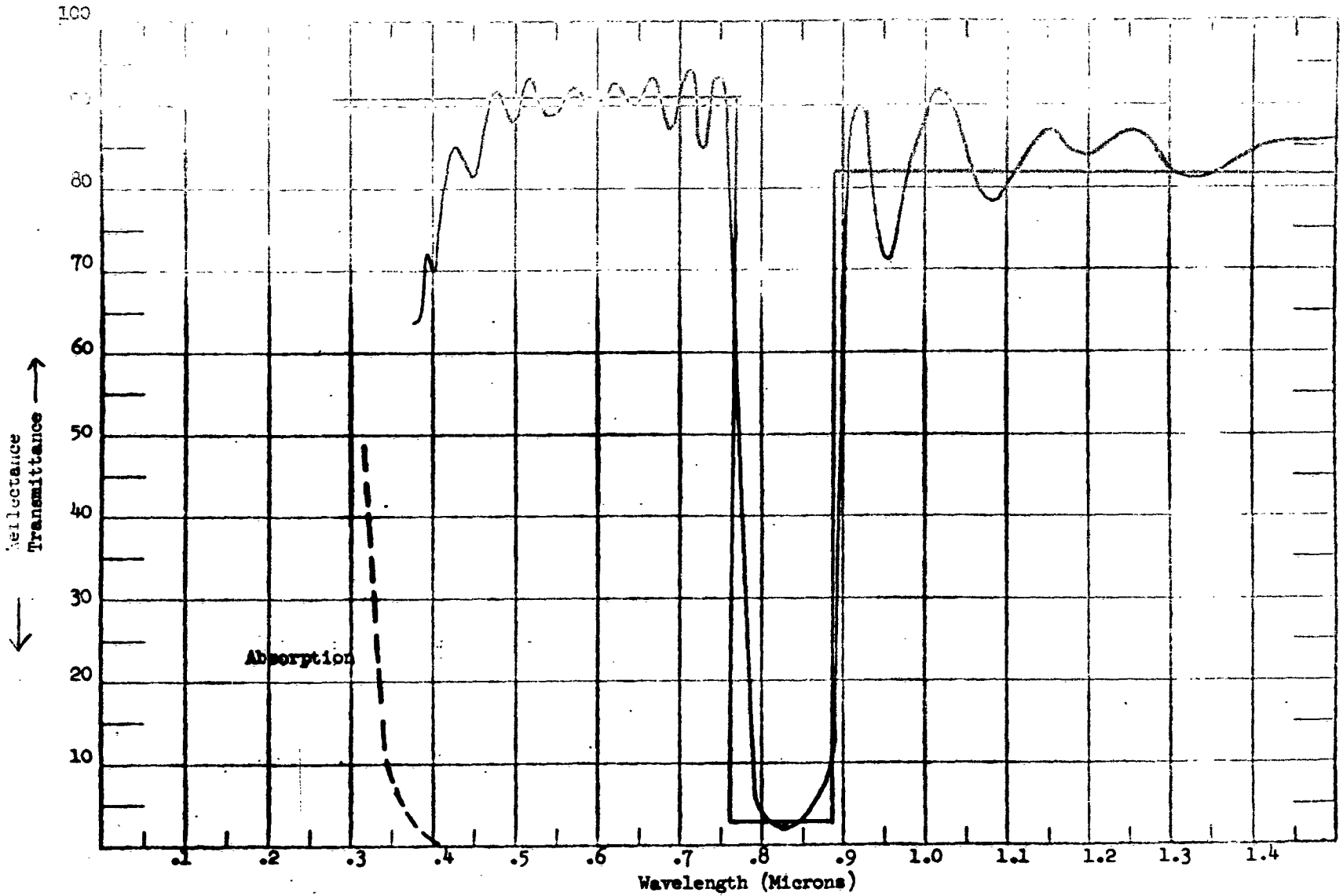


Figure 16. Concentrator Filter of "Red" Cells - Type SL 120/83.

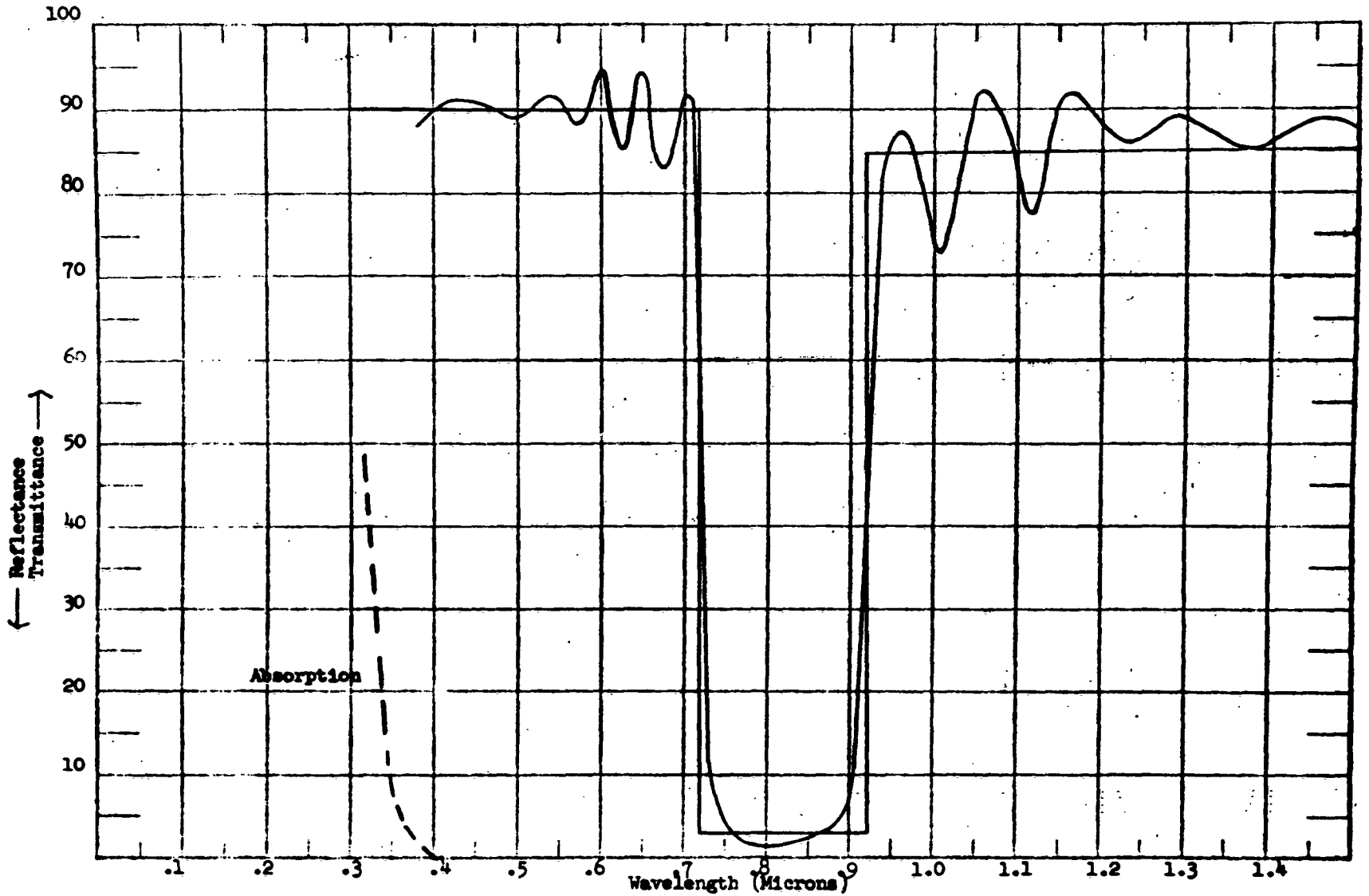


Figure 17. Concentrator Filter for "Red" Cells - Type SL 200/82.

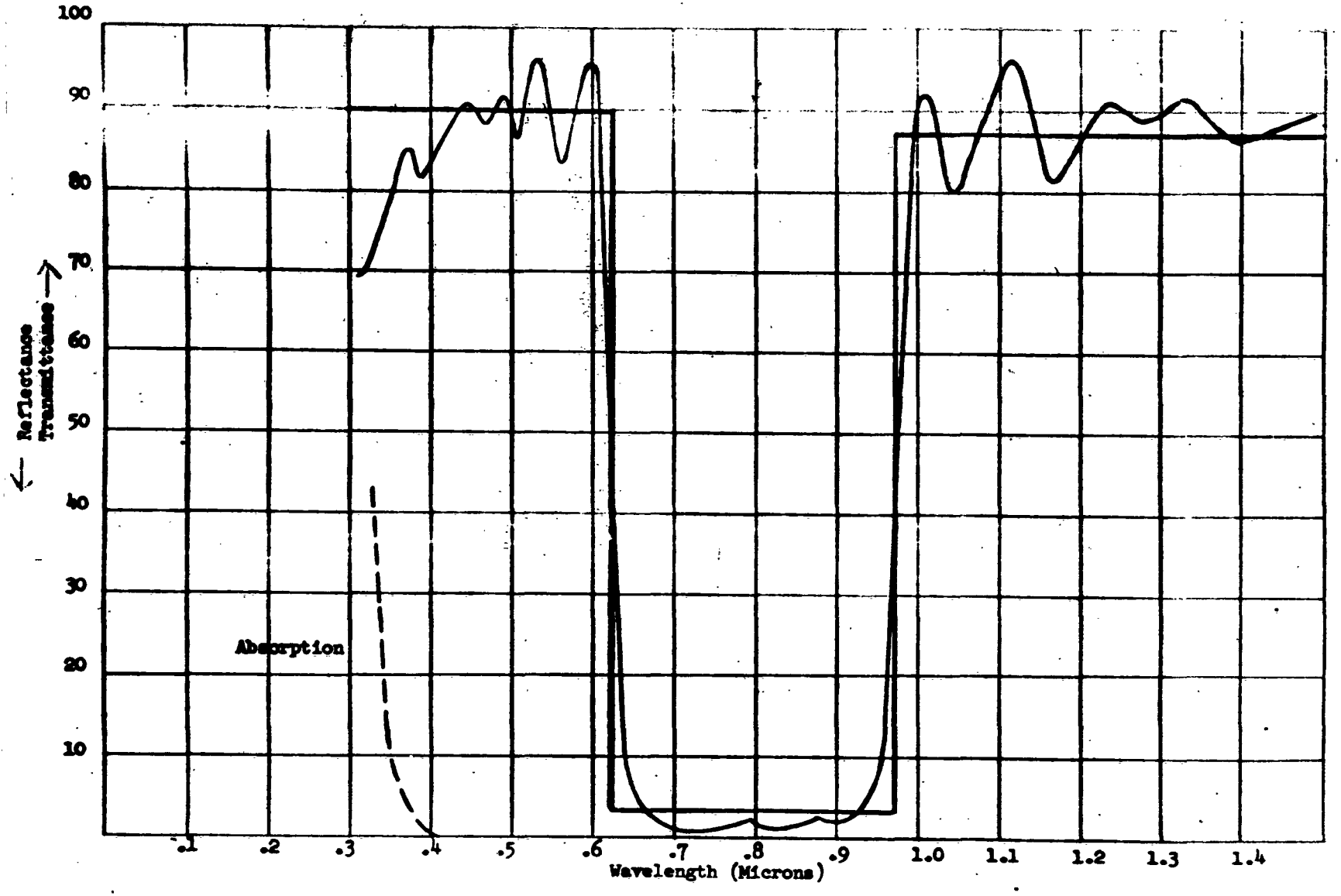


Figure 18. Concentrator Filter for "Red" Cells - Type SL350/80.

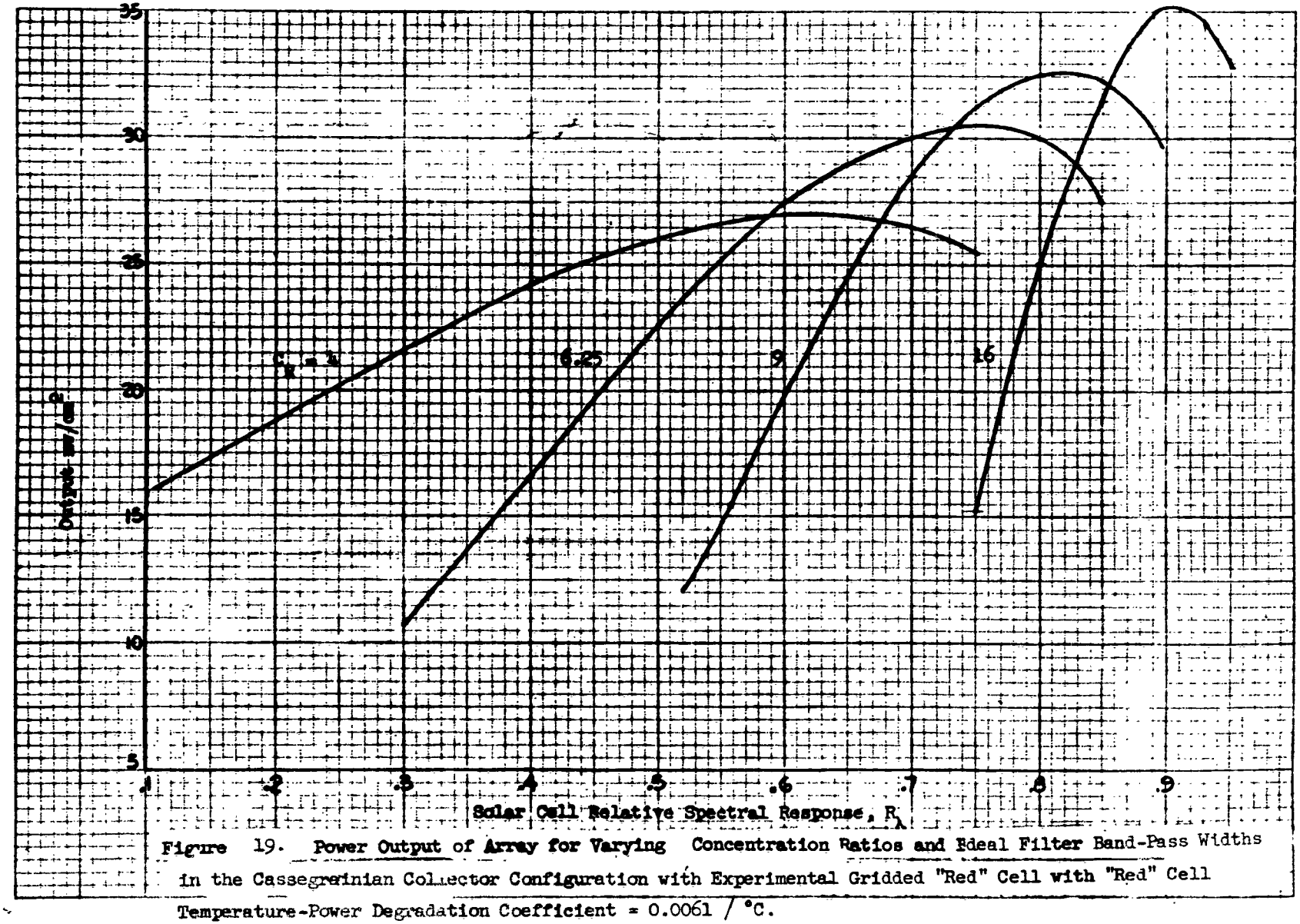


Figure 19. Power Output of Array for Varying Concentration Ratios and Ideal Filter Band-Pass Widths in the Cassegrainian Collector Configuration with Experimental Gridded "Red" Cell with "Red" Cell Temperature-Power Degradation Coefficient = 0.0061 / °C.

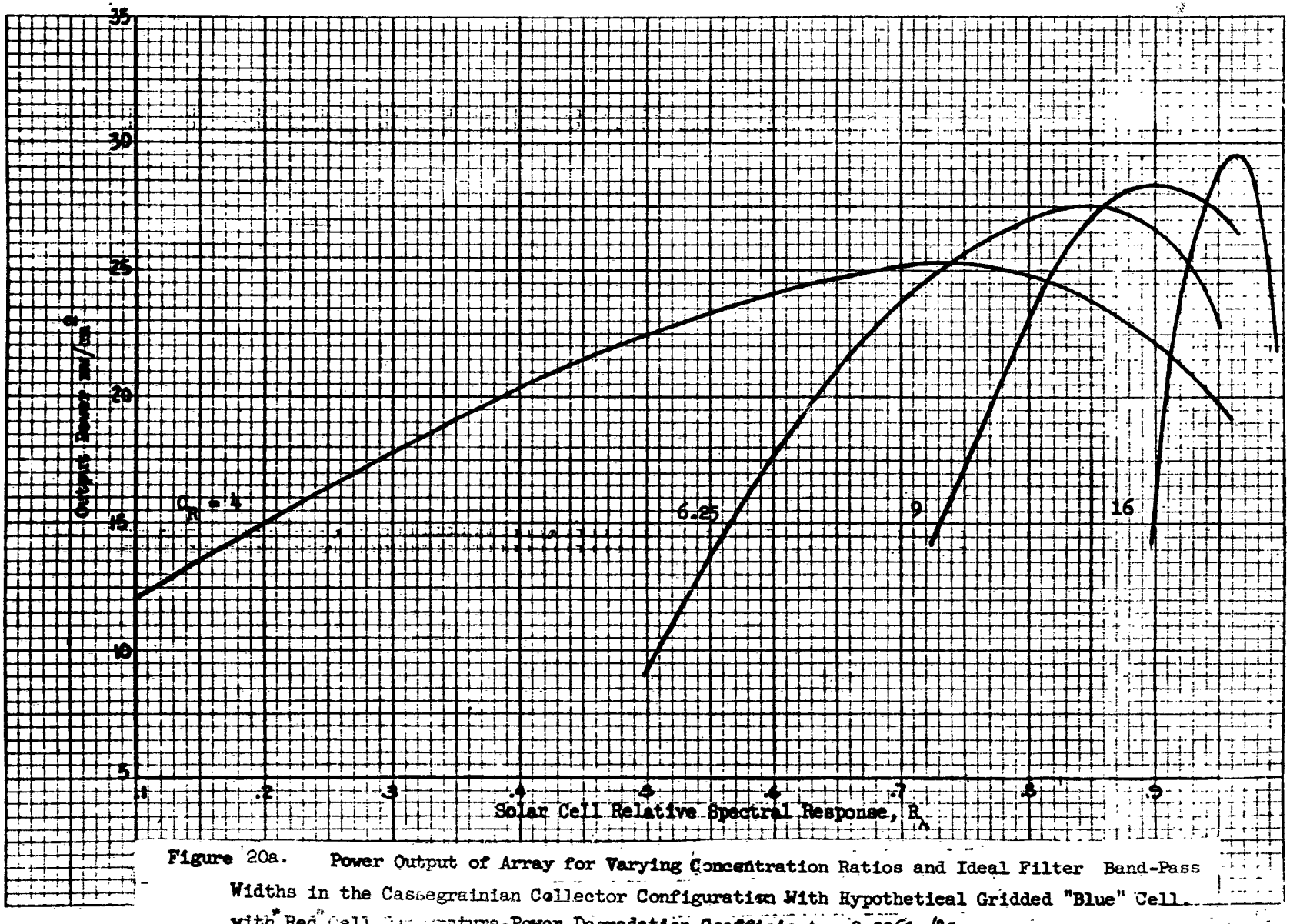


Figure 20a. **Power Output of Array for Varying Concentration Ratios and Ideal Filter Band-Pass Widths in the Cassegrainian Collector Configuration With Hypothetical Gridded "Blue" Cell with Red Cell Temperature-Power Degradation Coefficient = 0.0060 /°C.**

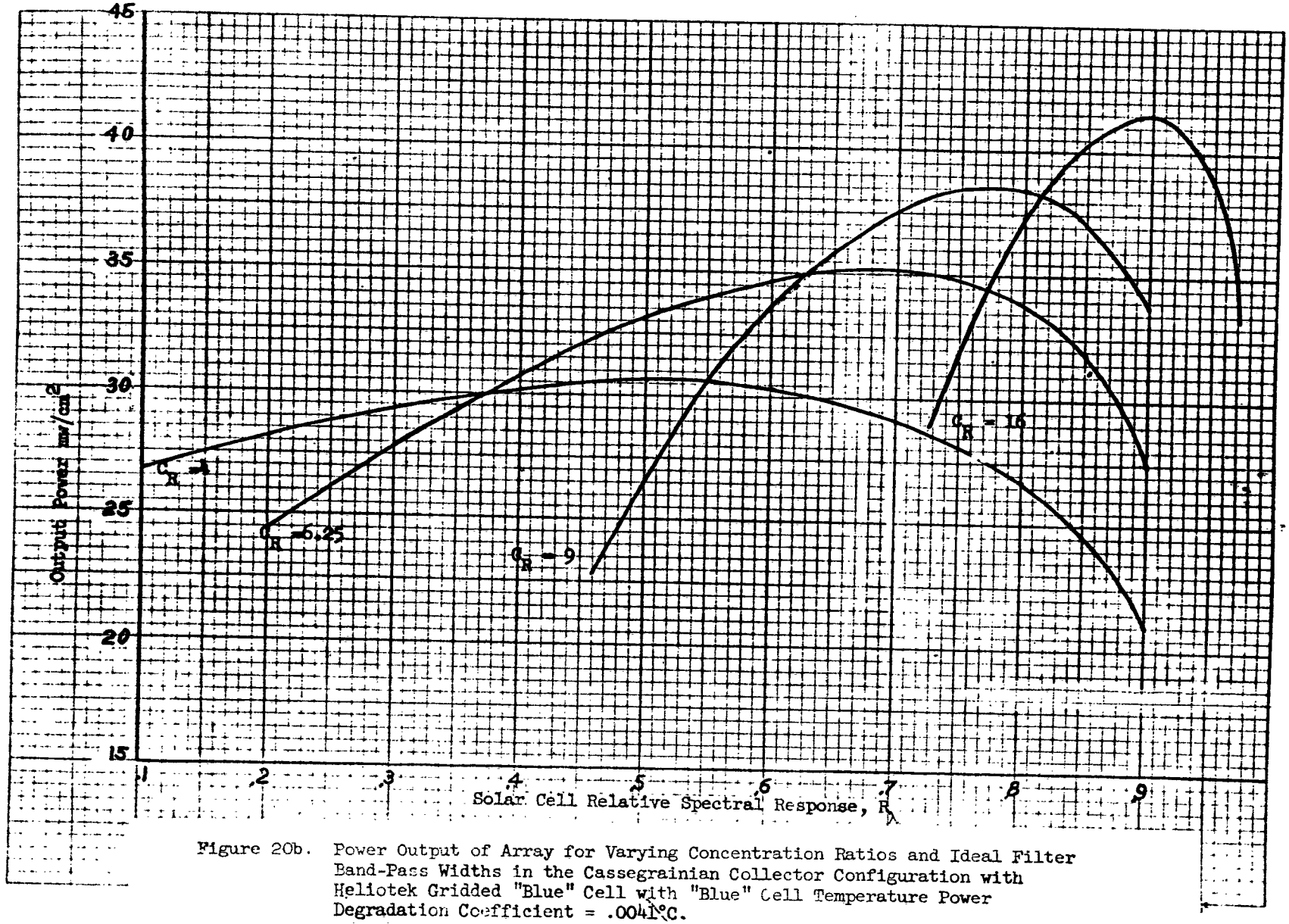


Figure 20b. Power Output of Array for Varying Concentration Ratios and Ideal Filter Band-Pass Widths in the Cassegrainian Collector Configuration with Heliotek Gridded "Blue" Cell with "Blue" Cell Temperature Power Degradation Coefficient = .0041°C.

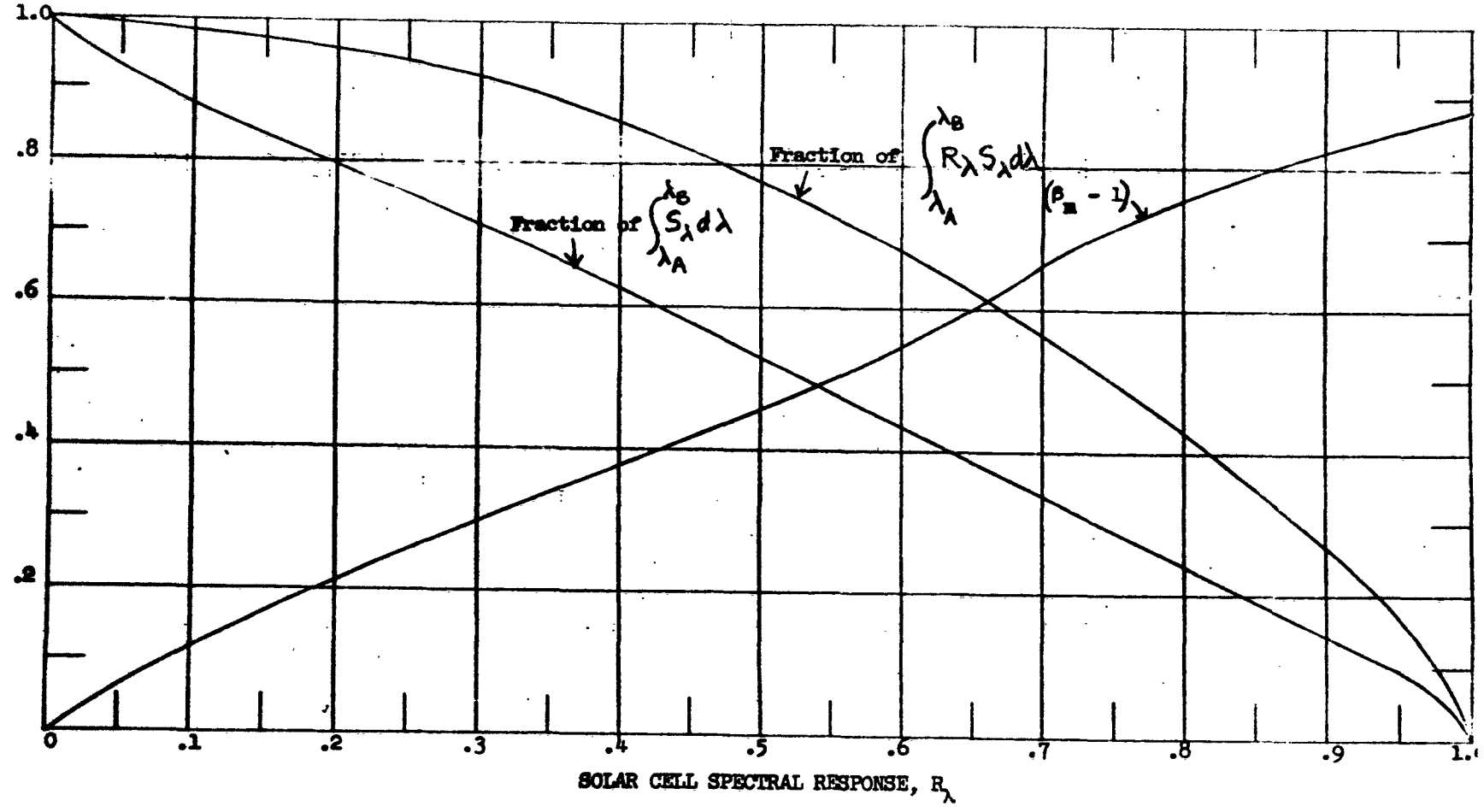


FIGURE 21. FRACTION OF THE SOLAR ENERGY AND CELL POWER OUTPUT OCCURRING IN REGION FOUND BY CHOOSING FILTER BAND-PASS LIMITS AT EQUAL HEIGHT ON THE RESPONSE CURVE OF THE EXPERIMENTAL GRIDDED "RED" SILICON SOLAR CELL. ALSO, $(\beta_m - 1)$, WHERE β_m IS THE MULTIPLIER OF THE AVERAGE ABSOLUTE EFFICIENCY (AT THE REFERENCE TEMPERATURE) BETWEEN λ_A AND λ_B TO GIVE THE AVERAGE EFFICIENCY WITHIN THE R_λ LIMITS.

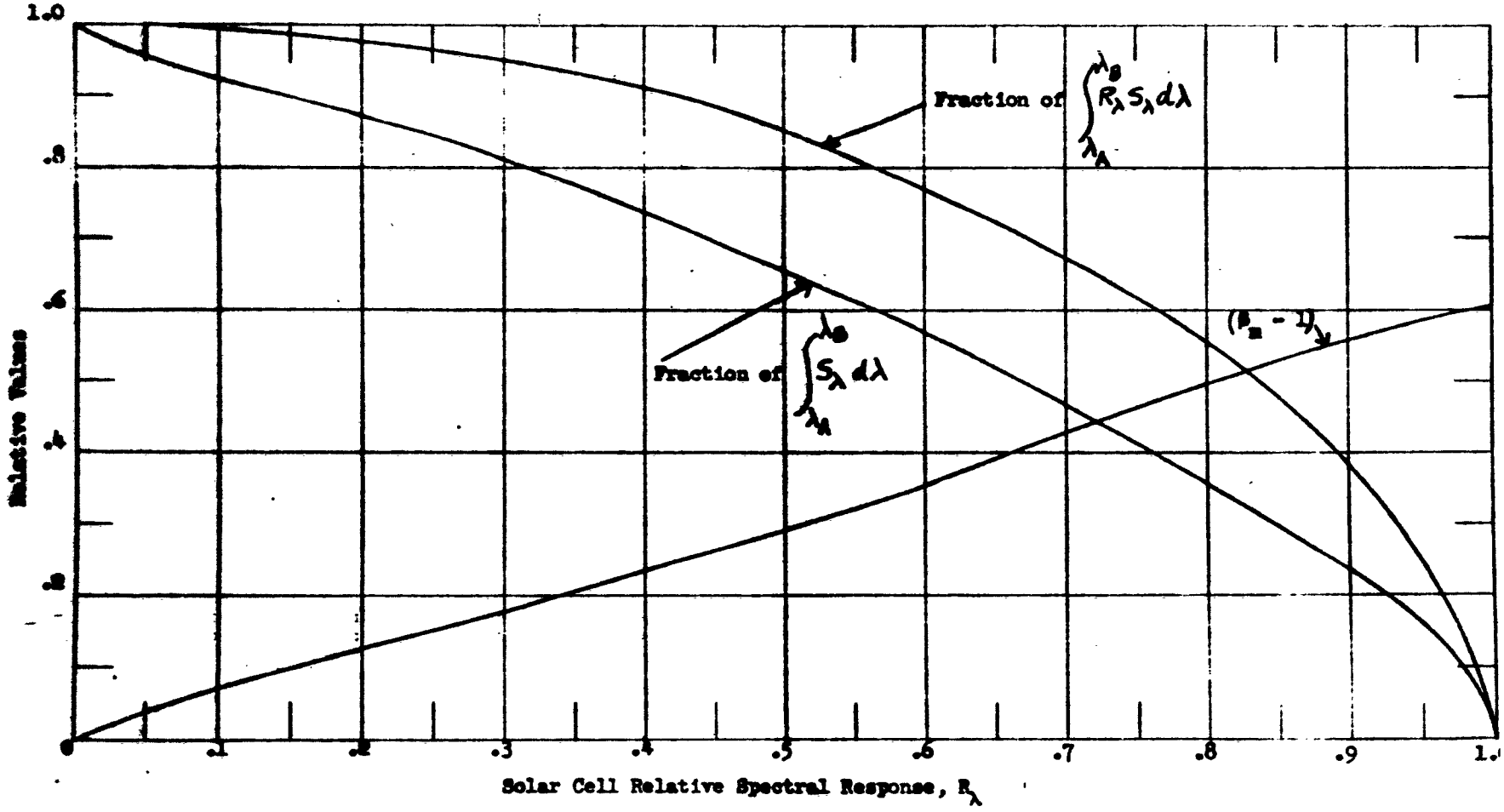


Figure 22. Fraction of the Solar Energy and Cell Power Output Occurring in Region Found by Choosing Filter Band-Pass Limits at Equal Height on the Response Curve of the Helistek Gridded "Blue" Silicon Solar Cell. Also, $(\beta_m - 1)$, where β_m is the Multiplier of the Average Absolute Efficiency (at the Reference Temperature) Between λ_A and λ_B to Give the Average Efficiency Within the R_λ Limits.

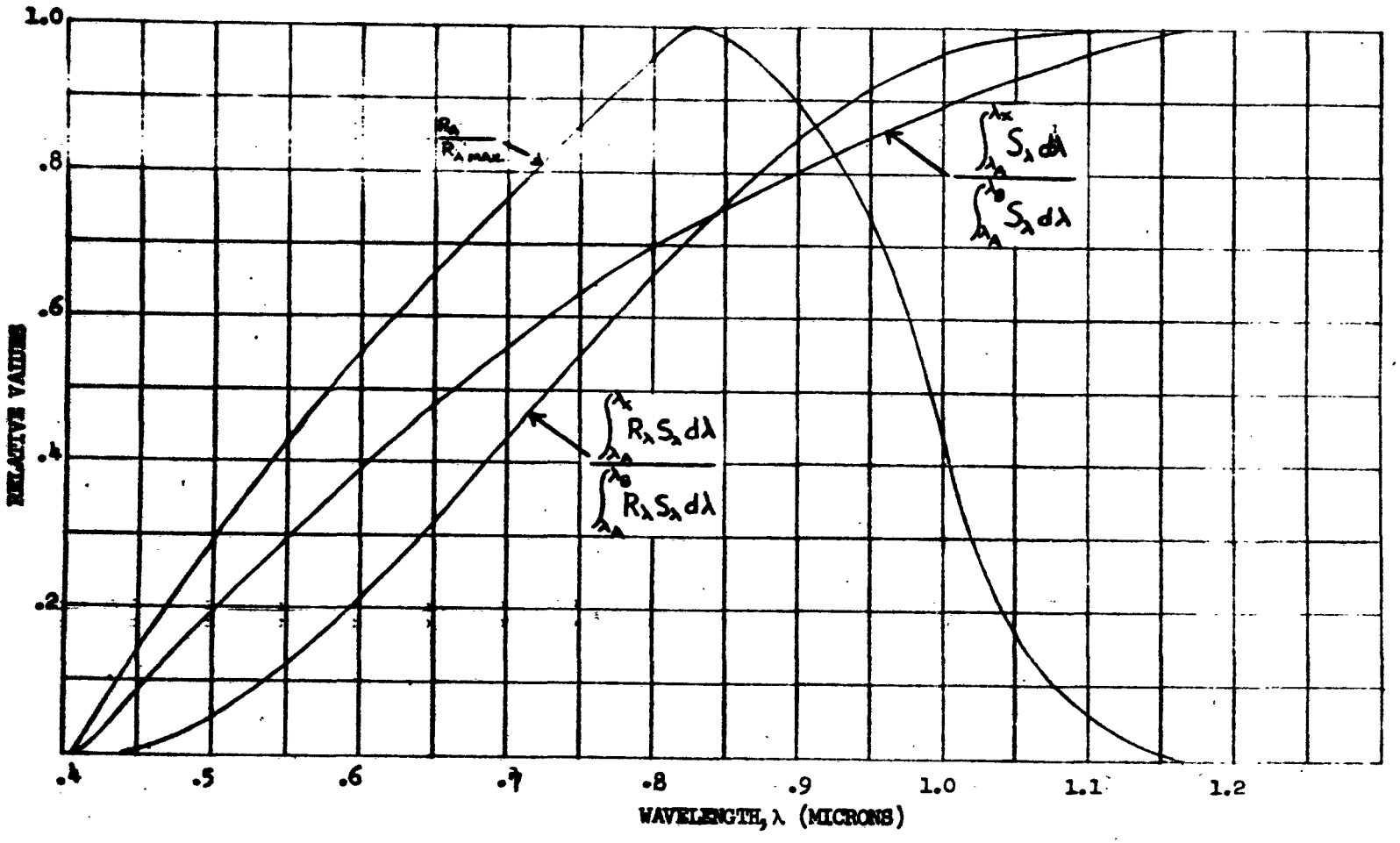


FIGURE 23. NORMALIZED RESPONSE AND CUMULATIVE SOLAR ENERGY AND POWER OUTPUT OF EXPERIMENTAL GRIDDED "RED" SILICON SOLAR CELL AS A FRACTION OF THE TOTAL BETWEEN λ_A AND λ_B.

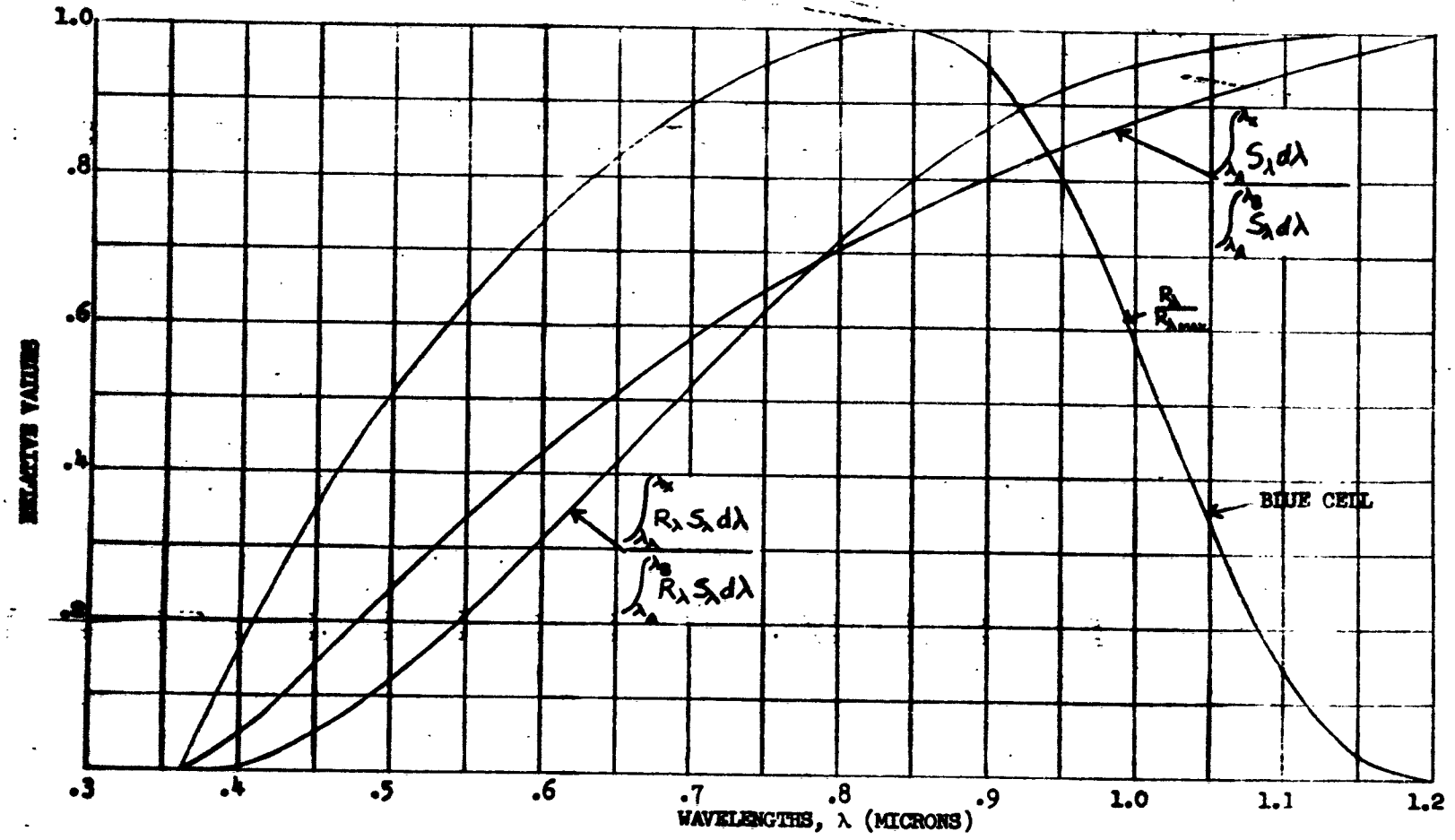


FIGURE 24. NORMALIZED RESPONSE AND CUMULATIVE SOLAR ENERGY AND POWER OUTPUT OF HELIOTEK GRIDDED "BLUE" SILICON SOLAR CELL AS A FRACTION OF THE TOTAL BETWEEN λ_A AND λ_B.

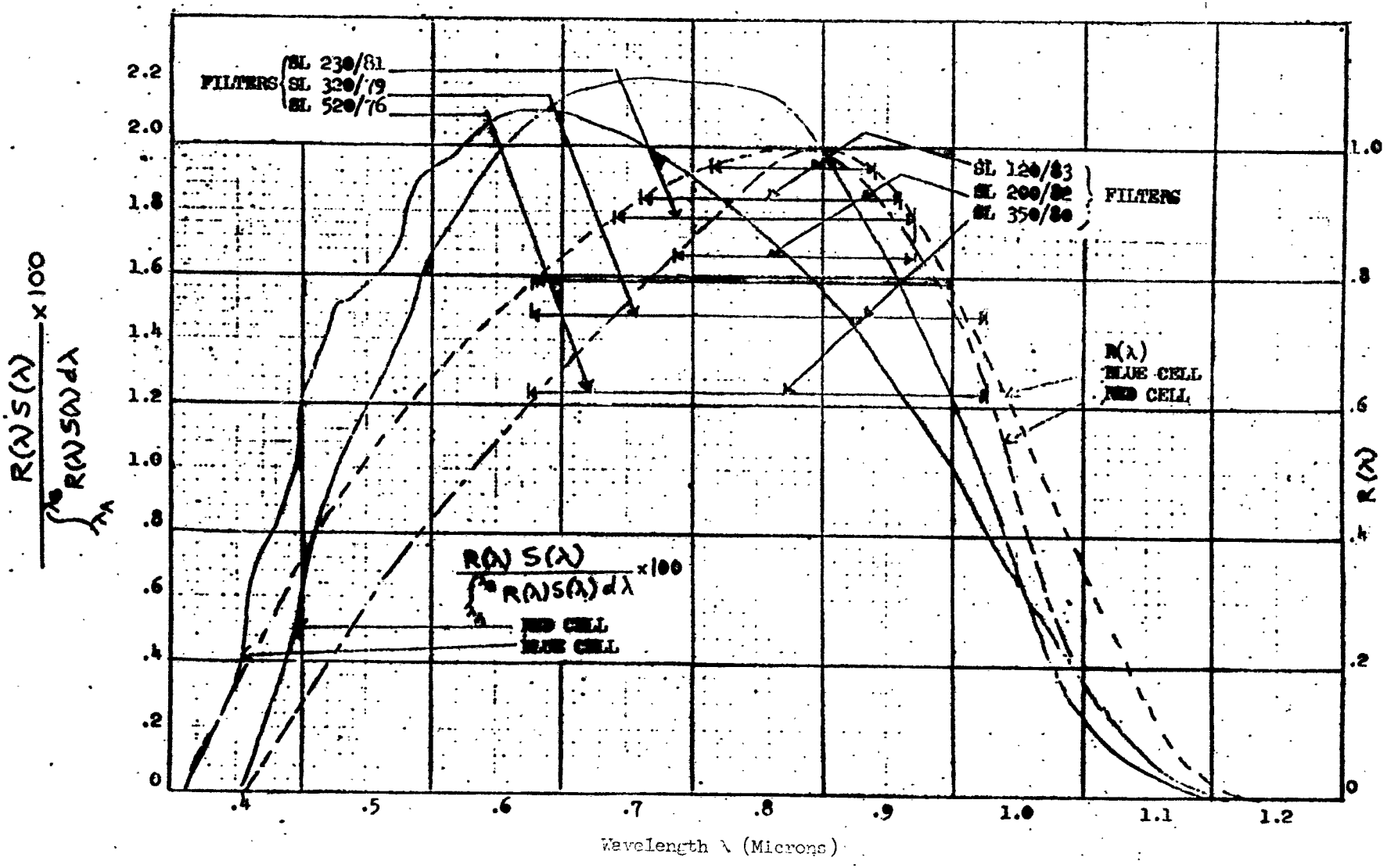


FIGURE 3. SPECTRAL DISTRIBUTION OF SOLAR CELL RESPONSE AND FILTER TRANSMISSION.

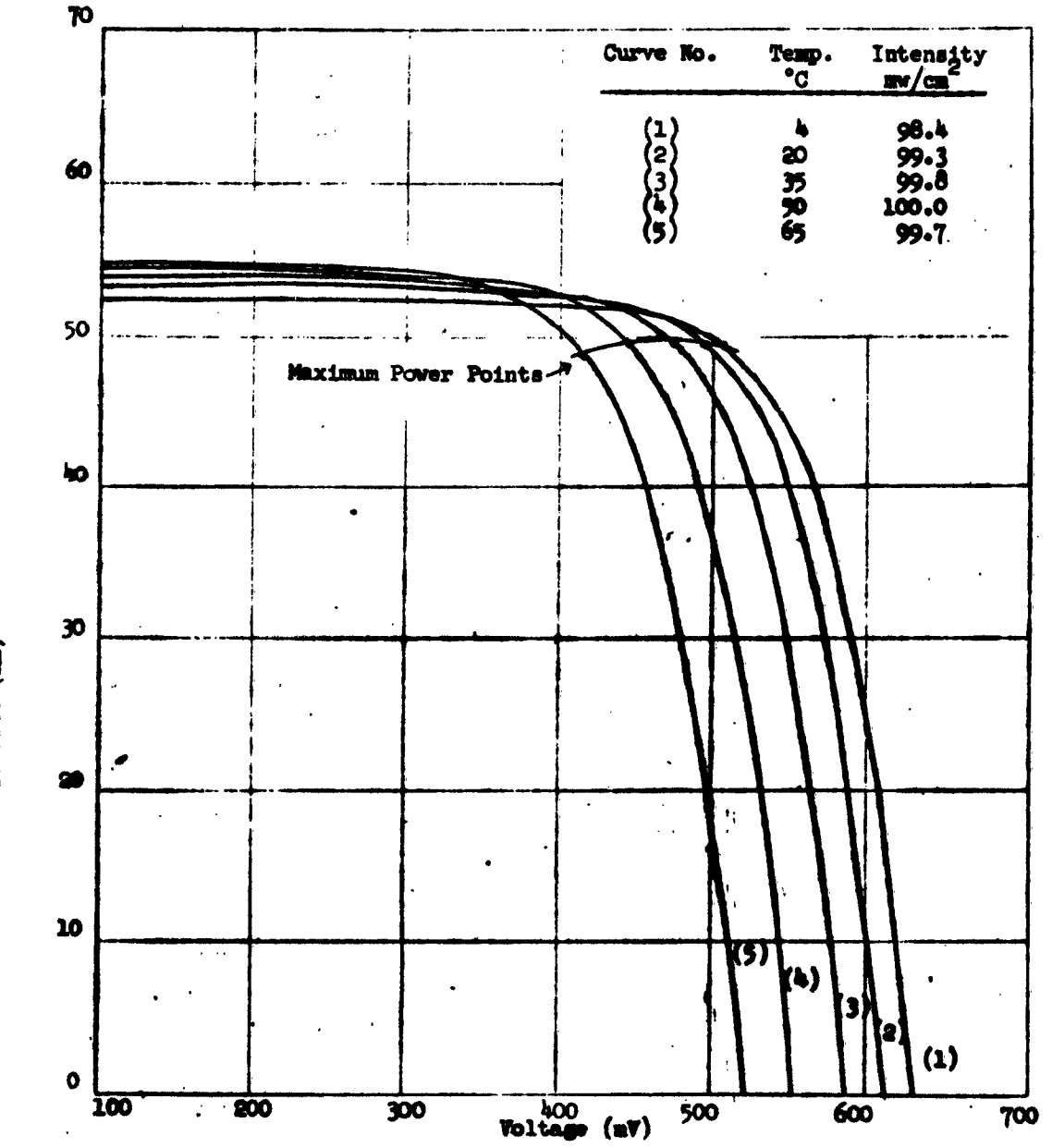


Figure 26. Solar Cell Power Output vs Temperature and Incident Energy for Heliotek Gridded "Blue" Cell (Sunlight at Table Mountain).

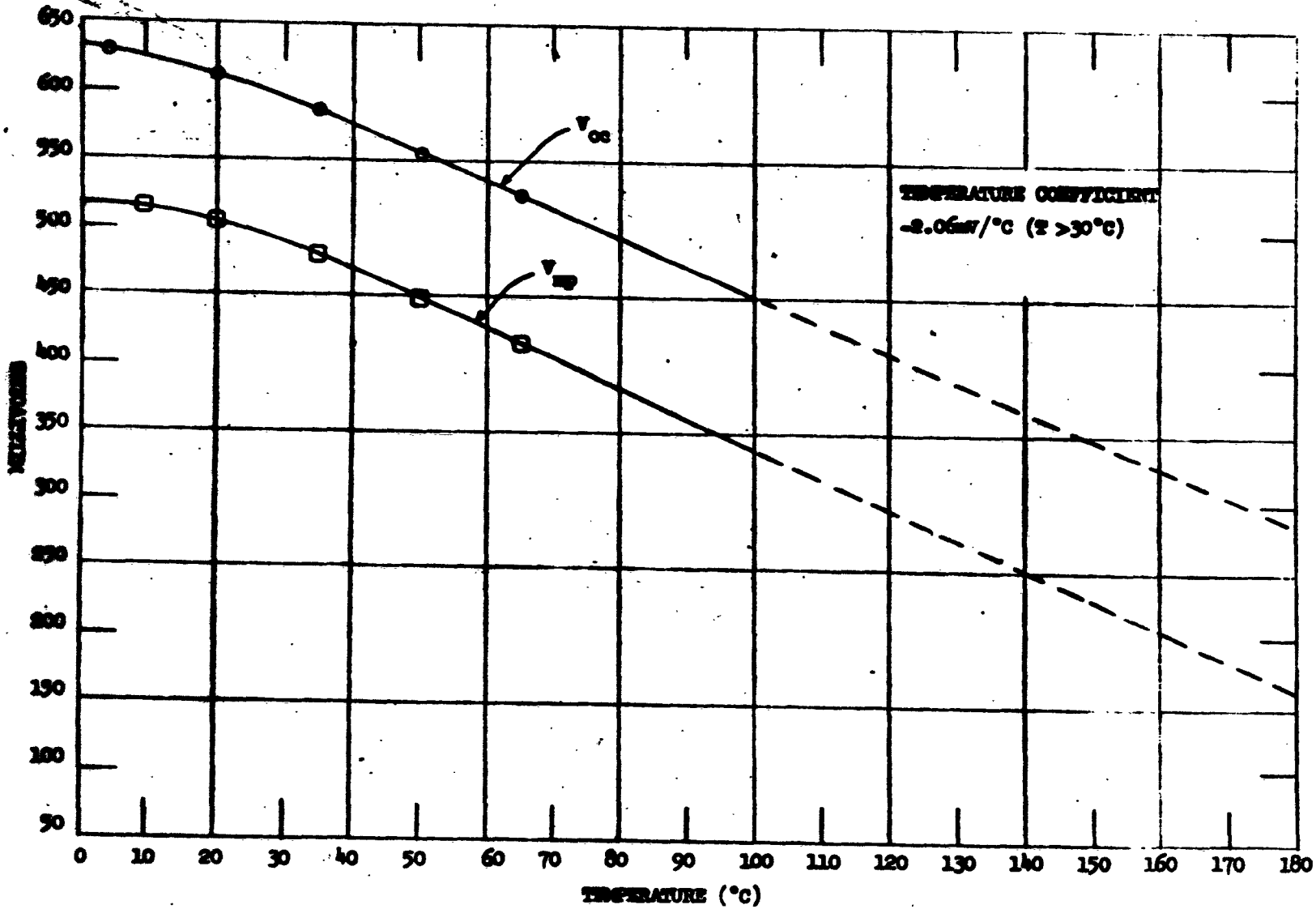


FIGURE 27. SOLAR CELL MAXIMUM POWER VOLTAGE AND OPEN CIRCUIT VOLTAGE VS. TEMPERATURE (SUNLIGHT ON TABLE MTN) FOR HELIOTEK GRIDDED "BLUE" CELL.

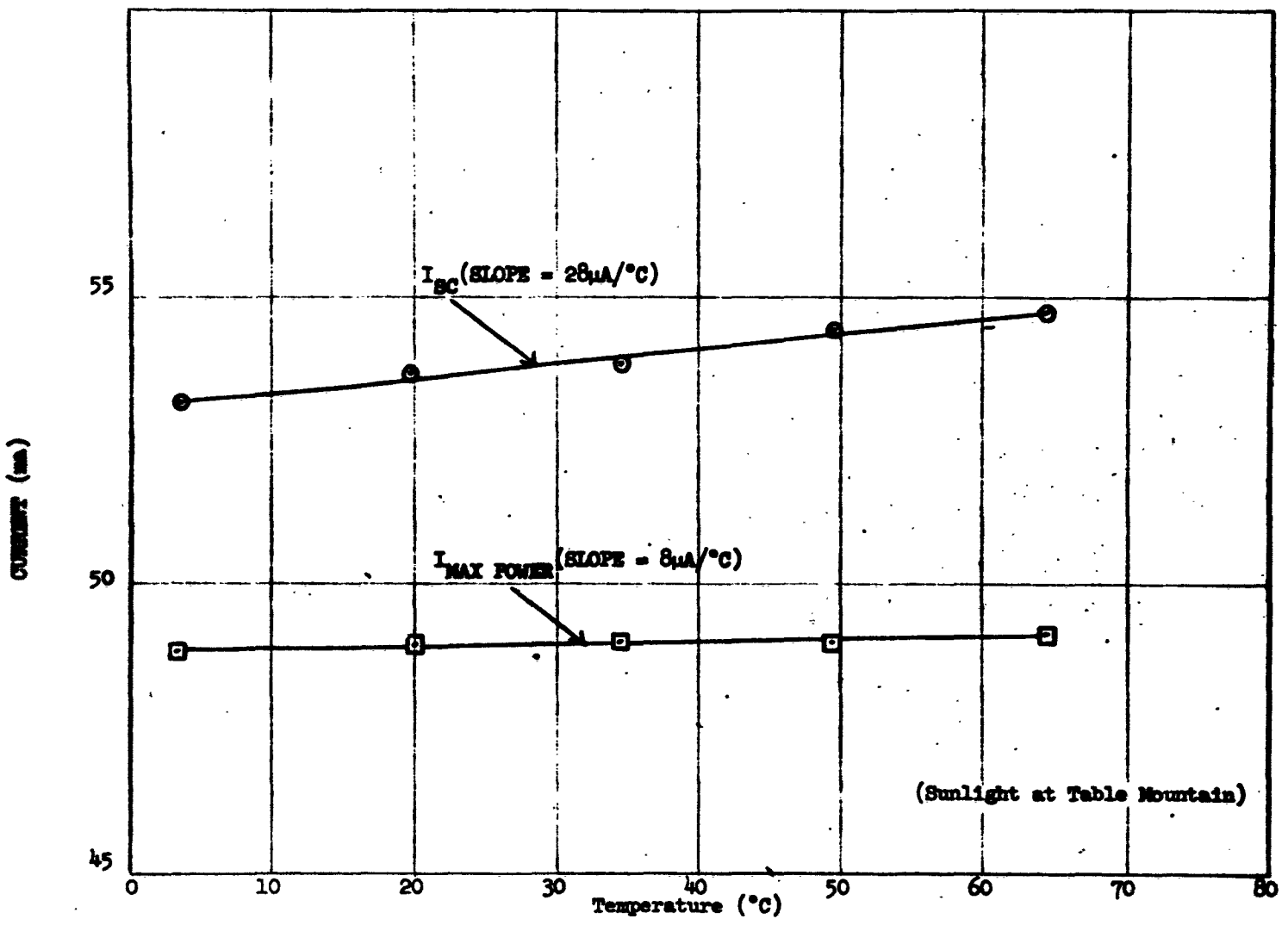


Figure 28. SOLAR CELL CURRENT vs TEMPERATURE FOR HELIOTEK GRIDDED "BLUE" CELL.

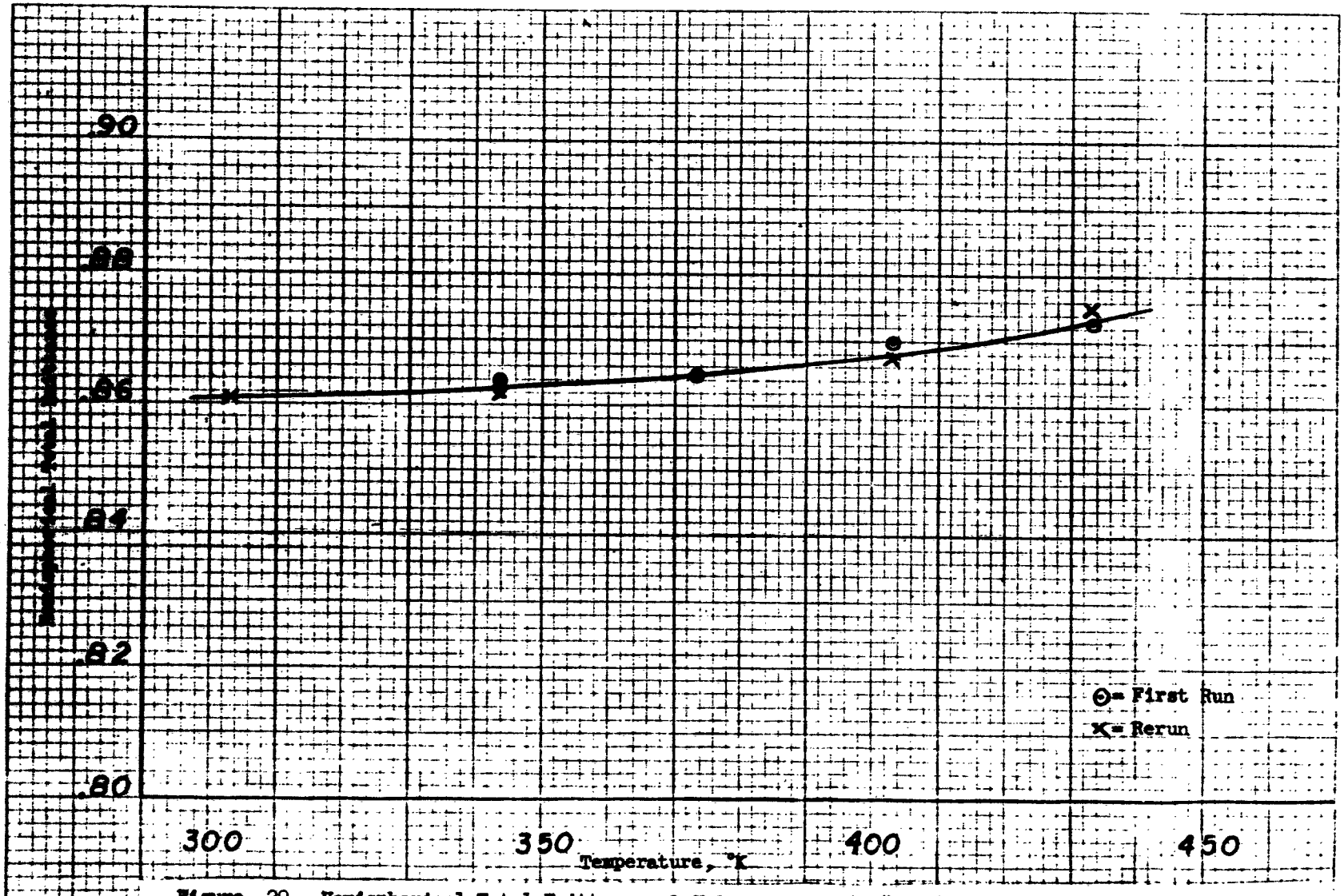


Figure 29. Hemispherical Total Emittance of Heliotek Gridded "Blue" Cell with Solakote "B" Filter.

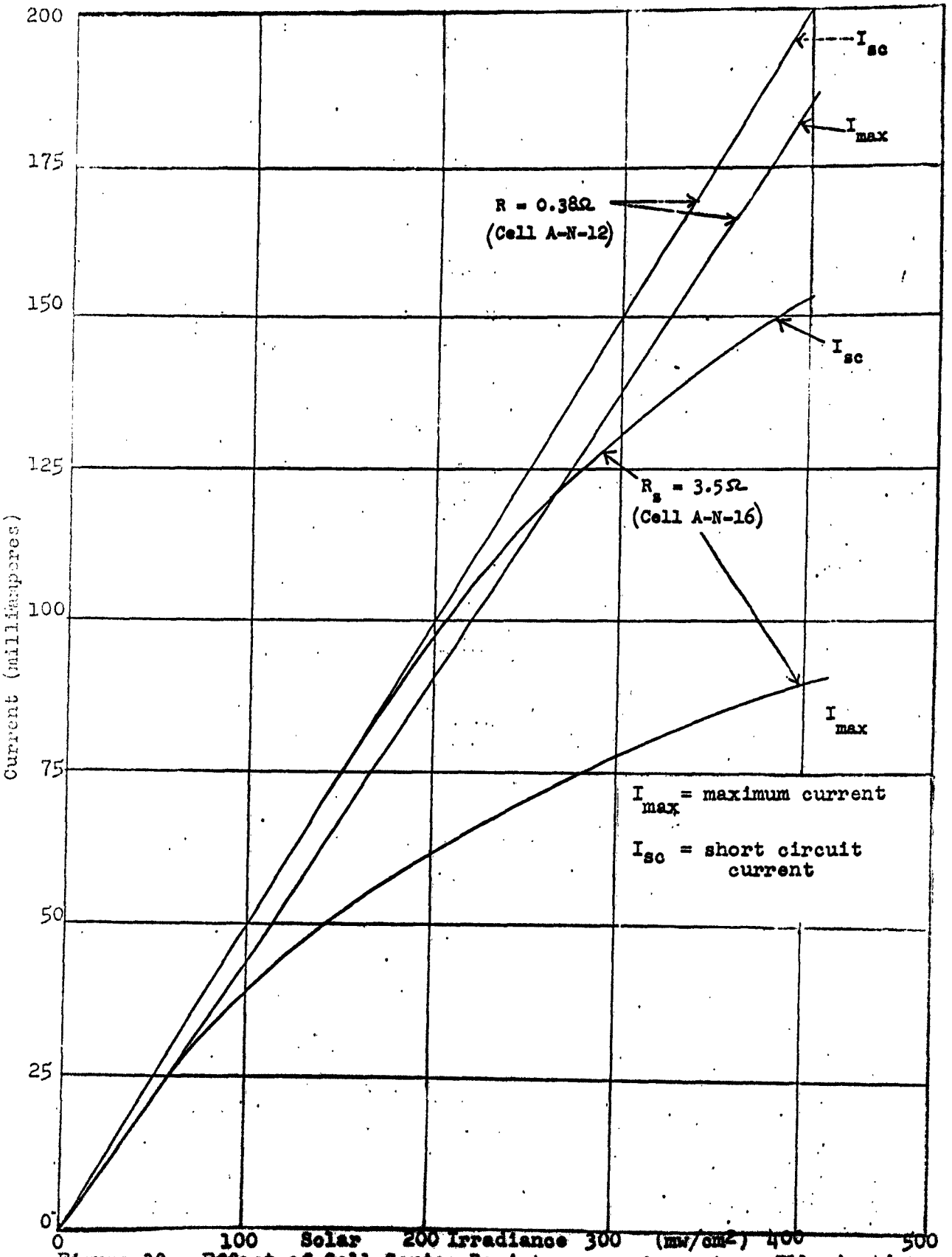


Figure 30. Effect of Cell Series Resistance on Current vs Illumination.
(From Wolf and Rauschenbach report, see footnote p. 4-29. Fig. 3 rev.)

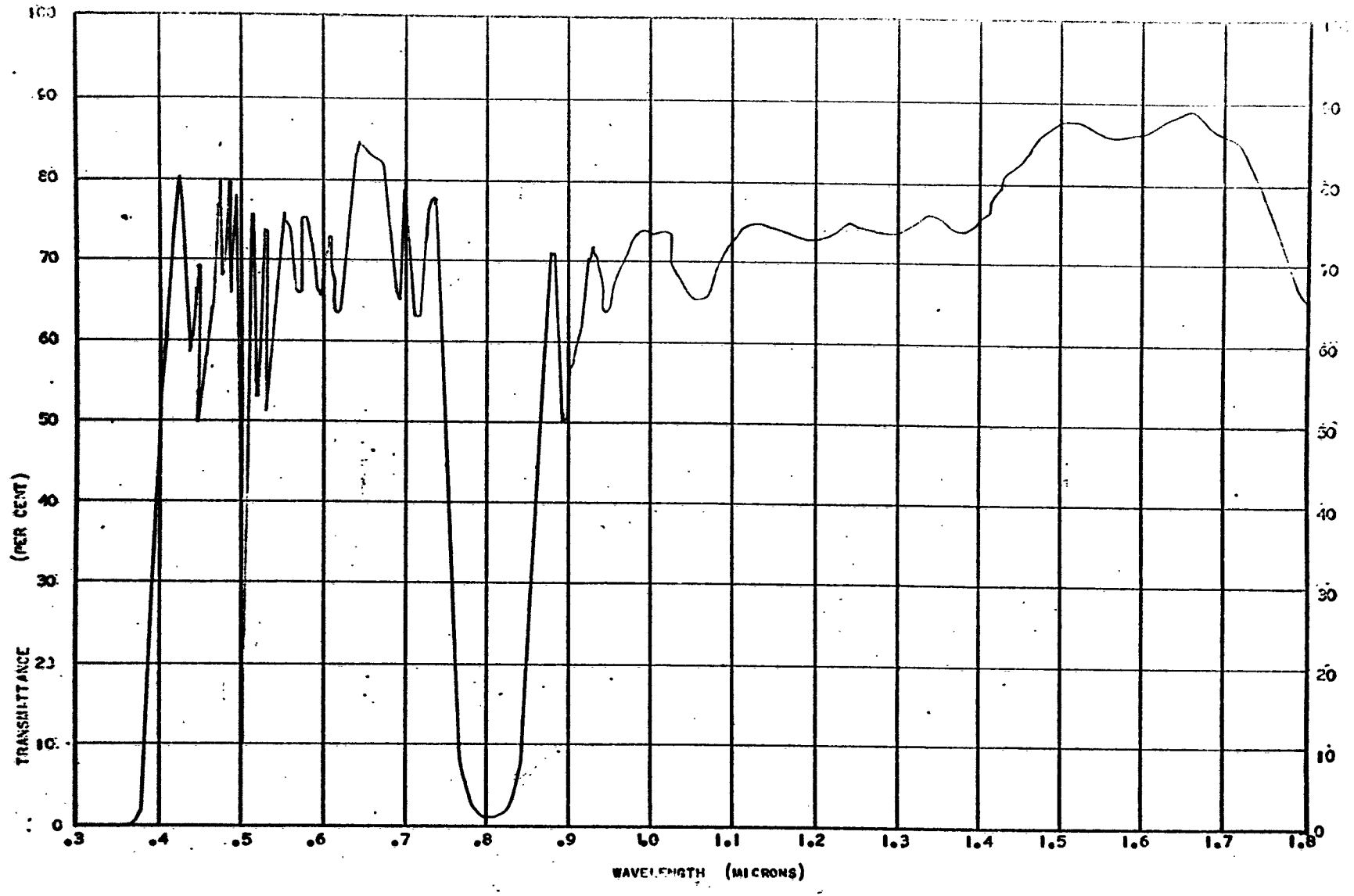


FIGURE 31. SPECTRAL TRANSMITTANCE OF TYPICAL SL-120 REFLECTING FILTER.

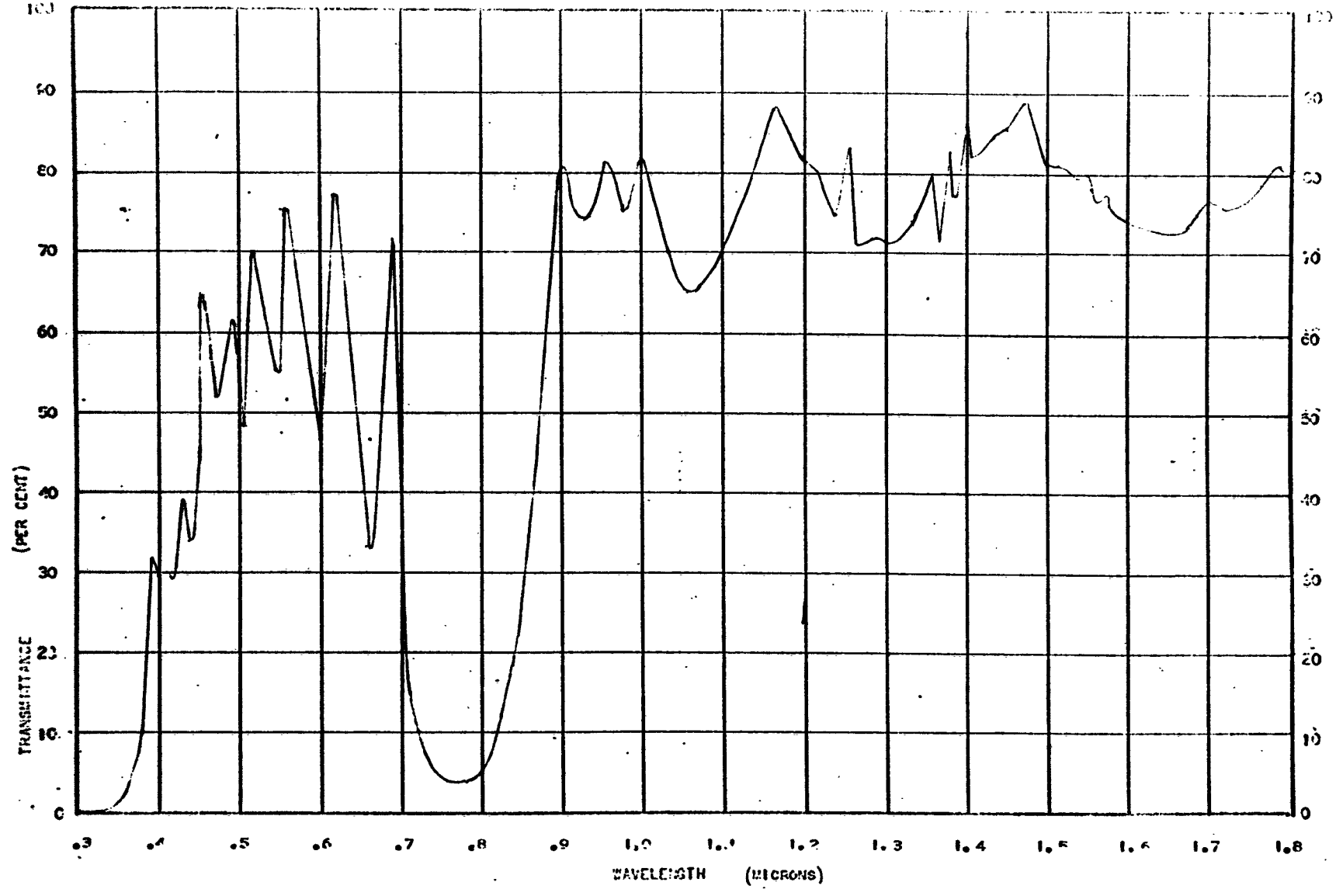


FIGURE 32. SPECTRAL TRANSMITTANCE OF TYPICAL SL-200(I) REFLECTING FILTER.

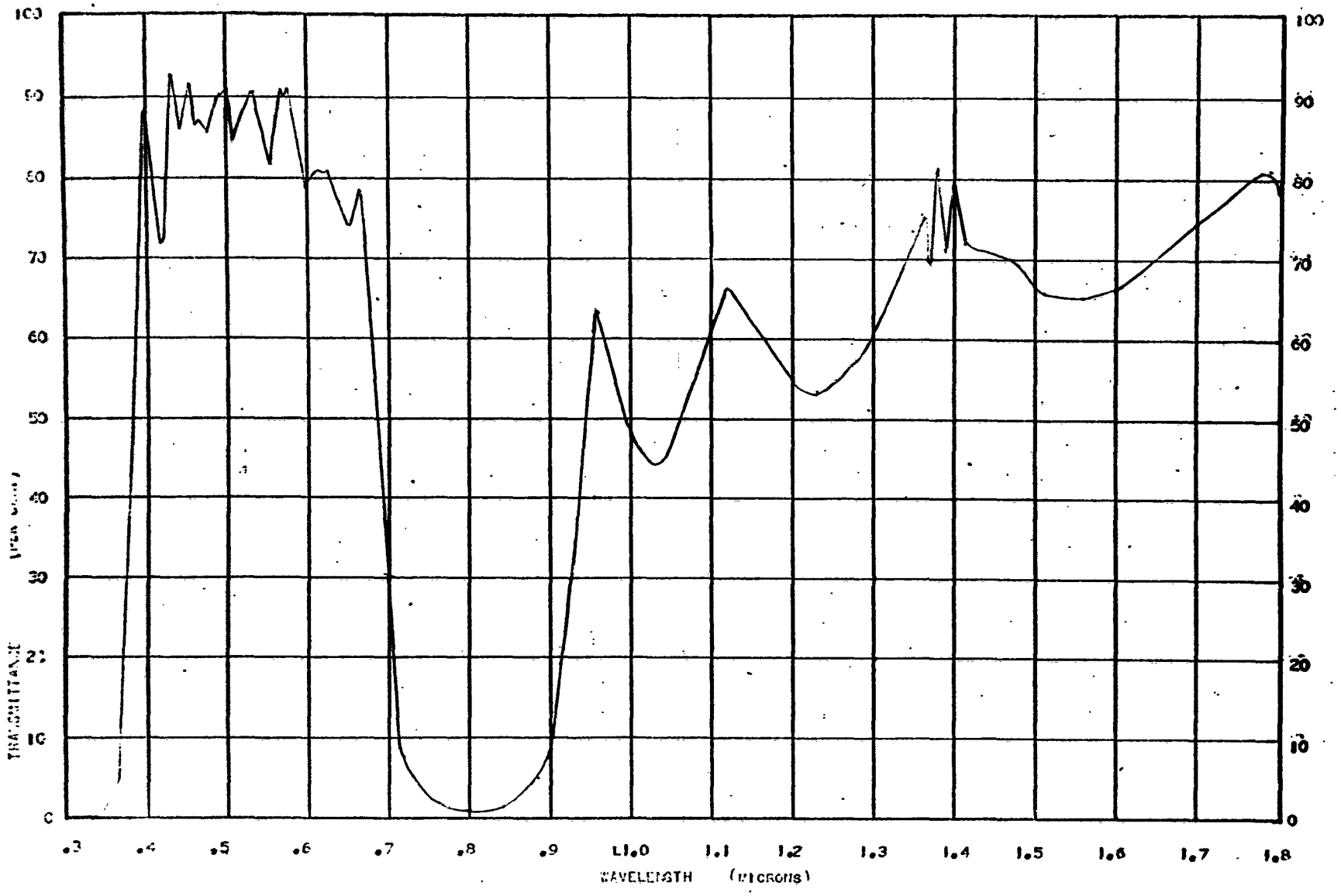


FIGURE 33. SPECTRAL TRANSMITTANCE OF TYPICAL SL-200 (II) REFLECTING FILTER.

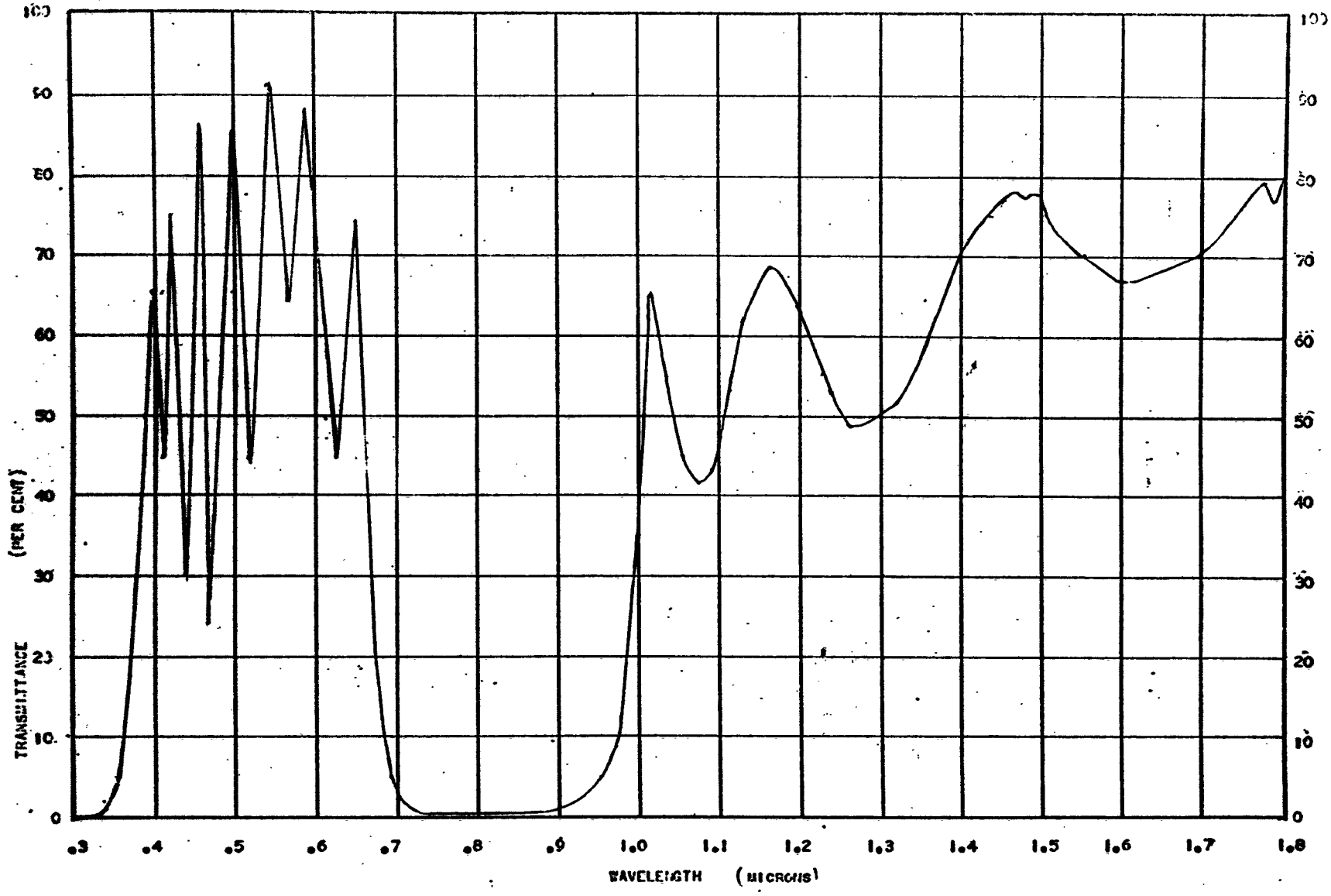


FIGURE 34. SPECTRAL TRANSMITTANCE OF TYPICAL SL-350 REFLECTING FILTER.

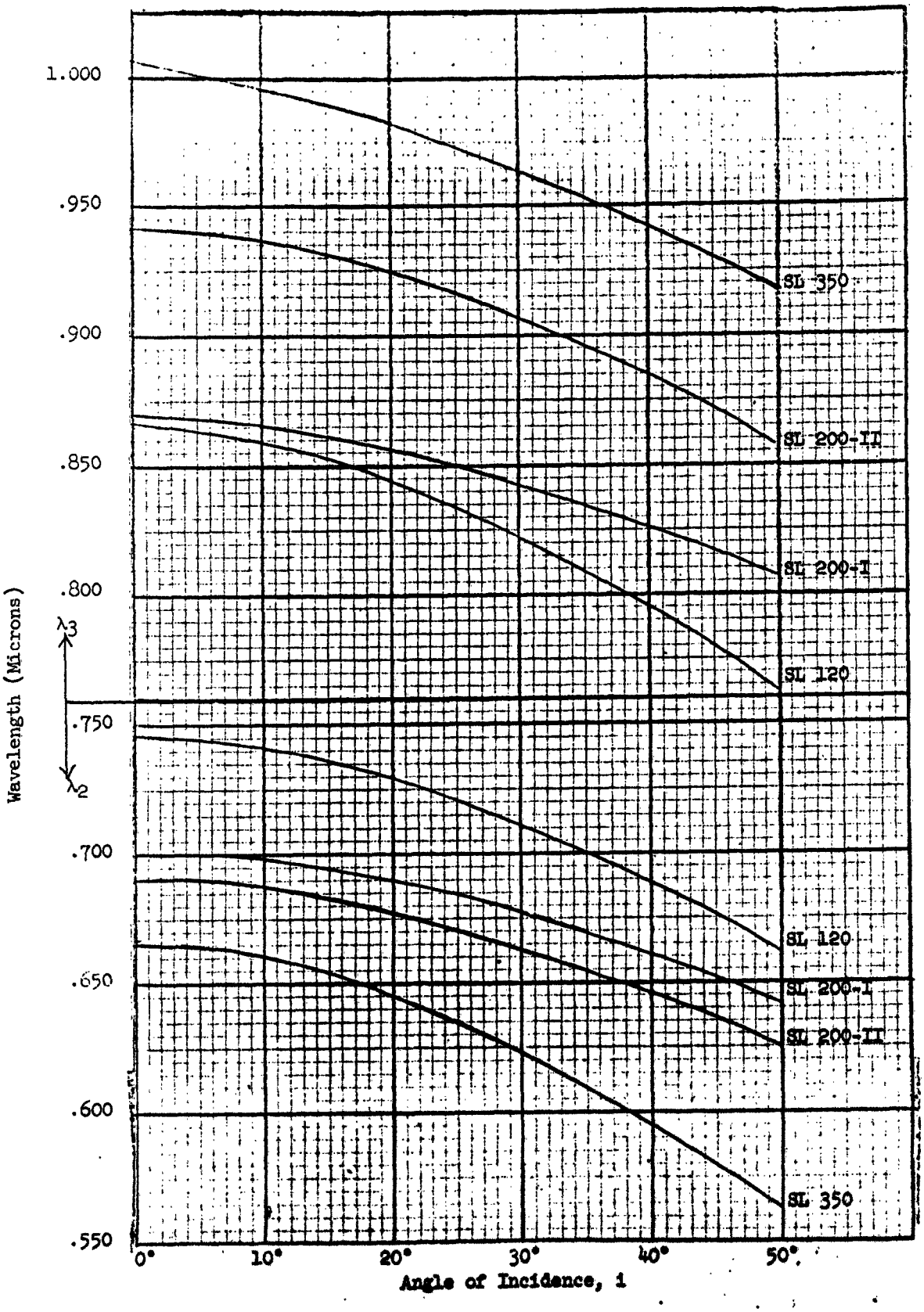


Figure 35. Variation in Cut-Off Wavelengths, λ_2 and λ_3, with Angle of Incidence

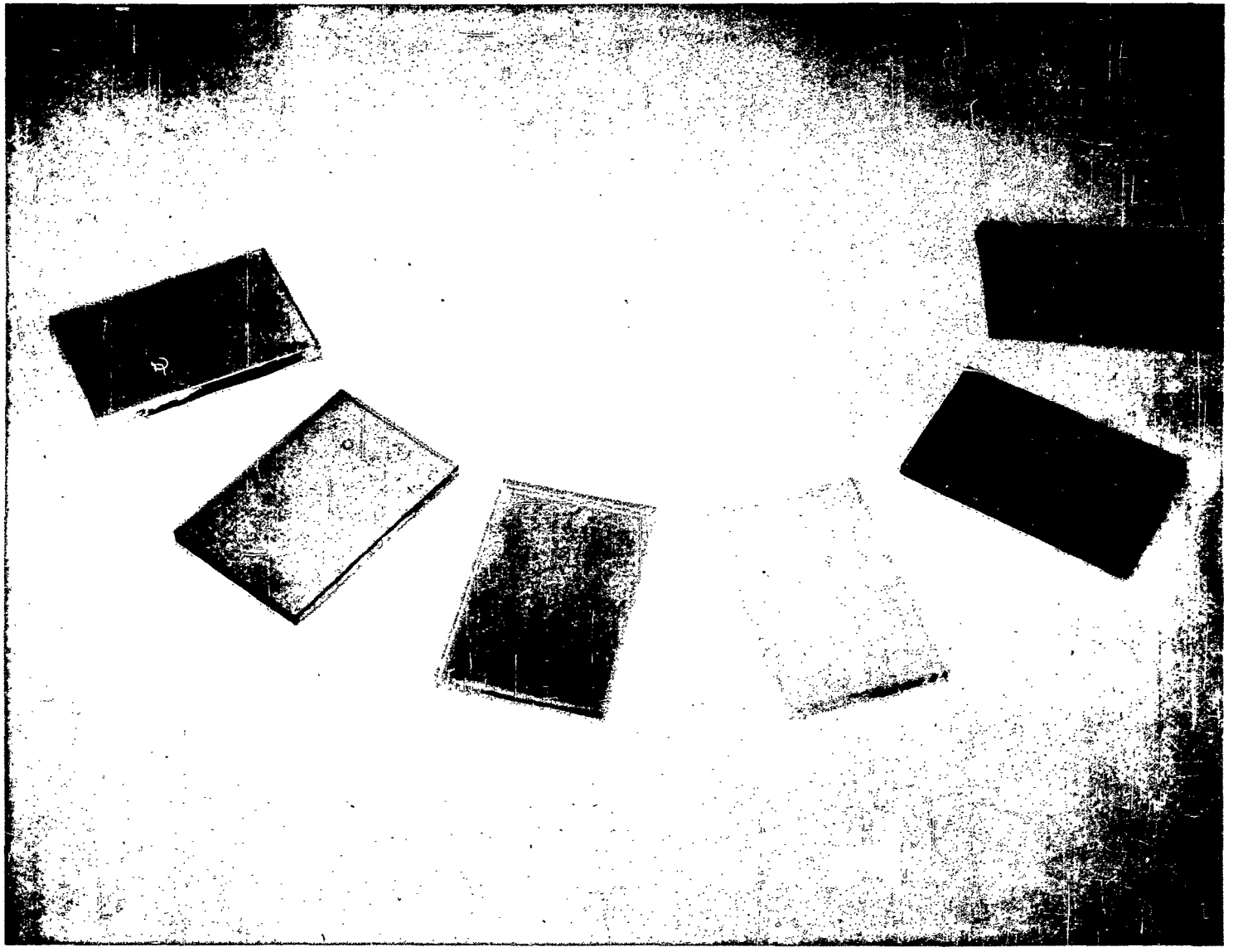


FIGURE 36 SL-350 REFLECTING FILTERS

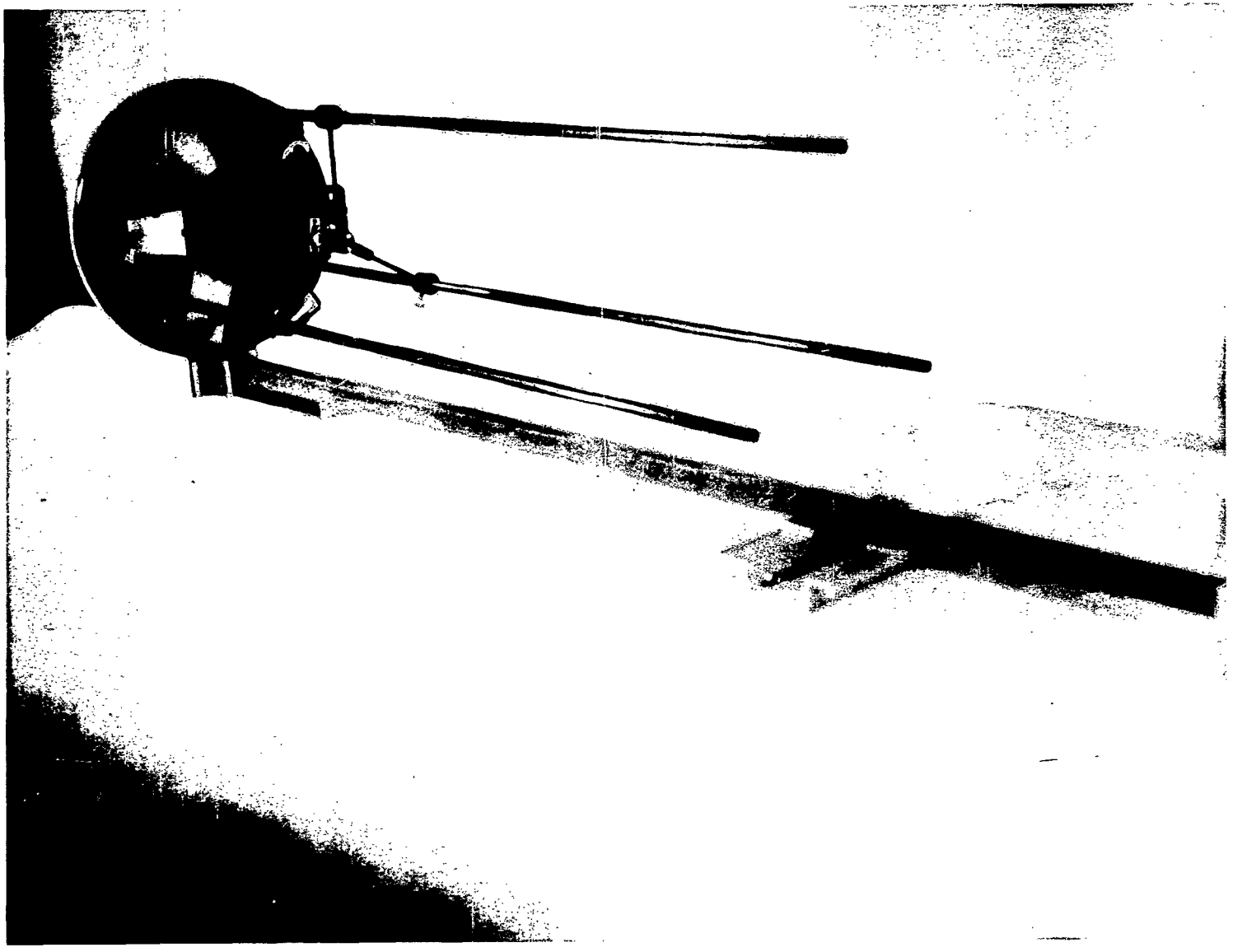


FIGURE 37 REFLECTING FILTER TEST APPARATUS

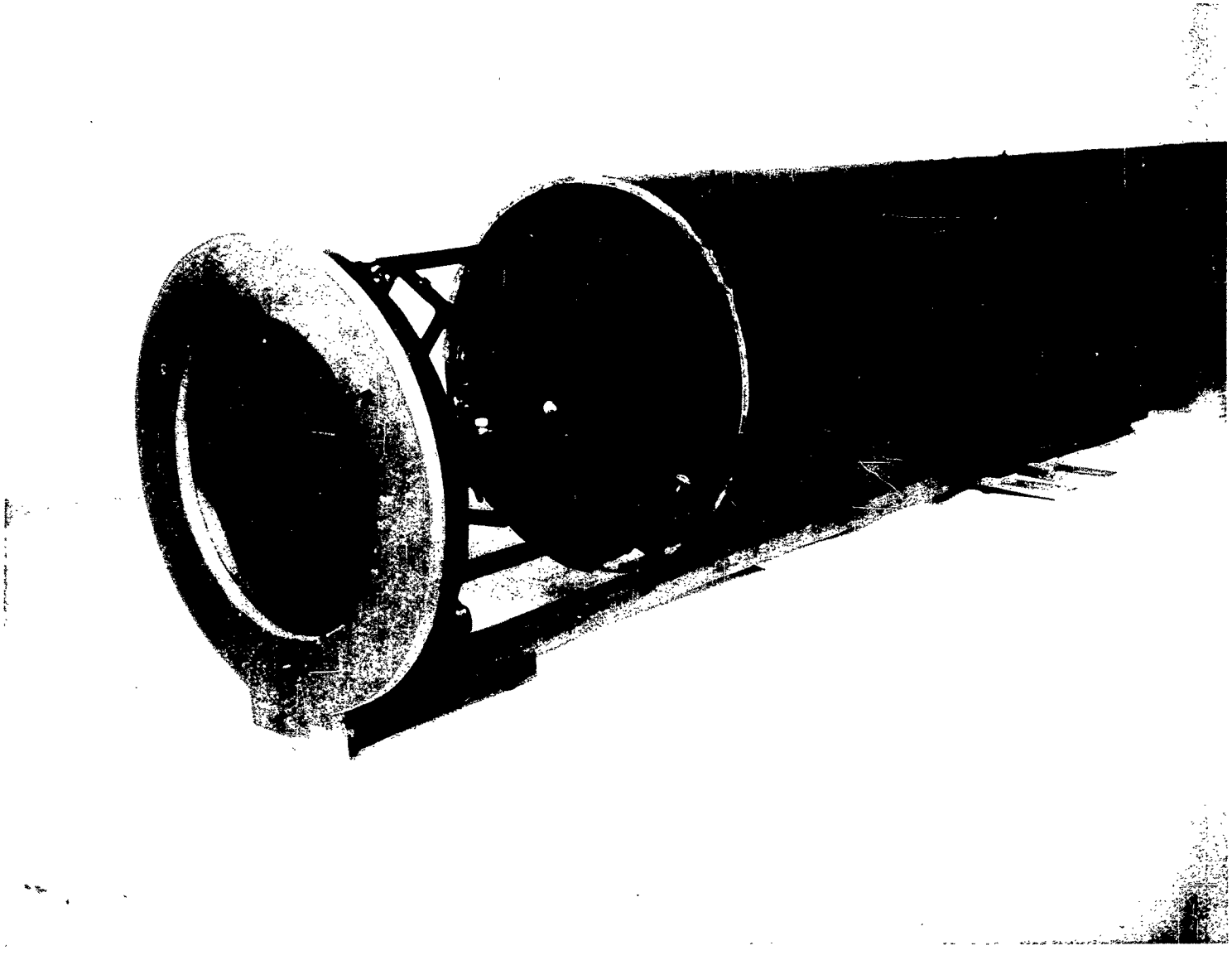


FIGURE 38 REFLECTING FILTER TEST APPARATUS WITH COLLIMATOR

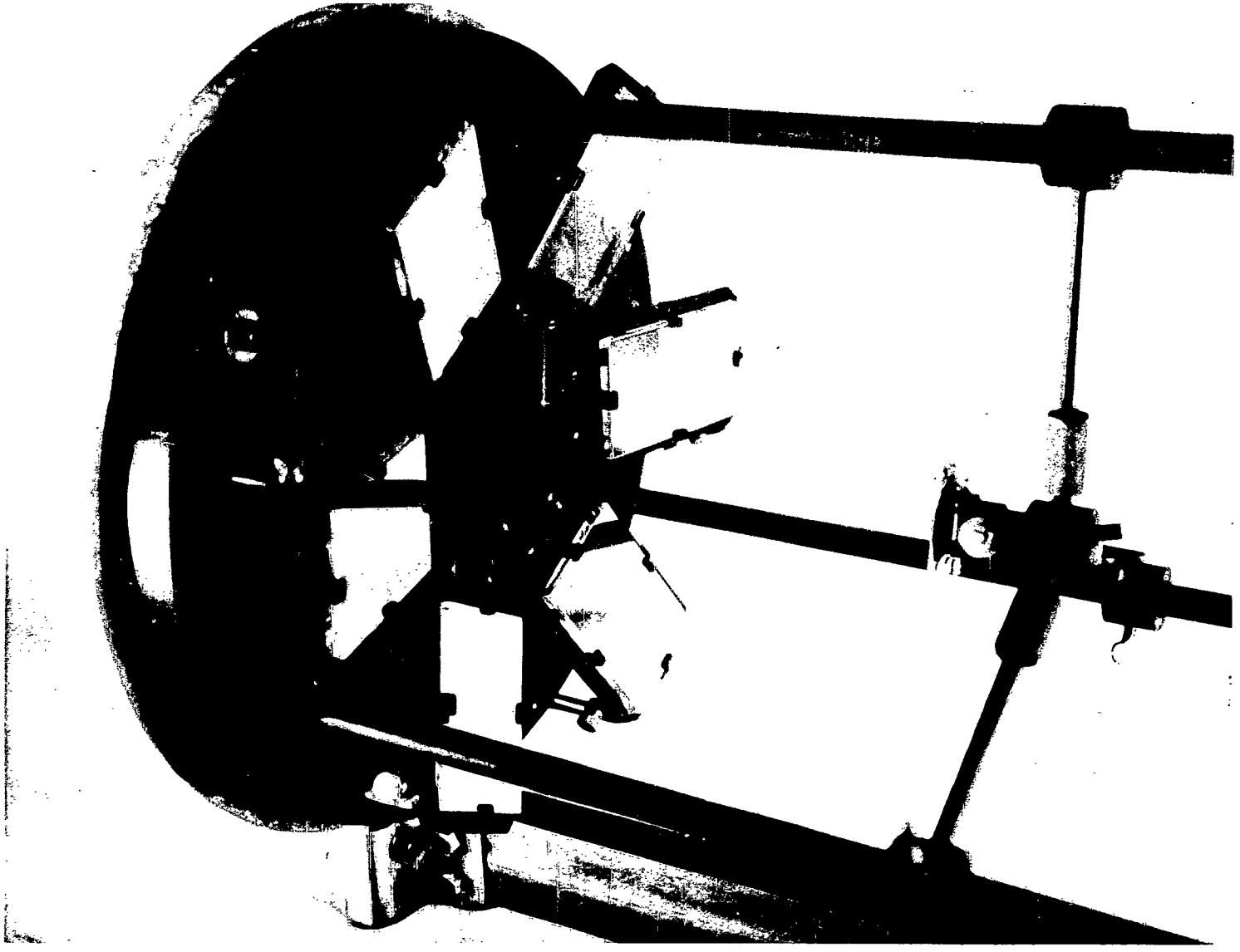


FIGURE 39 CLOSE-UP OF REFLECTING FILTER TEST APPARATUS

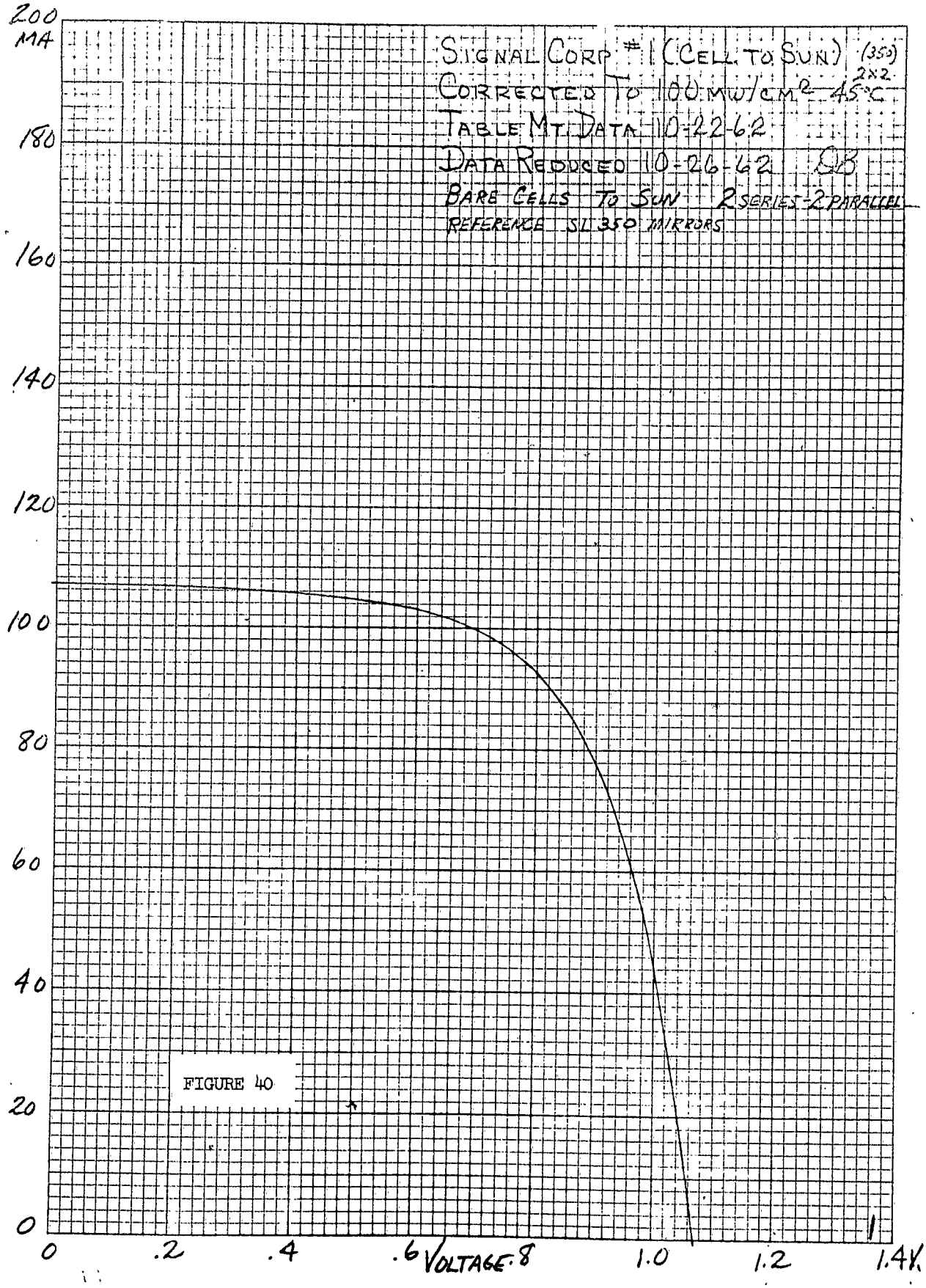

SIGNAL CORP. # 1 (CELL TO SUN) (350)
CORRECTED TO 100 MW/CM² 45°C 2X2
TABLE MT. DATA 10-22-62
DATA REDUCED 10-26-62 QS
BARE CELLS TO SUN 2 SERIES-2 PARALLEL
REFERENCE SL 350 MIRRORS
200 MA
180
160
140
120
100
80
60
40
20
0
CURRENT
0
.2
.4
.6
.8
1.0
1.2
1.4V
VOLTAGE

FIGURE 40

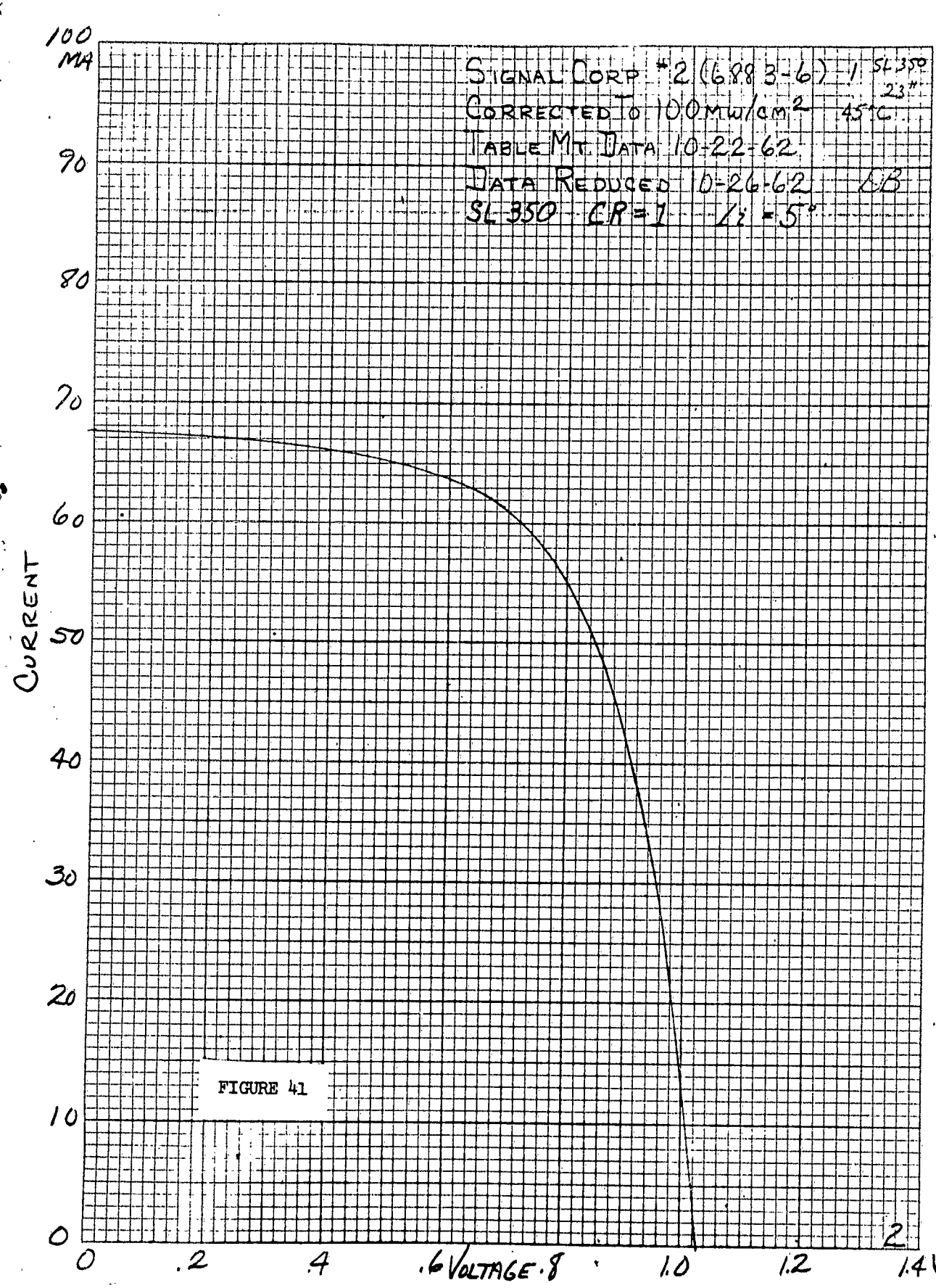


FIGURE 41

PRINTED IN U.S.A. ON CLEARPRINT TECHNICAL PAPER NO. 1015
CLEARPRINT PAPER CO. C35-10 X 10 DIVISIONS PER INCH. 70 X 100 DIVISIONS.

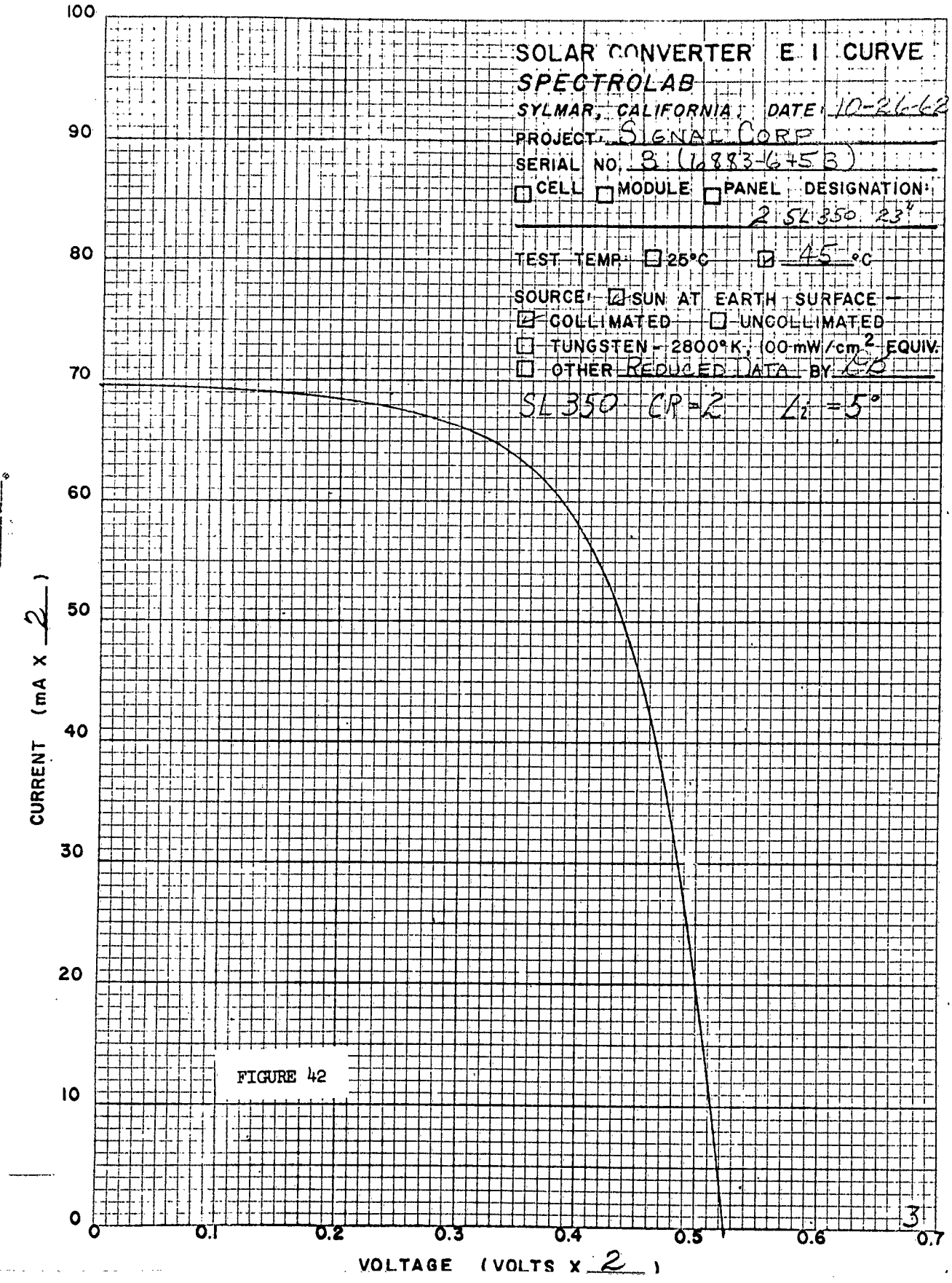

SOLAR CONVERTER E I CURVE
SPECTROLAB
SYLMAR, CALIFORNIA
DATE 10-26-62
PROJECT SIGNAL CORP
SERIAL NO. B (1883-6+5 B)
☐ CELL ☐ MODULE ☐ PANEL DESIGNATION:
2 SL 350 23⁴
TEST TEMP ☐ 25°C ☑ 45 °C
SOURCE: ☑ SUN AT EARTH SURFACE —
☑ COLLIMATED ☐ UNCOLLIMATED
☐ TUNGSTEN - 2800°K, 100 mW/cm² EQUIV.
☐ OTHER REDUCED DATA BY LB
SL 350 CR=2 Δi=5°
CURRENT (mA X 2)
VOLTAGE (VOLTS X 2)
100
90
80
70
60
50
40
30
20
10
0
0
0.1
0.2
0.3
0.4
0.5
0.6
0.7

FIGURE 42

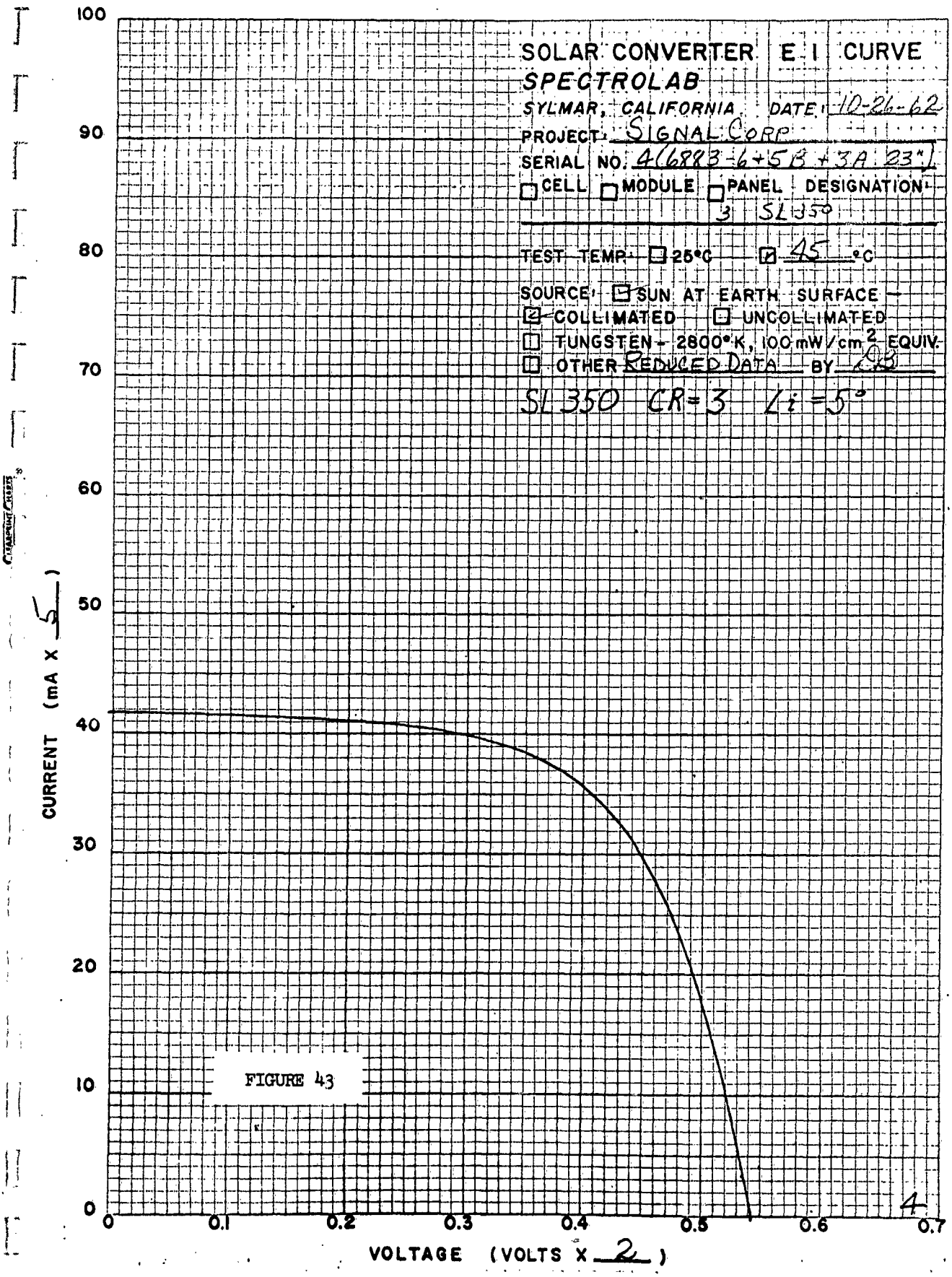

SOLAR CONVERTER E I CURVE
SPECTROLAB
SYLMAR, CALIFORNIA DATE: 10-26-62
PROJECT: SIGNAL CORP
SERIAL NO: 4(6883-6+5B+3A 23")
☐ CELL ☐ MODULE ☐ PANEL DESIGNATION: 3 SL 350
TEST TEMP: ☐ 25°C ☒ 45 °C
SOURCE: ☐ SUN AT EARTH SURFACE
☒ COLLIMATED ☐ UNCOLLIMATED
☐ TUNGSTEN - 2800°K, 100 mW/cm² EQUIV.
☐ OTHER REDUCED DATA BY DB
SL 350 CR=3 Li=5°
CURRENT (mA X 5)
VOLTAGE (VOLTS X 2)
100
90
80
70
60
50
40
30
20
10
0
0
0.1
0.2
0.3
0.4
0.5
0.6
0.7
4

FIGURE 43

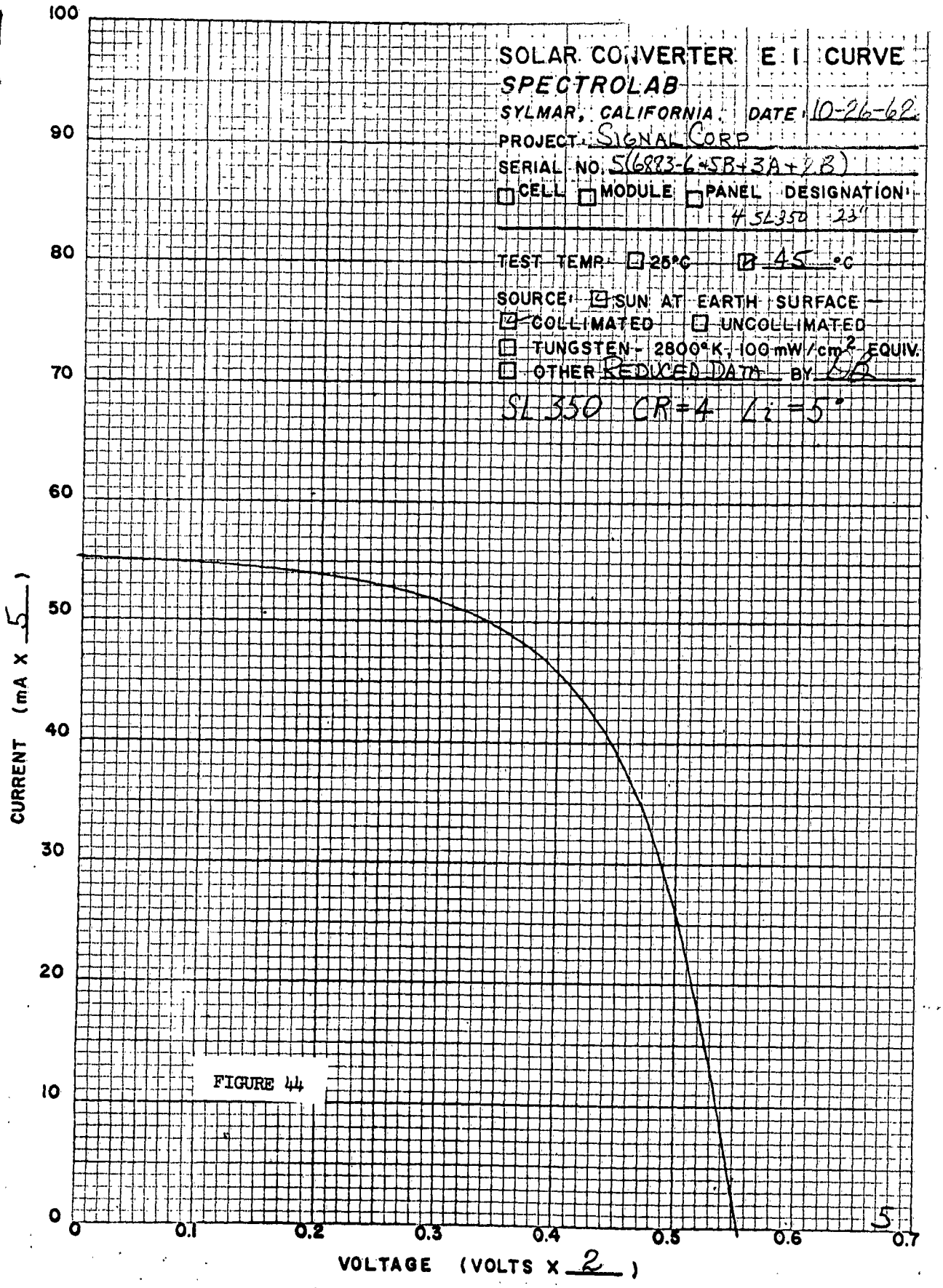


FIGURE 44

CLEARPRINT PAPER CO. C35. 10 X 10 DIVISIONS PER INCH. 70 X 100 DIVISIONS.

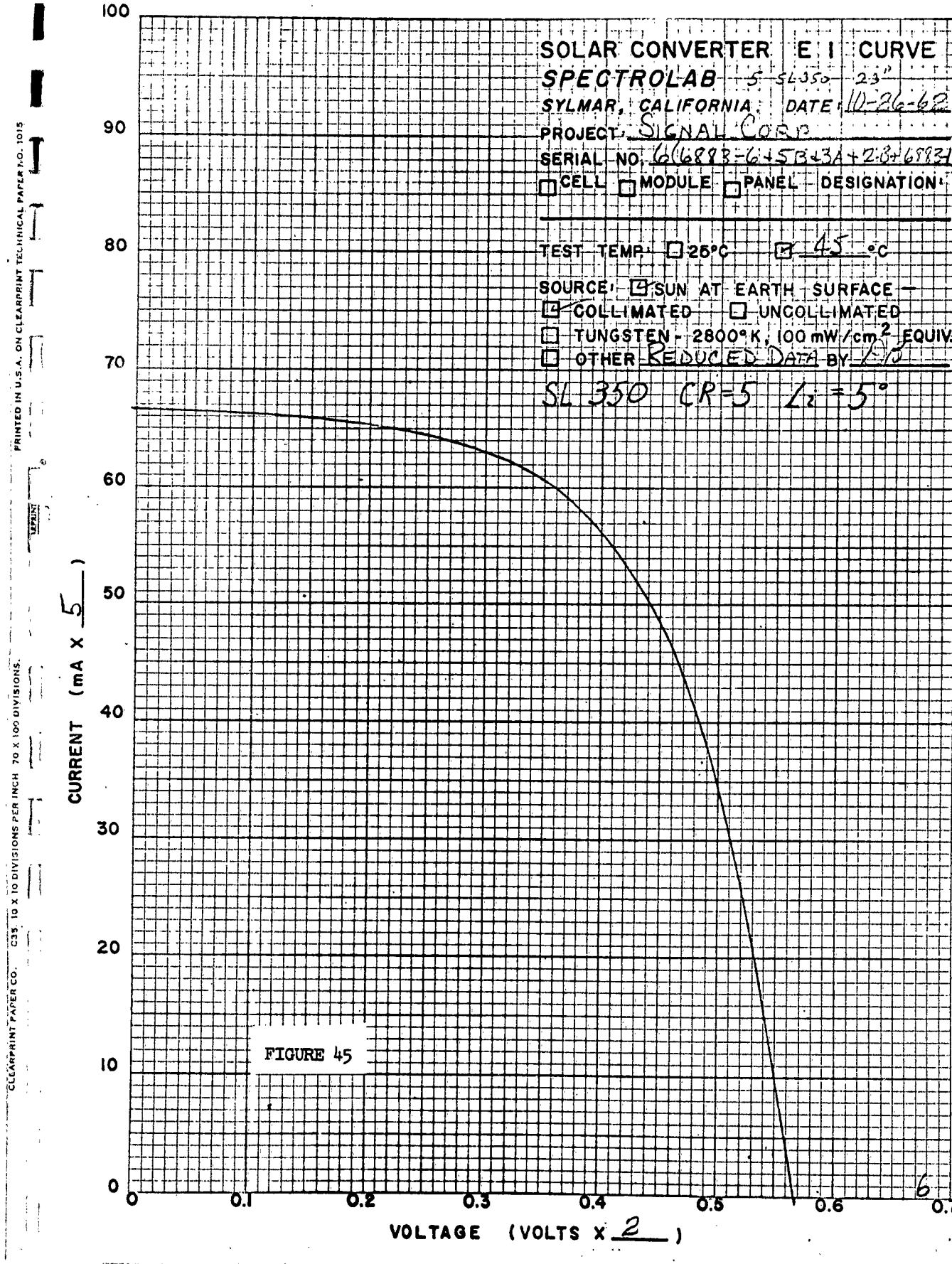


FIGURE 45

CLEARPRINT PAPER CO. C35, 10 X 10 DIVISIONS PER INCH, 70 X 100 DIVISIONS. PRINTED IN U.S.A. ON CLEARPRINT TECHNICAL PAPER NO. 1015

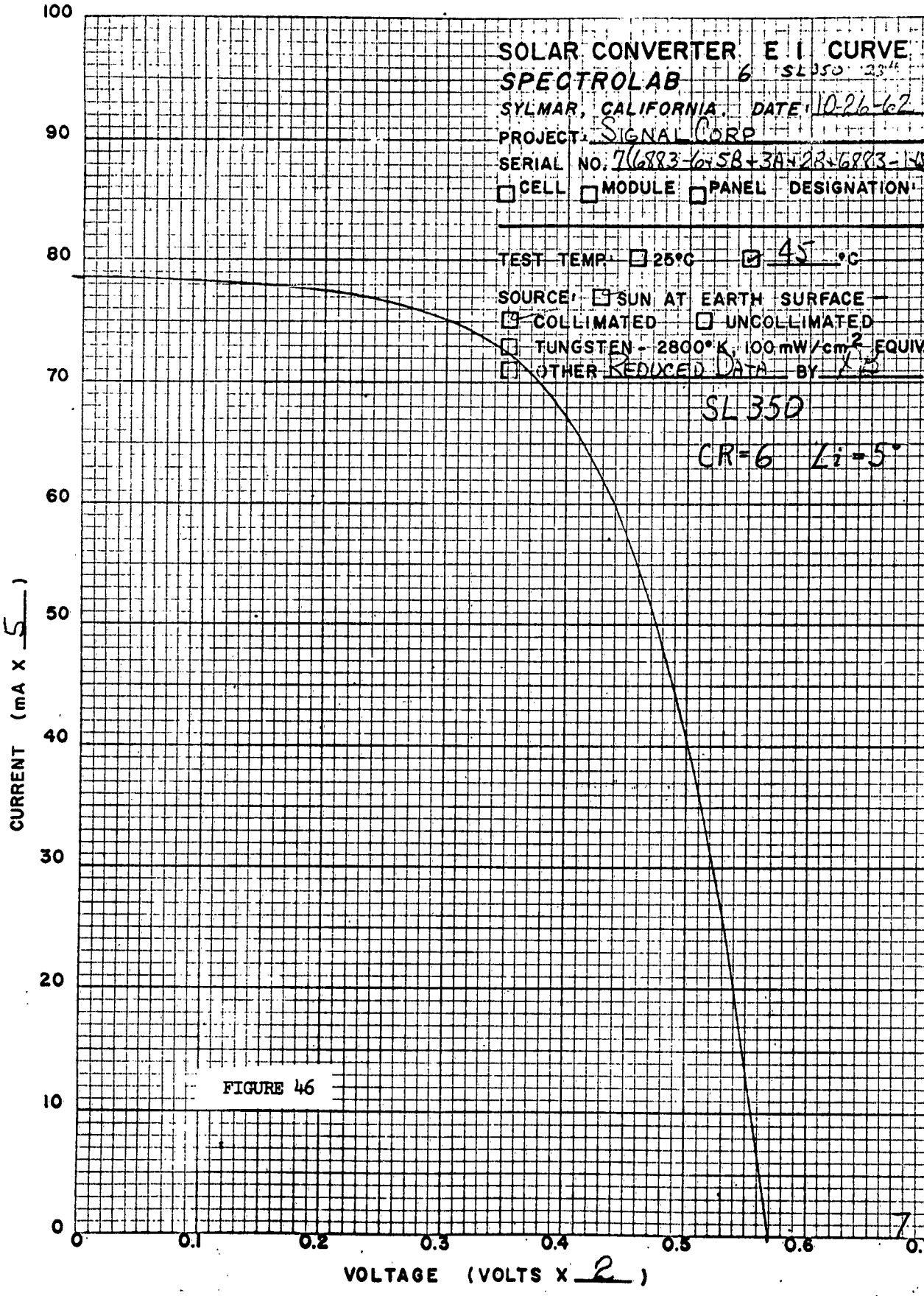


FIGURE 46

PRINTED IN U.S.A. ON CLEARPRINT TECHNICAL PAPER NO. 1015

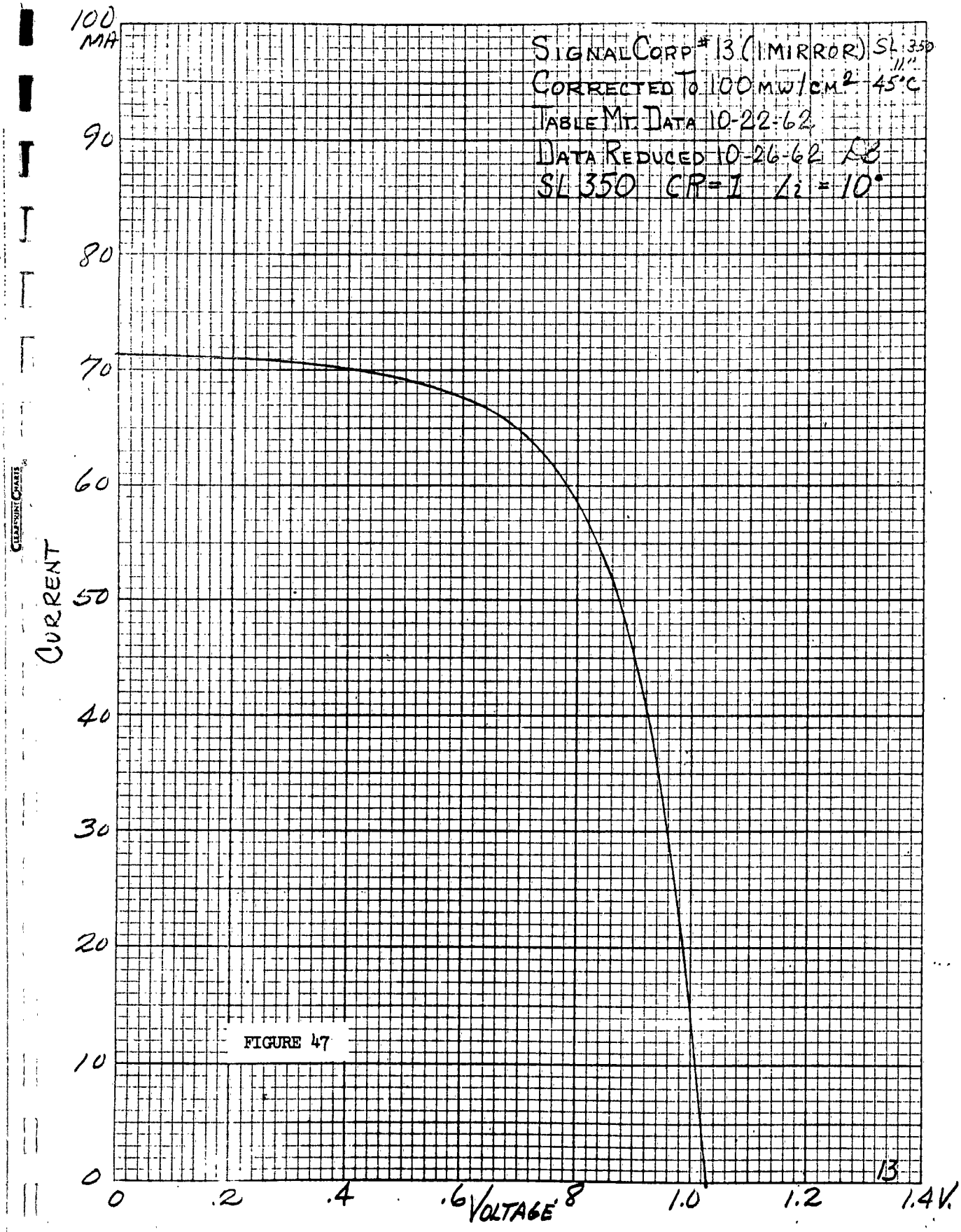

SIGNAL CORP #13 (MIRROR) SL 350
CORRECTED TO 100 MW/CM² 45°C
TABLE MT. DATA 10-22-62
DATA REDUCED 10-26-62
SL 350 CR=1 Li = 10°
100 MA
90
80
70
60
50
40
30
20
10
0
CURRENT
0
.2
.4
.6
.8
1.0
1.2
1.4 V.
VOLTAGE
13

FIGURE 47

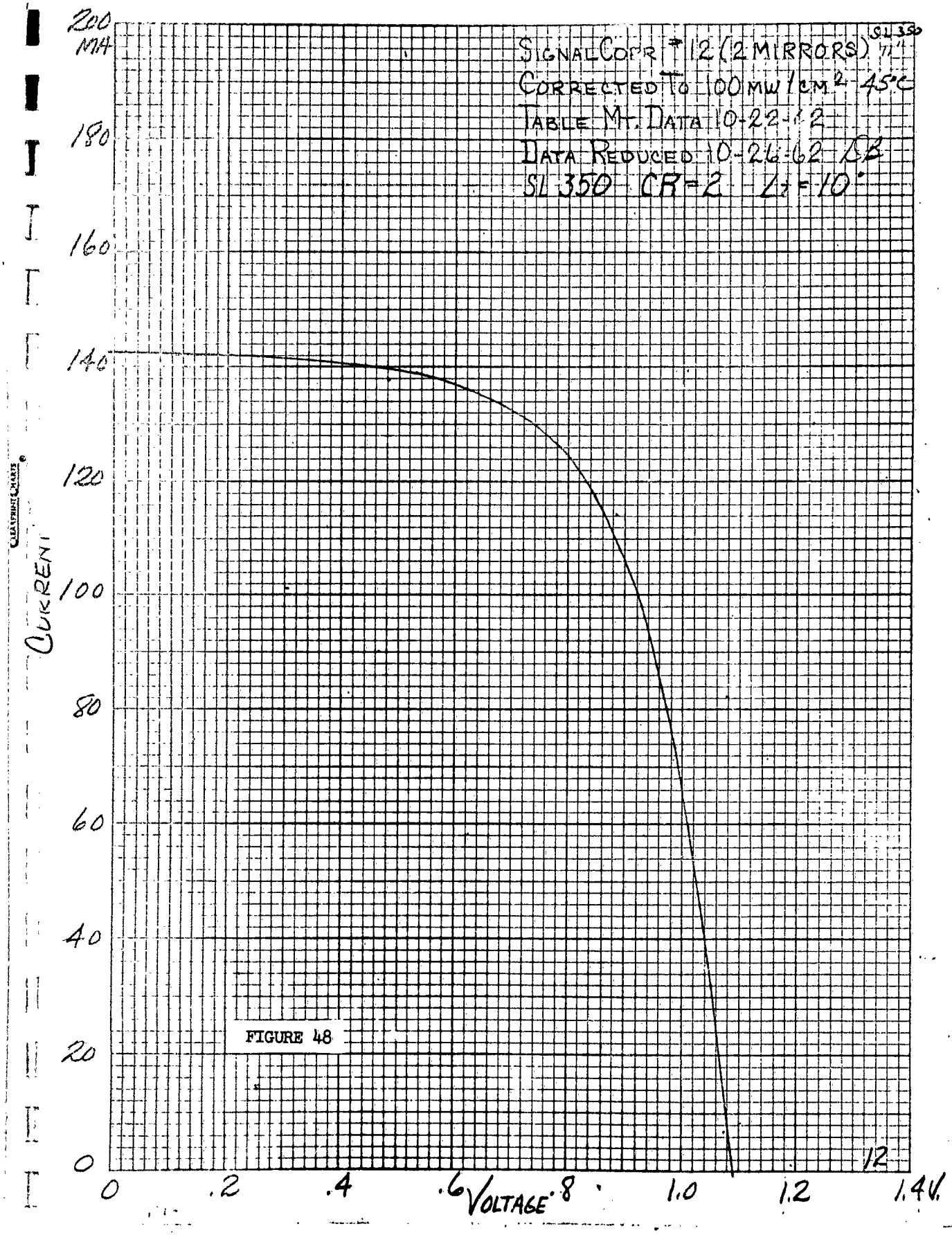

SL350
Signal Corr. 12 (2 Mirrors) 71
Corrected To 100 mw/cm² 45°C
Table Mt. Data 10-22-62
Data Reduced 10-24-62 DB
SL 350 CR-2 Δt = 10°
200 MA
180
160
140
120
100
80
60
40
20
0
Current
0
.2
.4
.6
.8
1.0
1.2
1.4V
Voltage
12

FIGURE 48

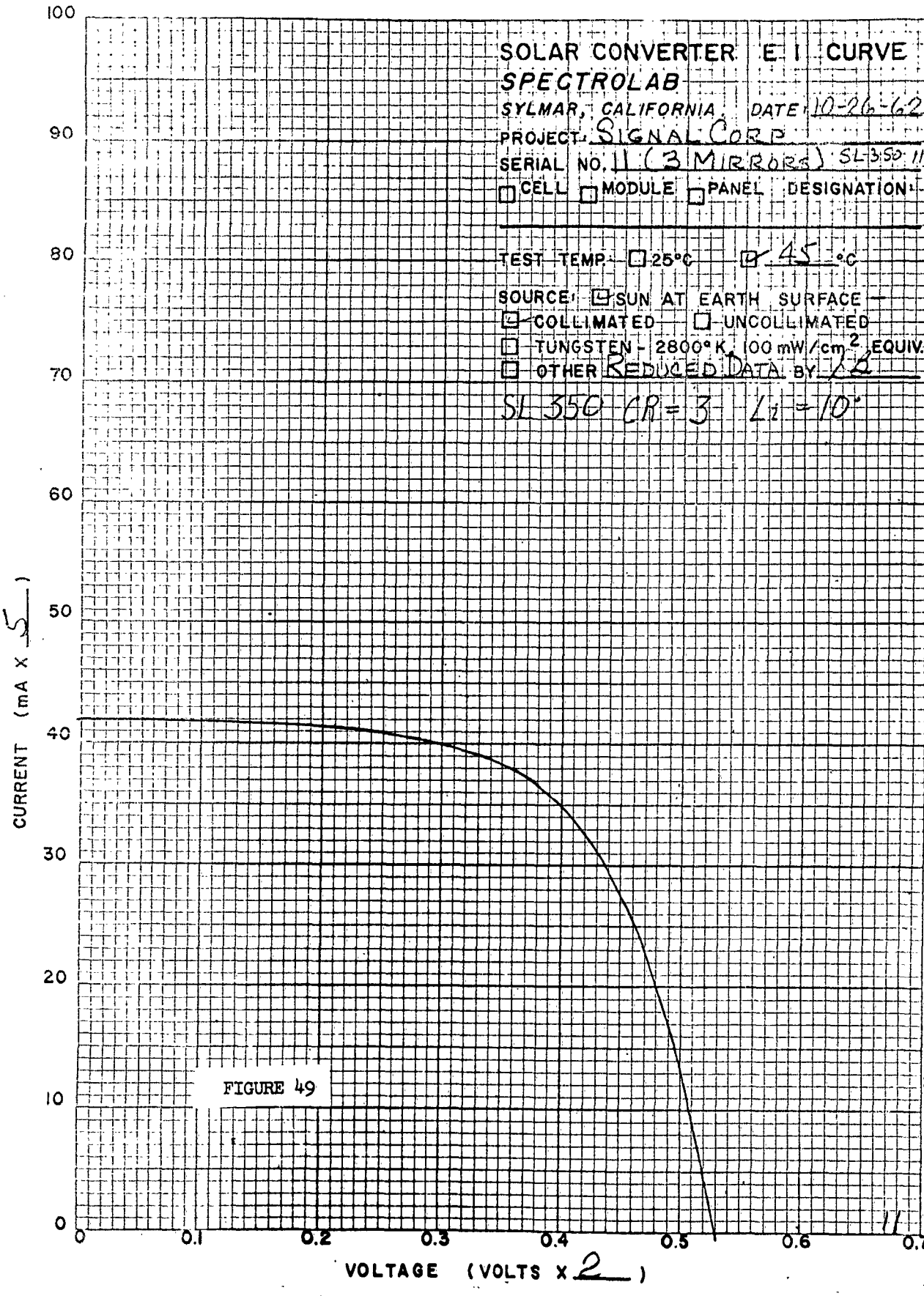

SOLAR CONVERTER E I CURVE
SPECTROLAB
SYLMAR, CALIFORNIA. DATE: 10-26-62
PROJECT: SIGNAL CORP
SERIAL NO. 11 (3 MIRRORS) SL-350 11"
☐ CELL ☐ MODULE ☐ PANEL DESIGNATION:
TEST TEMP: ☐ 25°C ☒ 45 °C
SOURCE: ☒ SUN AT EARTH SURFACE —
☒ COLLIMATED ☐ UNCOLLIMATED
☐ TUNGSTEN - 2800°K, 100 mW/cm² EQUIV.
☐ OTHER REDUCED DATA BY CA
SL 350 CR=3 Li=10"
CURRENT (mA X 5)
VOLTAGE (VOLTS X 2)
100
90
80
70
60
50
40
30
20
10
0
0
0.1
0.2
0.3
0.4
0.5
0.6
0.7
11

FIGURE 49

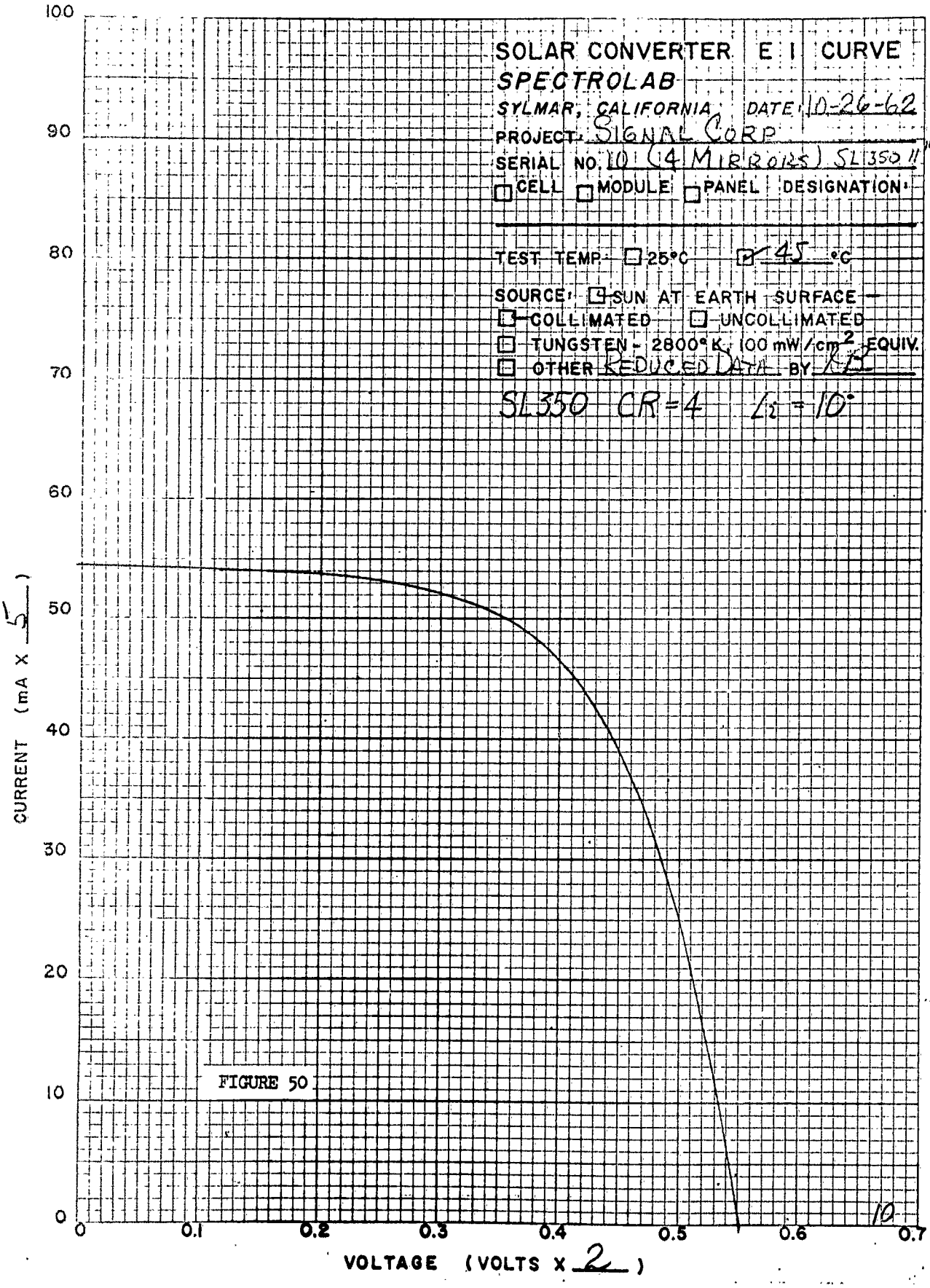

SOLAR CONVERTER E I CURVE
SPECTROLAB
SYLMAR, CALIFORNIA DATE 10-26-62
PROJECT SIGNAL CORP
SERIAL NO. 10 (4 MIRRORS) SL350 II
CELL MODULE PANEL DESIGNATION
TEST TEMP 25°C 45 °C
SOURCE SUN AT EARTH SURFACE
COLLIMATED UNCOLLIMATED
TUNGSTEN - 2800°K, 100 mW/cm² EQUIV.
OTHER REDUCED DATA BY
SL350 CR=4 Δ=10°
CURRENT (mA X 5)
VOLTAGE (VOLTS X 2)
0
10
20
30
40
50
60
70
80
90
100
0.1
0.2
0.3
0.4
0.5
0.6
0.7
10

FIGURE 50

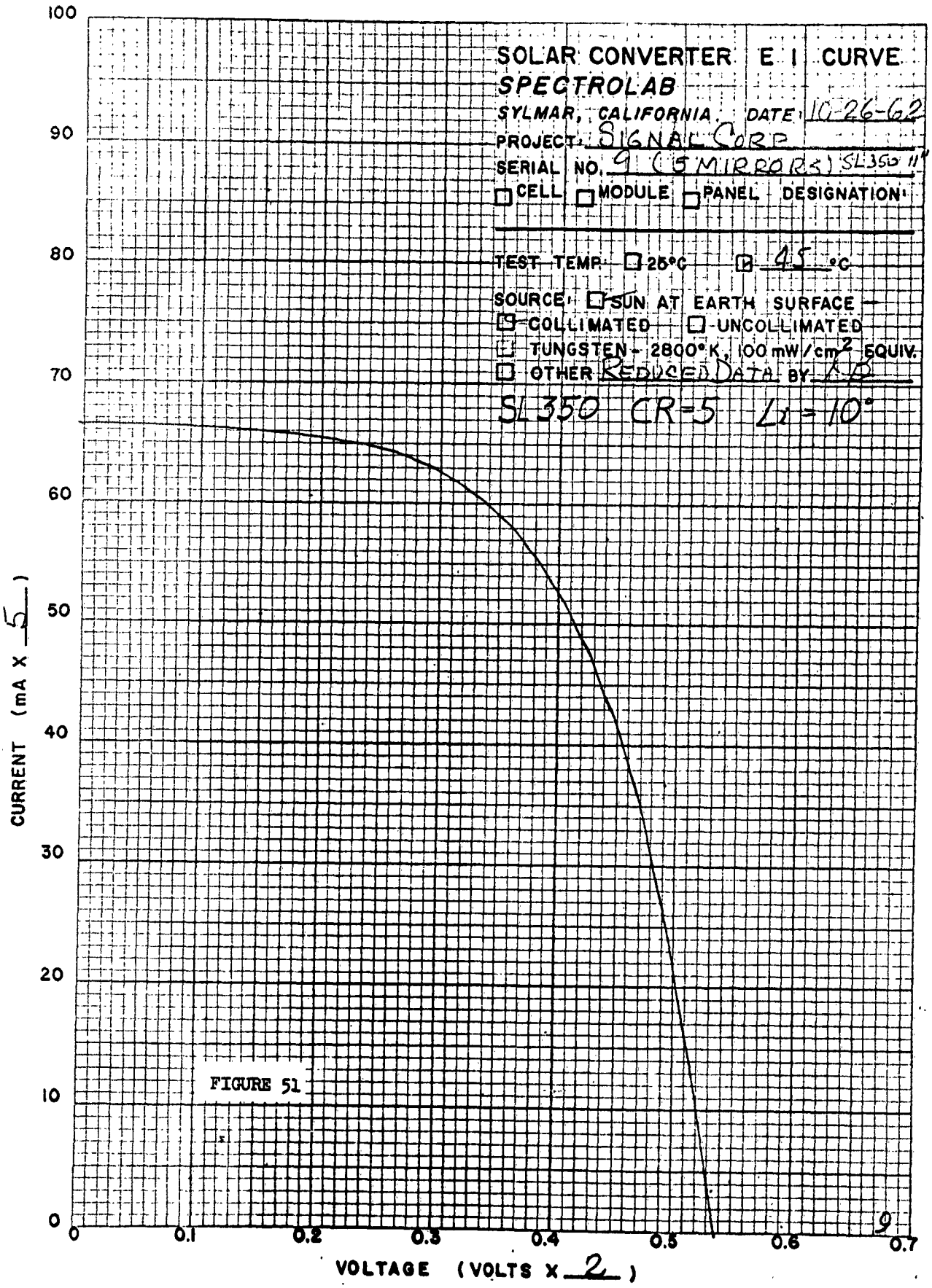
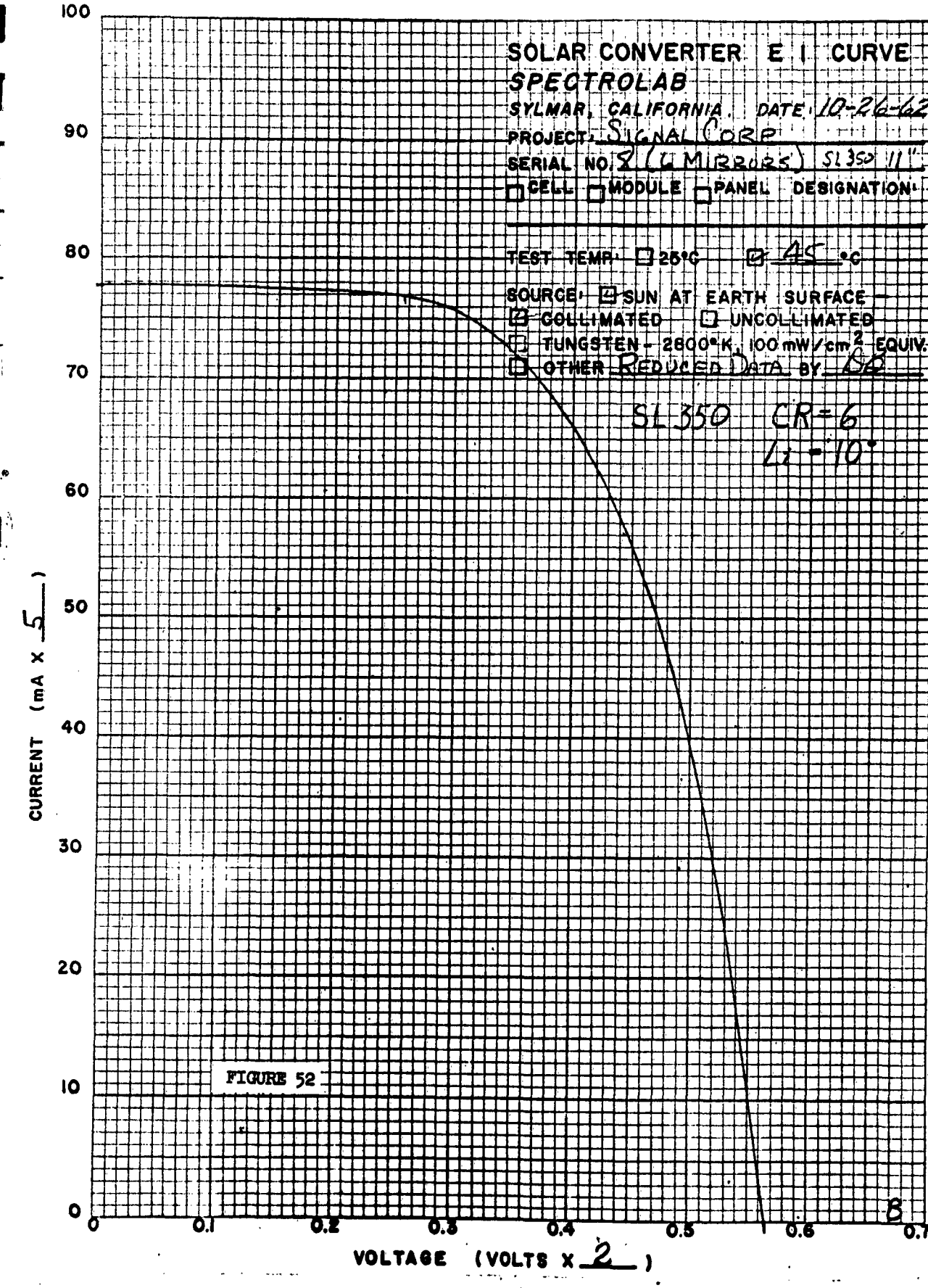

SOLAR CONVERTER E I CURVE
SPECTROLAB
SYLMAR, CALIFORNIA DATE 10-26-62
PROJECT SIGNAL CORP
SERIAL NO. 9 (5 MIRRORS) SL350 II"
CELL MODULE PANEL DESIGNATION
TEST TEMP. 25°C 45 °C
SOURCE: SUN AT EARTH SURFACE
COLLIMATED UNCOLLIMATED
TUNGSTEN - 2800°K, 100 mW/cm² EQUIV.
OTHER REDUCED DATA BY KB
SL350 CR-5 L2 = 10°
CURRENT (mA X 5)
VOLTAGE (VOLTS X 2)
0
10
20
30
40
50
60
70
80
90
100
0.1
0.2
0.3
0.4
0.5
0.6
0.7

FIGURE 51



CLEARPRINT PAPER CO. C-35 10 X 10 DIVISIONS PER INCH. 70 X 100 DIVISIONS. PRINTED IN U.S.A. ON CLEARPRINT TECHNICAL PAPER NO. 1015

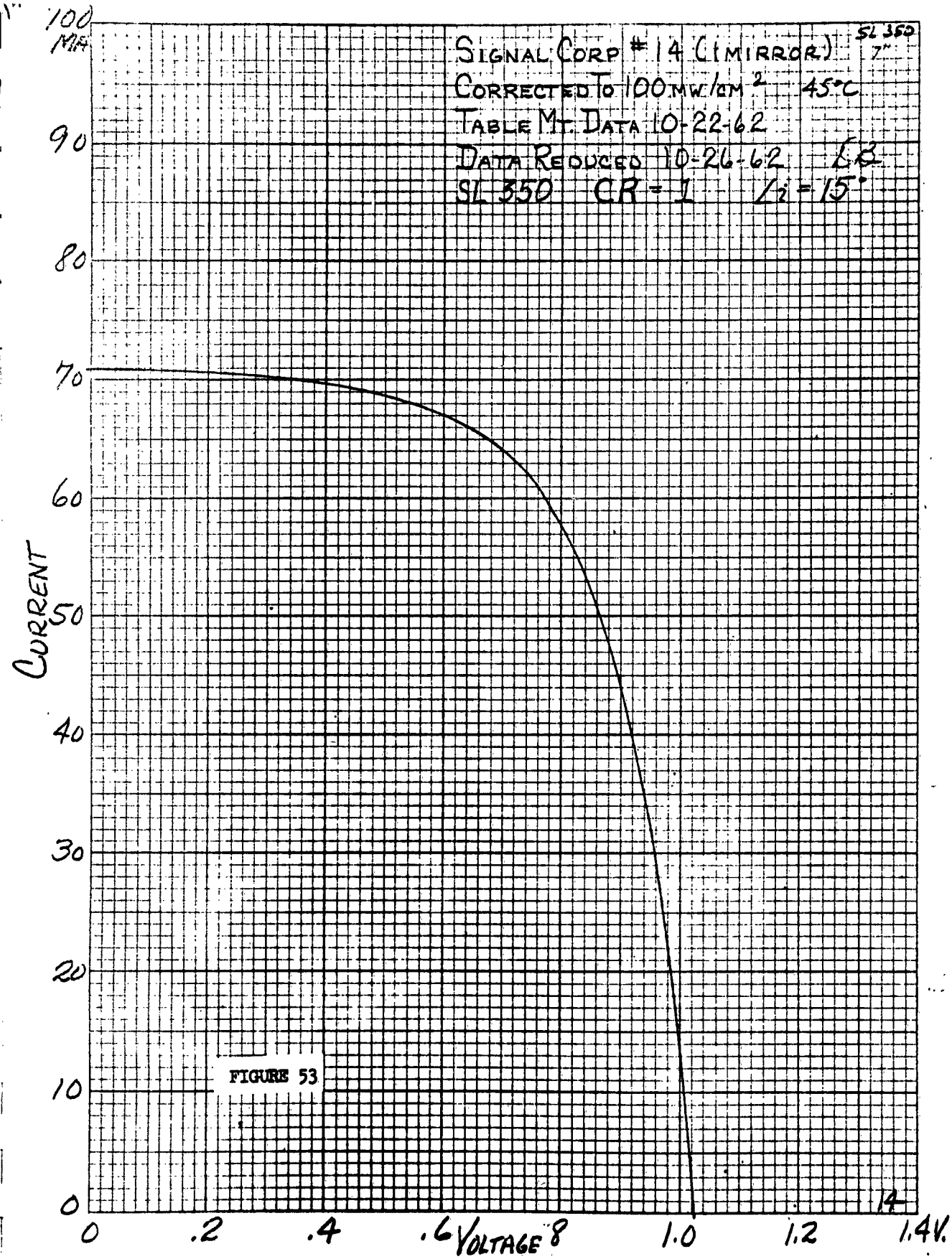


FIGURE 53

PRINTED IN U.S.A. ON CLEARPRINT TECHNICAL PAPER NO. 1015
CLEARPRINT PAPER CO. — 635 10 X 10 DIVISIONS PER INCH 70 X 100 DIVISIONS

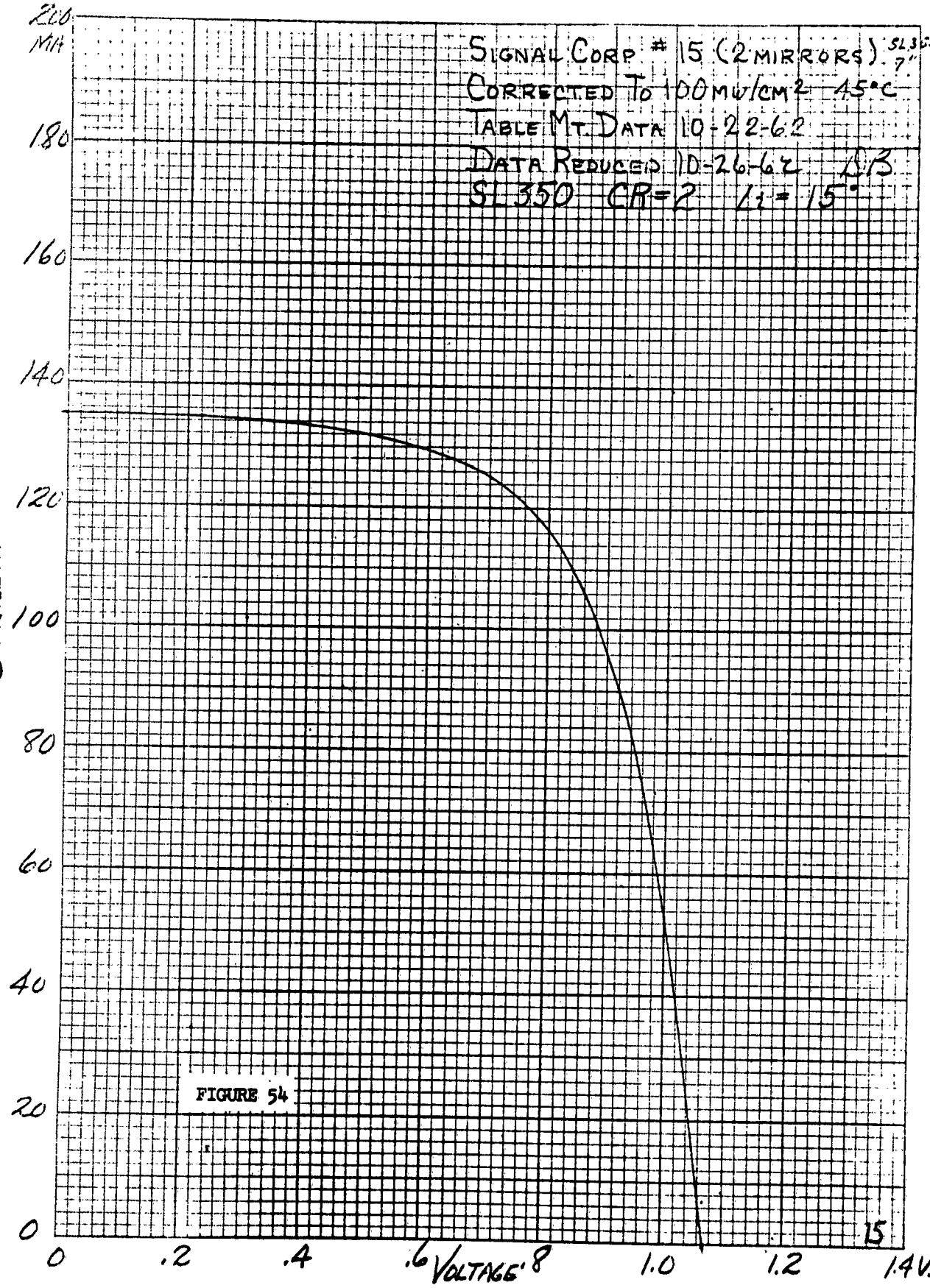

SIGNAL CORP # 15 (2 MIRRORS) SL350 7"
CORRECTED TO 100 MW/CM² 45°C
TABLE MT. DATA 10-22-62
DATA REDUCED 10-26-62 LB
SL 350 CR=2 Li = 15°
200 MA
180
160
140
120
100
80
60
40
20
0
CURRENT
0
.2
.4
.6
.8
1.0
1.2
1.4V.
VOLTAGE
15

FIGURE 54

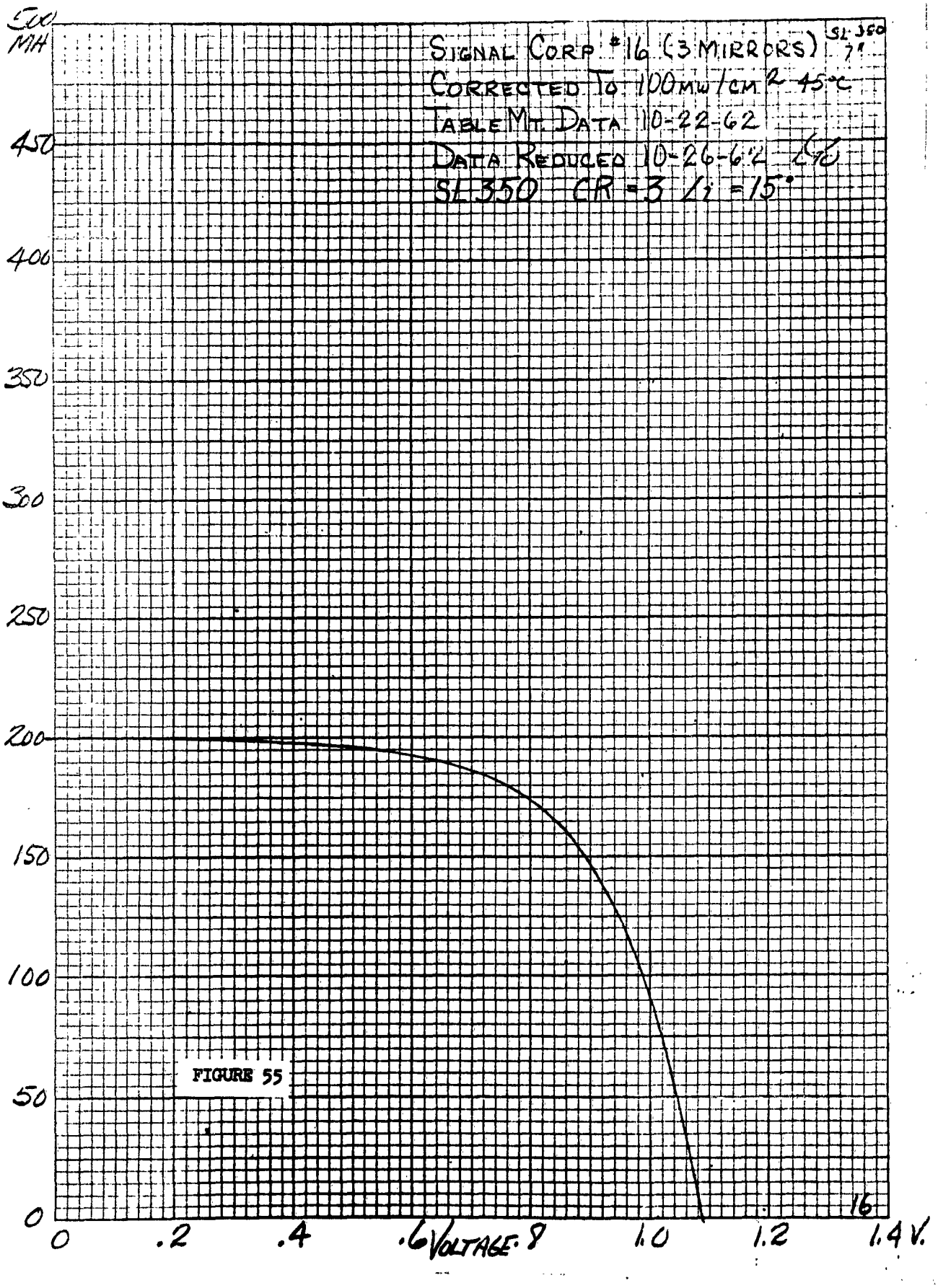


FIGURE 55

PRINTED IN U.S.A. ON CLEARPRINT TECHNICAL PAPER NO. 1015
CLEARPRINT PAPER CO C35 10 X 10 DIVISIONS PER INCH. 70 X 100 DIVISIONS.

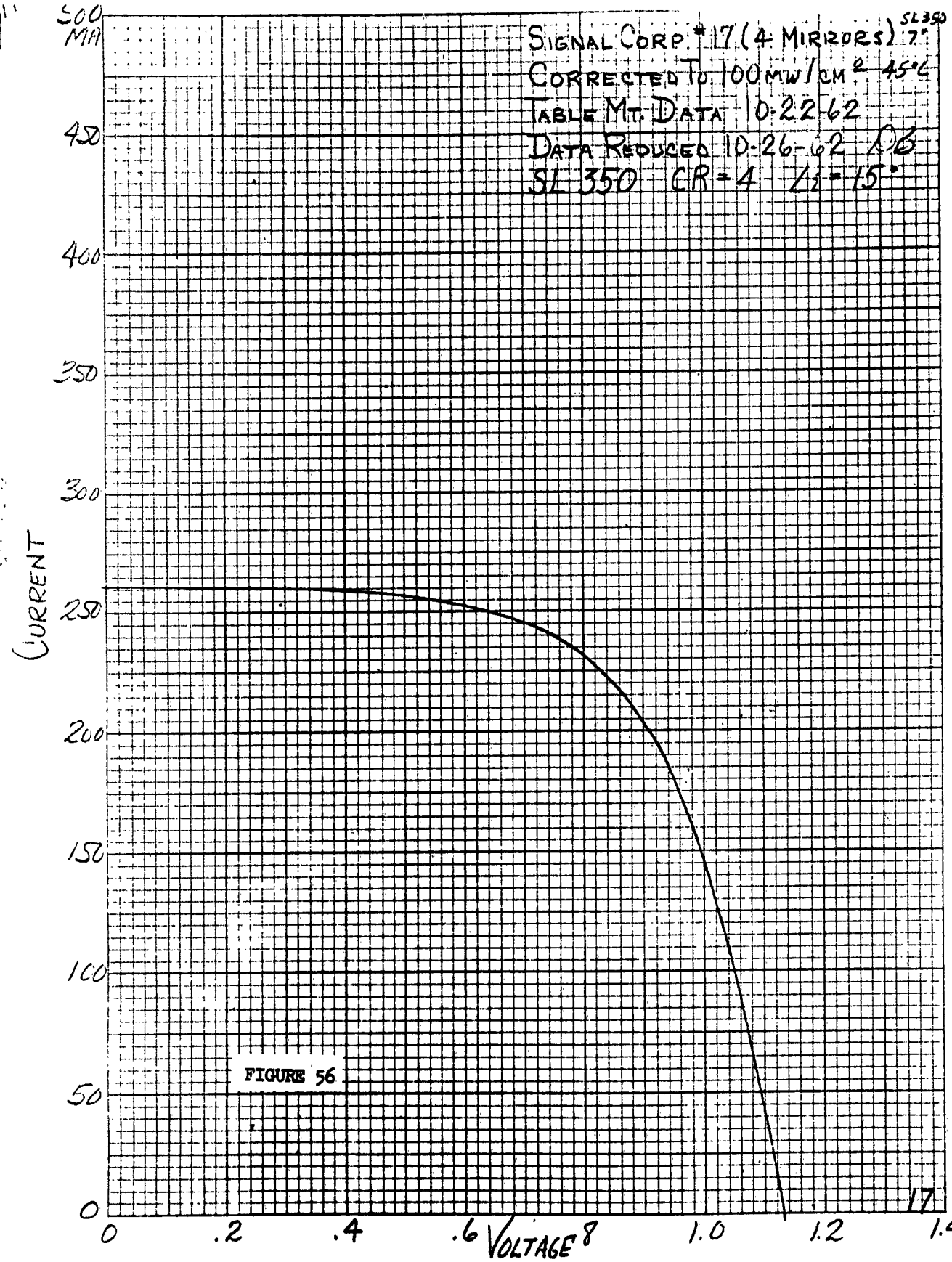

SL350
SIGNAL CORP. #17 (4 MIRRORS) 7"
CORRECTED TO 100 MW/CM² 45°C
TABLE MT. DATA 10-22-62
DATA REDUCED 10-26-62 AB
SL 350 CR=4 ½=15°
500 MA
450
400
350
300
250
200
150
100
50
0
CURRENT
0
.2
.4
.6
.8
1.0
1.2
1.4
VOLTAGE
17

FIGURE 56

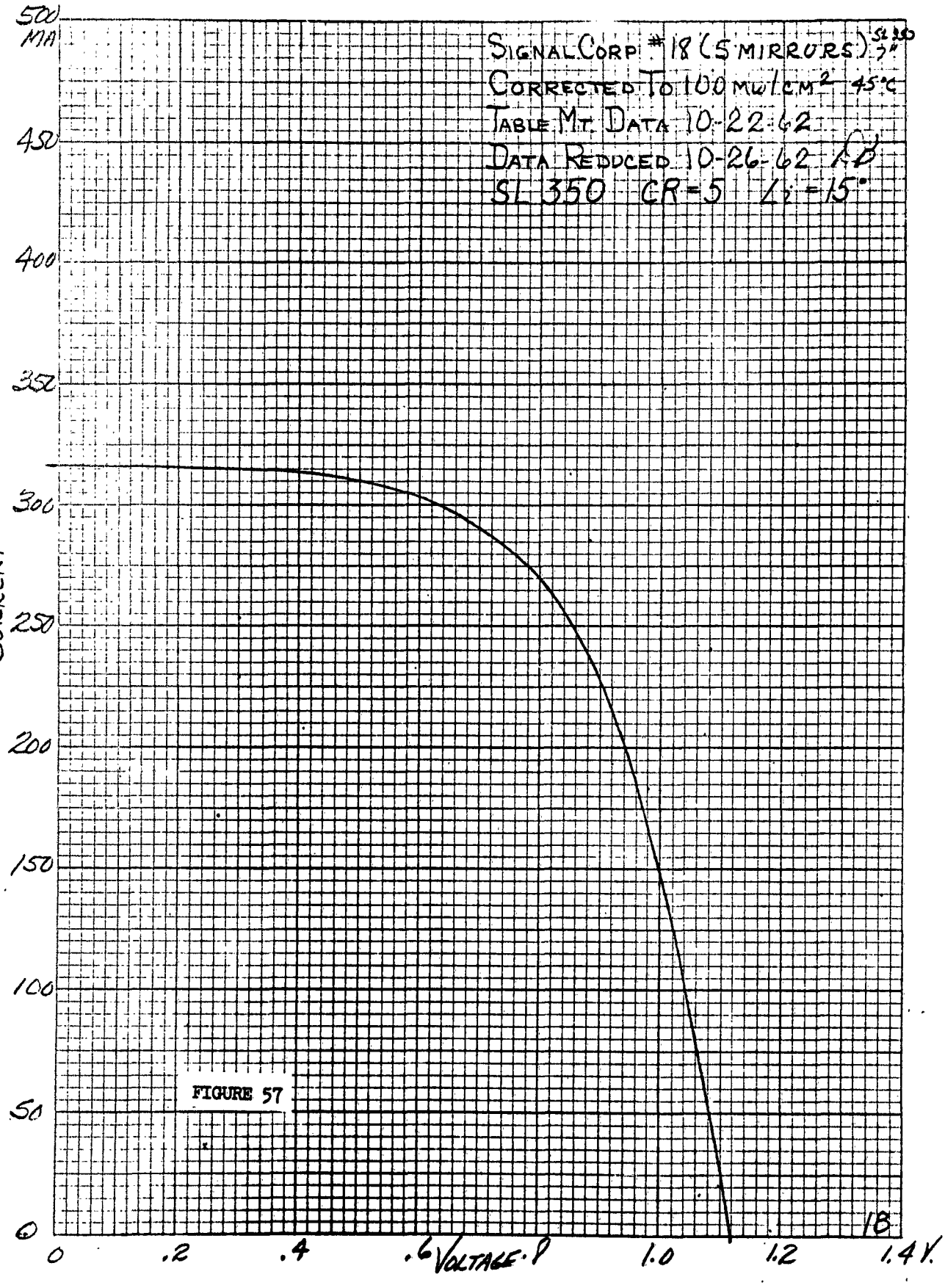


FIGURE 57

CLEARPRINT PAPER CO. PRINTED IN U.S.A. ON CLEARPRINT TECHNICAL PAPER NO. 10

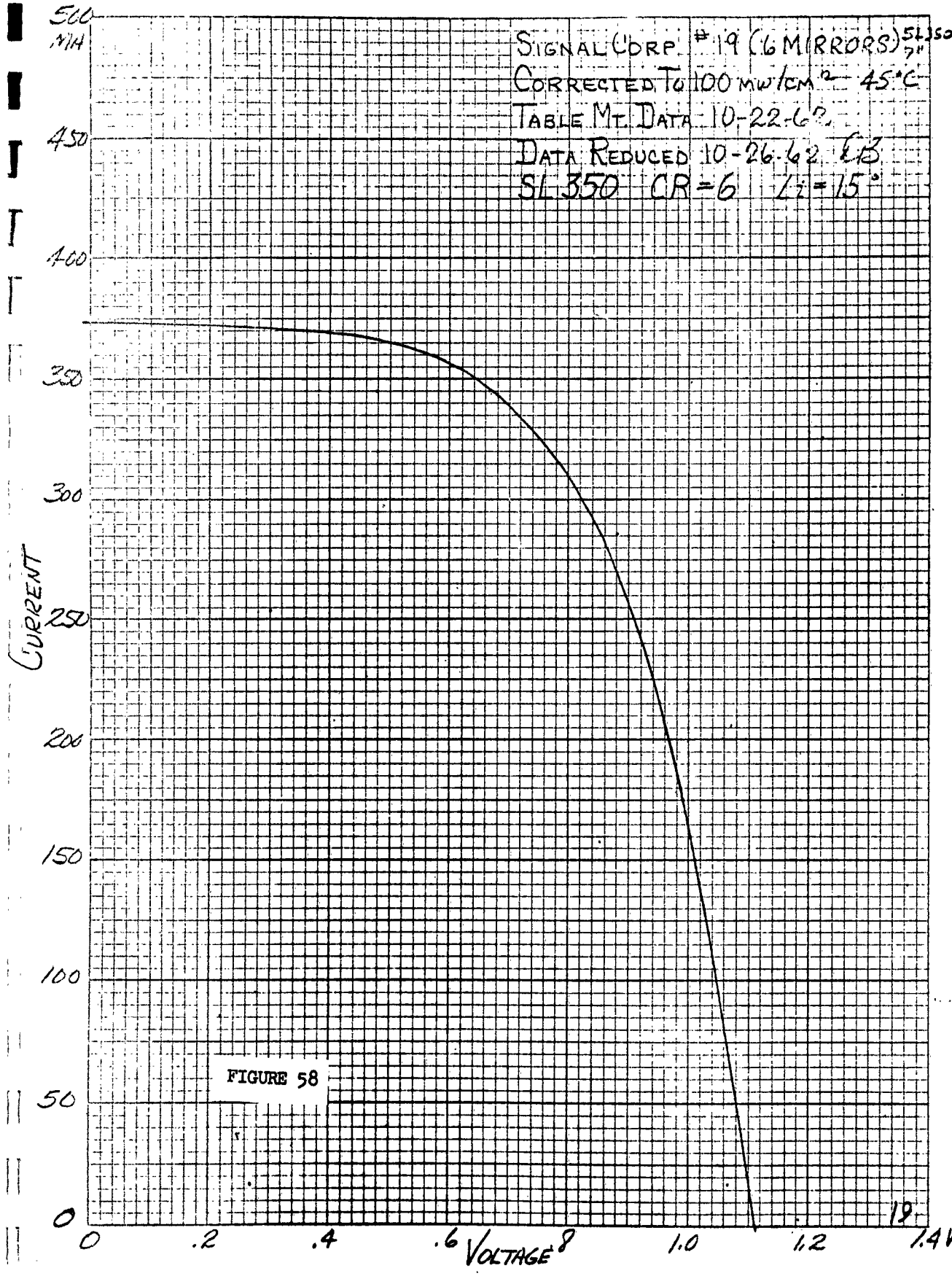

SIGNAL CORP. #19 (6 MIRRORS) SL350 7"
CORRECTED TO 100 mw/cm² — 45°C
TABLE MT. DATA 10-22-62
DATA REDUCED 10-26-62 EB
SL 350 CR=6 Li=15°
500 MA
450
400
350
300
250
200
150
100
50
0
CURRENT
0
.2
.4
.6
.8
1.0
1.2
1.4 V.
VOLTAGE
19

FIGURE 58

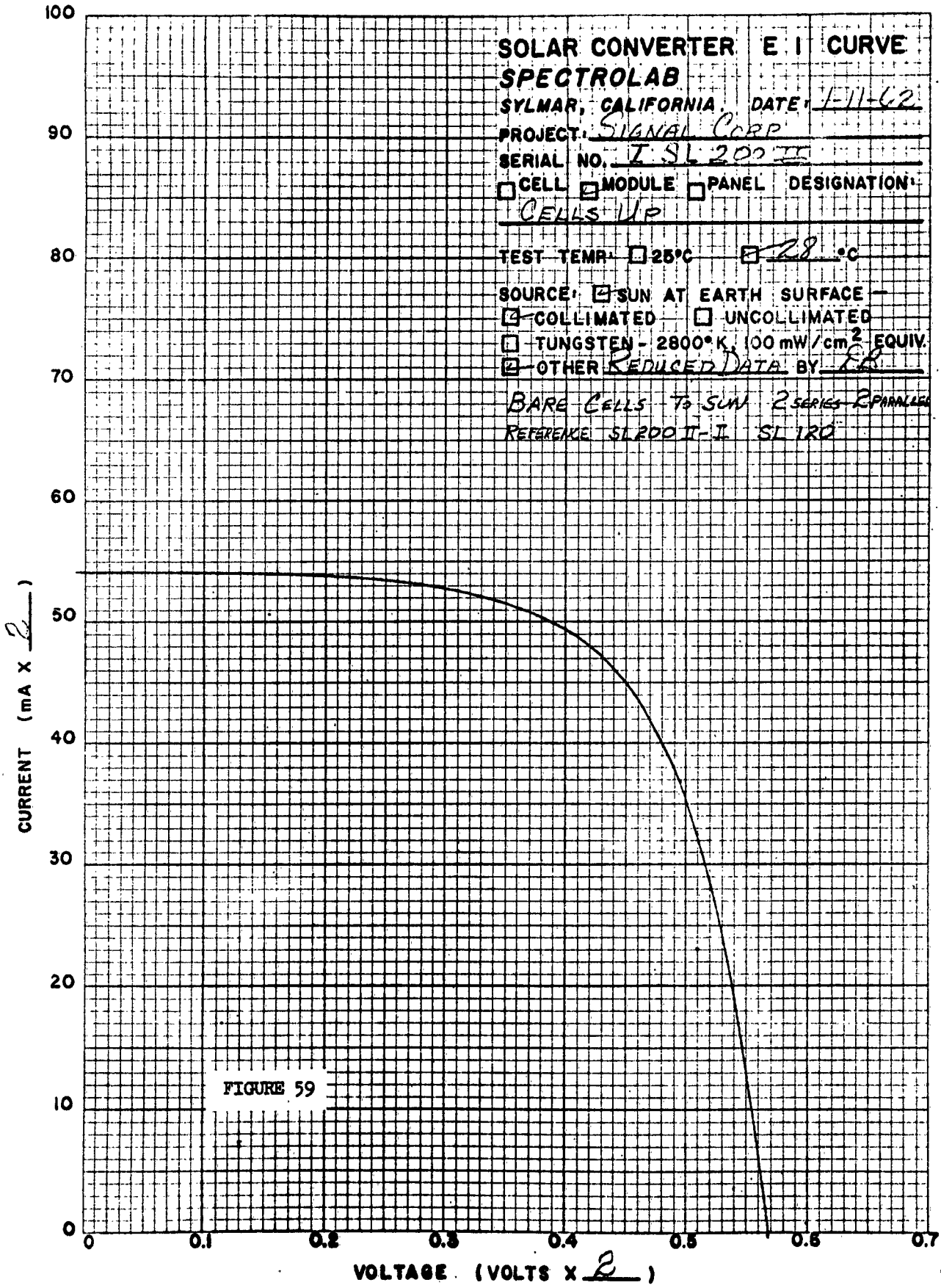

SOLAR CONVERTER E I CURVE
SPECTROLAB
SYLMAR, CALIFORNIA. DATE: 1-11-62
PROJECT: SIGNAL CORP
SERIAL NO. I SL 200 II
☐ CELL ☒ MODULE ☐ PANEL DESIGNATION:
CELLS UP
TEST TEMP: ☐ 25°C ☒ 28 °C
SOURCE: ☒ SUN AT EARTH SURFACE —
☒ COLLIMATED ☐ UNCOLLIMATED
☐ TUNGSTEN - 2800°K, 100 mW/cm² EQUIV.
☒ OTHER REDUCED DATA BY EB
BARE CELLS TO SUN 2 SERIES-2 PARALLEL
REFERENCE SL200 II-I SL 120
CURRENT (mA X 2)
VOLTAGE (VOLTS X 2)
100
90
80
70
60
50
40
30
20
10
0
0
0.1
0.2
0.3
0.4
0.5
0.6
0.7

FIGURE 59

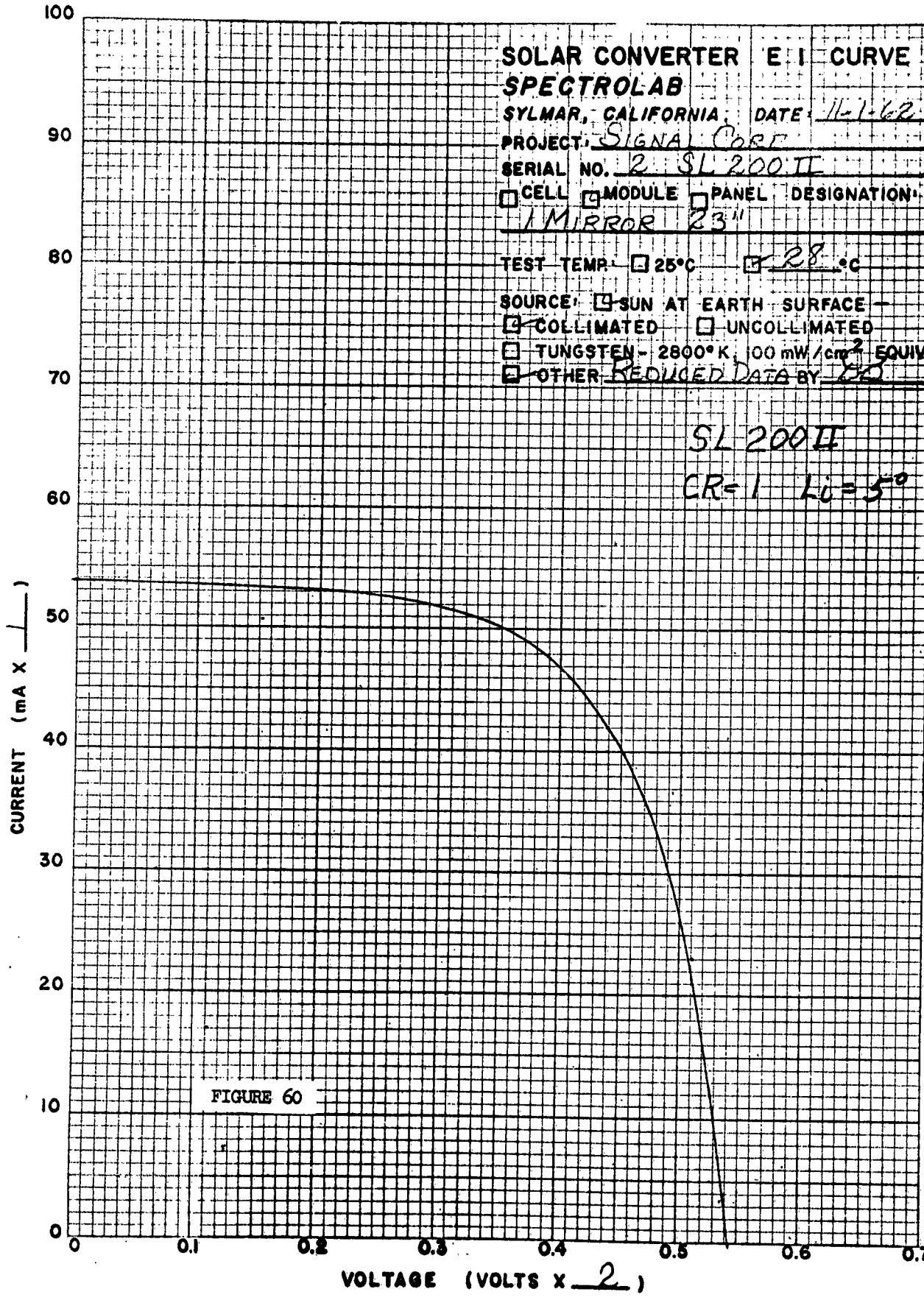

SOLAR CONVERTER E I CURVE
SPECTROLAB
SYLMAR, CALIFORNIA. DATE 11-1-62
PROJECT SIGNAL CORP
SERIAL NO. 2 SL 200 II
CELL MODULE PANEL DESIGNATION
1 MIRROR 23"
TEST TEMP 25°C 28 °C
SOURCE: SUN AT EARTH SURFACE
COLLIMATED UNCOLLIMATED
TUNGSTEN - 2800° K, 100 mW/cm² EQUIV.
OTHER REDUCED DATA BY
SL 200 II
CR=1 Li=5°
CURRENT (mA X 1)
VOLTAGE (VOLTS X 2)
0
10
20
30
40
50
60
70
80
90
100
0
0.1
0.2
0.3
0.4
0.5
0.6
0.7

FIGURE 60

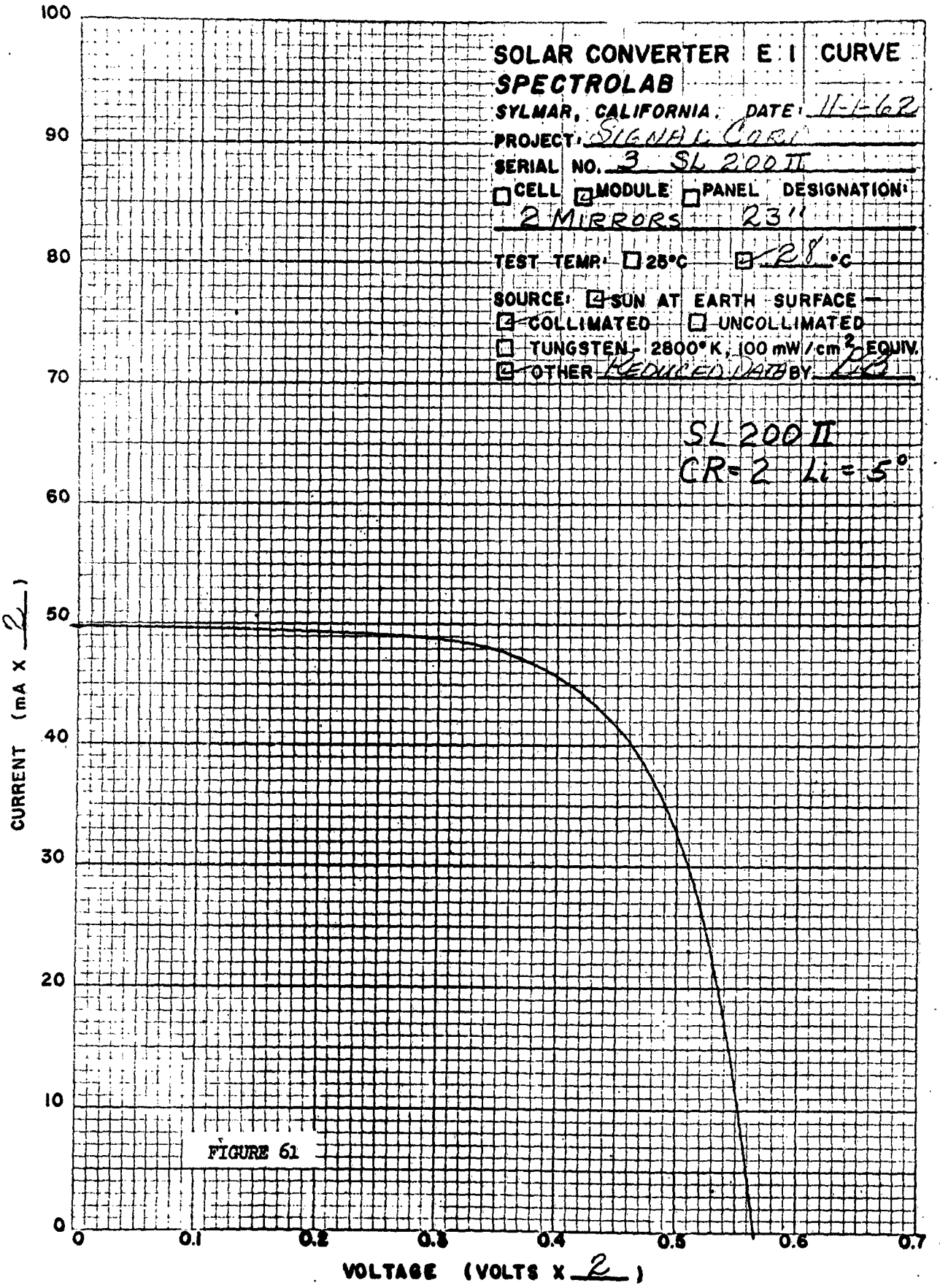

SOLAR CONVERTER E I CURVE
SPECTROLAB
SYLMAR, CALIFORNIA. DATE: 11-1-62
PROJECT: SIGNAL CORP
SERIAL NO. 3 SL 200 II
☐ CELL ☒ MODULE ☐ PANEL DESIGNATION:
2 MIRRORS 23"
TEST TEMP: ☐ 25°C ☒ 28 °C
SOURCE: ☒ SUN AT EARTH SURFACE —
☒ COLLIMATED ☐ UNCOLLIMATED
☐ TUNGSTEN - 2800°K, 100 mW/cm² EQUIV.
☒ OTHER REDUCED DATA BY
SL 200 II
CR=2 Li=5°
CURRENT (mA X 2)
VOLTAGE (VOLTS X 2)
100
90
80
70
60
50
40
30
20
10
0
0
0.1
0.2
0.3
0.4
0.5
0.6
0.7

FIGURE 61

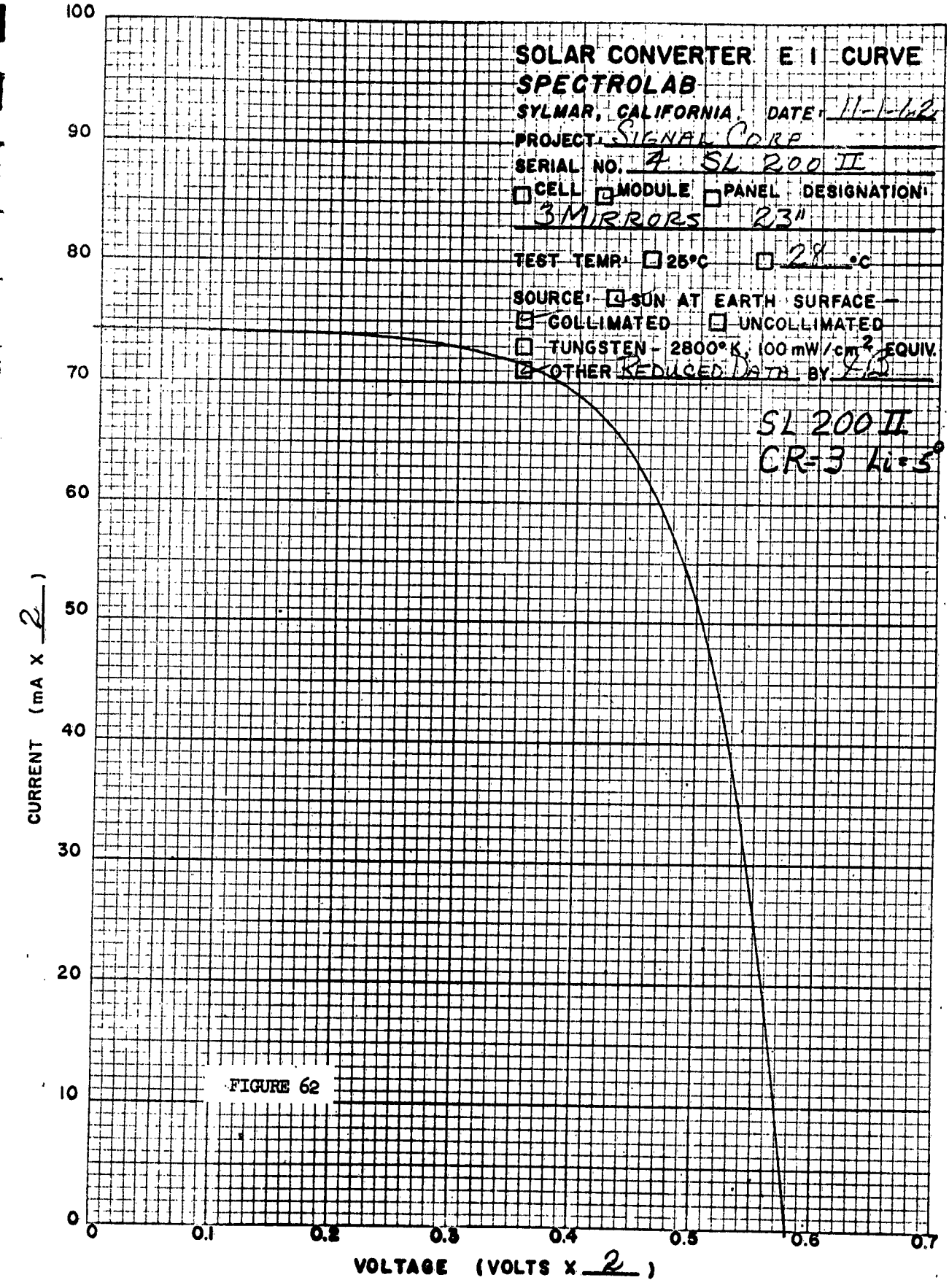

SOLAR CONVERTER E I CURVE
SPECTROLAB
SYLMAR, CALIFORNIA. DATE: 11-1-62
PROJECT: SIGNAL CORP
SERIAL NO. 4 SL 200 II
☐ CELL ☒ MODULE ☐ PANEL DESIGNATION:
3 MIRRORS 23"
TEST TEMP: ☐ 25°C ☐ 28 °C
SOURCE: ☒ SUN AT EARTH SURFACE —
☒ COLLIMATED ☐ UNCOLLIMATED
☐ TUNGSTEN - 2800°K, 100 mW/cm² EQUIV.
☒ OTHER REDUCED DATA BY: LB
SL 200 II
CR=3 Li=5°
CURRENT (mA X 2)
VOLTAGE (VOLTS X 2)
100
90
80
70
60
50
40
30
20
10
0
0
0.1
0.2
0.3
0.4
0.5
0.6
0.7

FIGURE 62

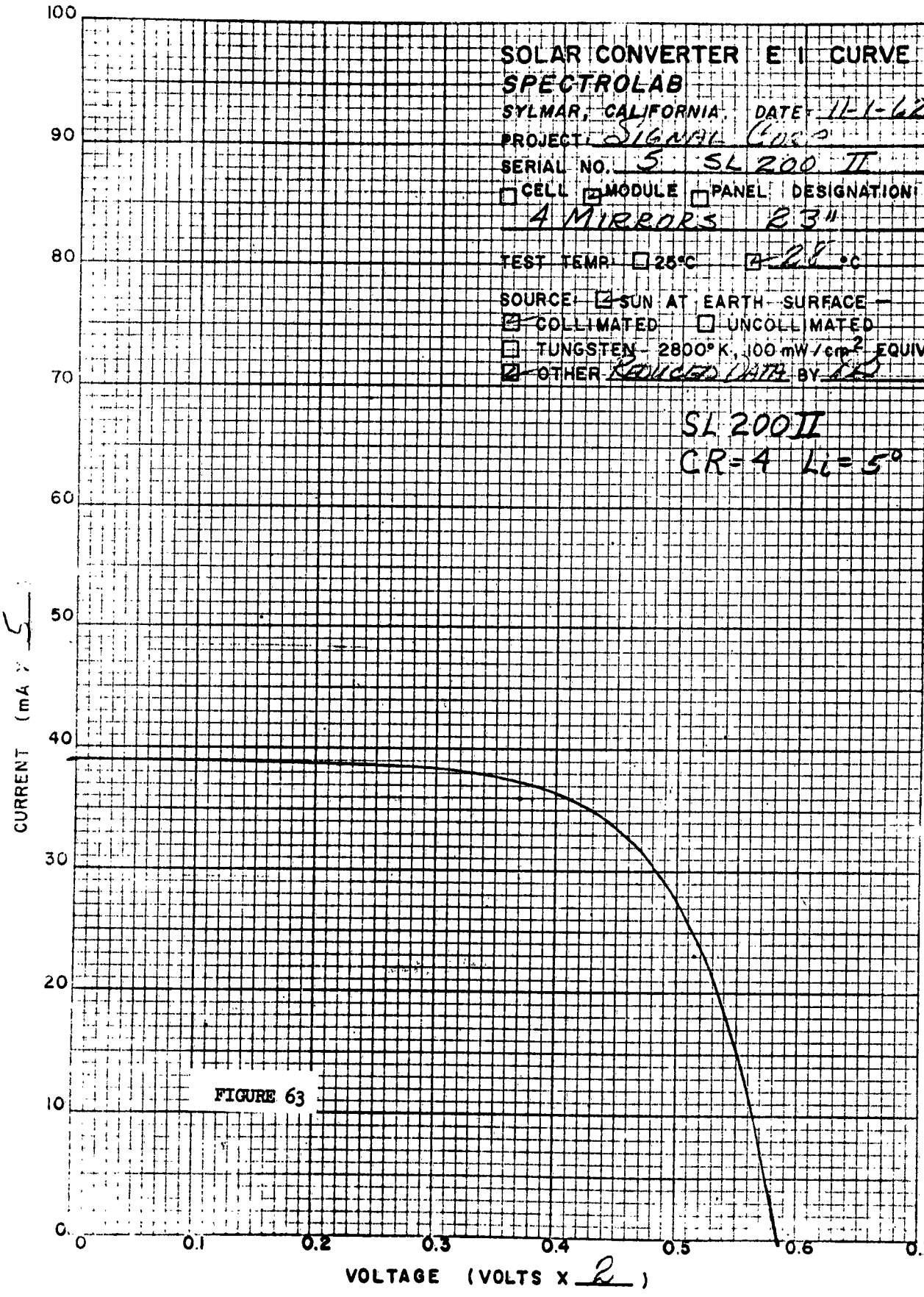

SOLAR CONVERTER E I CURVE
SPECTROLAB
SYLMAR, CALIFORNIA. DATE 11-1-62
PROJECT: SIGNAL CORPS
SERIAL NO. 5 SL 200 II
☐ CELL ☒ MODULE ☐ PANEL DESIGNATION:
4 MIRRORS 23"
TEST TEMP: ☐ 25°C ☒ 28 °C
SOURCE: ☒ SUN AT EARTH SURFACE —
☒ COLLIMATED ☐ UNCOLLIMATED
☐ TUNGSTEN - 2800° K, 100 mW/cm² EQUIV
☒ OTHER SOURCED DATA BY LES
SL 200 II
CR=4 Li=5°
CURRENT (mA X 5)
VOLTAGE (VOLTS X 2)
0
10
20
30
40
50
60
70
80
90
100
0
0.1
0.2
0.3
0.4
0.5
0.6
0.7

FIGURE 63

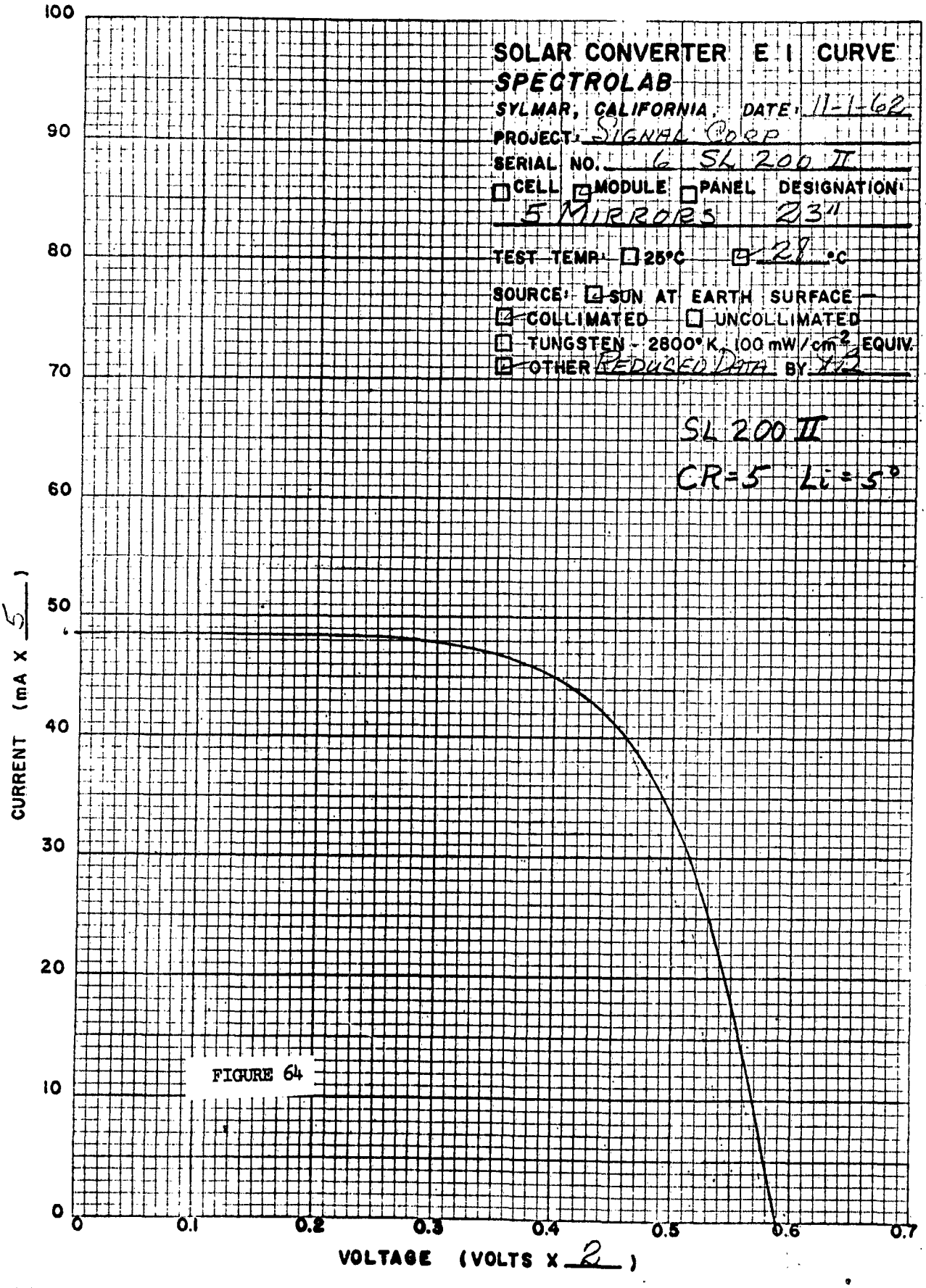

SOLAR CONVERTER E I CURVE
SPECTROLAB
SYLMAR, CALIFORNIA. DATE: 11-1-62
PROJECT: SIGNAL CORP
SERIAL NO. 6 SL 200 II
CELL MODULE PANEL DESIGNATION:
5 MIRRORS 23"
TEST TEMP: 25°C 21 °C
SOURCE: SUN AT EARTH SURFACE
COLLIMATED UNCOLLIMATED
TUNGSTEN - 2800° K, 100 mW/cm² EQUIV.
OTHER REDUCED DATA BY R.L.
SL 200 II
CR=5 Li=5°
CURRENT (mA X 5)
VOLTAGE (VOLTS X 2)
100
90
80
70
60
50
40
30
20
10
0
0
0.1
0.2
0.3
0.4
0.5
0.6
0.7

FIGURE 64

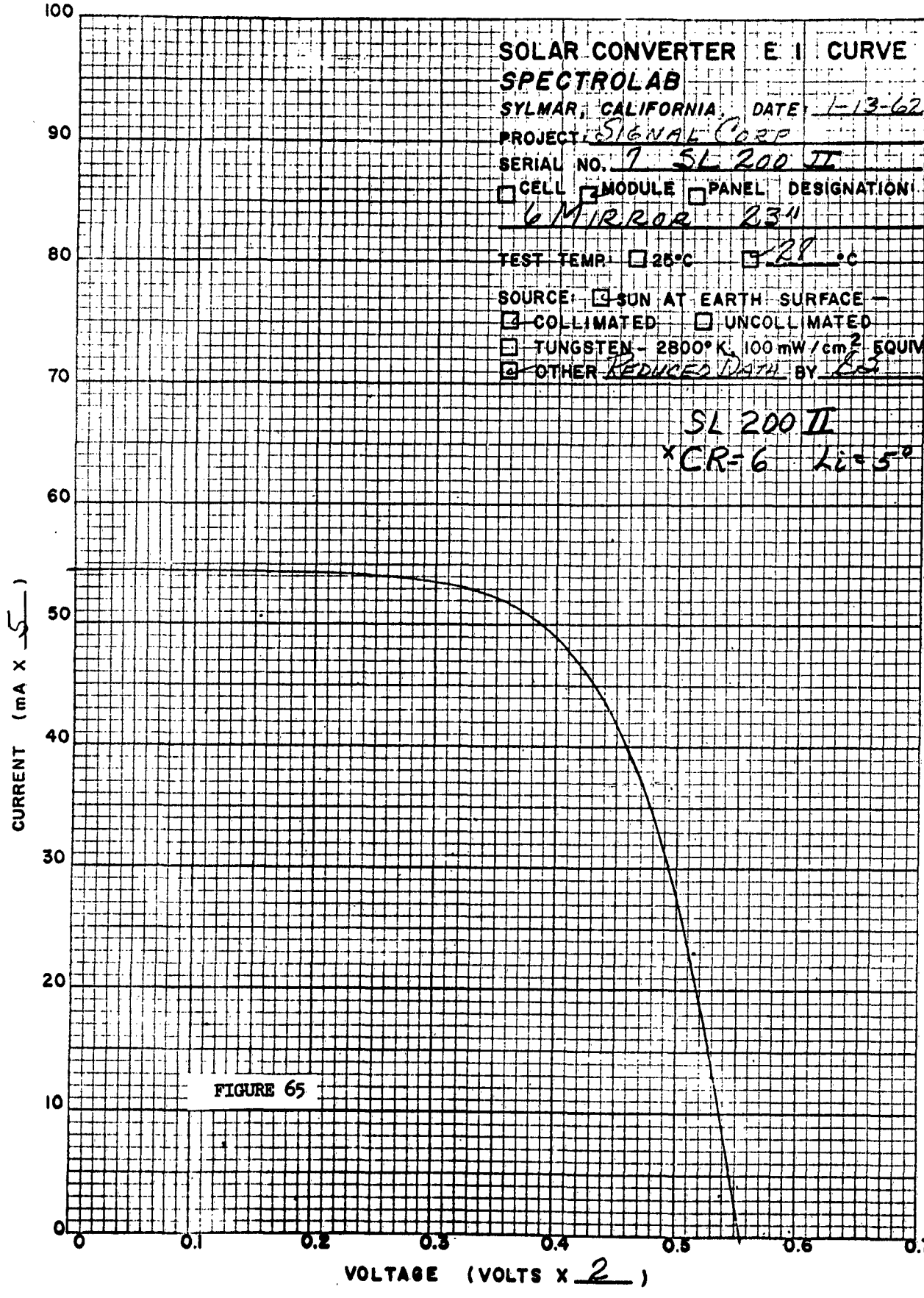

SOLAR CONVERTER E I CURVE
SPECTROLAB
SYLMAR, CALIFORNIA DATE: 1-13-62
PROJECT: SIGNAL CORP
SERIAL NO. 7 SL 200 II
CELL MODULE PANEL DESIGNATION
6 MIRROR 231
TEST TEMP: 25°C 28 °C
SOURCE: SUN AT EARTH SURFACE —
COLLIMATED UNCOLLIMATED
TUNGSTEN - 2800° K, 100 mW/cm² EQUIV
OTHER REDUCED PATH BY 8.3
SL 200 II
×CR=6 Li=5°
CURRENT (mA X 5)
VOLTAGE (VOLTS X 2)
0
10
20
30
40
50
60
70
80
90
100
0
0.1
0.2
0.3
0.4
0.5
0.6
0.7

FIGURE 65

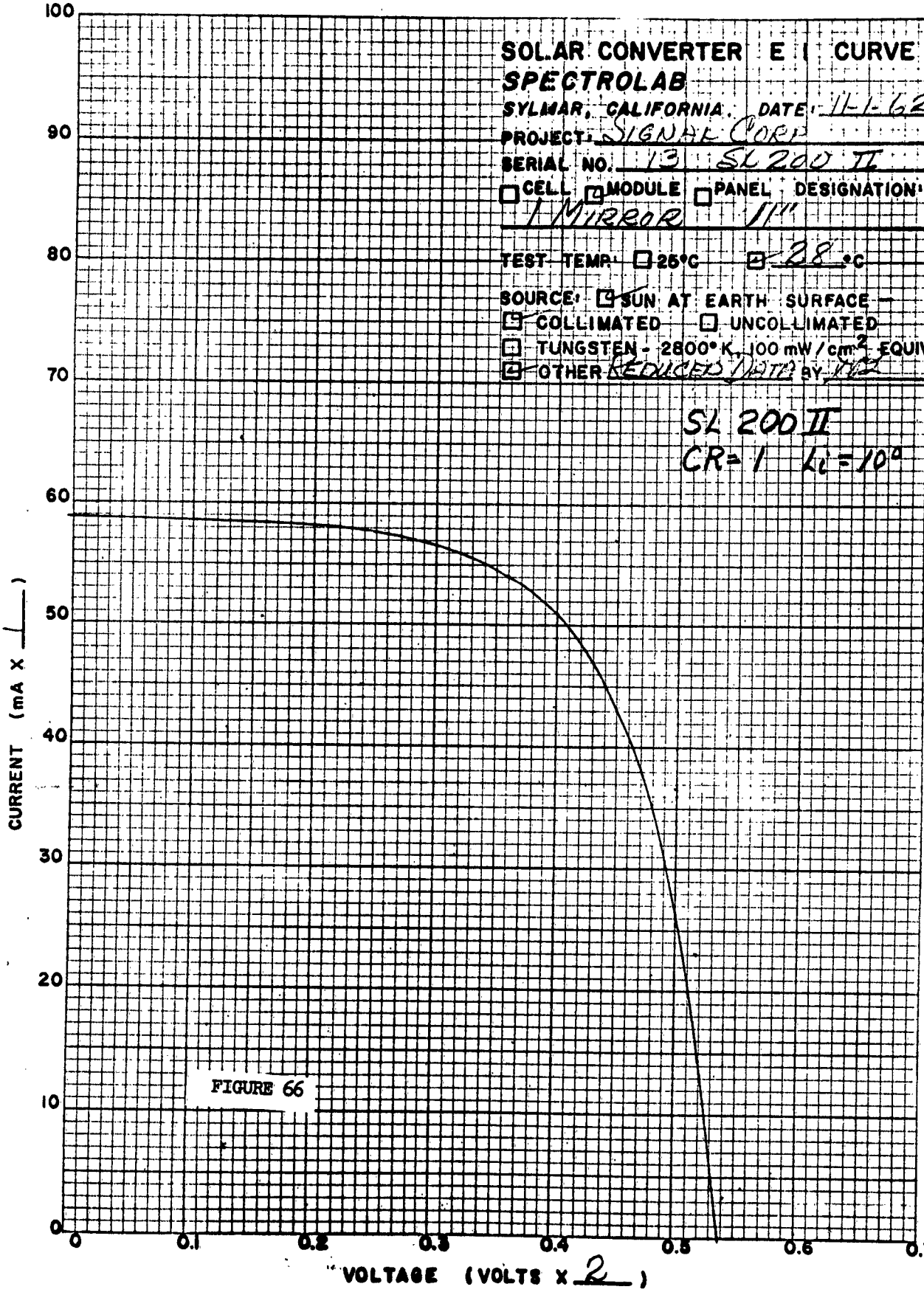

SOLAR CONVERTER E I CURVE
SPECTROLAB
SYLMAR, CALIFORNIA. DATE: 11-1-62
PROJECT: SIGNAL CORPS
SERIAL NO. 13 SL 200 II
CELL MODULE PANEL DESIGNATION:
1 MIRROR III
TEST TEMP: 25°C 28 °C
SOURCE: SUN AT EARTH SURFACE
COLLIMATED UNCOLLIMATED
TUNGSTEN - 2800° K, 100 mW/cm² EQUIV.
OTHER REDUCED DATA BY TRW
SL 200 II
CR=1 Li=10°
CURRENT (mA X 1)
VOLTAGE (VOLTS X 2)
0
10
20
30
40
50
60
70
80
90
100
0
0.1
0.2
0.3
0.4
0.5
0.6
0.7

FIGURE 66

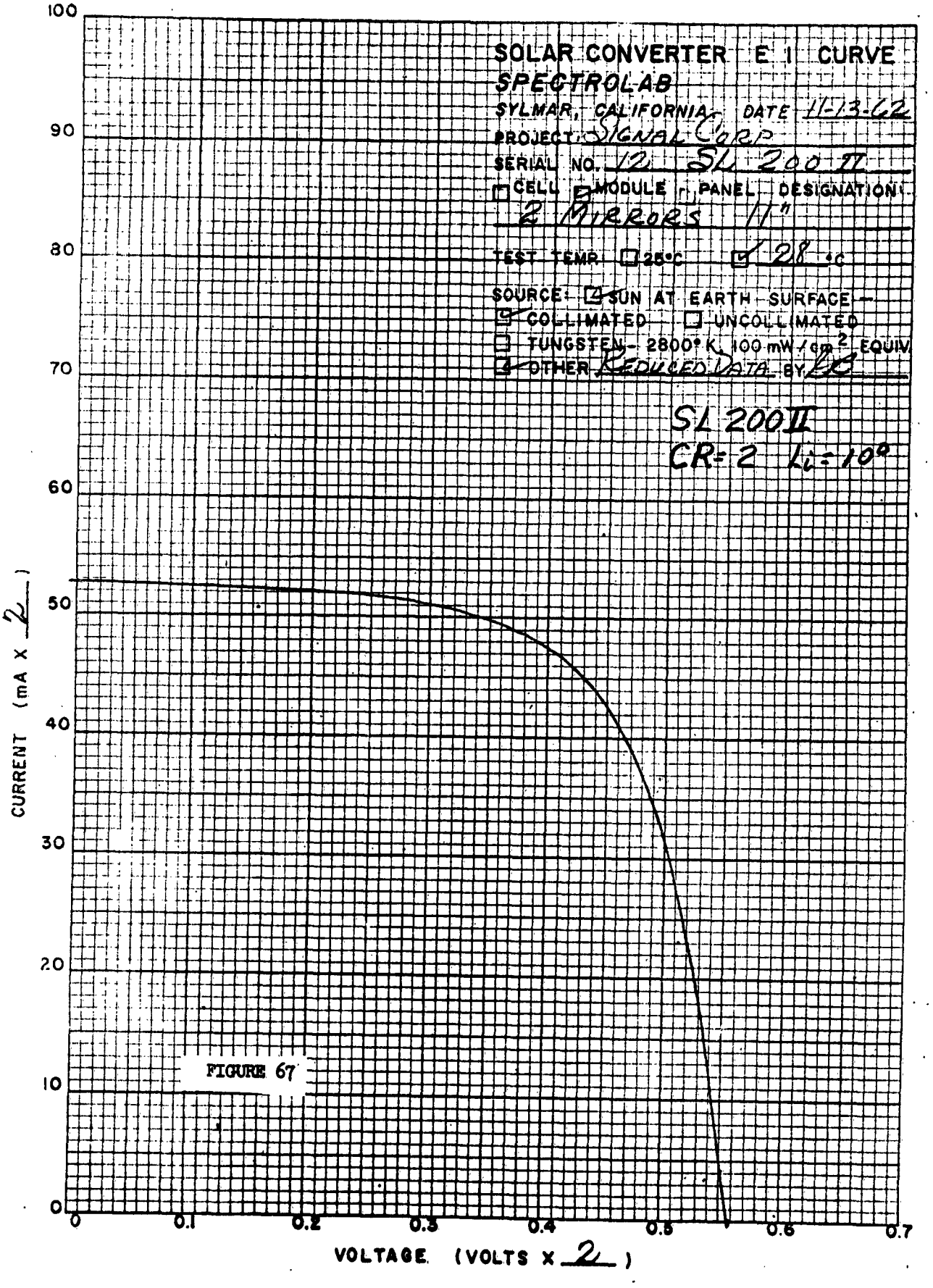

SOLAR CONVERTER E I CURVE
SPECTROLAB
SYLMAR, CALIFORNIA DATE 11-13-62
PROJECT SIGNAL CORP
SERIAL NO. 12 SL 200 II
☐ CELL ☑ MODULE ☐ PANEL DESIGNATION
2 MIRRORS 11"
TEST TEMP. ☐ 25°C ☑ 28 °C
SOURCE: ☑ SUN AT EARTH SURFACE —
☑ COLLIMATED ☐ UNCOLLIMATED
☐ TUNGSTEN - 2800° K, 100 mW/cm² EQUIV.
☑ OTHER REDUCED DATA BY LC
SL 200II
CR=2 Li=10°
CURRENT (mA x 2)
VOLTAGE (VOLTS x 2)
0
10
20
30
40
50
60
70
80
90
100
0
0.1
0.2
0.3
0.4
0.5
0.6
0.7

FIGURE 67

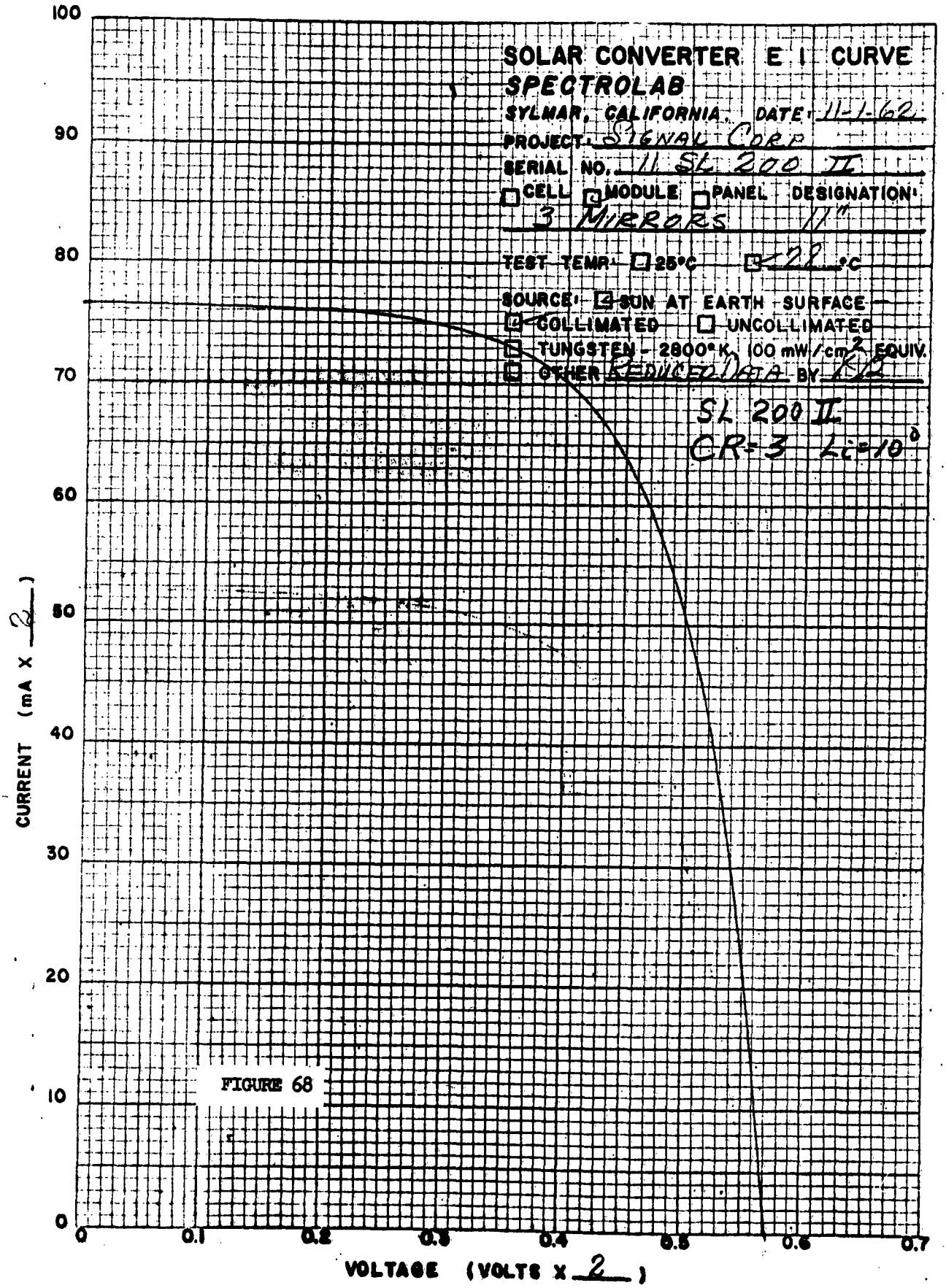

SOLAR CONVERTER E I CURVE
SPECTROLAB
SYLMAR, CALIFORNIA. DATE: 11-1-62
PROJECT: SIGNAL CORP
SERIAL NO. 11 SL 200 II
CELL MODULE PANEL DESIGNATION:
3 MIRRORS 11"
TEST TEMP: 25°C 22 °C
SOURCE: SUN AT EARTH SURFACE
COLLIMATED UNCOLLIMATED
TUNGSTEN - 2800°K, 100 mW/cm² EQUIV.
OTHER REDUCED DATA BY KL
SL 200 II
CR=3 Li=10Δ
CURRENT (mA X 2)
VOLTAGE (VOLTS X 2)
0
10
20
30
40
50
60
70
80
90
100
0
0.1
0.2
0.3
0.4
0.5
0.6
0.7

FIGURE 68

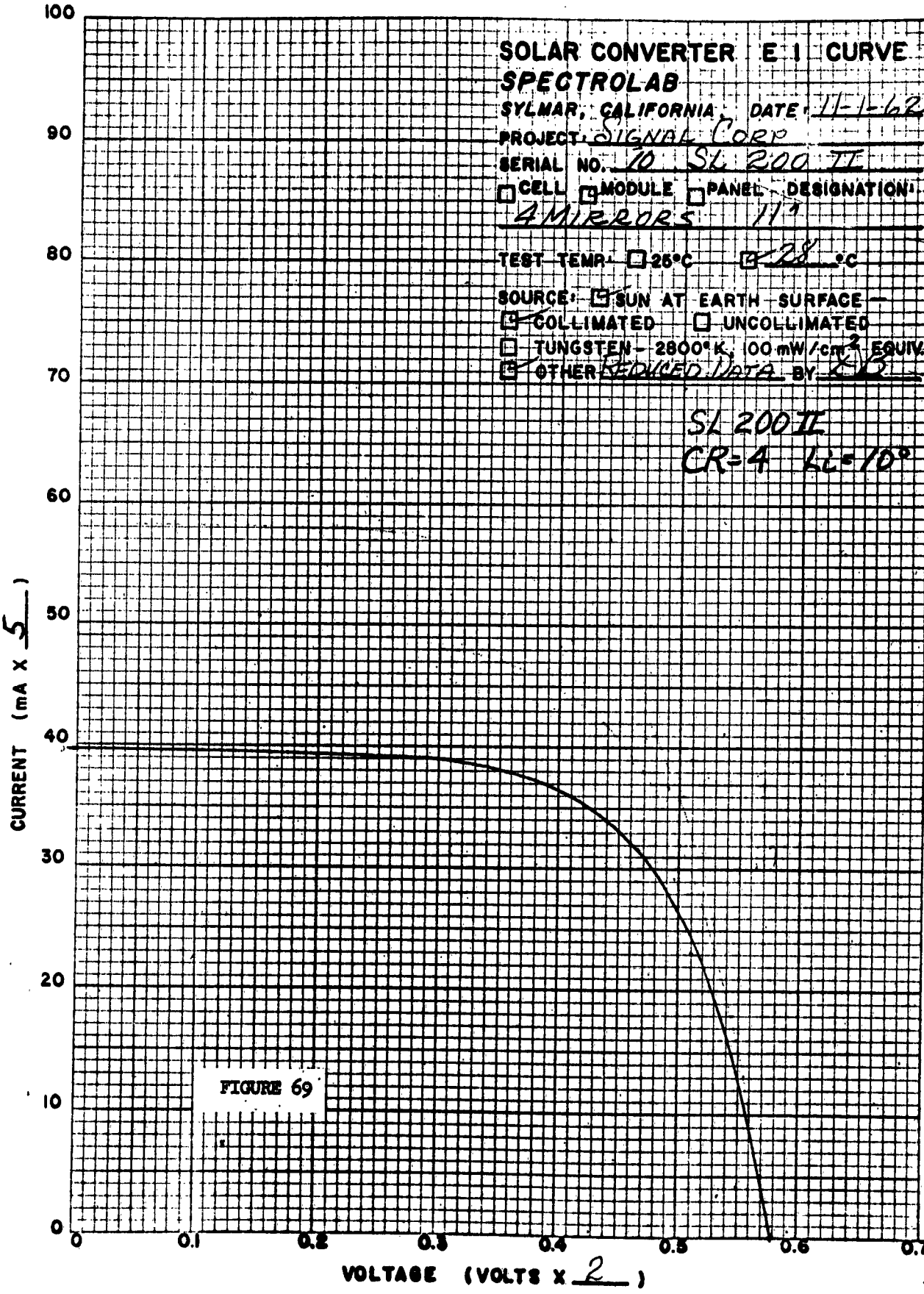

SOLAR CONVERTER E I CURVE
SPECTROLAB
SYLMAR, CALIFORNIA DATE: 11-1-62
PROJECT: SIGNAL CORP
SERIAL NO. 10 SL 200 II
☐ CELL ☒ MODULE ☐ PANEL DESIGNATION:
4 MIRRORS 11"
TEST TEMP: ☐ 25°C ☒ 28 °C
SOURCE: ☒ SUN AT EARTH SURFACE —
☒ COLLIMATED ☐ UNCOLLIMATED
☐ TUNGSTEN - 2800°K, 100 mW/cm² EQUIV.
☒ OTHER REDUCED DATA BY EJB
SL 200 II
CR=4 ½=10°
CURRENT (mA X 5)
VOLTAGE (VOLTS X 2)
0
10
20
30
40
50
60
70
80
90
100
0
0.1
0.2
0.3
0.4
0.5
0.6
0.7

FIGURE 69

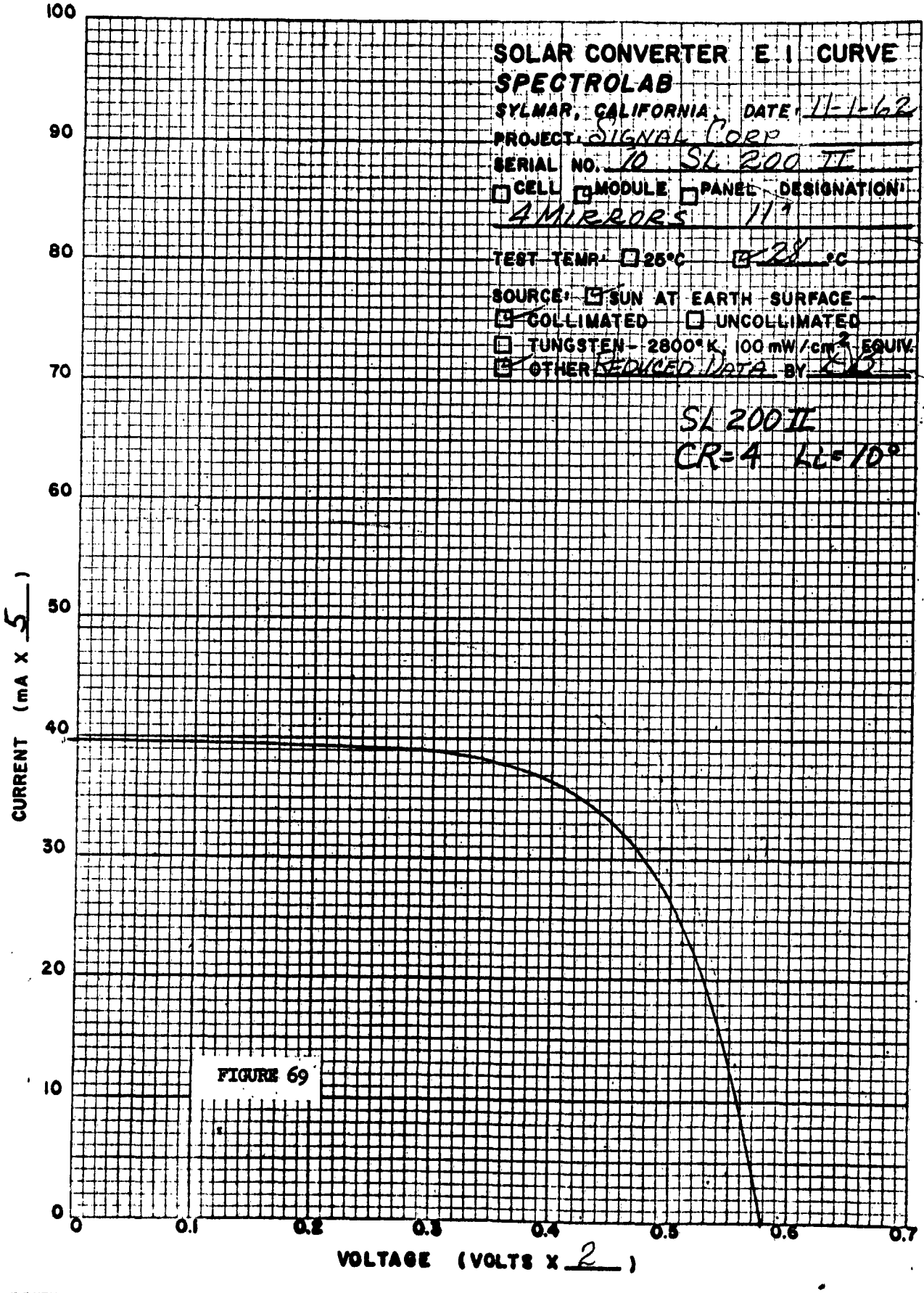

SOLAR CONVERTER E I CURVE
SPECTROLAB
SYLMAR, CALIFORNIA, DATE: 11-1-62
PROJECT: SIGNAL CORP
SERIAL NO. 10 SL 200 II
☐ CELL ☒ MODULE ☐ PANEL DESIGNATION:
4 MIRRORS 11°
TEST TEMP: ☐ 25°C ☒ 28 °C
SOURCE: ☒ SUN AT EARTH SURFACE —
☒ COLLIMATED ☐ UNCOLLIMATED
☐ TUNGSTEN - 2800°K, 100 mW/cm² EQUIV.
☒ OTHER REDUCED DATA BY
SL 200 II
CR=4 ½=10°
CURRENT (mA X 5)
VOLTAGE (VOLTS X 2)
0
10
20
30
40
50
60
70
80
90
100
0.1
0.2
0.3
0.4
0.5
0.6
0.7

FIGURE 69

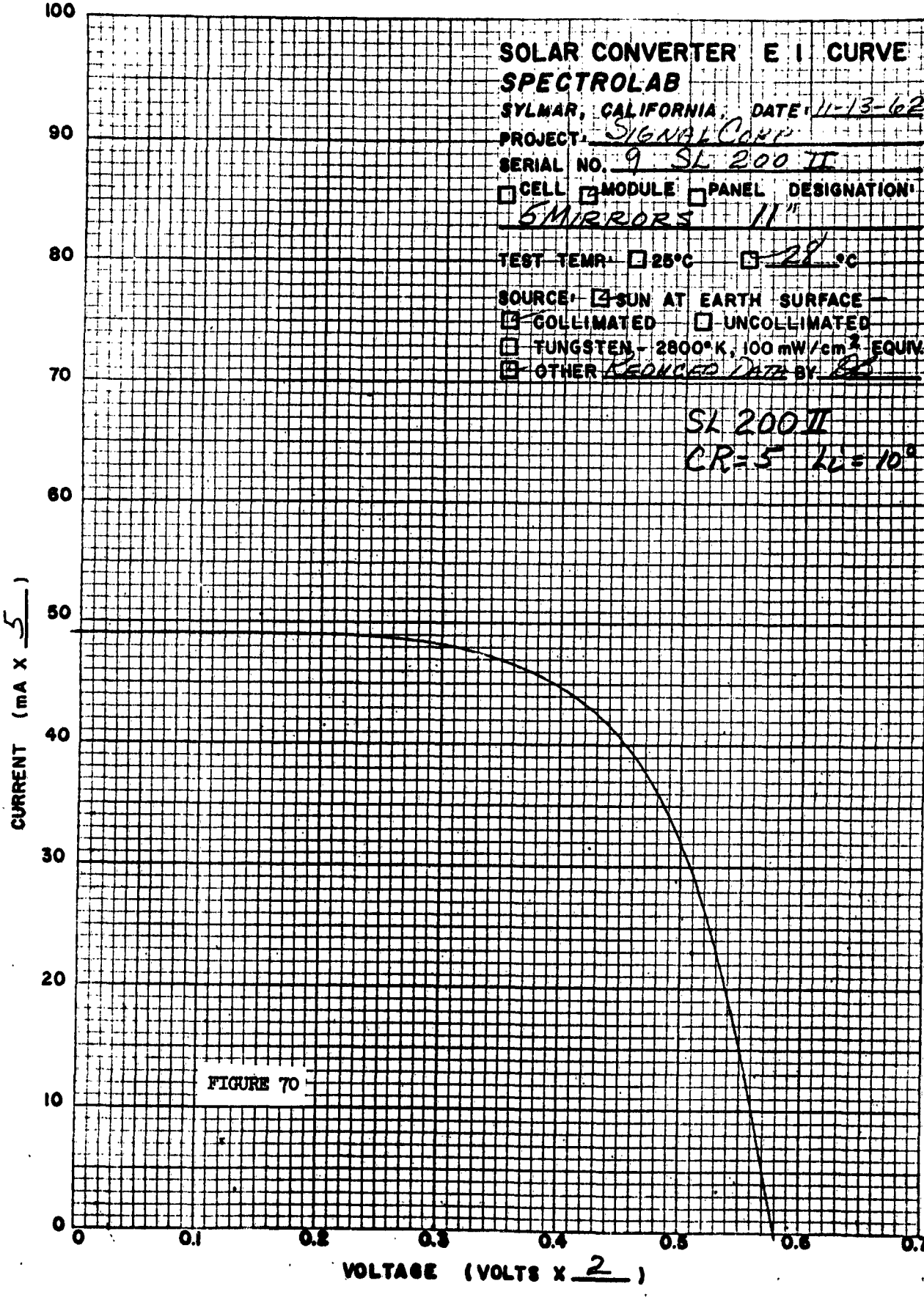

SOLAR CONVERTER E I CURVE
SPECTROLAB
SYLMAR, CALIFORNIA. DATE: 11-13-62
PROJECT: SIGNAL CORP.
SERIAL NO. 9 SL 200 II
☐ CELL ☒ MODULE ☐ PANEL DESIGNATION:
5 MIRRORS 11"
TEST TEMP: ☐ 25°C ☐ 28 °C
SOURCE: ☒ SUN AT EARTH SURFACE —
☒ COLLIMATED ☐ UNCOLLIMATED
☐ TUNGSTEN - 2800°K, 100 mW/cm² EQUIV.
☒ OTHER REDUCED DATA BY: BB
SL 200 II
CR=5 ½=10°
CURRENT (mA X 5)
VOLTAGE (VOLTS X 2)
100
90
80
70
60
50
40
30
20
10
0
0
0.1
0.2
0.3
0.4
0.5
0.6
0.7

FIGURE 70

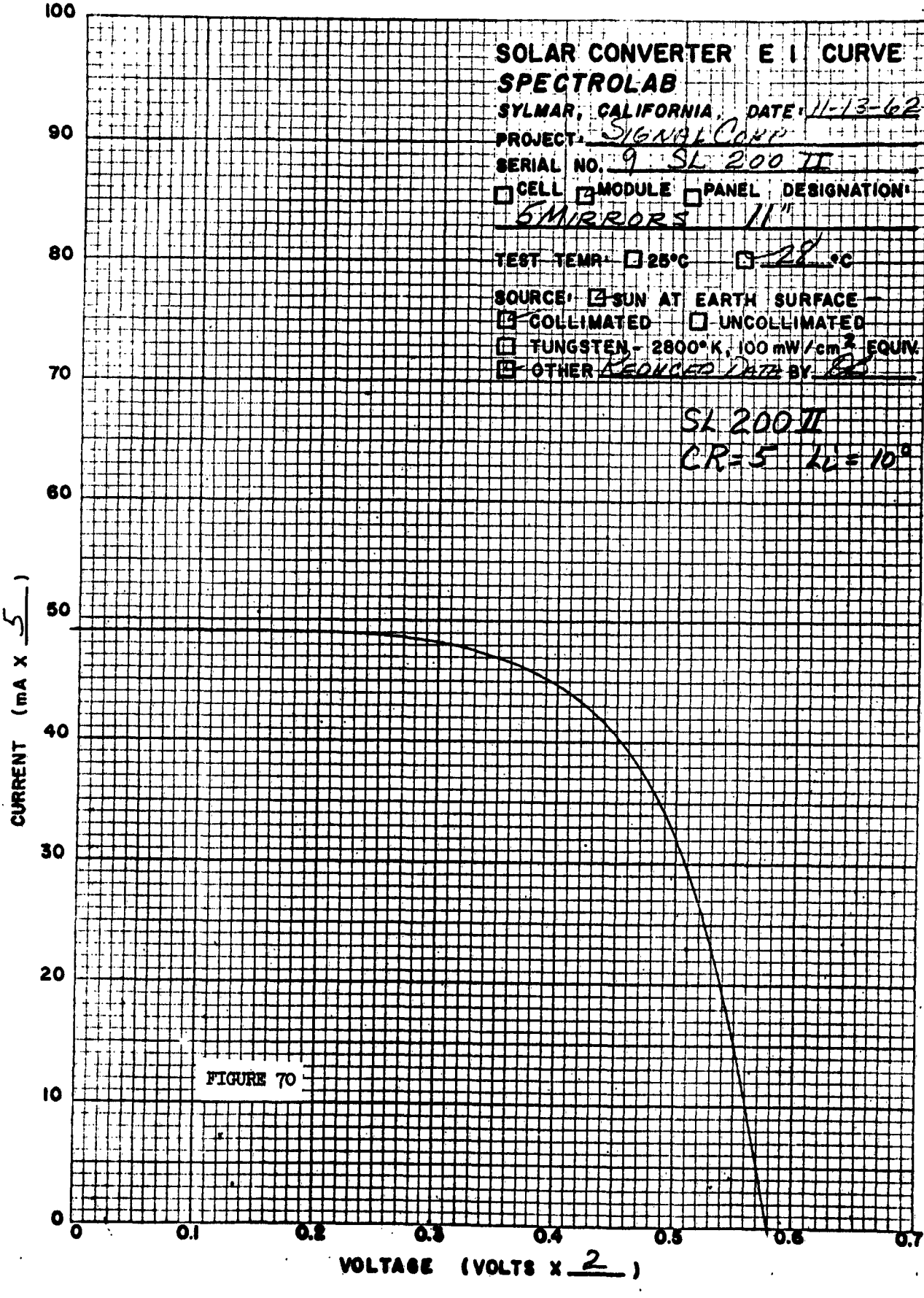

SOLAR CONVERTER E I CURVE
SPECTROLAB
SYLMAR, CALIFORNIA, DATE 11-13-62
PROJECT Signal Corp
SERIAL NO. 9 SL 200 II
CELL MODULE PANEL DESIGNATION
5 MIRRORS 11"
TEST TEMP. 25°C 28 °C
SOURCE: SUN AT EARTH SURFACE
COLLIMATED UNCOLLIMATED
TUNGSTEN - 2800°K, 100 mW/cm² EQUIV.
OTHER ACCURACY DATA BY
SL 200 II
CR=5 2½=10°
CURRENT (mA x 5)
VOLTAGE (VOLTS x 2)
100
90
80
70
60
50
40
30
20
10
0
0
0.1
0.2
0.3
0.4
0.5
0.6
0.7

FIGURE 70

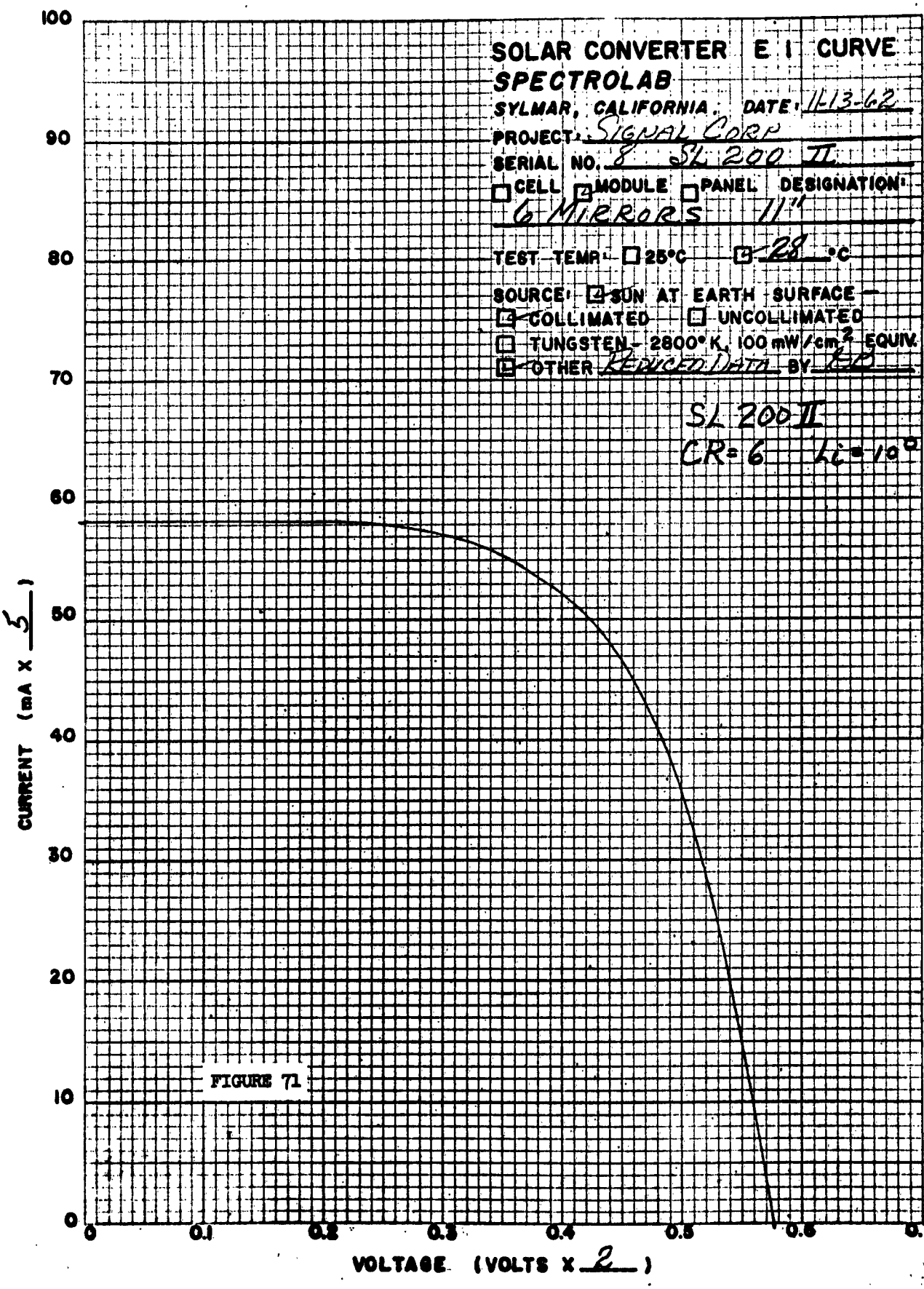

SOLAR CONVERTER E I CURVE
SPECTROLAB
SYLMAR, CALIFORNIA. DATE: 11-13-62
PROJECT: SIGNAL CORP
SERIAL NO. 8 SL 200 II
☐ CELL ☒ MODULE ☐ PANEL DESIGNATION:
6 MIRRORS 11"
TEST TEMP: ☐ 25°C ☒ 28 °C
SOURCE: ☒ SUN AT EARTH SURFACE —
☒ COLLIMATED ☐ UNCOLLIMATED
☐ TUNGSTEN - 2800° K, 100 mW/cm² EQUIV.
☒ OTHER REDUCED DATA BY RD
SL 200 II
CR = 6 Li = 10°
CURRENT (mA X 5)
VOLTAGE (VOLTS X 2)
0
10
20
30
40
50
60
70
80
90
100
0
0.1
0.2
0.3
0.4
0.5
0.6
0.7

FIGURE 71

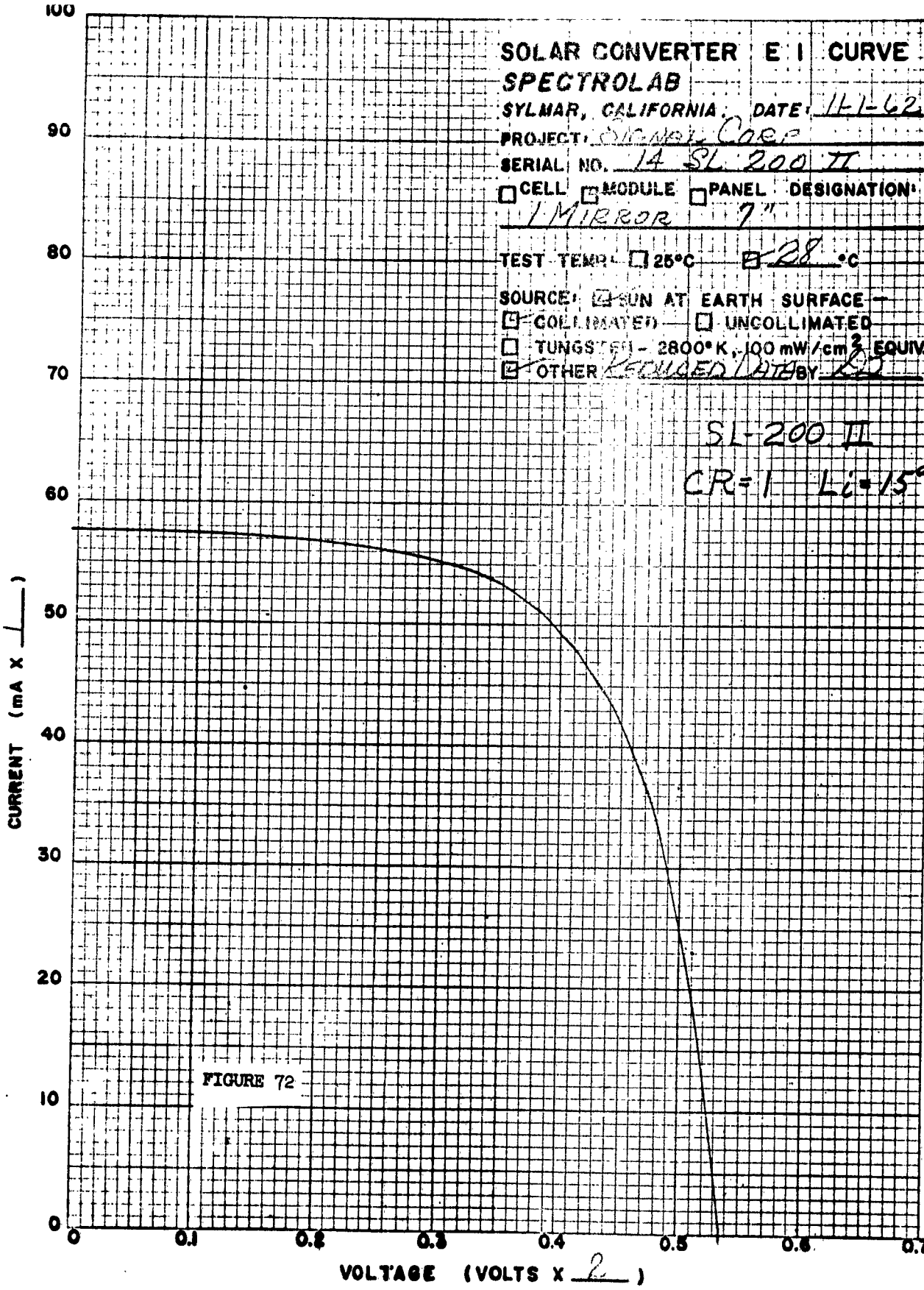

SOLAR CONVERTER E I CURVE
SPECTROLAB
SYLMAR, CALIFORNIA. DATE 11-1-62
PROJECT: SUNKIST CORP
SERIAL NO. 14 SL 200 II
CELL MODULE PANEL DESIGNATION:
1 MIRROR 7"
TEST TEMP: 25°C 28 °C
SOURCE: SUN AT EARTH SURFACE —
COLLIMATED — UNCOLLIMATED
TUNGSTEN - 2800°K, 100 mW/cm² EQUIV.
OTHER REDUCED DATA BY RD
SL-200 II
CR=1 Li=15°
CURRENT (mA X 1)
VOLTAGE (VOLTS X 2)
0
10
20
30
40
50
60
70
80
90
100
0
0.1
0.2
0.3
0.4
0.5
0.6
0.7

FIGURE 72

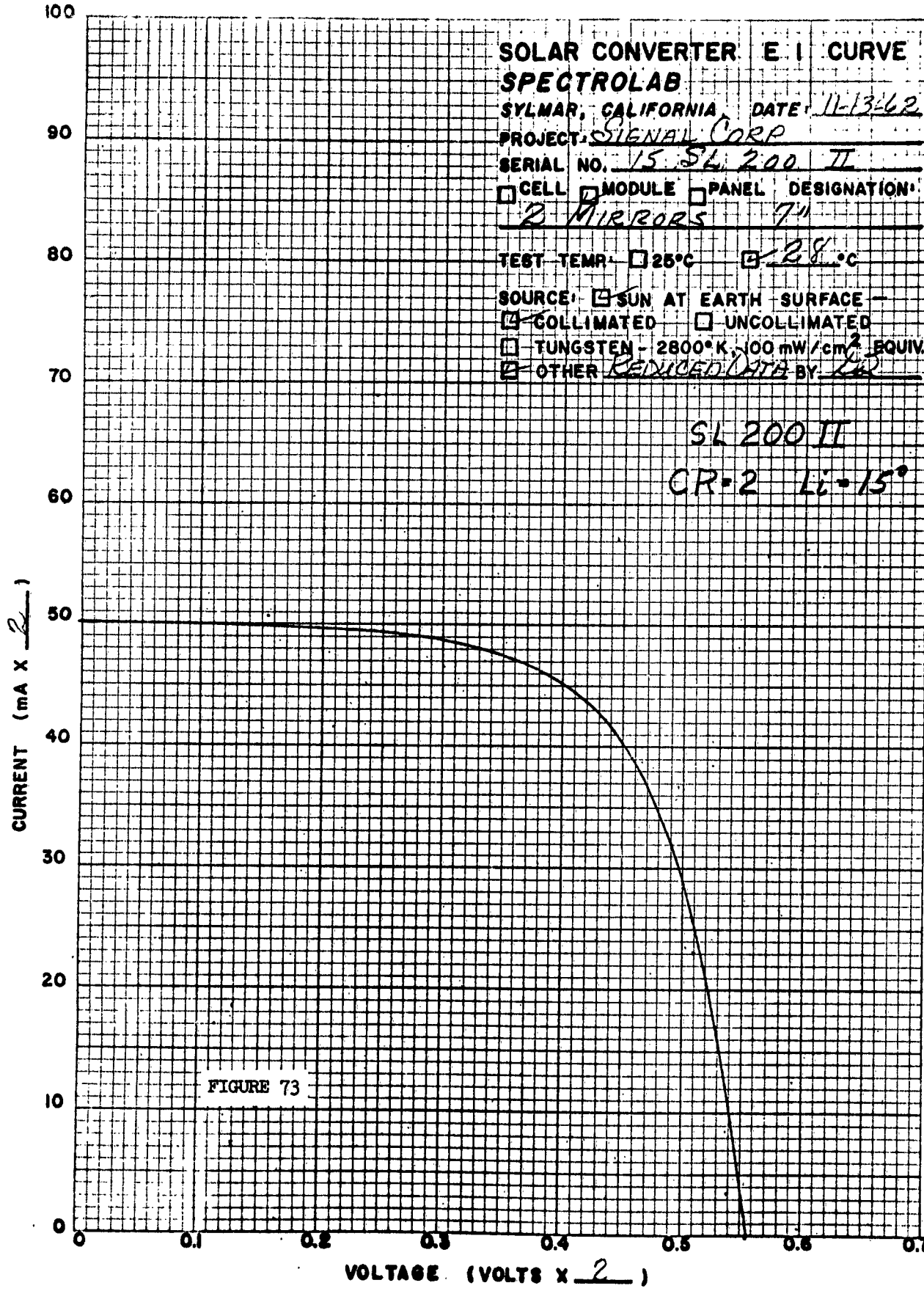

SOLAR CONVERTER E I CURVE
SPECTROLAB
SYLMAR, CALIFORNIA DATE 11-13-62
PROJECT SIGNAL CORP
SERIAL NO. 15 SL 200 II
CELL MODULE PANEL DESIGNATION
2 MIRRORS 7"
TEST TEMP 25°C 28 °C
SOURCE SUN AT EARTH SURFACE
COLLIMATED UNCOLLIMATED
TUNGSTEN - 2800°K, 100 mW/cm² EQUIV.
OTHER REDUCED DATA BY
SL 200 II
CR-2 Li-15°
CURRENT (mA X 2)
VOLTAGE (VOLTS X 2)
0
10
20
30
40
50
60
70
80
90
100
0
0.1
0.2
0.3
0.4
0.5
0.6
0.7

FIGURE 73

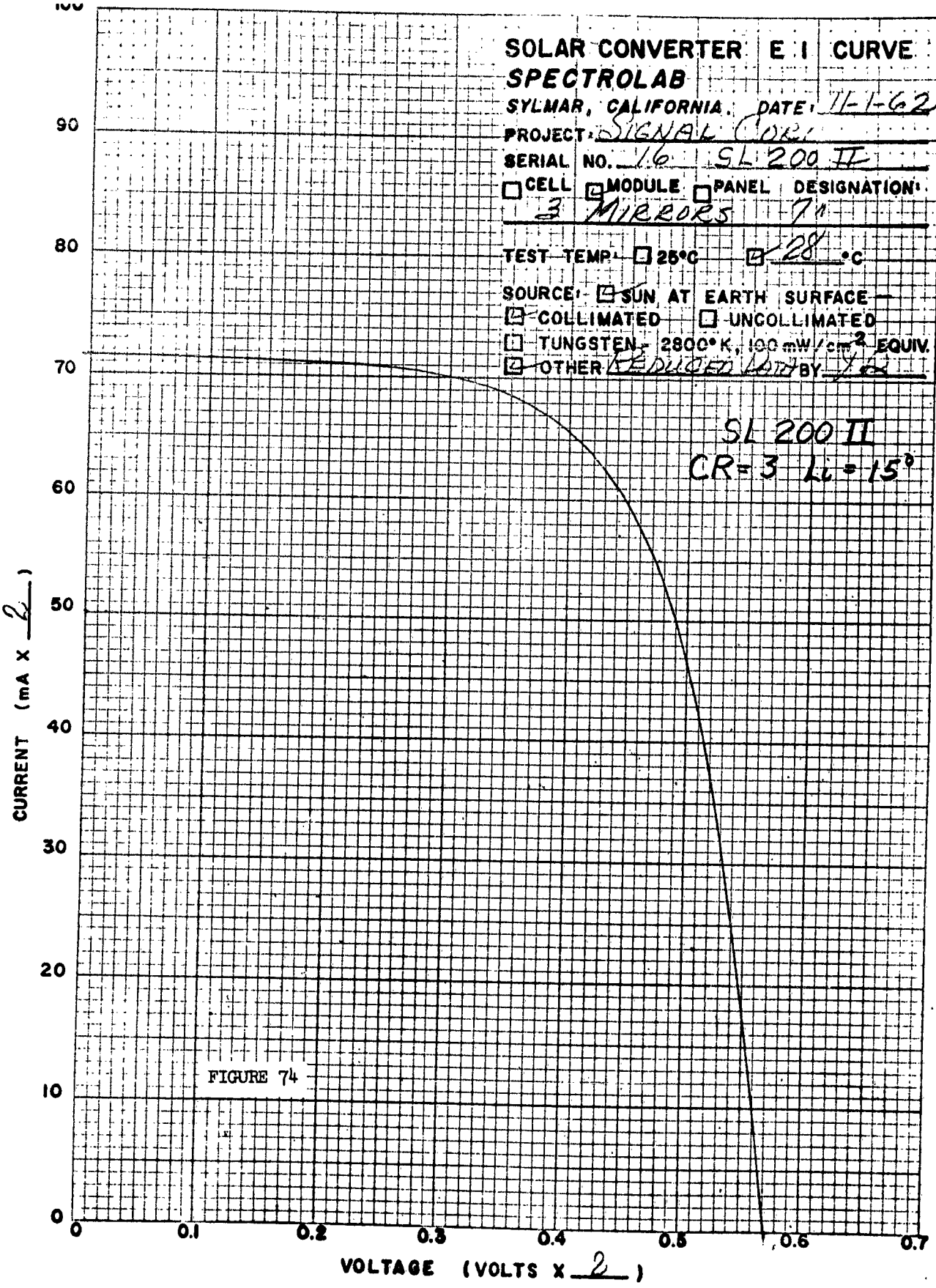

SOLAR CONVERTER E I CURVE
SPECTROLAB
SYLMAR, CALIFORNIA. DATE: 11-1-62
PROJECT: SIGNAL CORP.
SERIAL NO. 16 SL 200 II
☐ CELL ☒ MODULE ☐ PANEL DESIGNATION:
3 MIRRORS 7A
TEST TEMP: ☐ 25°C ☒ 28 °C
SOURCE: ☒ SUN AT EARTH SURFACE —
☒ COLLIMATED ☐ UNCOLLIMATED
☐ TUNGSTEN - 2800° K, 100 mW/cm² EQUIV.
☒ OTHER REDUCED 10% BY MIR
SL 200 II
CR=3 Li=15°
CURRENT (mA X 2)
VOLTAGE (VOLTS X 2)
0
10
20
30
40
50
60
70
80
90
100
0
0.1
0.2
0.3
0.4
0.5
0.6
0.7

FIGURE 74

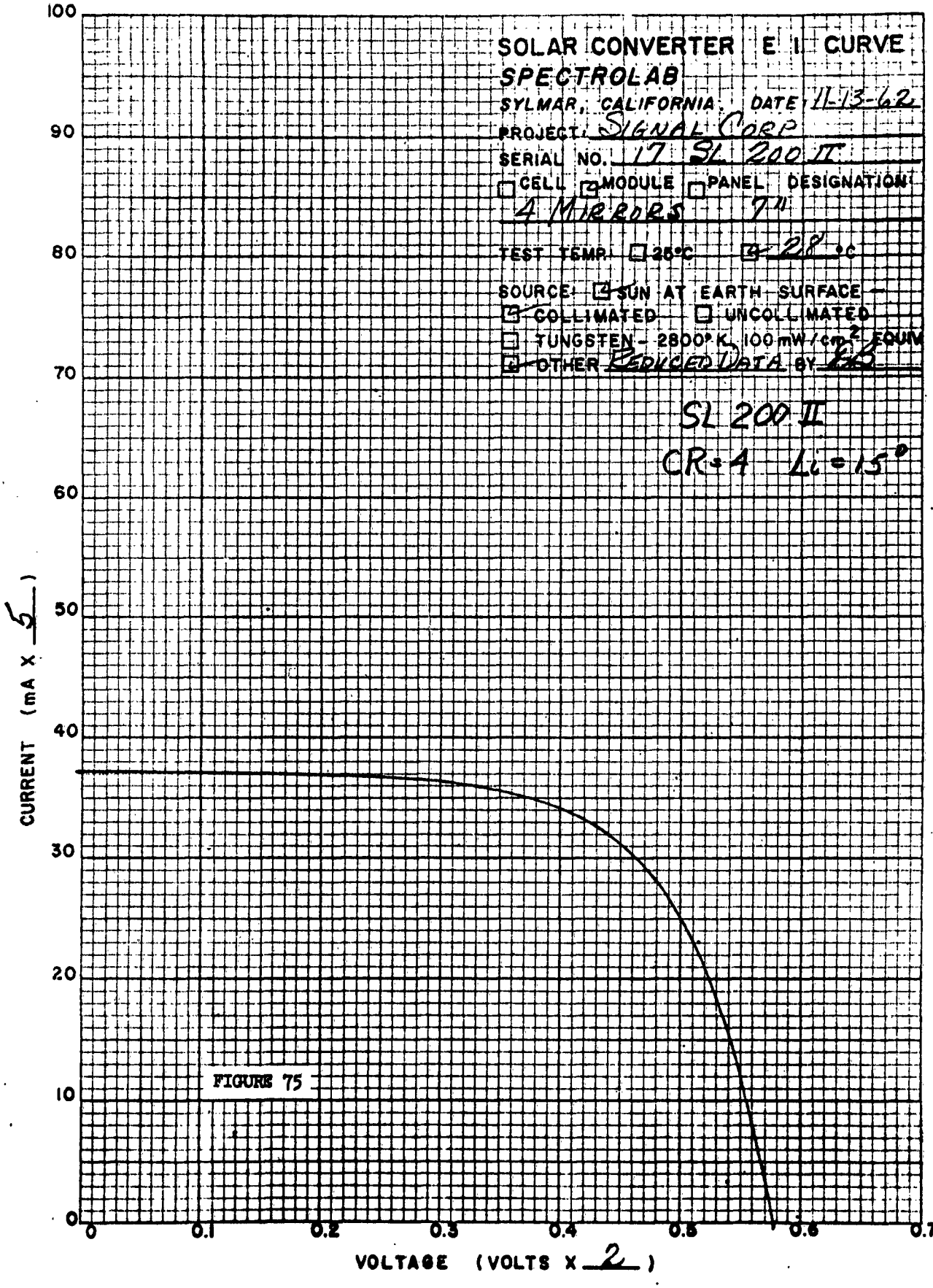

SOLAR CONVERTER E I CURVE
SPECTROLAB
SYLMAR, CALIFORNIA. DATE 11-13-62
PROJECT: SIGNAL CORP
SERIAL NO. 17 SL 200 II
☐ CELL ☒ MODULE ☐ PANEL DESIGNATION
4 MIRRORS 7"
TEST TEMP: ☐ 25°C ☒ 28 °C
SOURCE: ☒ SUN AT EARTH SURFACE —
☒ COLLIMATED ☐ UNCOLLIMATED
☐ TUNGSTEN - 2800° K, 100 mW/cm² EQUIV
☒ OTHER REDUCED DATA BY EAS
SL 200 II
CR=4 Li=15°
CURRENT (mA X 5)
VOLTAGE (VOLTS X 2)
0
10
20
30
40
50
60
70
80
90
100
0
0.1
0.2
0.3
0.4
0.5
0.6
0.7

FIGURE 75

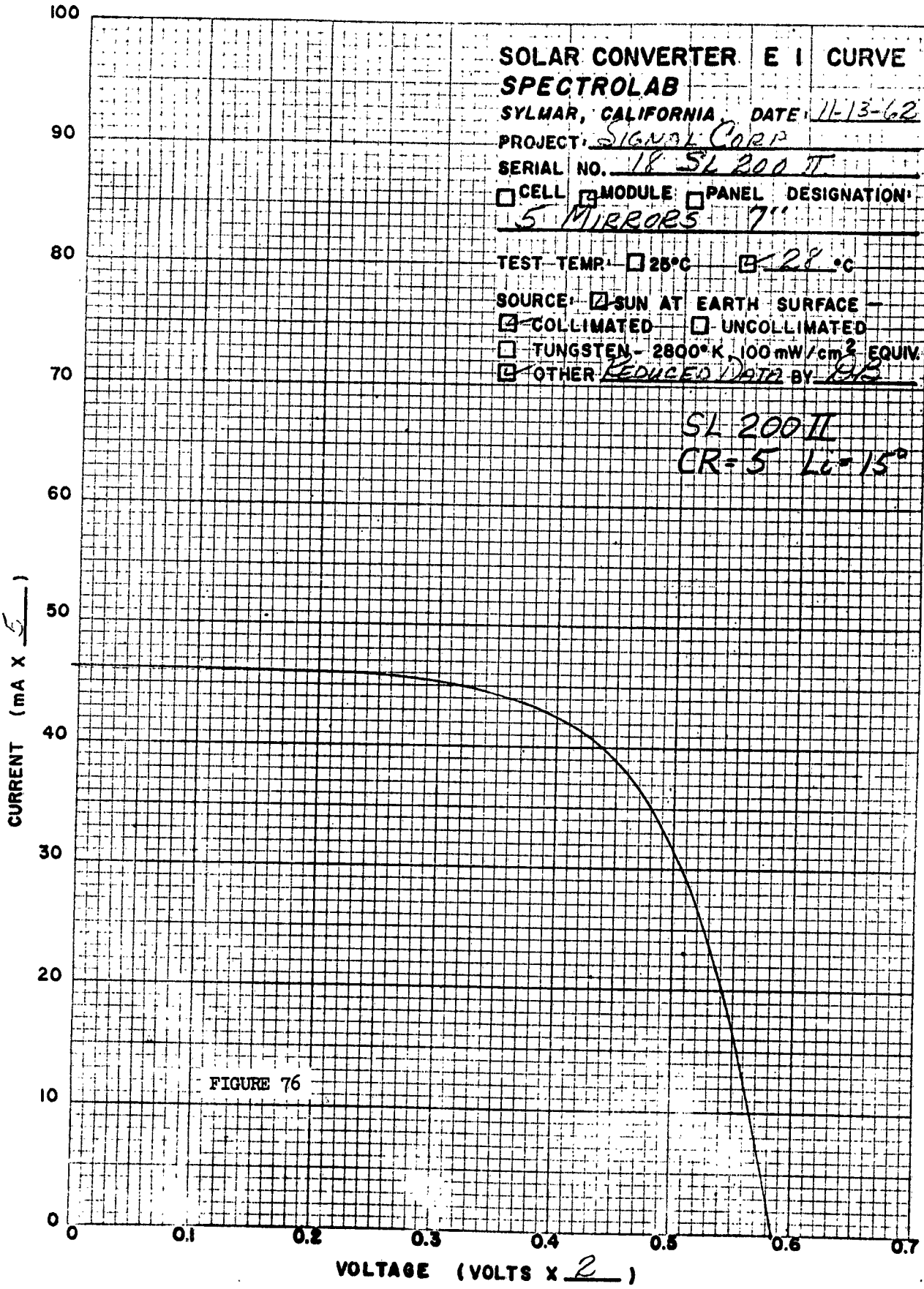


FIGURE 76

PRINTED IN U.S.A. ON CLEARPRINT TECHNICAL PAPER NO. 1015

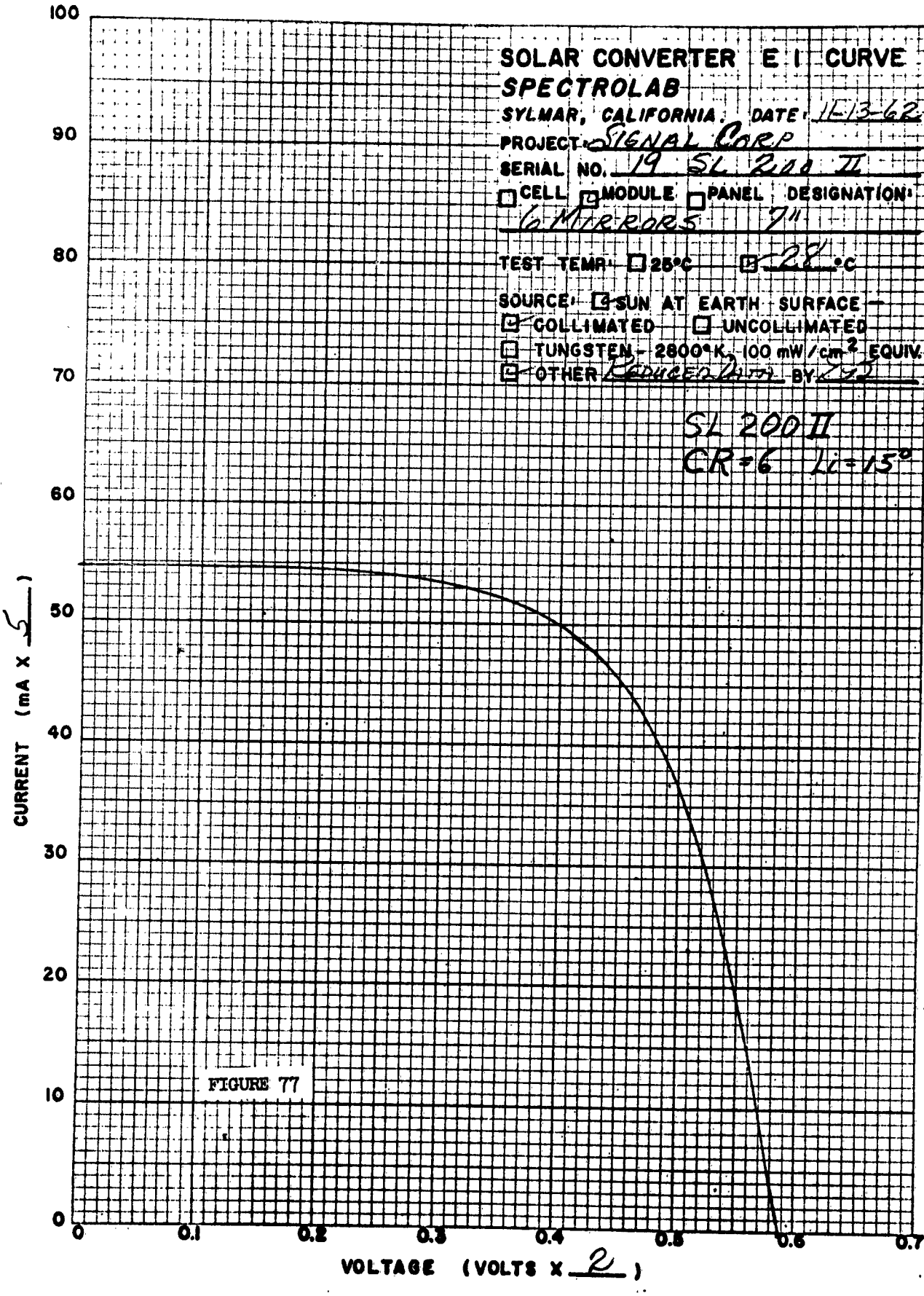

SOLAR CONVERTER E I CURVE
SPECTROLAB
SYLMAR, CALIFORNIA. DATE: 11-13-62
PROJECT: SIGNAL CORP
SERIAL NO. 19 SL 200 II
☐ CELL ☒ MODULE ☐ PANEL DESIGNATION:
6 MIRRORS 7"
TEST TEMP: ☐ 25°C ☒ 28 °C
SOURCE: ☒ SUN AT EARTH SURFACE —
☒ COLLIMATED ☐ UNCOLLIMATED
☐ TUNGSTEN - 2800°K, 100 mW/cm² EQUIV.
☒ OTHER REDUCED WITH BY
SL 200 II
CR=6 Li=15°
CURRENT (mA X 5)
VOLTAGE (VOLTS X 2)
0
10
20
30
40
50
60
70
80
90
100
0
0.1
0.2
0.3
0.4
0.5
0.6
0.7

FIGURE 77

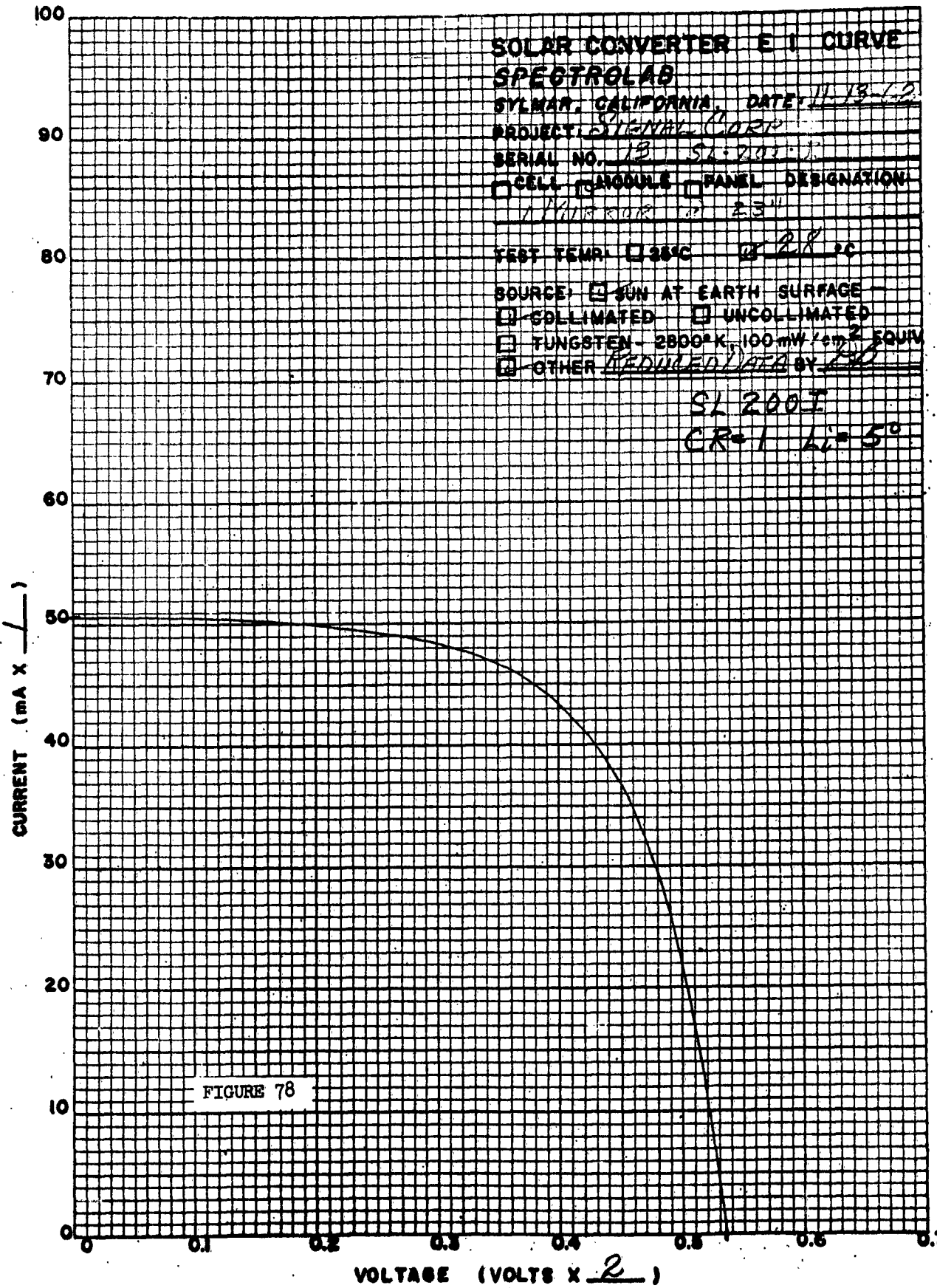

SOLAR CONVERTER E I CURVE
SPECTROLAB
SYLMAR, CALIFORNIA. DATE: 11-13-62
PROJECT: SYNAP Case
SERIAL NO. 13 SL 200 I
☐ CELL ☒ MODULE ☐ PANEL DESIGNATION:
1 Mini-Sun 23"
TEST TEMP: ☐ 25°C ☒ 28 °C
SOURCE: ☒ SUN AT EARTH SURFACE —
☒ COLLIMATED ☐ UNCOLLIMATED
☐ TUNGSTEN - 2800°K, 100 mW/cm² EQUIV.
☒ OTHER REDUCED DATA BY
SL 200 I
CR=1 Li=5°
CURRENT (mA X 1)
VOLTAGE (VOLTS X 2)
100
90
80
70
60
50
40
30
20
10
0
0
0.1
0.2
0.3
0.4
0.5
0.6
0.7

FIGURE 78

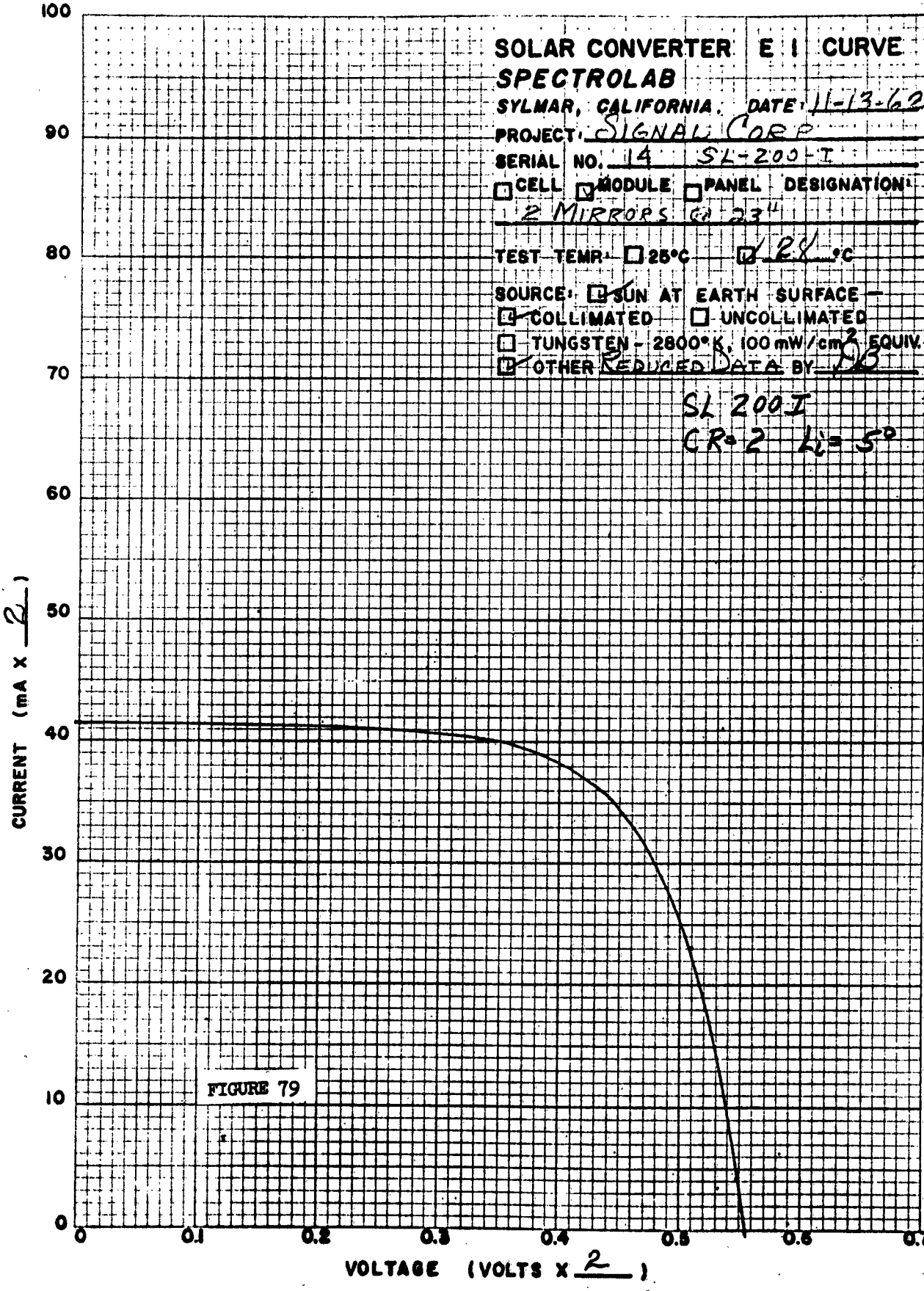

SOLAR CONVERTER E I CURVE
SPECTROLAB
SYLMAR, CALIFORNIA. DATE 11-13-62
PROJECT SIGNAL CORP
SERIAL NO. 14 SL-200-I
CELL MODULE PANEL DESIGNATION
2 MIRRORS @ 23"
TEST TEMP 25°C 28 °C
SOURCE SUN AT EARTH SURFACE —
COLLIMATED UNCOLLIMATED
TUNGSTEN - 2800°K, 100 mW/cm² EQUIV.
OTHER REDUCED DATA BY RB
SL 200 I
CR=2 Li=5°
CURRENT (mA X 2)
VOLTAGE (VOLTS X 2)
0
10
20
30
40
50
60
70
80
90
100
0
0.1
0.2
0.3
0.4
0.5
0.6
0.7

FIGURE 79

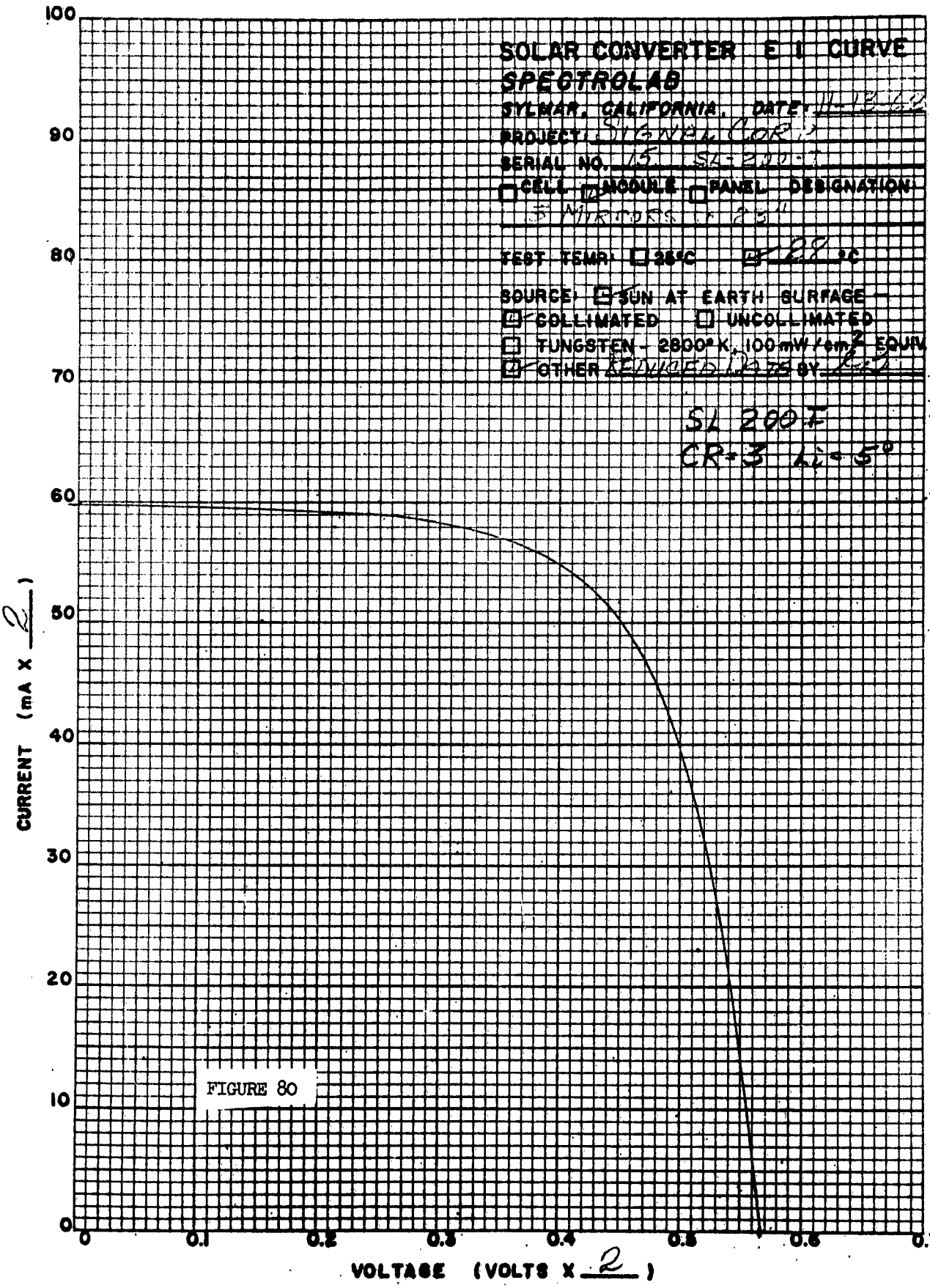

SOLAR CONVERTER E I CURVE
SPECTROLAB
SYLMAR, CALIFORNIA. DATE: 11-12-82
PROJECT: Sylvania Corp.
SERIAL NO. 15 SL-200-T
☐ CELL ☑ MODULE ☐ PANEL DESIGNATION:
3" Mirrors + 2"
TEST TEMP: ☐ 25°C ☑ 28 °C
SOURCE: ☑ SUN AT EARTH SURFACE —
☑ COLLIMATED ☐ UNCOLLIMATED
☐ TUNGSTEN - 2800°K, 100 mW/cm² EQUIV.
☑ OTHER REVERSED BIAS BY
SL 200T
CR=3 Δi=5°
CURRENT (mA X 2)
VOLTAGE (VOLTS X 2)
100
90
80
70
60
50
40
30
20
10
0
0
0.1
0.2
0.3
0.4
0.5
0.6
0.7

FIGURE 80

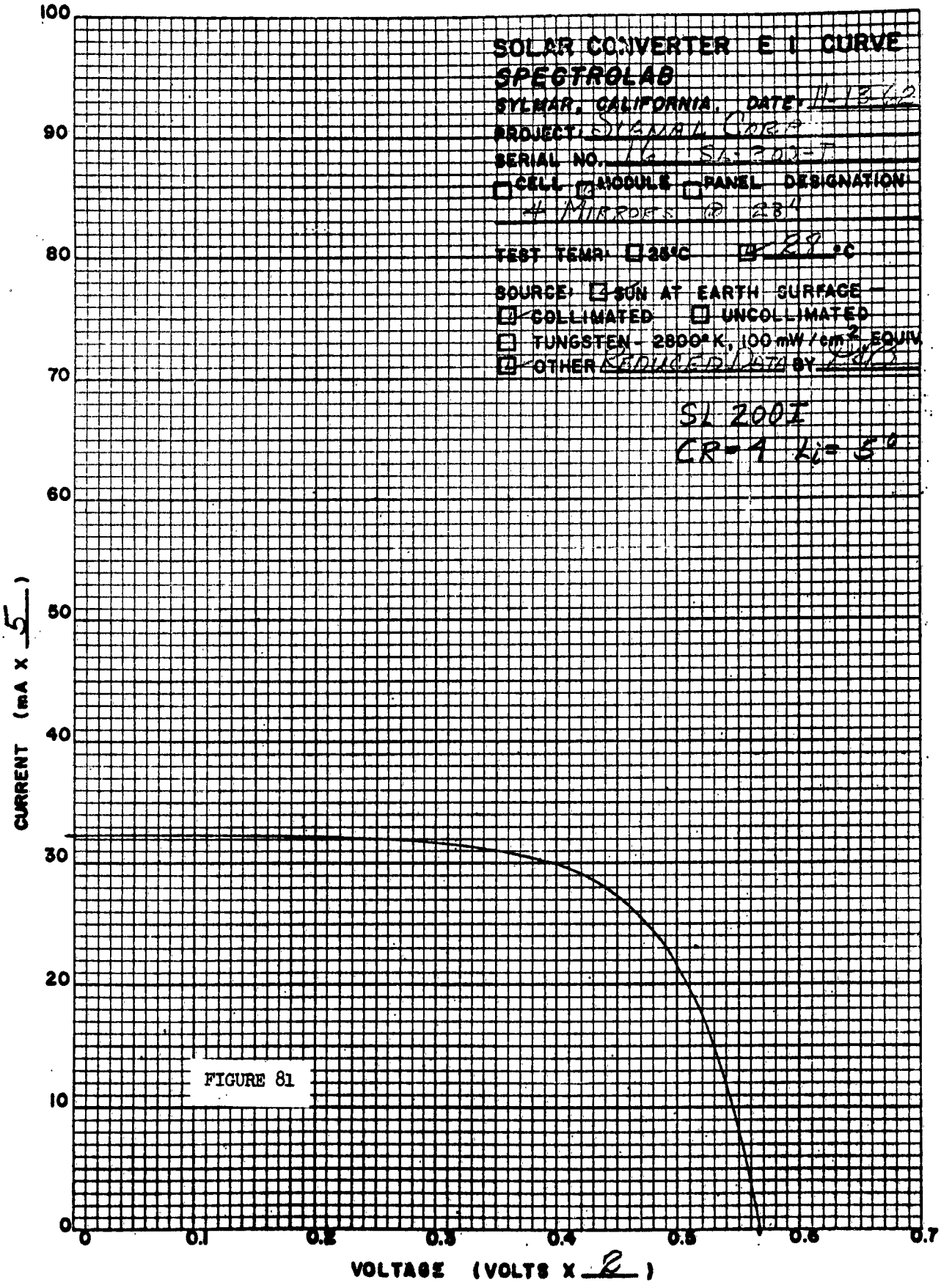

SOLAR CONVERTER E I CURVE
SPECTROLAB
SYLMAR, CALIFORNIA. DATE: 11-13-62
PROJECT: Syncom Corp
SERIAL NO. 16 SL 200 T
☐ CELL ☑ MODULE ☐ PANEL DESIGNATION:
4 MIRRORS @ 23X
TEST TEMP: ☐ 25°C ☑ 28 °C
SOURCE: ☐ SUN AT EARTH SURFACE
☑ COLLIMATED ☐ UNCOLLIMATED
☐ TUNGSTEN - 2800°K, 100 mW/cm² EQUIV
☑ OTHER REDUCED DATA BY
SL 200T
CR-1 Li= 5°
CURRENT (mA X 5)
VOLTAGE (VOLTS X 2)
100
90
80
70
60
50
40
30
20
10
0
0
0.1
0.2
0.3
0.4
0.5
0.6
0.7

FIGURE 81

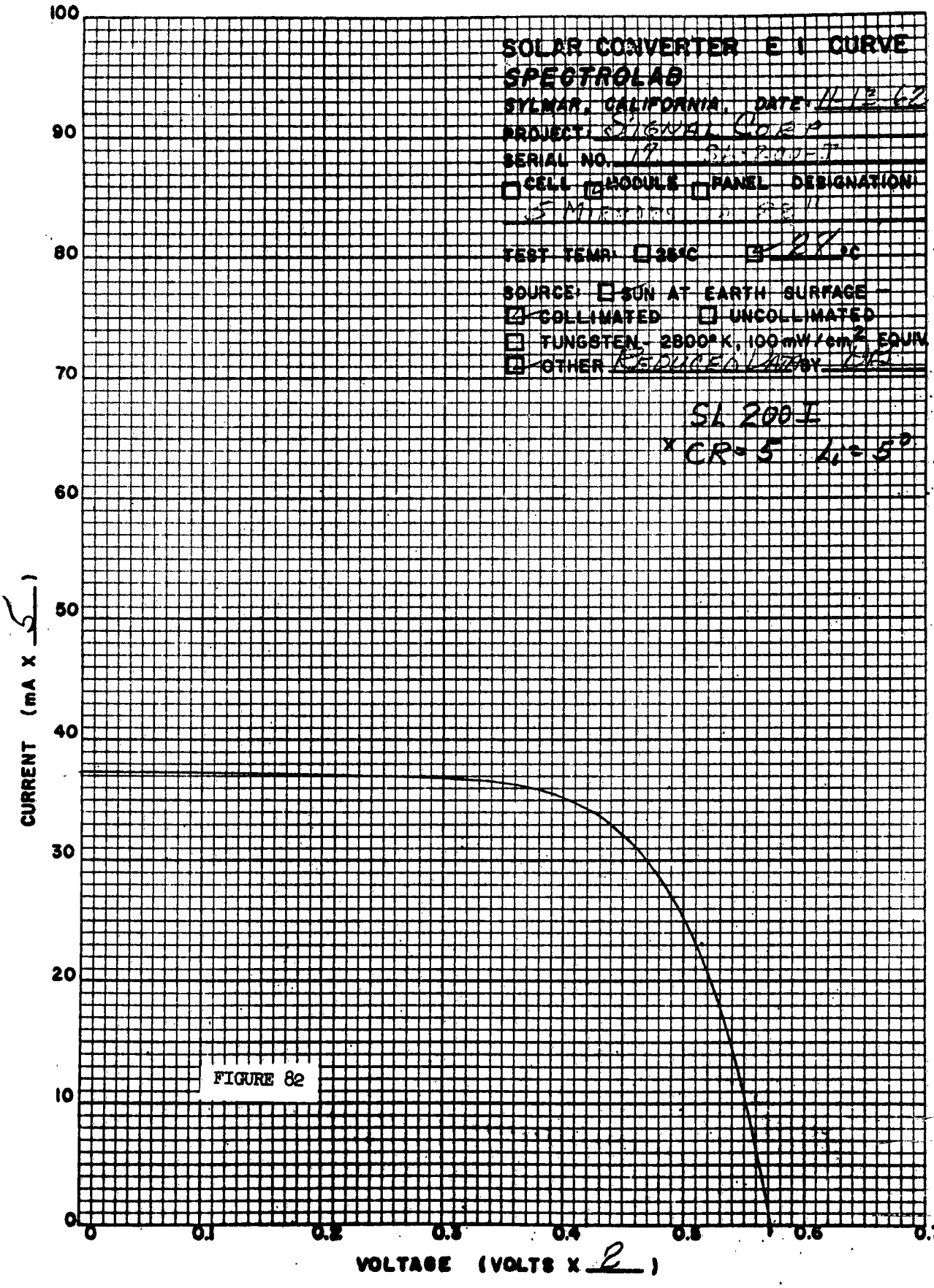

SOLAR CONVERTER E I CURVE
SPECTROLAB
SYLMAR, CALIFORNIA. DATE: 4-12-62
PROJECT: Sidewall Solar
SERIAL NO. 12 Bypassed
☐ CELL ☒ MODULE ☐ PANEL DESIGNATION:
5 Mil Cover Glass
TEST TEMP: ☐ 25°C ☒ 28 °C
SOURCE: ☐ SUN AT EARTH SURFACE
☑ COLLIMATED ☐ UNCOLLIMATED
☐ TUNGSTEN - 2800°K, 100 mW/cm² EQUIV.
☐ OTHER REDUCED INTENSITY
SA 200-L
X CR = 5 Li = 5°
CURRENT (mA X 5)
VOLTAGE (VOLTS X 2)
100
90
80
70
60
50
40
30
20
10
0
0
0.1
0.2
0.3
0.4
0.5
0.6
0.7

FIGURE 82

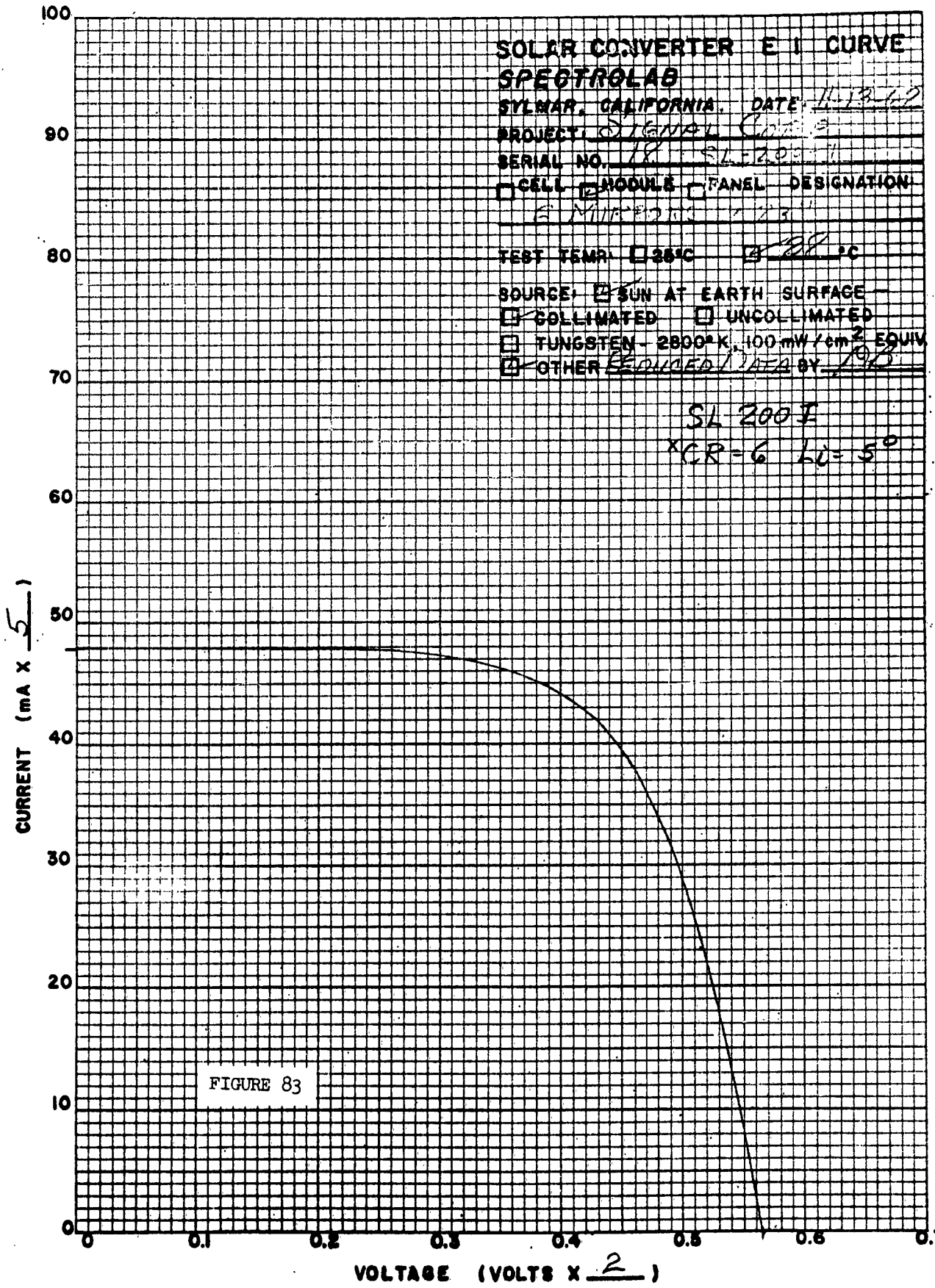

SOLAR CONVERTER E I CURVE
SPECTROLAB
SYLMAR, CALIFORNIA. DATE: 11-12-62
PROJECT: SIGNAL
SERIAL NO. SL-200
CELL MODULE PANEL DESIGNATION:
TEST TEMP: 25°C 28 °C
SOURCE: SUN AT EARTH SURFACE
COLLIMATED UNCOLLIMATED
TUNGSTEN - 2800°K, 100 mW/cm² EQUIV.
OTHER REDUCED DATA BY
SL 200 F
XCR = 6 Li = 5°
CURRENT (mA X 5)
VOLTAGE (VOLTS X 2)
100
90
80
70
60
50
40
30
20
10
0
0
0.1
0.2
0.3
0.4
0.5
0.6
0.7

FIGURE 83

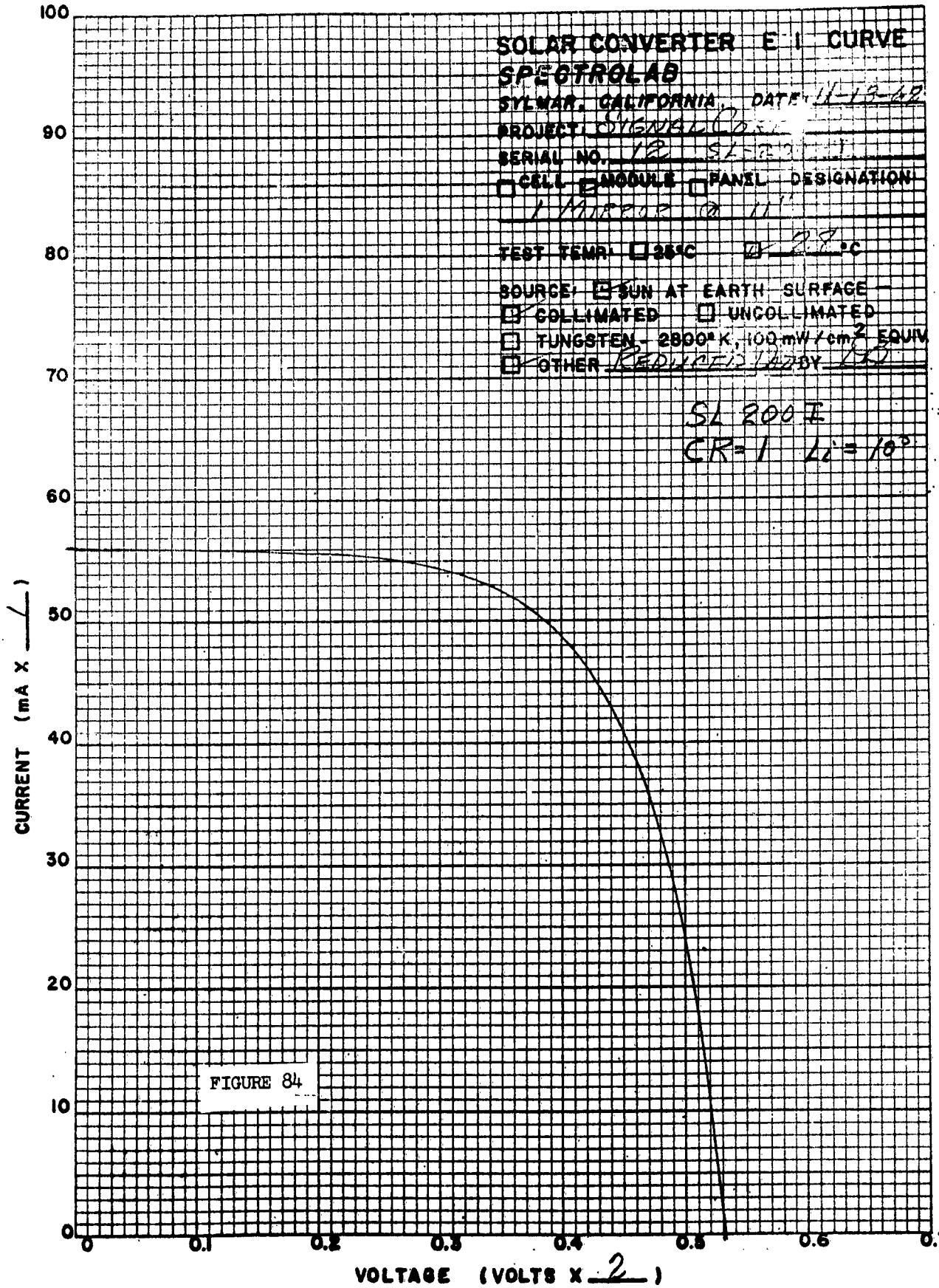

SOLAR CONVERTER E I CURVE
SPECTROLAB
SYLMAR, CALIFORNIA, DATE 11-13-62
PROJECT: SNAP 2
SERIAL NO. 12 SL-
CELL MODULE PANEL DESIGNATION
1 MIL @ 11
TEST TEMP: 28°C 28 °C
SOURCE: SUN AT EARTH SURFACE
COLLIMATED UNCOLLIMATED
TUNGSTEN, 2800° K, 100 mW/cm² EQUIV.
OTHER REDUCED TO BY
SL 200 I
CR=1 Li = 10°
CURRENT (mA X 1)
VOLTAGE (VOLTS X 2)
100
90
80
70
60
50
40
30
20
10
0
0
0.1
0.2
0.3
0.4
0.5
0.6
0.7

FIGURE 84

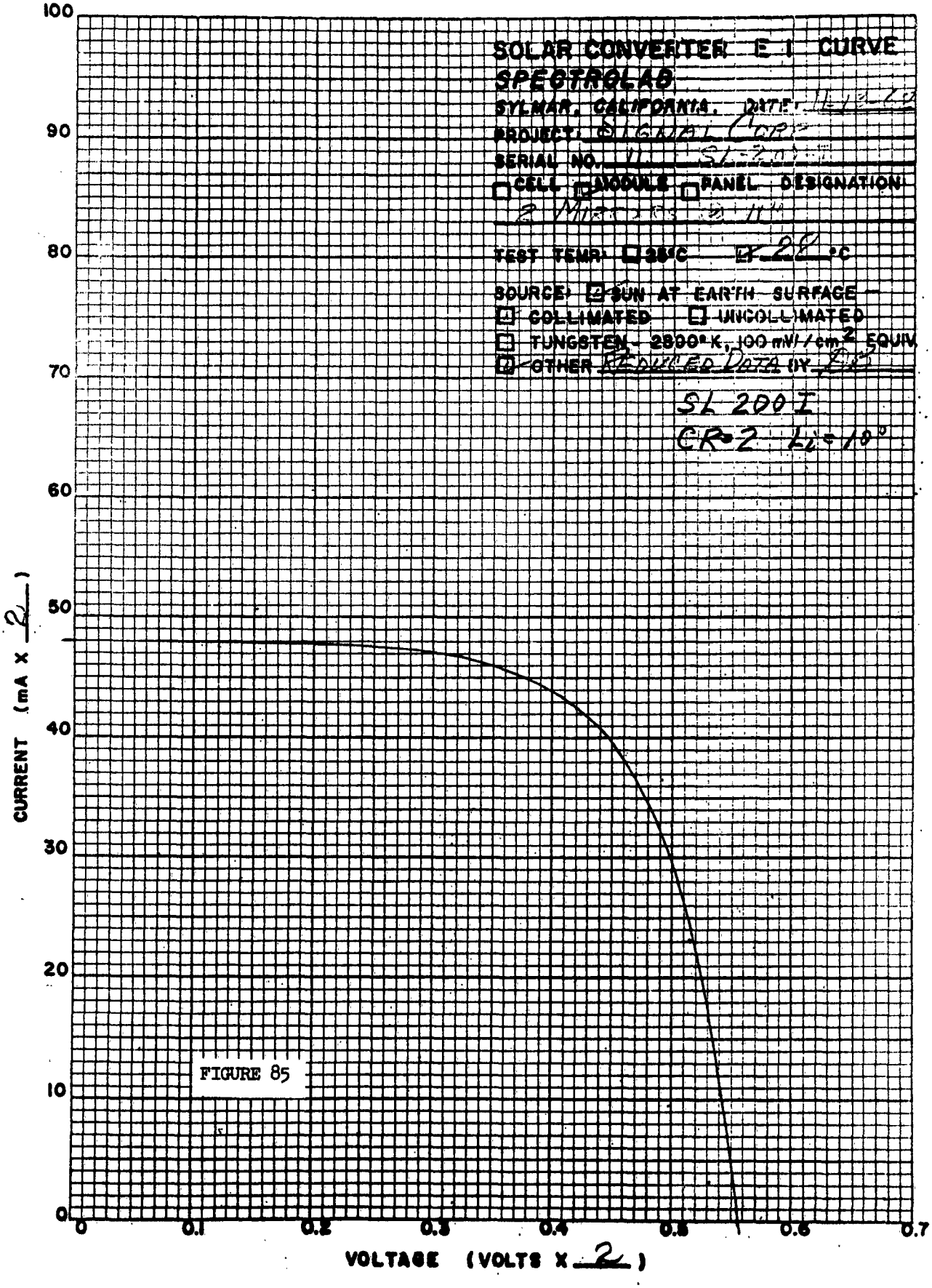

SOLAR CONVERTER E I CURVE
SPECTROLAB
SYLMAR, CALIFORNIA. DATE:
PROJECT:
SERIAL NO.
CELL MODULE PANEL DESIGNATION
TEST TEMP: 28°C °C
SOURCE: SUN AT EARTH SURFACE
COLLIMATED UNCOLLIMATED
TUNGSTEN - 2800°K, 100 mW/cm² EQUIV.
OTHER REDUCED DATA BY
SL 200 I
CR-2 Li = 10°
CURRENT (mA X 2)
VOLTAGE (VOLTS X 2)
100
90
80
70
60
50
40
30
20
10
0
0
0.1
0.2
0.3
0.4
0.5
0.6
0.7

FIGURE 85

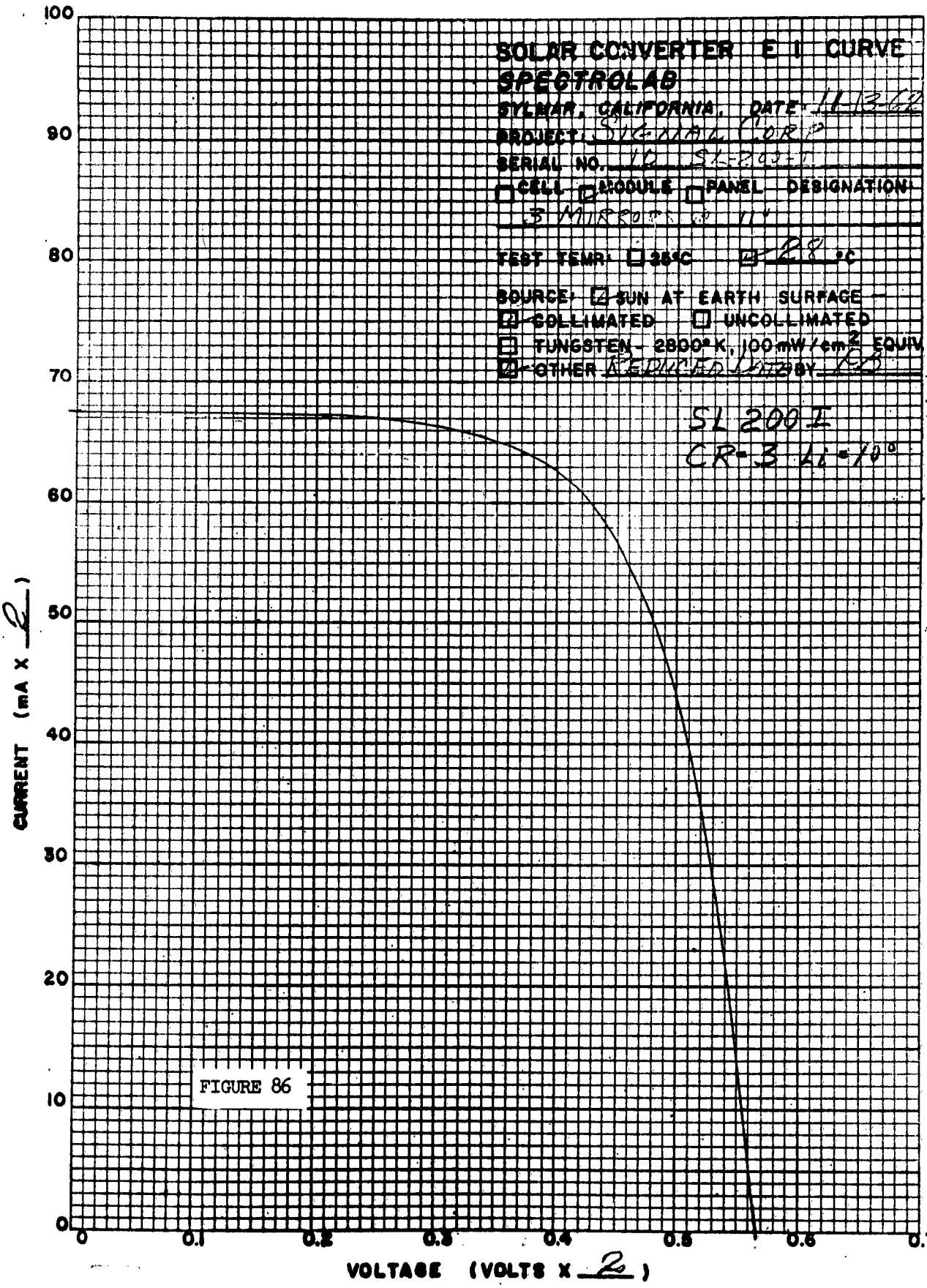

SOLAR CONVERTER E I CURVE
SPECTROLAB
SYLMAR, CALIFORNIA. DATE: 11-13-62
PROJECT: Sylmar CPR
SERIAL NO. 12 SL-200-I
☐ CELL ☑ MODULE ☐ PANEL DESIGNATION:
3 MIRRORS @ 11"
TEST TEMP: ☐ 25°C ☑ 28 °C
SOURCE: ☑ SUN AT EARTH SURFACE
☑ COLLIMATED ☐ UNCOLLIMATED
☐ TUNGSTEN - 2800°K, 100 mW/cm² EQUIV
☑ OTHER REFLECTED LIGHT BY AL
SL 200 I
CR-3 Ai = 10°
CURRENT (mA X 2)
VOLTAGE (VOLTS X 2)
0
10
20
30
40
50
60
70
80
90
100
0
0.1
0.2
0.3
0.4
0.5
0.6
0.7

FIGURE 86

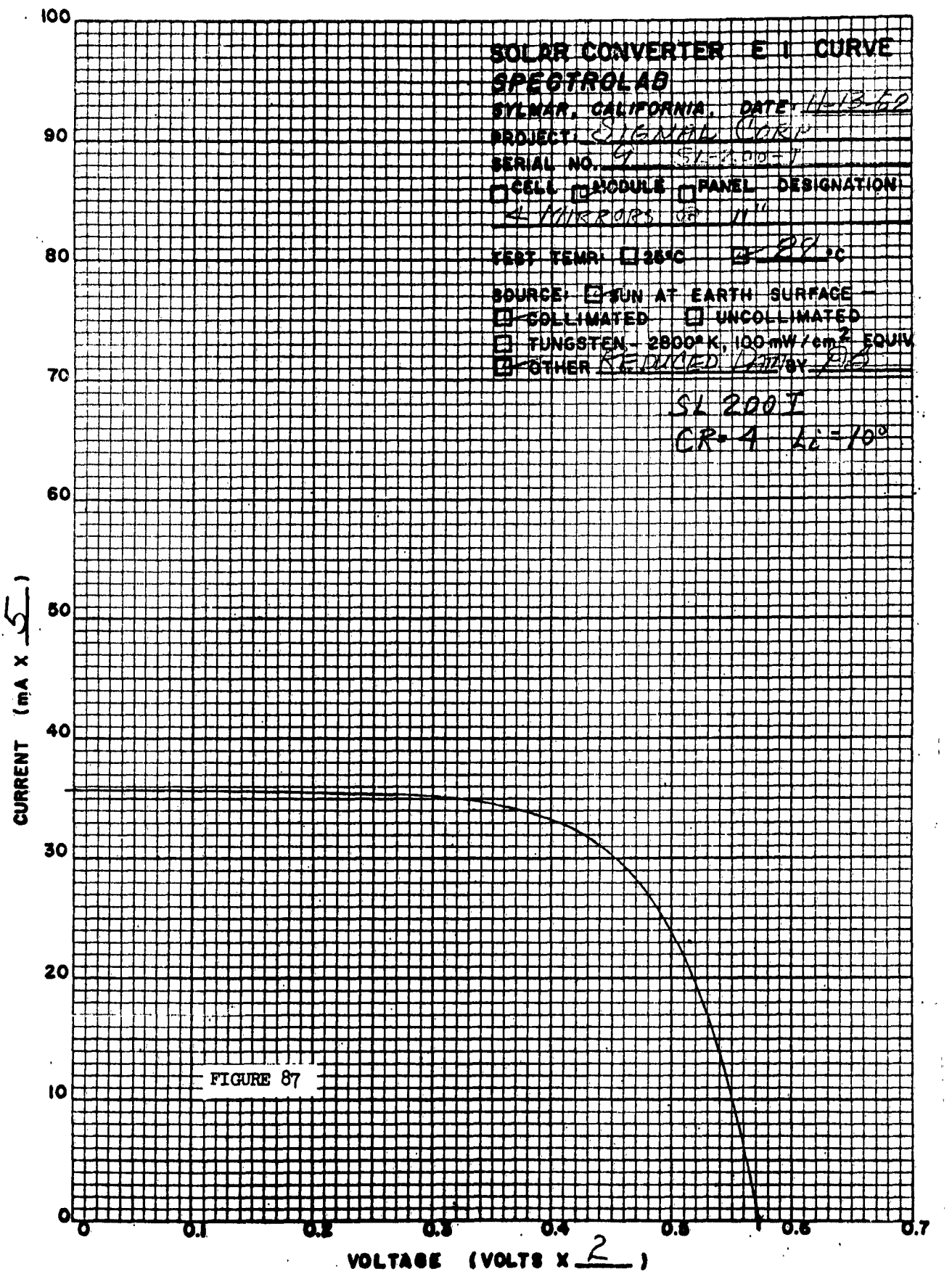

SOLAR CONVERTER E I CURVE
SPECTROLAB
SYLMAR, CALIFORNIA. DATE: 4-13-62
PROJECT: SIGNAL CORP
SERIAL NO. 4 SL-200-T
☐ CELL ☐ MODULE ☐ PANEL DESIGNATION
4 MICROPACS OF 11
TEST TEMP: ☐ 25°C ☒ 22 °C
SOURCE: ☒ SUN AT EARTH SURFACE —
☐ COLLIMATED ☐ UNCOLLIMATED
☐ TUNGSTEN - 2800° K, 100 mW/cm² EQUIV
☒ OTHER REDUCED LAMP BY 2.6
SL 200 T
CR-4 Ai = 70°
CURRENT (mA X 5)
VOLTAGE (VOLTS X 2)
0
10
20
30
40
50
60
70
80
90
100
0.1
0.2
0.3
0.4
0.5
0.6
0.7

FIGURE 87

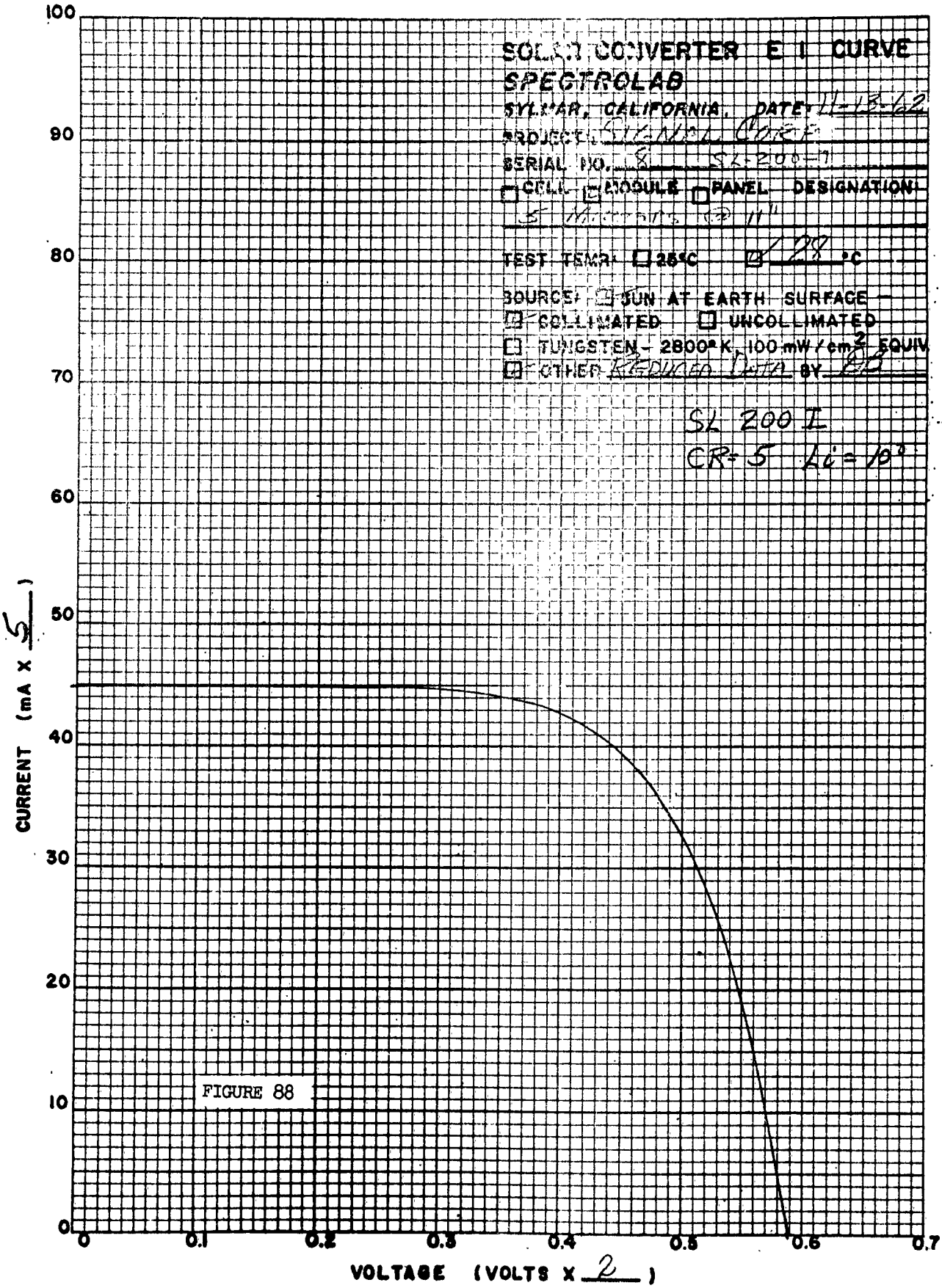

SOLAR CONVERTER E I CURVE
SPECTROLAB
SYLMAR, CALIFORNIA. DATE: 11-13-62
PROJECT: SIGNAL CORPS
SERIAL NO. SL-200-7
☐ CELL ☑ MODULE ☐ PANEL DESIGNATION:
5 Mwatts @ 11"
TEST TEMP: ☐ 25°C ☑ 28 °C
SOURCE: ☐ SUN AT EARTH SURFACE —
☑ COLLIMATED ☐ UNCOLLIMATED
☐ TUNGSTEN - 2800°K, 100 mW/cm² EQUIV
☑ OTHER REDUCED DATA BY DS
SL 200 I
CR-5 Ai = 10°
CURRENT (mA X 5)
VOLTAGE (VOLTS X 2)
100
90
80
70
60
50
40
30
20
10
0
0
0.1
0.2
0.3
0.4
0.5
0.6
0.7

FIGURE 88

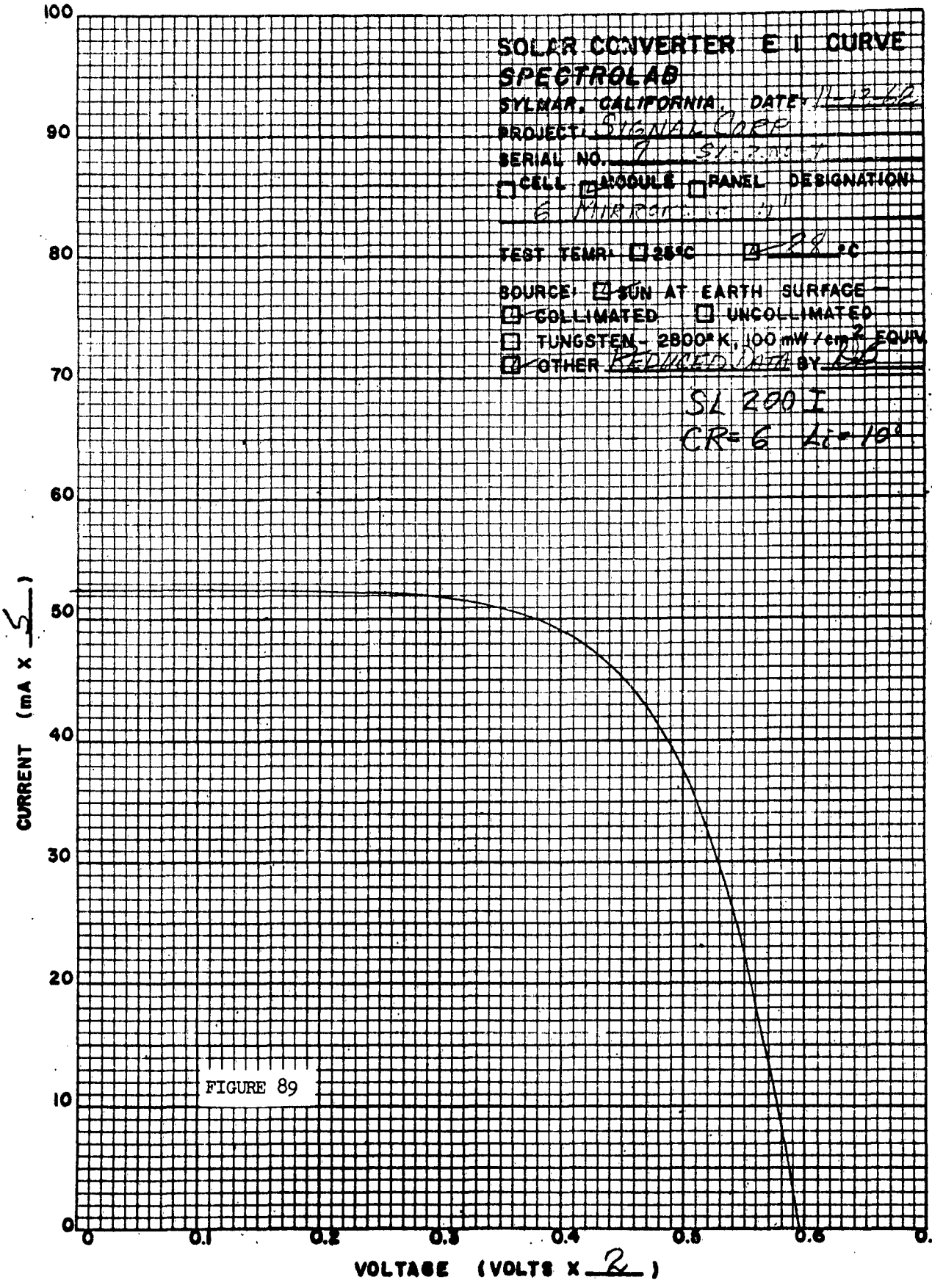

SOLAR CONVERTER E I CURVE
SPECTROLAB
SYLMAR, CALIFORNIA. DATE: 11-12-62
PROJECT: SIGNAL CORP
SERIAL NO. 2 SL 200 I
☐ CELL ☒ MODULE ☐ PANEL DESIGNATION:
6 MIRROR
TEST TEMP: ☐ 25°C ☒ 28 °C
SOURCE: ☒ SUN AT EARTH SURFACE
☐ COLLIMATED ☐ UNCOLLIMATED
☐ TUNGSTEN - 2800° K, 100 mW/cm² EQUIV.
☒ OTHER REDUCED WITH BY LAB
SL 200 I
CR=6 Ai=10°
CURRENT (mA X 5)
VOLTAGE (VOLTS X 2)
0
10
20
30
40
50
60
70
80
90
100
0
0.1
0.2
0.3
0.4
0.5
0.6
0.7

FIGURE 89

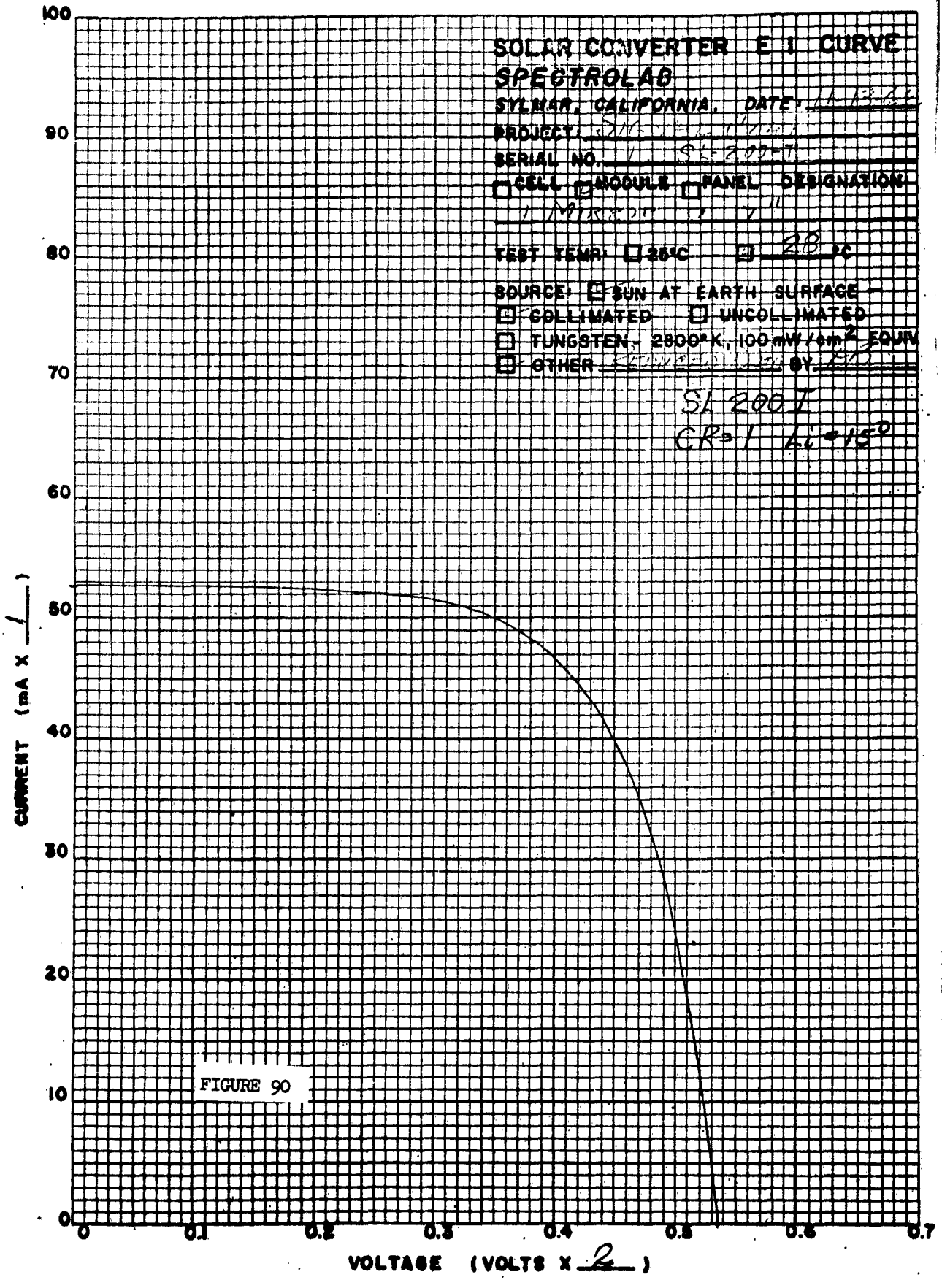

SOLAR CONVERTER E I CURVE
SPECTROLAB
SYLMAR, CALIFORNIA. DATE:
PROJECT:
SERIAL NO.
CELL MODULE PANEL DESIGNATION:
TEST TEMP: 25°C 28 °C
SOURCE: SUN AT EARTH SURFACE
COLLIMATED UNCOLLIMATED
TUNGSTEN, 2800°K, 100 mW/cm² EQUIV.
OTHER BY
SL 200 T
CR=1 Ai=15°
CURRENT (mA X 1)
VOLTAGE (VOLTS X 2)
0
10
20
30
40
50
60
70
80
90
100
0.1
0.2
0.3
0.4
0.5
0.6
0.7

FIGURE 90

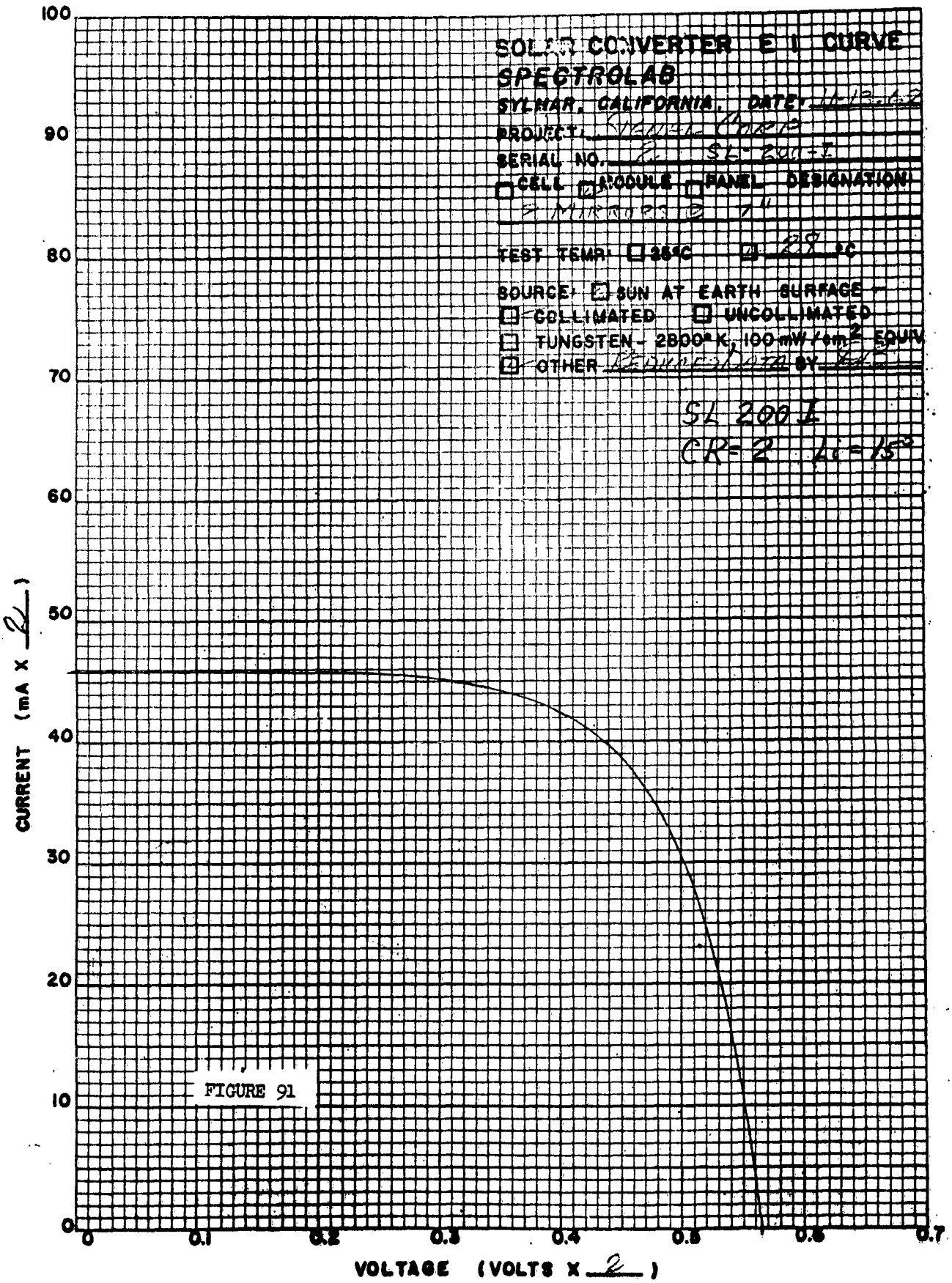

SOLAR CONVERTER E I CURVE
SPECTROLAB
SYLMAR, CALIFORNIA. DATE:
PROJECT:
SERIAL NO.
CELL MODULE PANEL DESIGNATION:
TEST TEMP: 25°C
SOURCE: SUN AT EARTH SURFACE
COLLIMATED UNCOLLIMATED
TUNGSTEN - 2800° K, 100 mW/cm² EQUIV
OTHER
SL 200 L
CR=2 Ai=15
CURRENT (mA X 2)
VOLTAGE (VOLTS X 2)
100
90
80
70
60
50
40
30
20
10
0
0
0.1
0.2
0.3
0.4
0.5
0.6
0.7

FIGURE 91

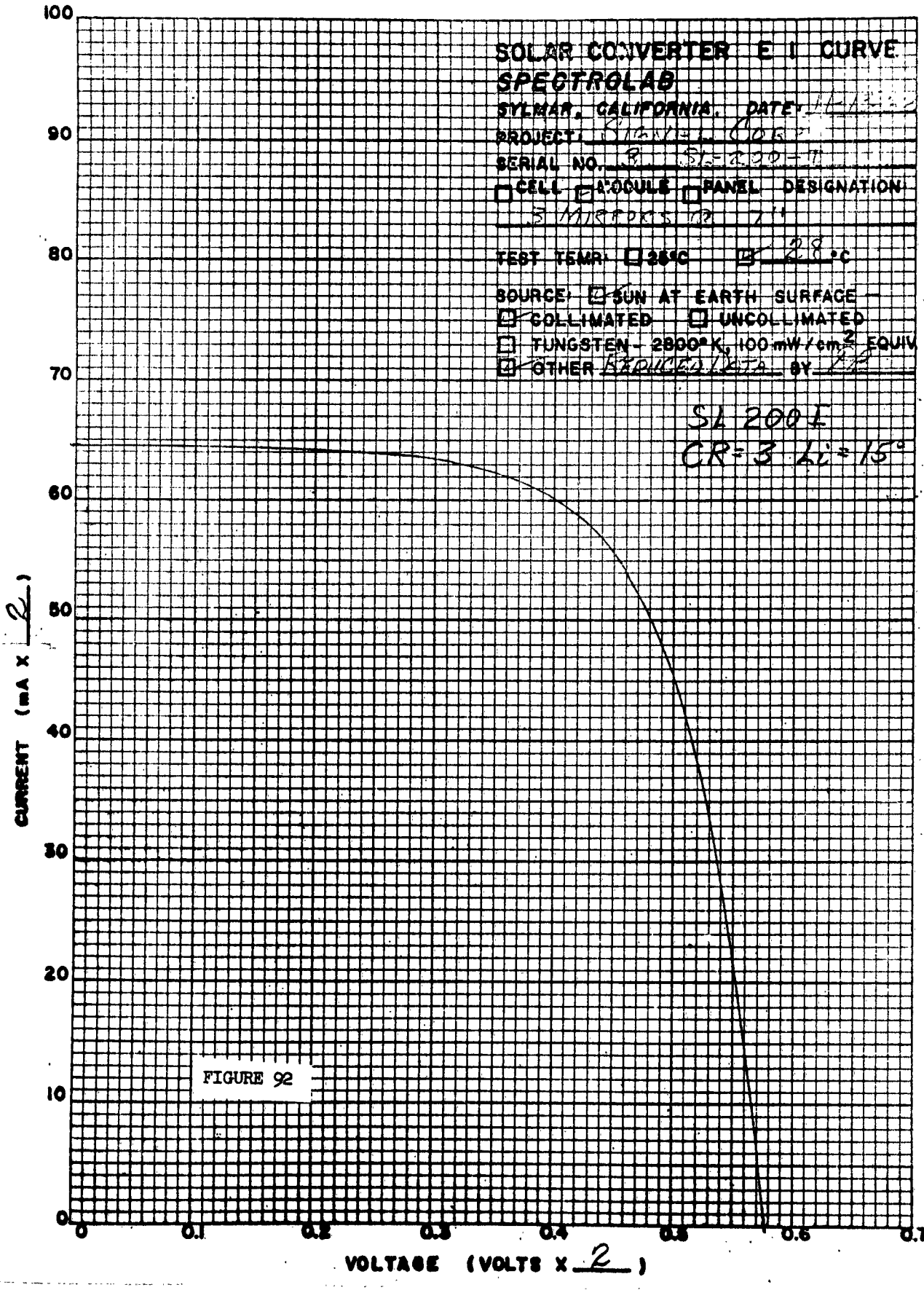

SOLAR CONVERTER E I CURVE
SPECTROLAB
SYLMAR, CALIFORNIA. DATE:
PROJECT:
SERIAL NO.
☐ CELL ☐ COUPON ☐ PANEL DESIGNATION
TEST TEMP: ☐ 25°C ☐ °C
SOURCE: ☐ SUN AT EARTH SURFACE —
☐ COLLIMATED ☐ UNCOLLIMATED
☐ TUNGSTEN - 2800°K, 100 mW/cm² EQUIV
☐ OTHER BALLOON DATA BY
SI 200 E
CR=3 Li=15°
CURRENT (mA X 2)
VOLTAGE (VOLTS X 2)
0
10
20
30
40
50
60
70
80
90
100
0.1
0.2
0.3
0.4
0.5
0.6
0.7

FIGURE 92

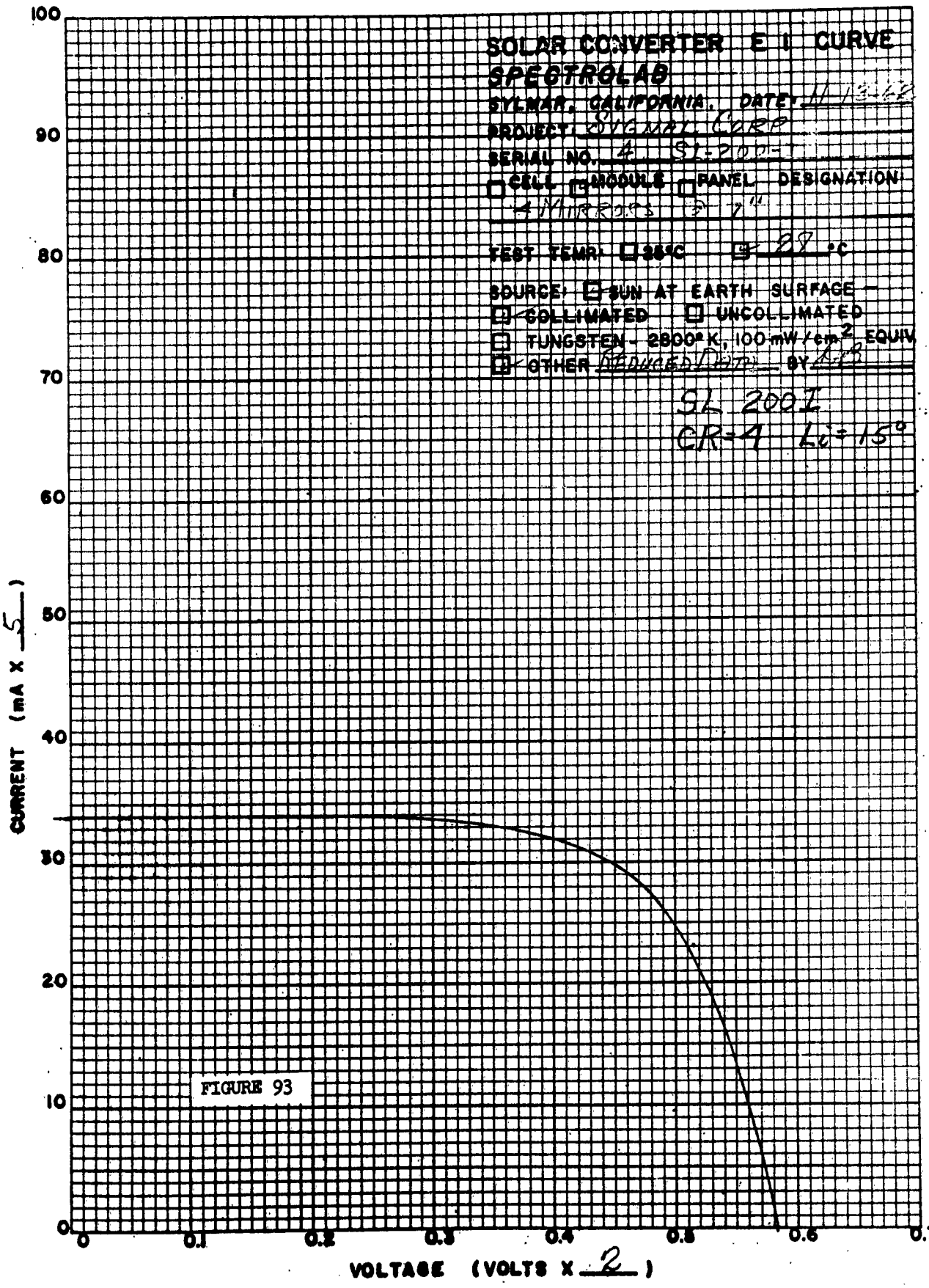

SOLAR CONVERTER E I CURVE
SPECTROLAB
SYLMAR, CALIFORNIA. DATE: 11/13/62
PROJECT: Sylmar Cure
SERIAL NO. 4 SL-200I-
☐ CELL ☒ MODULE ☐ PANEL DESIGNATION:
4 Mirrors 2" x 2"
TEST TEMP: ☐ 25°C ☒ 28 °C
SOURCE: ☒ SUN AT EARTH SURFACE —
☒ COLLIMATED ☐ UNCOLLIMATED
☐ TUNGSTEN - 2800°K, 100 mW/cm² EQUIV
☒ OTHER Reduced Data BY A.B.
SL 200I
CR=4 Li=15°
CURRENT (mA X 5)
VOLTAGE (VOLTS X 2)
100
90
80
70
60
50
40
30
20
10
0
0
0.1
0.2
0.3
0.4
0.5
0.6
0.7

FIGURE 93

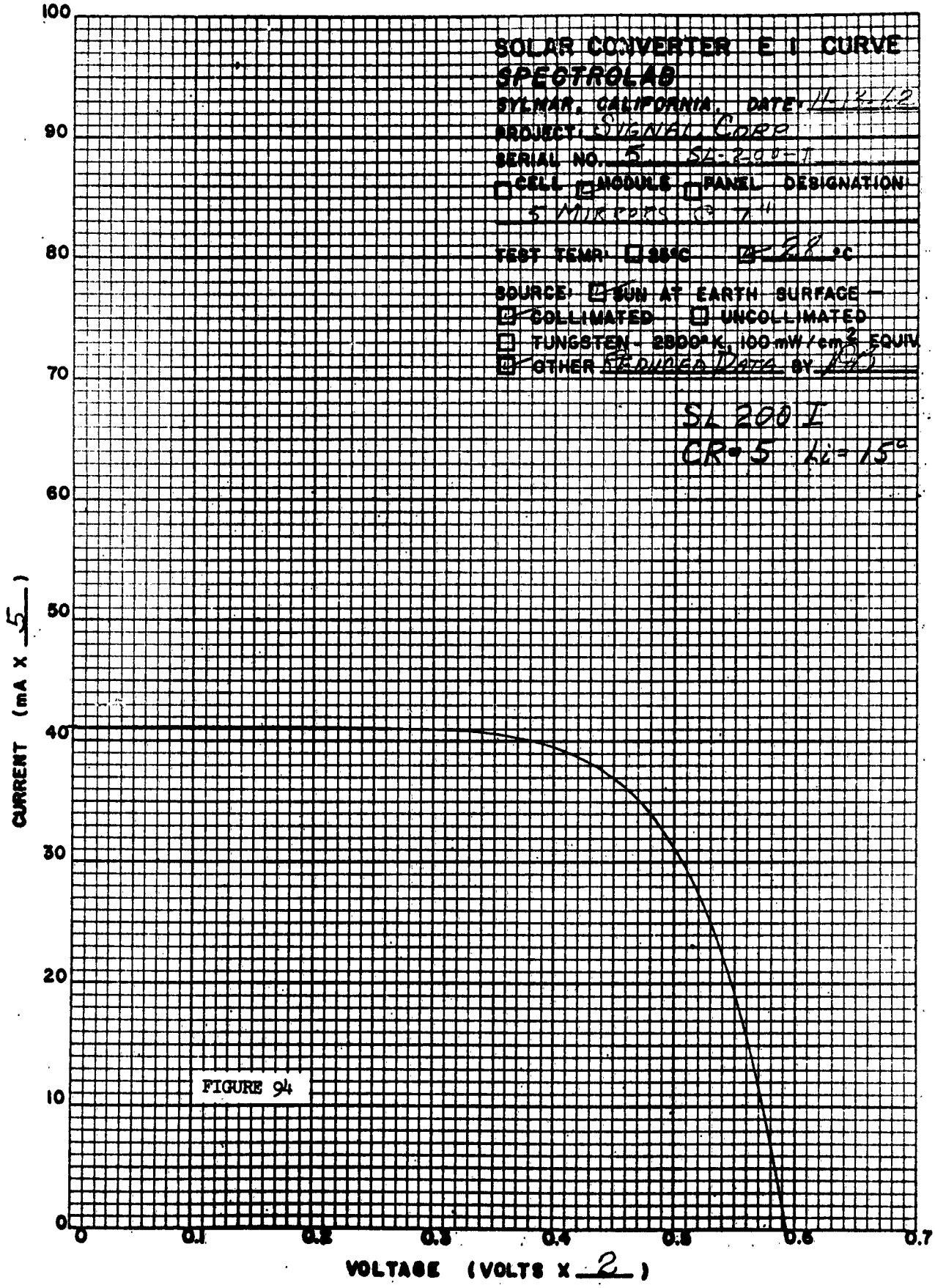

SOLAR CONVERTER E I CURVE
SPECTROLAB
SYLMAR, CALIFORNIA. DATE: 11-2-72
PROJECT: SIGNAL CORP
SERIAL NO. 5 SL-200-I
☐ CELL ☒ MODULE ☐ PANEL DESIGNATION:
5 MIRRORS @ 7"
TEST TEMP: ☐ 25°C ☒ 28 °C
SOURCE: ☒ SUN AT EARTH SURFACE —
☒ COLLIMATED ☐ UNCOLLIMATED
☐ TUNGSTEN - 2800°K, 100 mW/cm² EQUIV.
☒ OTHER REDUCED DATA BY LRC
SL 200 I
CR=5 Li=15°
CURRENT (mA X 5)
VOLTAGE (VOLTS X 2)
100
90
80
70
60
50
40
30
20
10
0
0
0.1
0.2
0.3
0.4
0.5
0.6
0.7

FIGURE 94

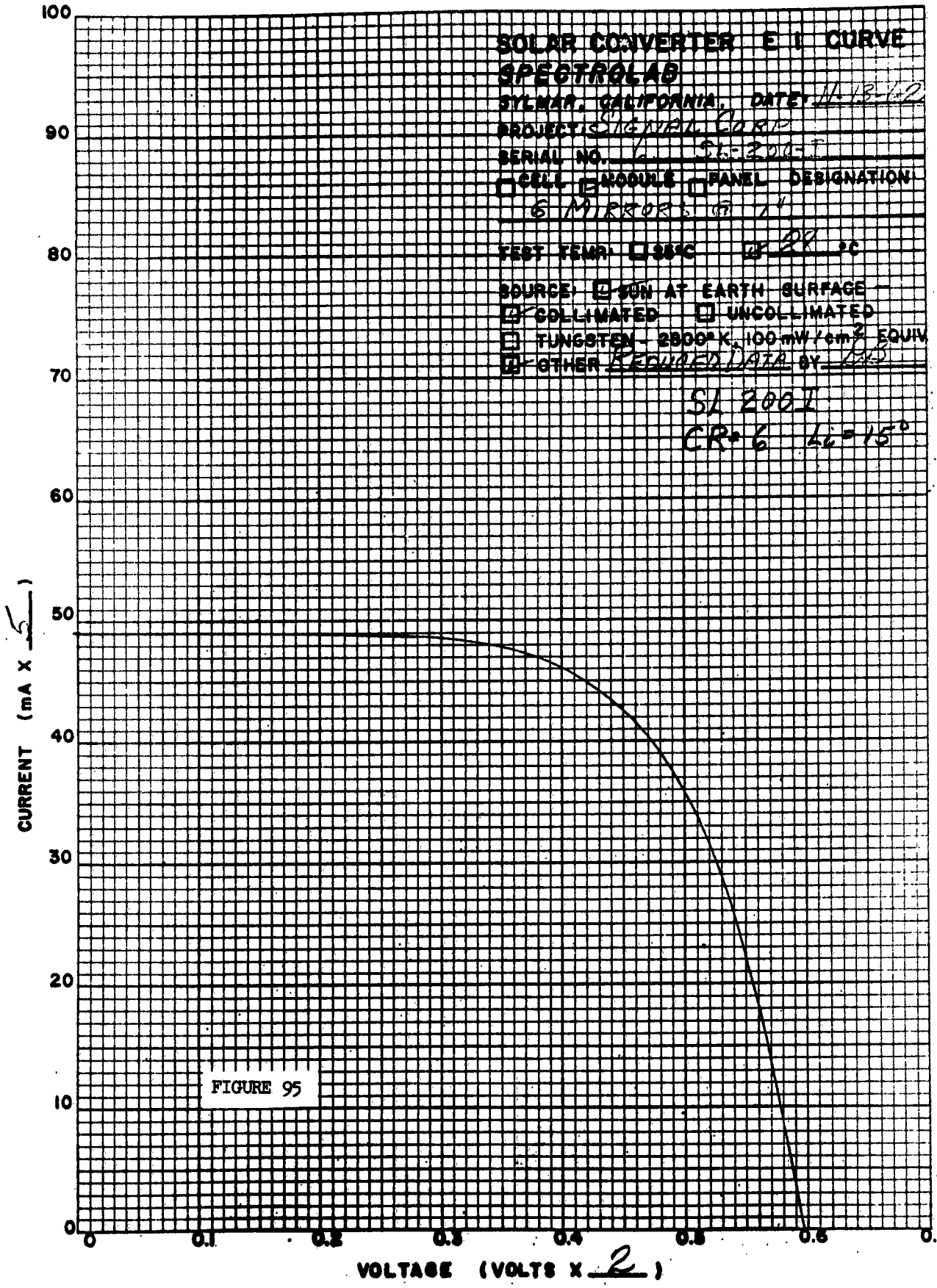

SOLAR CONVERTER E I CURVE
SPECTROLAB
SYLMAR, CALIFORNIA, DATE: 11-13-72
PROJECT: SIGMA 4 ORP
SERIAL NO. 4 SL-2001
CELL MODULE PANEL DESIGNATION
6 MIRRORS @ 1"
TEST TEMP: 25°C 22 °C
SOURCE: SUN AT EARTH SURFACE
COLLIMATED UNCOLLIMATED
TUNGSTEN - 2800°K, 100 mW/cm² EQUIV
OTHER REDUCED DATA BY
SL 2001
CR=6 4c=15°
CURRENT (mA X 5)
VOLTAGE (VOLTS X 2)
0
10
20
30
40
50
60
70
80
90
100
0
0.1
0.2
0.3
0.4
0.5
0.6
0.7

FIGURE 95

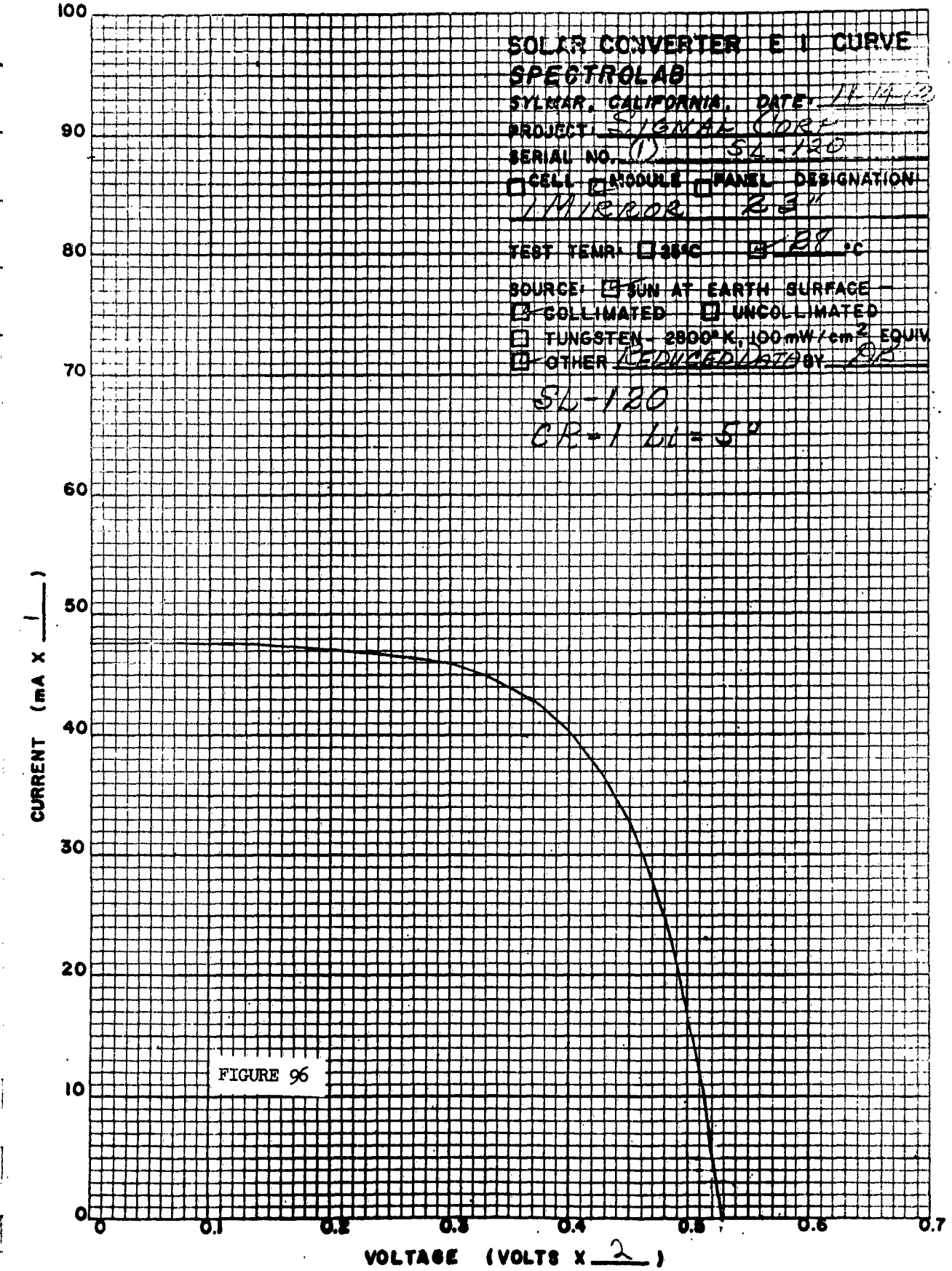

SOLAR CONVERTER E I CURVE
SPECTROLAB
SYLMAR, CALIFORNIA. DATE: 11-14-72
PROJECT: SYNCHRO CORP
SERIAL NO. 01 SL-120
☐ CELL ☒ MODULE ☐ PANEL DESIGNATION:
1 MIRROR 2 3"
TEST TEMP: ☐ 25°C ☒ 28 °C
SOURCE: ☒ SUN AT EARTH SURFACE
☒ COLLIMATED ☐ UNCOLLIMATED
☐ TUNGSTEN - 2800°K, 100 mW/cm² EQUIV
☒ OTHER REDUCED INTO BY 2
SL-120
CR-1 Li = 5°
CURRENT (mA X 1)
VOLTAGE (VOLTS X 2)
100
90
80
70
60
50
40
30
20
10
0
0
0.1
0.2
0.3
0.4
0.5
0.6
0.7

FIGURE 96

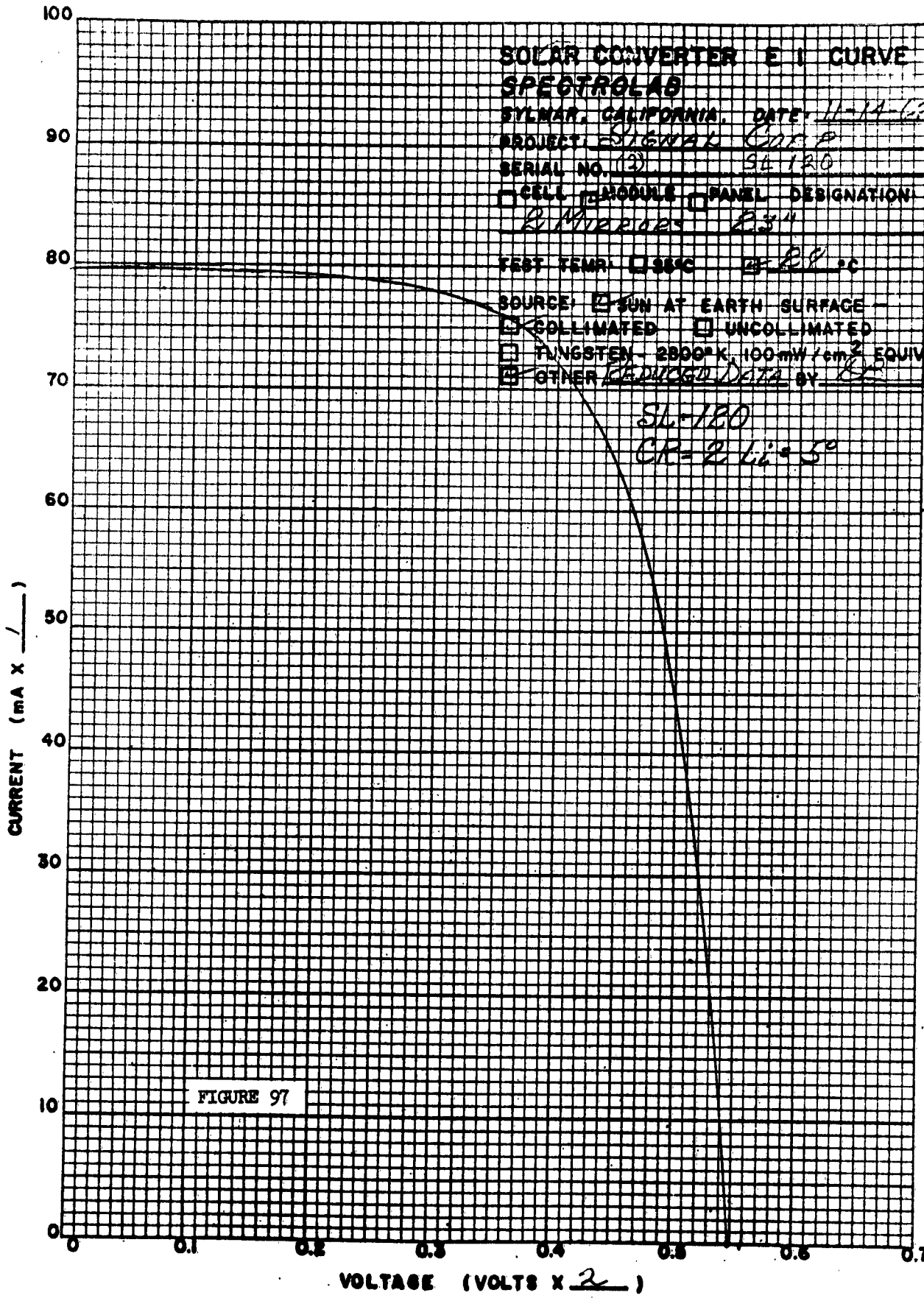

SOLAR CONVERTER E I CURVE
SPECTROLAB
SYLMAR, CALIFORNIA. DATE: 11-14-62
PROJECT: SIGMA 5 Corp
SERIAL NO. (2) SL-120
CELL MODULE PANEL DESIGNATION:
2 Mirrors 2.34
TEST TEMP: 28°C 28 °C
SOURCE: SUN AT EARTH SURFACE -
COLLIMATED UNCOLLIMATED
TUNGSTEN - 2800°K, 100 mW/cm² EQUIV
OTHER Reduced Data BY
SL-120
CR-2 Li=5°
CURRENT (mA X 1)
VOLTAGE (VOLTS X 2)
0
10
20
30
40
50
60
70
80
90
100
0.1
0.2
0.3
0.4
0.5
0.6
0.7

FIGURE 97

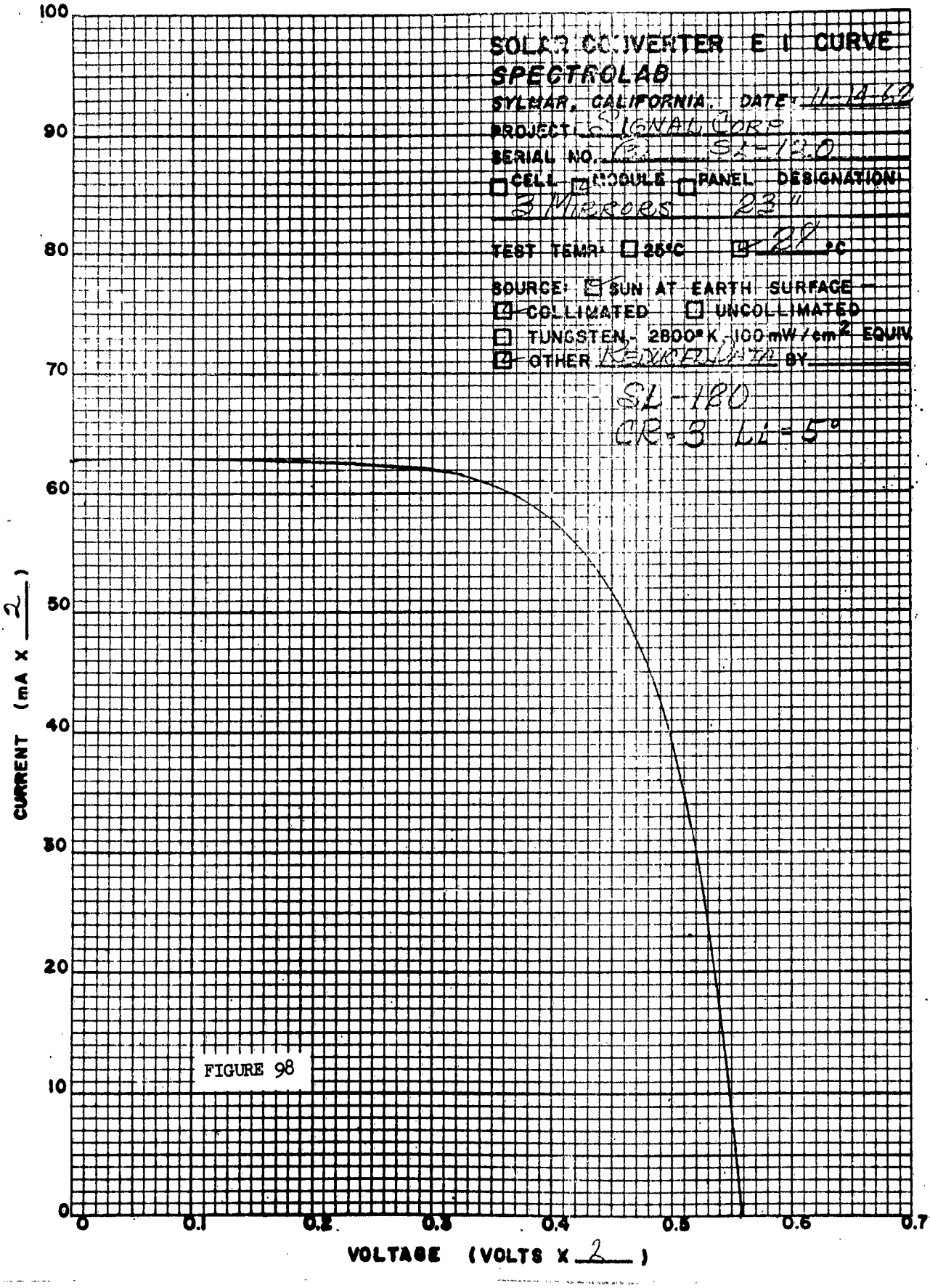

SOLAR CONVERTER E I CURVE
SPECTROLAB
SYLMAR, CALIFORNIA. DATE 11-14-62
PROJECT SIGNAL CORPS
SERIAL NO. SL-180
☐ CELL ☒ MODULE ☐ PANEL DESIGNATION
3 MICRONS 23"
TEST TEMP: ☐ 25°C ☒ 28 °C
SOURCE: ☒ SUN AT EARTH SURFACE —
☒ COLLIMATED ☐ UNCOLLIMATED
☐ TUNGSTEN - 2800°K - 100 mW/cm² EQUIV.
☒ OTHER KENTRON BY
SL-180
CR-3 Li=5°
CURRENT (mA x 2)
VOLTAGE (VOLTS x 2)
100
90
80
70
60
50
40
30
20
10
0
0
0.1
0.2
0.3
0.4
0.5
0.6
0.7

FIGURE 98

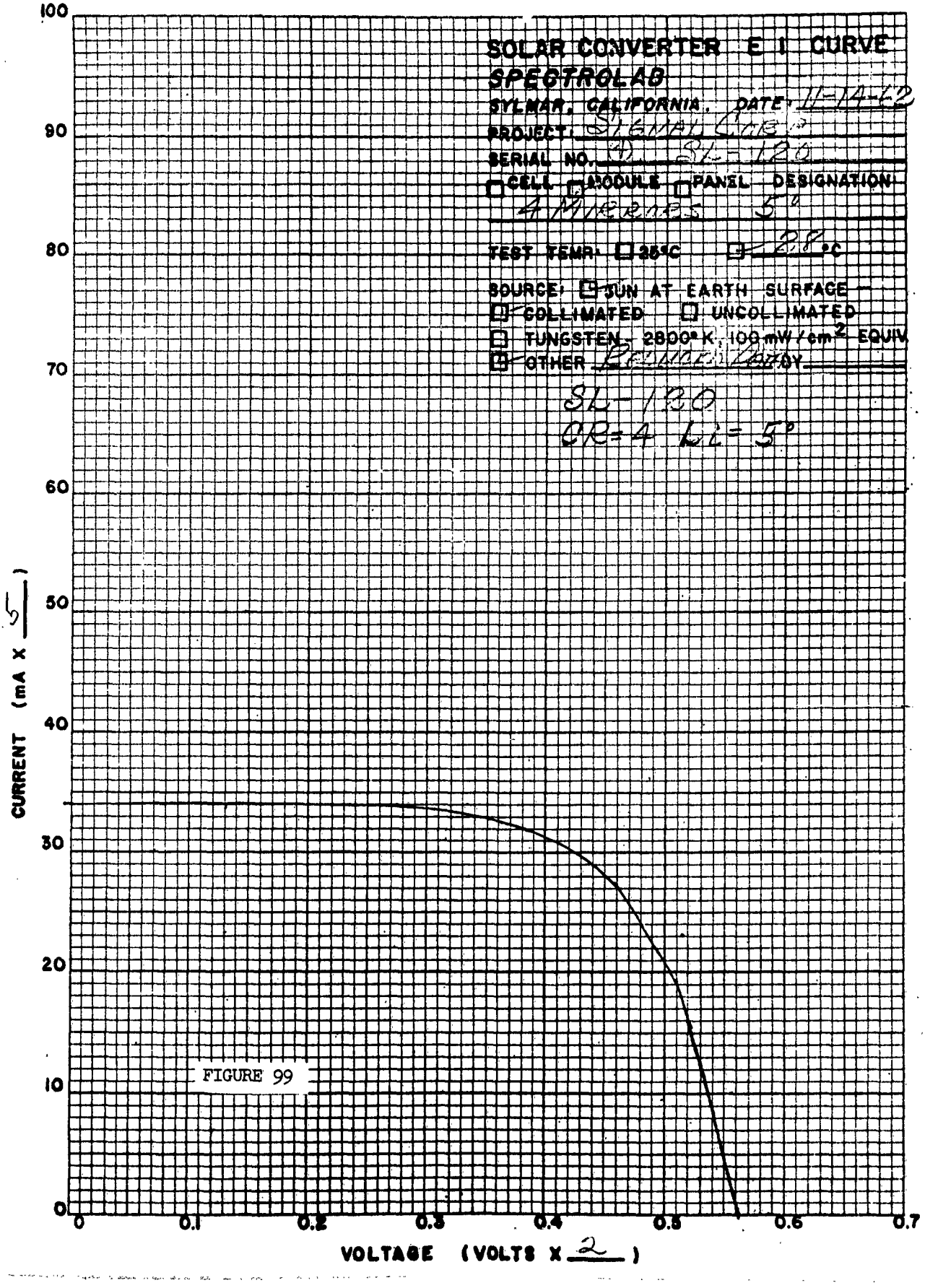

SOLAR CONVERTER E I CURVE
SPECTROLAB
SYLMAR, CALIFORNIA. DATE: 11-14-62
PROJECT: Sylmar Cells
SERIAL NO. (4) SL-120
☐ CELL ☐ MODULE ☐ PANEL DESIGNATION:
4 Minerals 5°
TEST TEMP: ☐ 25°C ☒ 28 °C
SOURCE: ☒ SUN AT EARTH SURFACE
☐ COLLIMATED ☐ UNCOLLIMATED
☐ TUNGSTEN - 2800° K, 100 mW/cm² EQUIV.
☒ OTHER Beam Laboy
SL-130
OR=4 Li=5°
CURRENT (mA X 5)
VOLTAGE (VOLTS X 2)
100
90
80
70
60
50
40
30
20
10
0
0
0.1
0.2
0.3
0.4
0.5
0.6
0.7

FIGURE 99

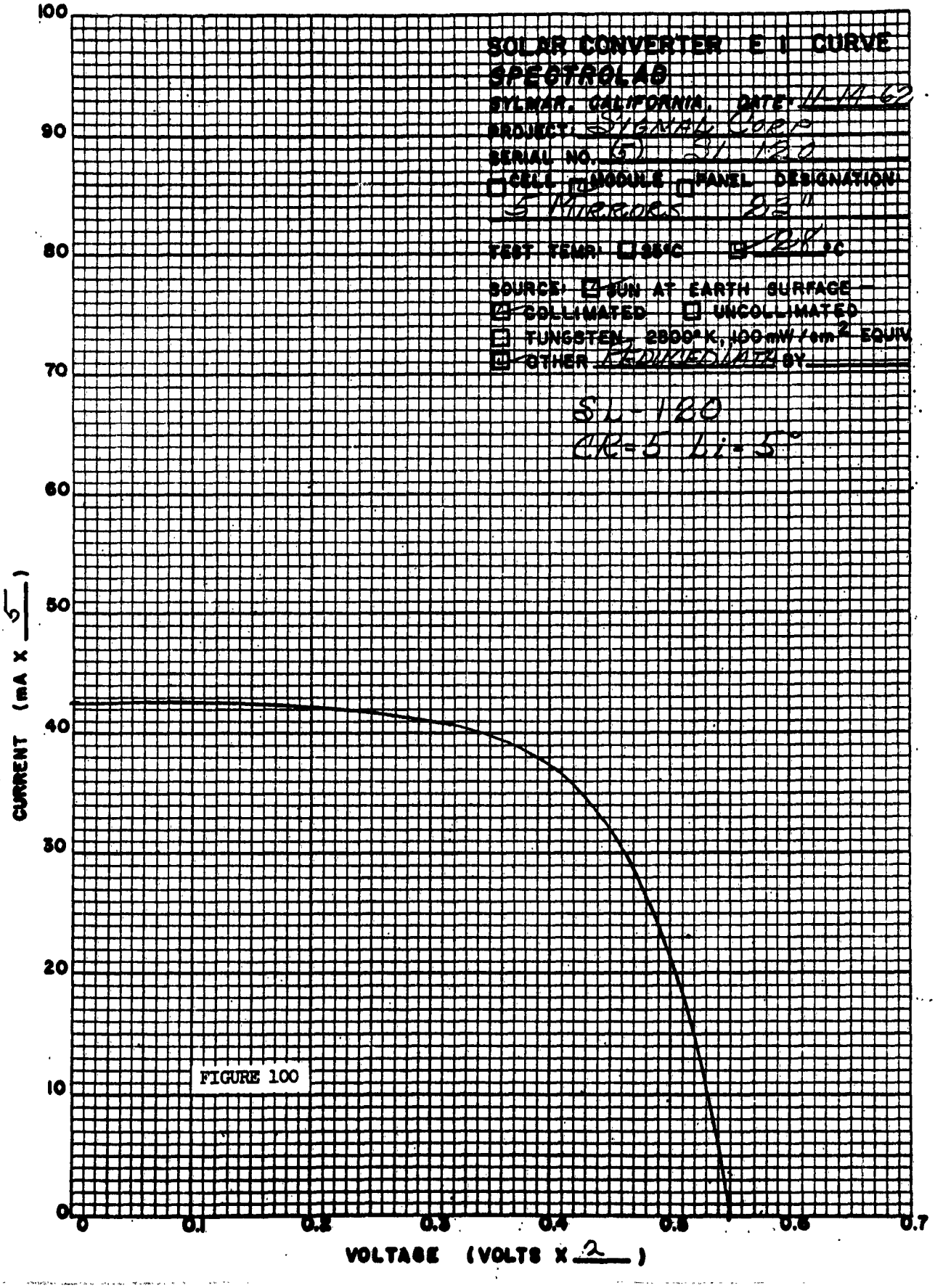

SOLAR CONVERTER E I CURVE
SPECTROLAB
SYLMAR, CALIFORNIA. DATE: 4-14-62
PRODUCT: Sigma Corp
SERIAL NO. (5) SL 120
☐ CELL ☒ MODULE ☐ PANEL DESIGNATION:
5 Micros 2 Ω
TEST TEMP: ☐ 25°C ☒ 28° C
SOURCE: ☒ SUN AT EARTH SURFACE —
☒ COLLIMATED ☐ UNCOLLIMATED
☐ TUNGSTEN, 2800°K, 100 mW/cm² EQUIV.
☐ OTHER EQUIVALENT BY
SL-120
AR-5 Li-5
CURRENT (mA X 5)
VOLTAGE (VOLTS X 2)
100
90
80
70
60
50
40
30
20
10
0
0
0.1
0.2
0.3
0.4
0.5
0.6
0.7

FIGURE 100

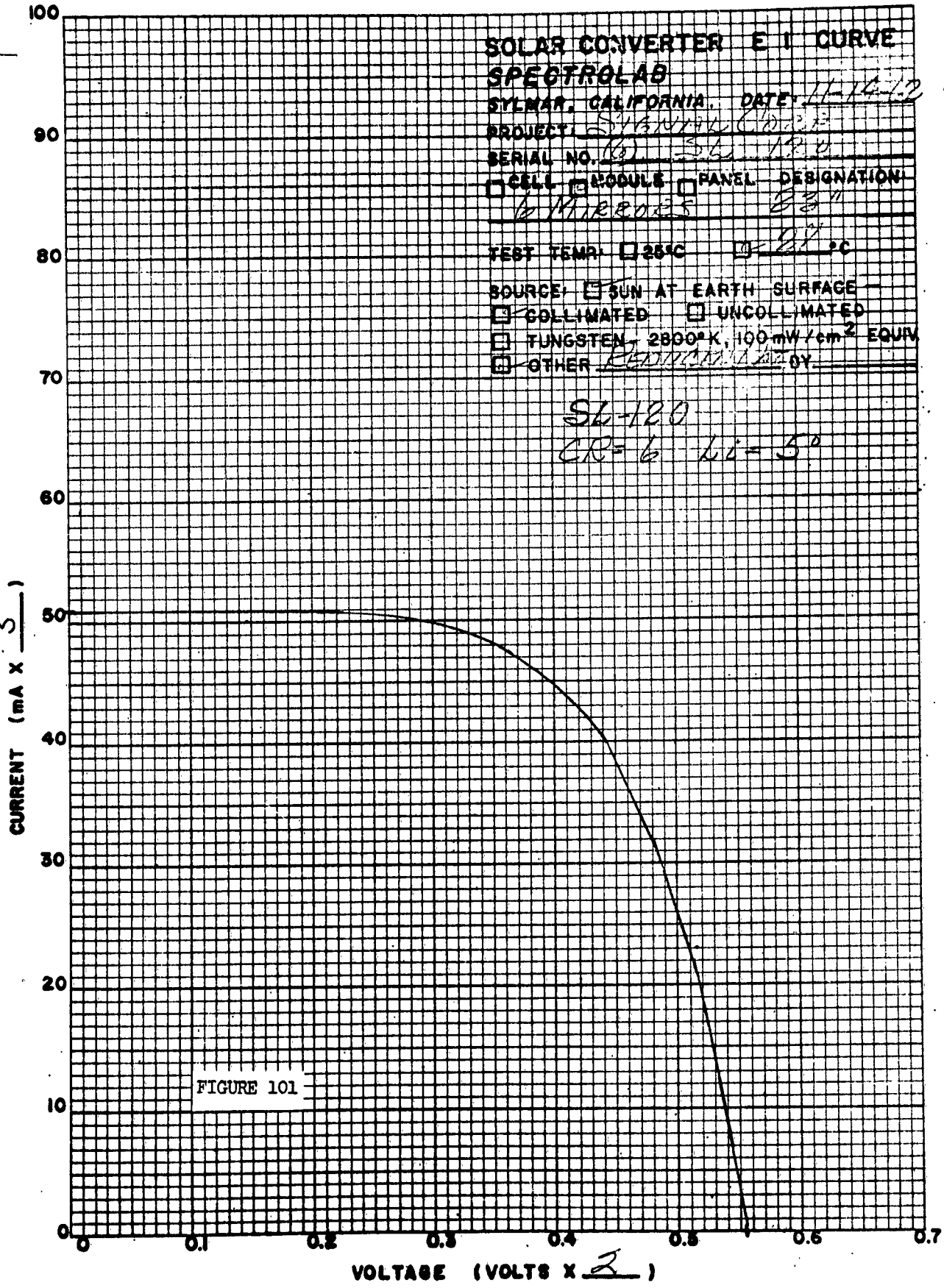

SOLAR CONVERTER E I CURVE
SPECTROLAB
SYLMAR, CALIFORNIA. DATE: 11-14-12
PROJECT:
SERIAL NO.
CELL MODULE PANEL DESIGNATION:
TEST TEMP: 25°C °C
SOURCE: SUN AT EARTH SURFACE
COLLIMATED UNCOLLIMATED
TUNGSTEN 2800°K, 100 mW/cm² EQUIV.
OTHER
SL-120
CR= 6 Li= 5°
CURRENT (mA X 5)
VOLTAGE (VOLTS X 2)
100
90
80
70
60
50
40
30
20
10
0
0
0.1
0.2
0.3
0.4
0.5
0.6
0.7

FIGURE 101

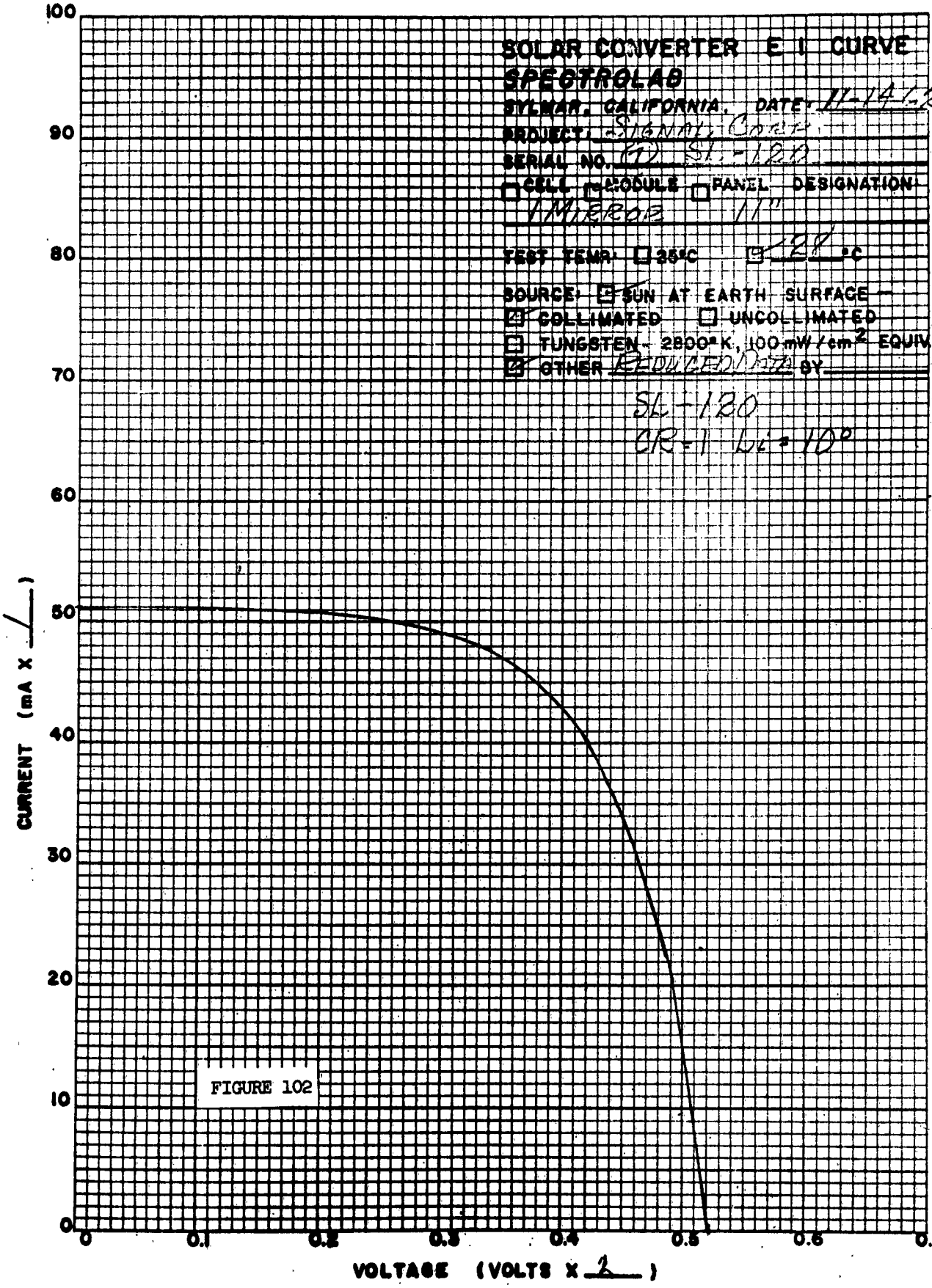

SOLAR CONVERTER E I CURVE
SPECTROLAB
SYLMAR, CALIFORNIA. DATE: 11-14-62
PROJECT: SIGMA, Corp.
SERIAL NO. 60 SL-120
☐ CELL ☐ MODULE ☐ PANEL DESIGNATION:
1 MICRO 11"
TEST TEMP: ☐ 25°C ☑ 28 °C
SOURCE: ☑ SUN AT EARTH SURFACE —
☑ COLLIMATED ☐ UNCOLLIMATED
☐ TUNGSTEN - 2800°K, 100 mW/cm² EQUIV.
☑ OTHER REDUCED DATA BY
SL-120
OR=1 Li=10°
CURRENT (mA X 1)
VOLTAGE (VOLTS X 1)
0
10
20
30
40
50
60
70
80
90
100
0
0.1
0.2
0.3
0.4
0.5
0.6
0.7

FIGURE 102

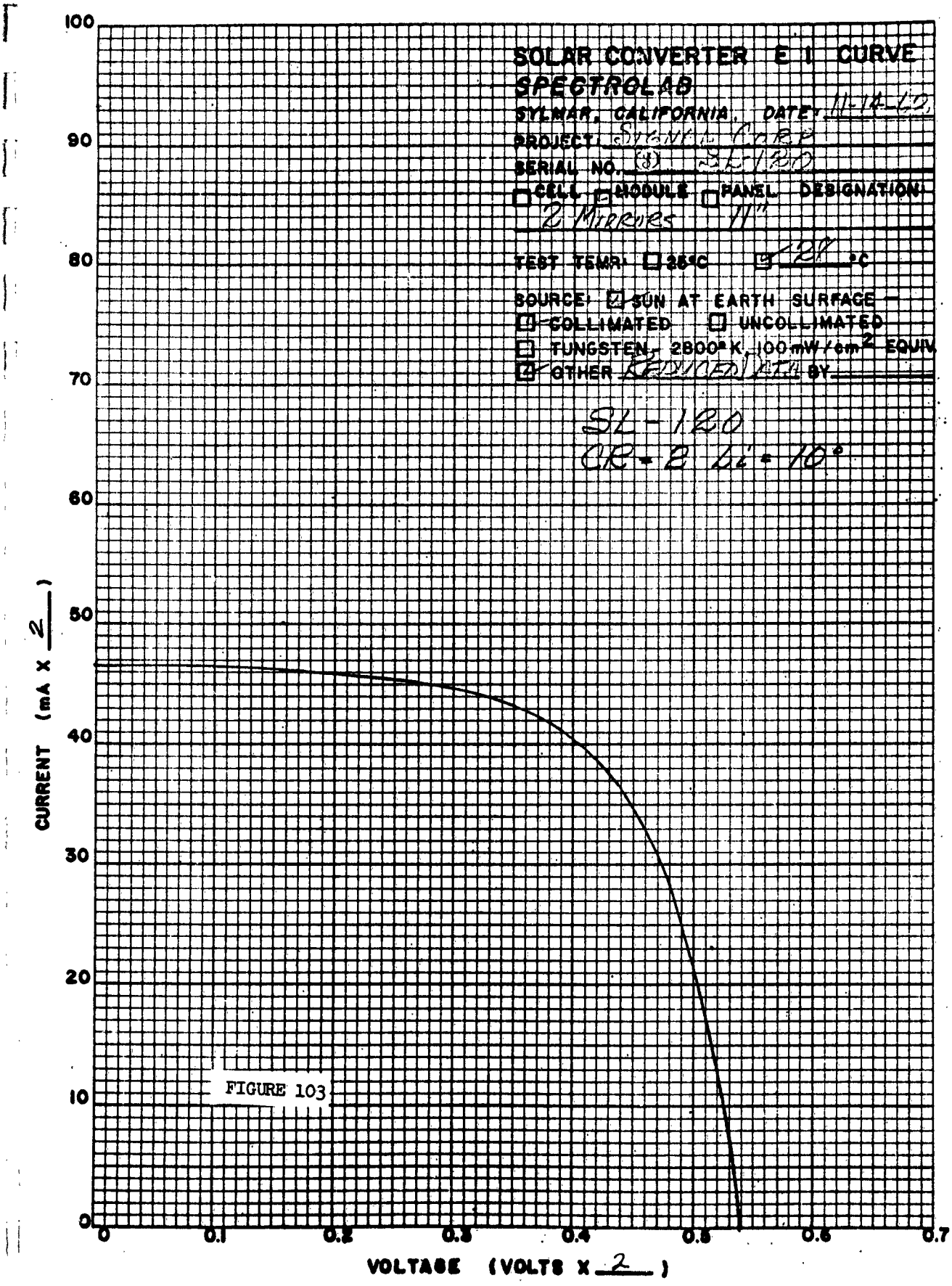

SOLAR CONVERTER E I CURVE
SPECTROLAB
SYLMAR, CALIFORNIA. DATE: 11-14-69
PROJECT: Synch. Knee
SERIAL NO. (8) SL-180
☐ CELL ☐ MODULE ☐ PANEL DESIGNATION:
2 Mirrors 11"
TEST TEMP: ☐ 25°C ☑ 28 °C
SOURCE: ☑ SUN AT EARTH SURFACE —
☐ COLLIMATED ☐ UNCOLLIMATED
☐ TUNGSTEN, 2800°K, 100 mW/cm² EQUIV.
☑ OTHER REDUCED INTO BY
SL-180
CR-2 Ai = 10°
CURRENT (mA X 2)
VOLTAGE (VOLTS X 2)
100
90
80
70
60
50
40
30
20
10
0
0
0.1
0.2
0.3
0.4
0.5
0.6
0.7

FIGURE 103

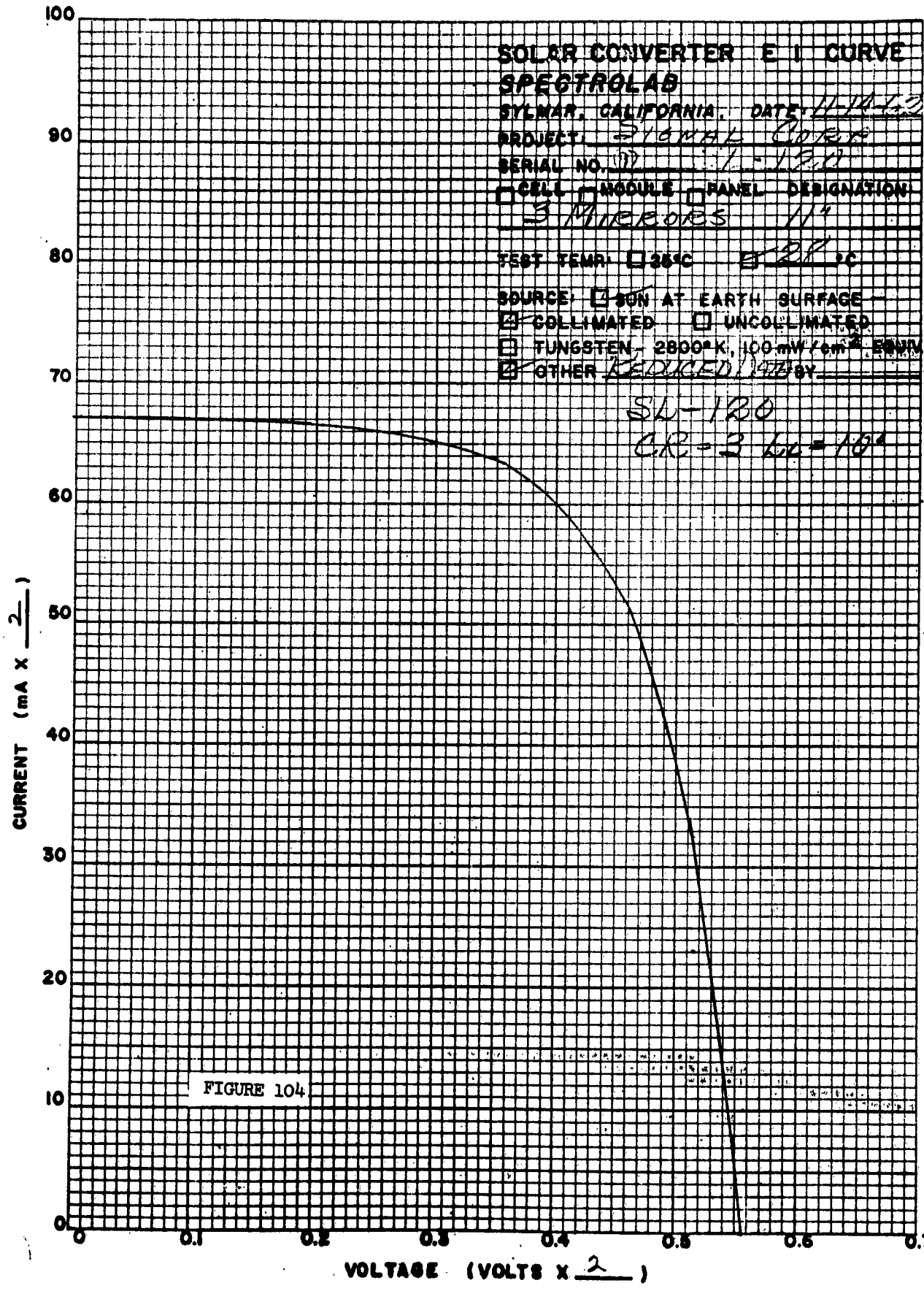

SOLAR CONVERTER E I CURVE
SPECTROLAB
SYLMAR, CALIFORNIA. DATE: 11-14-62
PROJECT: Signal Corps
SERIAL NO. M 1-1522
☐ CELL ☐ MODULE ☐ PANEL DESIGNATION
3 Mineroes 1N4
TEST TEMP: ☐ 35°C ☑ 28 °C
SOURCE: ☐ SUN AT EARTH SURFACE —
☑ COLLIMATED ☐ UNCOLLIMATED
☐ TUNGSTEN - 2800°K, 100 mW/cm² EQUIV.
☑ OTHER REDUCED Voltage
SL-120
CR-3 Ku = 10⁴
CURRENT (mA X 2)
VOLTAGE (VOLTS X 2)
0
10
20
30
40
50
60
70
80
90
100
0.1
0.2
0.3
0.4
0.5
0.6
0.7

FIGURE 104

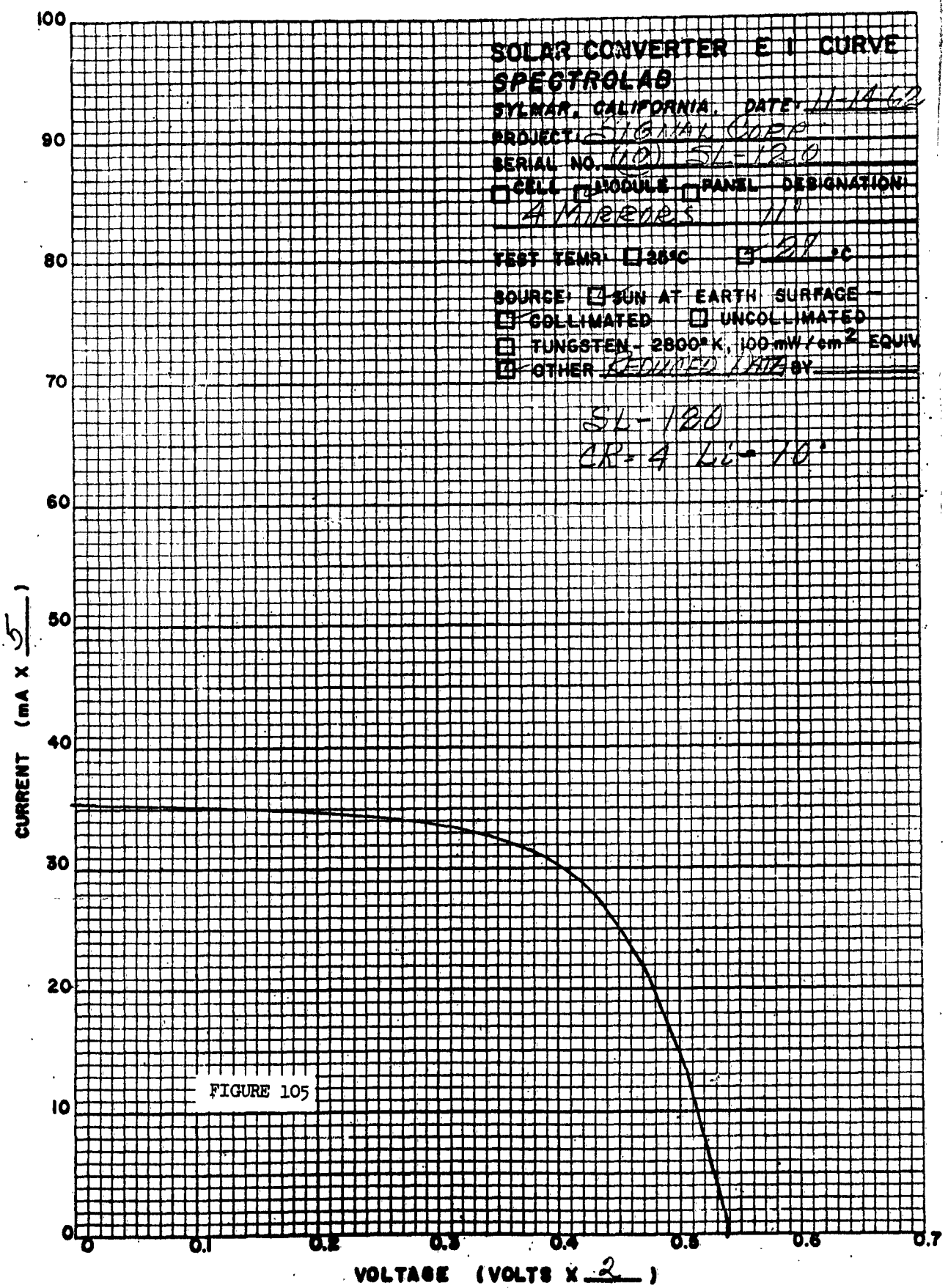

SOLAR CONVERTER E I CURVE
SPECTROLAB
SYLMAR, CALIFORNIA. DATE: 11-14-62
PROJECT: SOLAR CORP
SERIAL NO. (10) SL-120
☐ CELL ☒ MODULE ☐ PANEL DESIGNATION:
4 Minerals 11"
TEST TEMP: ☐ 25°C ☒ 21 °C
SOURCE: ☒ SUN AT EARTH SURFACE
☐ COLLIMATED ☐ UNCOLLIMATED
☐ TUNGSTEN - 2800° K, 100 mW/cm² EQUIV
☒ OTHER REDUCED LIGHT BY
SL-120
AR=4 Li=10'
CURRENT (mA X 5)
VOLTAGE (VOLTS X 2)
100
90
80
70
60
50
40
30
20
10
0
0
0.1
0.2
0.3
0.4
0.5
0.6
0.7

FIGURE 105

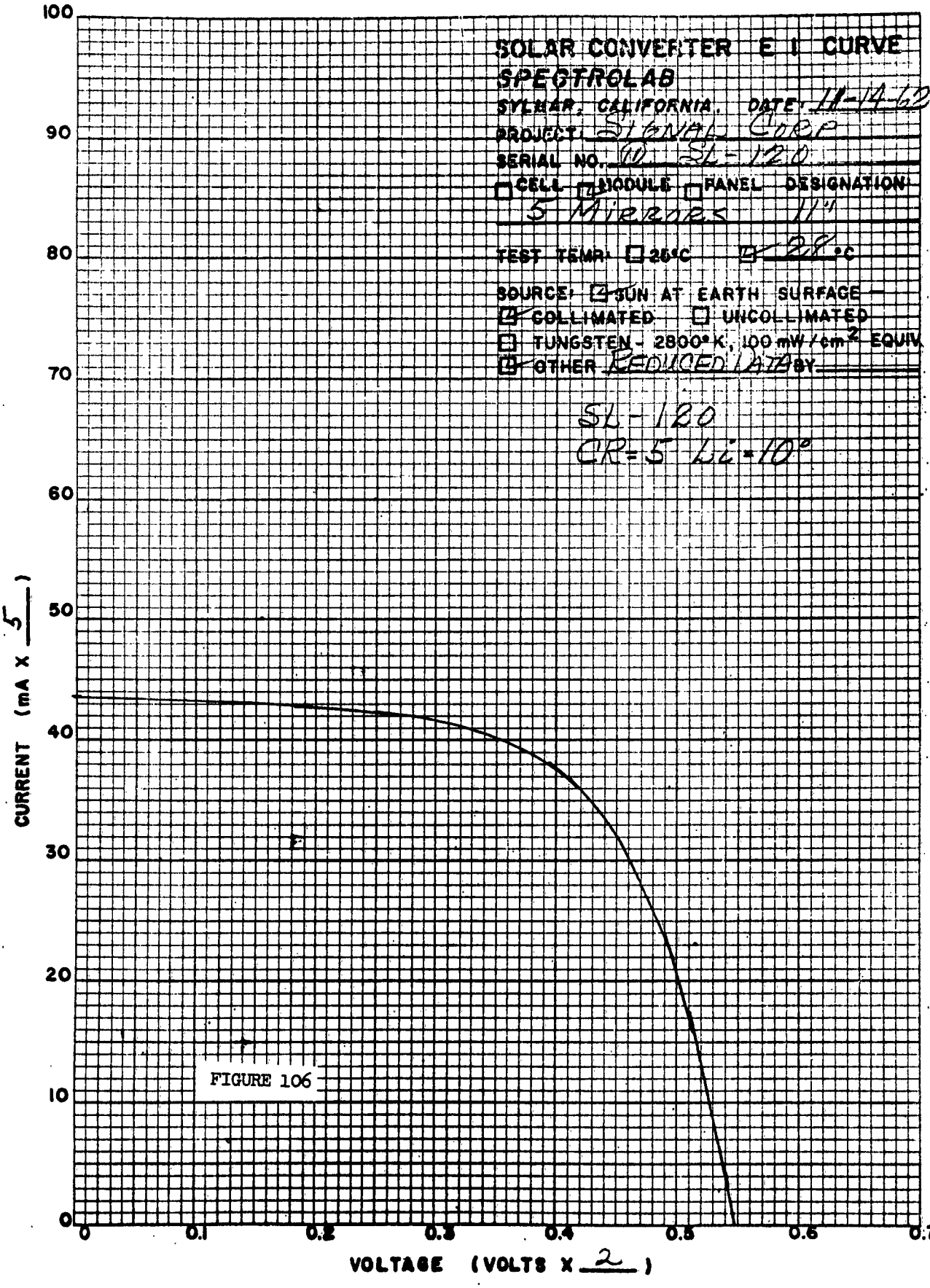

SOLAR CONVERTER E I CURVE
SPECTROLAB
SYLMAR, CALIFORNIA. DATE: 11-14-62
PROJECT: Signal Corp
SERIAL NO. 10 SL-120
CELL MODULE PANEL DESIGNATION:
5 Mirrors 11"
TEST TEMP: 25°C 28°C
SOURCE: SUN AT EARTH SURFACE
COLLIMATED UNCOLLIMATED
TUNGSTEN - 2800°K, 100 mW/cm² EQUIV.
OTHER REDUCED DATA BY
SL-120
CR=5 Li=10°
CURRENT (mA x 5)
VOLTAGE (VOLTS x 2)
0
10
20
30
40
50
60
70
80
90
100
0
0.1
0.2
0.3
0.4
0.5
0.6
0.7

FIGURE 106

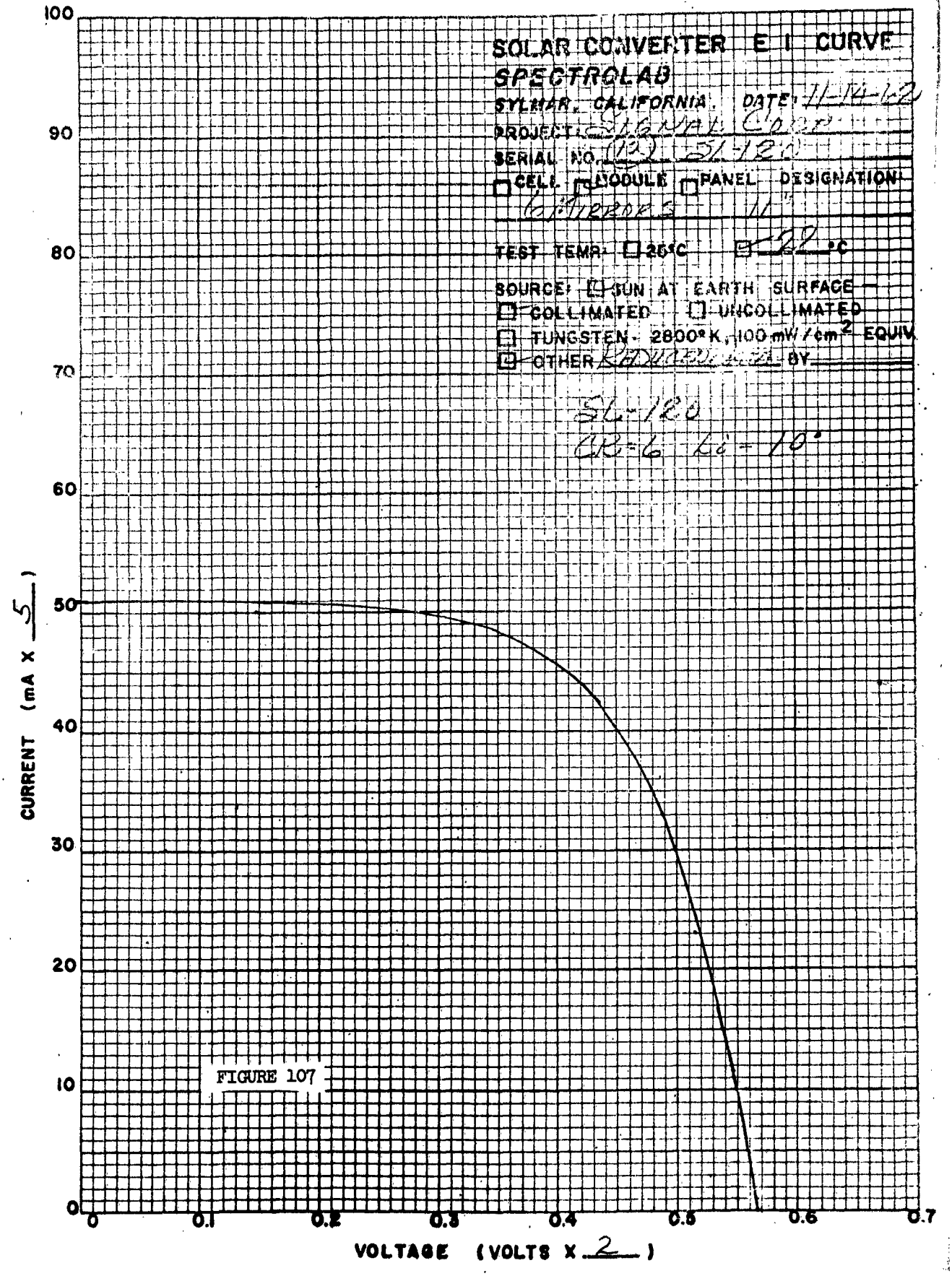

SOLAR CONVERTER E I CURVE
SPECTROLAB
SYLMAR, CALIFORNIA
DATE: 11-14-62
PROJECT: Signal Corps
SERIAL NO. (12) SL-120
CELL MODULE PANEL DESIGNATION:
California 5 11"
TEST TEMP: 25°C 62 °C
SOURCE: SUN AT EARTH SURFACE
COLLIMATED UNCOLLIMATED
TUNGSTEN - 2800°K, 100 mW/cm² EQUIV.
OTHER Xenon arc BY
SL-120
AR=6 Li=10°
CURRENT (mA X 5)
VOLTAGE (VOLTS X 2)
0
10
20
30
40
50
60
70
80
90
100
0
0.1
0.2
0.3
0.4
0.5
0.6
0.7

FIGURE 107

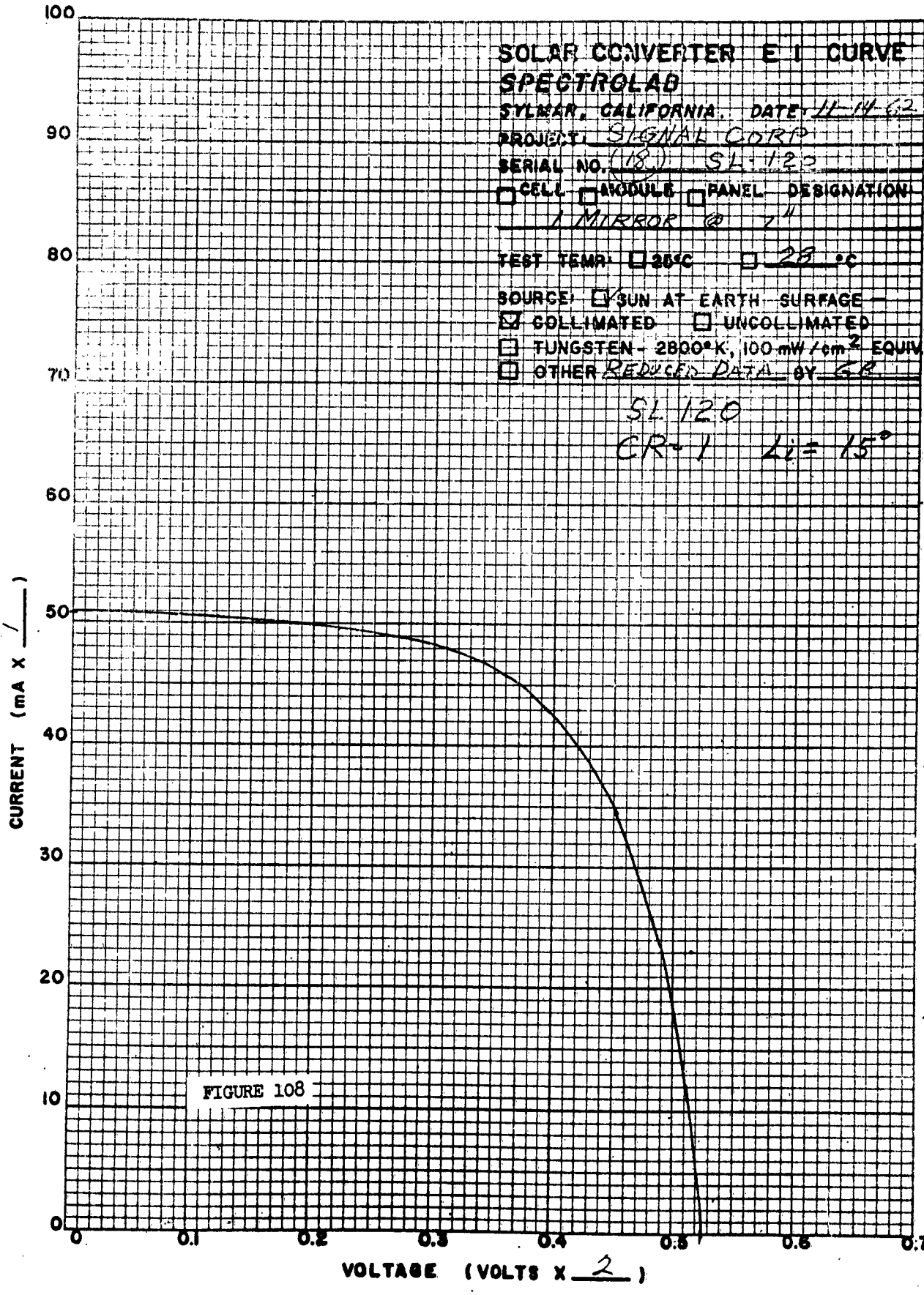

SOLAR CONVERTER E I CURVE
SPECTROLAB
SYLMAR, CALIFORNIA. DATE 11-14-62
PROJECT: SIGNAL CORP
SERIAL NO. (18) SL-120
☐ CELL ☐ MODULE ☐ PANEL DESIGNATION
1 MIRROR @ 7"
TEST TEMP: ☐ 25°C ☐ 28 °C
SOURCE: ☐ SUN AT EARTH SURFACE
☑ COLLIMATED ☐ UNCOLLIMATED
☐ TUNGSTEN - 2800°K, 100 mW/cm² EQUIV
☐ OTHER REDUCED DATA BY GR
SL 120
CR-1 Li = 15°
CURRENT (mA X 1)
VOLTAGE (VOLTS X 2)
100
90
80
70
60
50
40
30
20
10
0
0
0.1
0.2
0.3
0.4
0.5
0.6
0.7

FIGURE 108

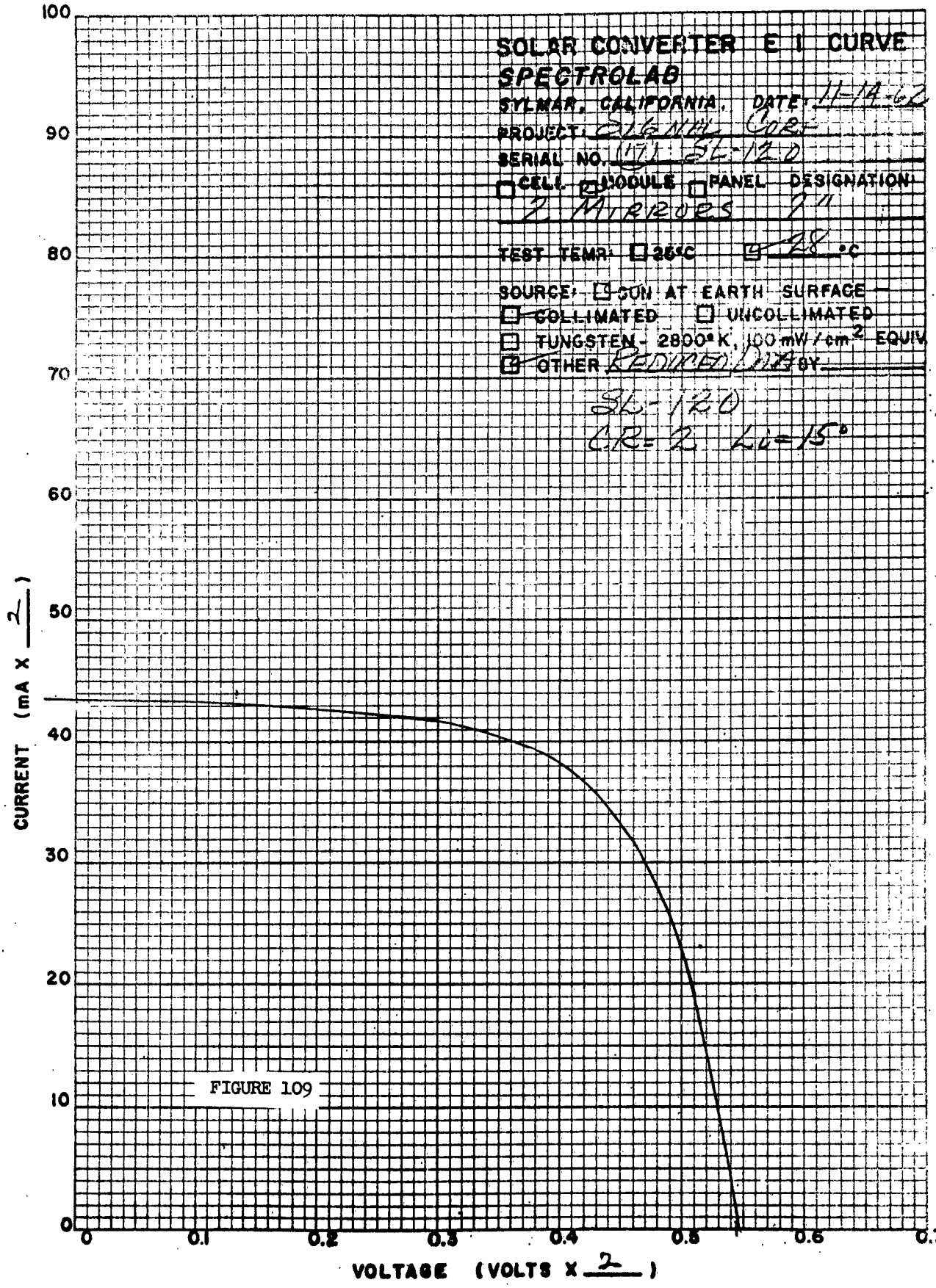

SOLAR CONVERTER E I CURVE
SPECTROLAB
SYLMAR, CALIFORNIA. DATE: 11-14-62
PROJECT: GOES
SERIAL NO. 171 SL-120
CELL MODULE PANEL DESIGNATION:
2 MIRRORS 1"
TEST TEMP: 25°C 28 °C
SOURCE: SUN AT EARTH SURFACE
COLLIMATED UNCOLLIMATED
TUNGSTEN - 2800°K, 100 mW/cm² EQUIV.
OTHER REDUCED DATA BY
SL-120
C.R.= 2 Lu=15°
CURRENT (mA X 2)
VOLTAGE (VOLTS X 2)
100
90
80
70
60
50
40
30
20
10
0
0
0.1
0.2
0.3
0.4
0.5
0.6
0.7

FIGURE 109

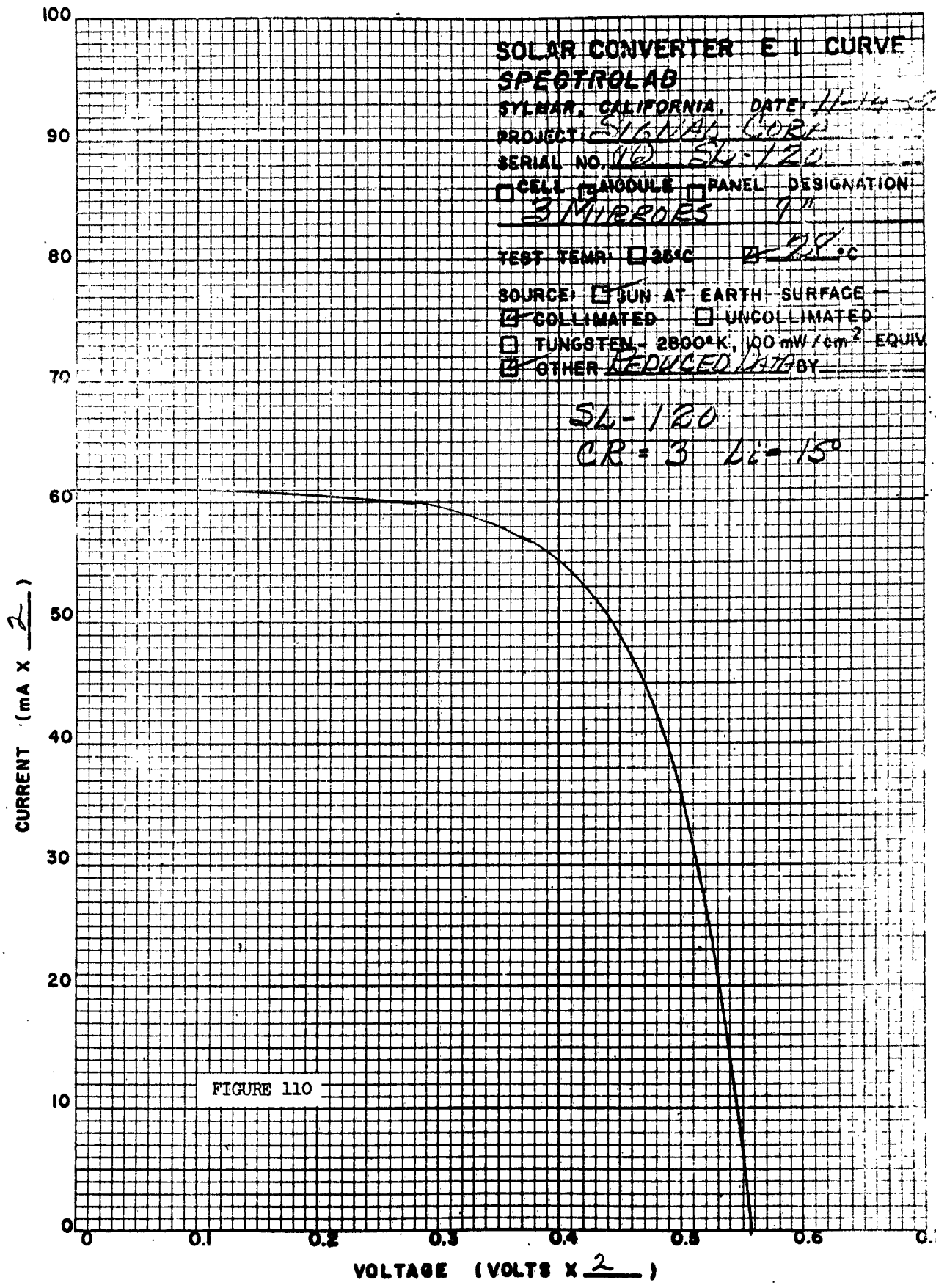

SOLAR CONVERTER E I CURVE
SPECTROLAB
SYLMAR, CALIFORNIA. DATE: 11-14-
PROJECT: SYLMAR CORE
SERIAL NO. 46 SL-120
CELL MODULE PANEL DESIGNATION
3 MIRRORS 1"
TEST TEMP: 28°C 28°C
SOURCE: SUN AT EARTH SURFACE
COLLIMATED UNCOLLIMATED
TUNGSTEN - 2800°K, 100 mW/cm² EQUIV.
OTHER REDUCED DATA BY
SL-120
CR=3 Li=15°
CURRENT (mA X 2)
VOLTAGE (VOLTS X 2)
0
10
20
30
40
50
60
70
80
90
100
0
0.1
0.2
0.3
0.4
0.5
0.6
0.7

FIGURE 110

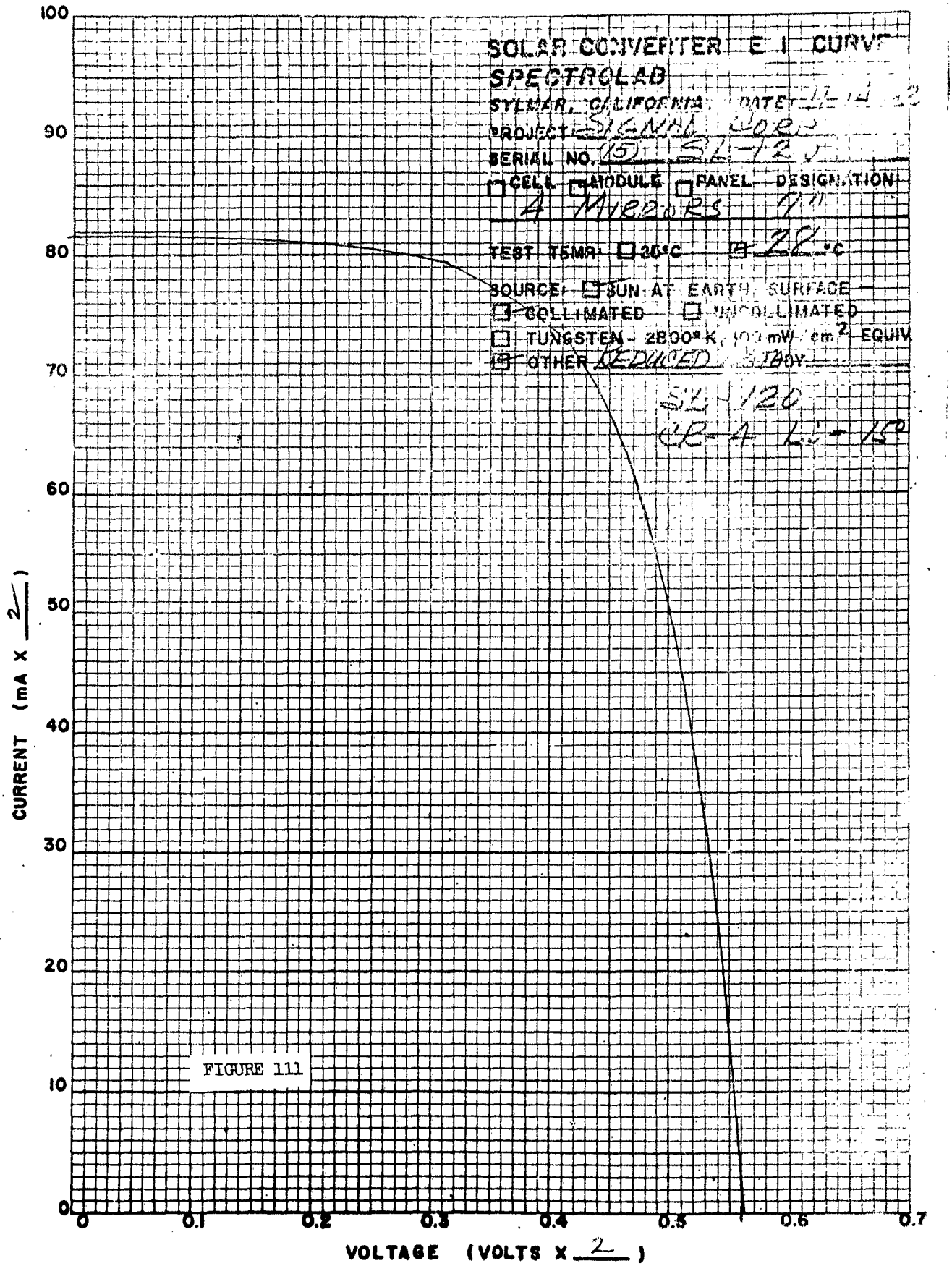

SOLAR CONVERTER E I CURVE
SPECTROLAB
SYLMAR, CALIFORNIA
DATE
PROJECT SIGNAL
SERIAL NO. 05 SL-12
CELL MODULE PANEL DESIGNATION
4 MIRRORS
TEST TEMP: 20°C 28°C
SOURCE: SUN AT EARTH SURFACE
COLLIMATED UNCOLLIMATED
TUNGSTEN - 2800°K, mW/cm² EQUIV.
OTHER REDUCED 1 SUN
SL-120
AR-4 L = 15°
CURRENT (mA X 2)
VOLTAGE (VOLTS X 2)
0
10
20
30
40
50
60
70
80
90
100
0
0.1
0.2
0.3
0.4
0.5
0.6
0.7

FIGURE 111

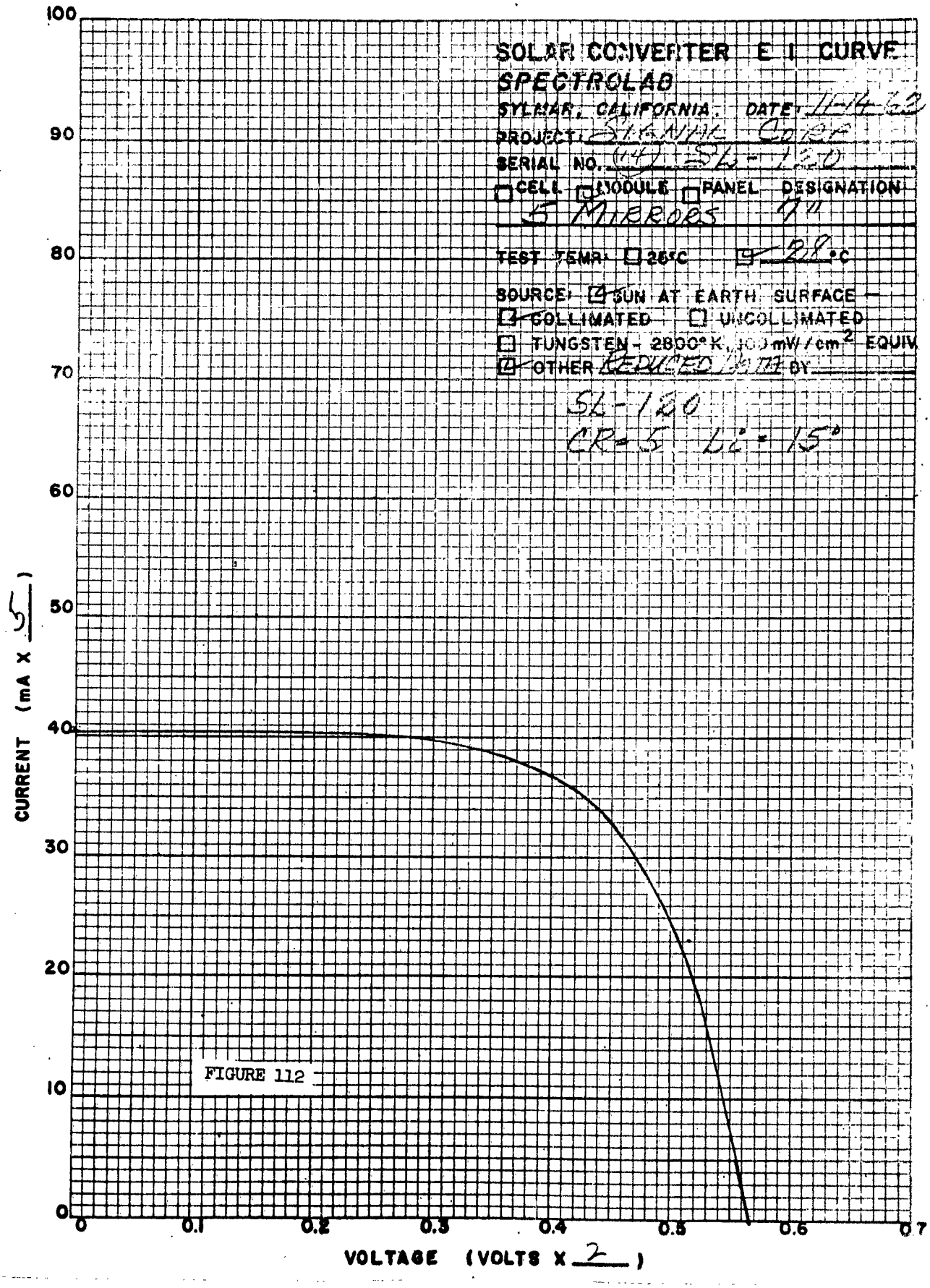

SOLAR CONVERTER E I CURVE
SPECTROLAB
SYLMAR, CALIFORNIA. DATE: 11-4-63
PROJECT: SYNAC Corp
SERIAL NO. (4) SL-120
CELL MODULE PANEL DESIGNATION
5 Mirrors 4"
TEST TEMP: 26°C 28°C
SOURCE: SUN AT EARTH SURFACE
COLLIMATED UNCOLLIMATED
TUNGSTEN - 2800°K, 100 mW/cm² EQUIV
OTHER REDUCED BY
SL-120
CR=5 Li=15°
CURRENT (mA X 5)
VOLTAGE (VOLTS X 2)
0
10
20
30
40
50
60
70
80
90
100
0
0.1
0.2
0.3
0.4
0.5
0.6
0.7

FIGURE 112

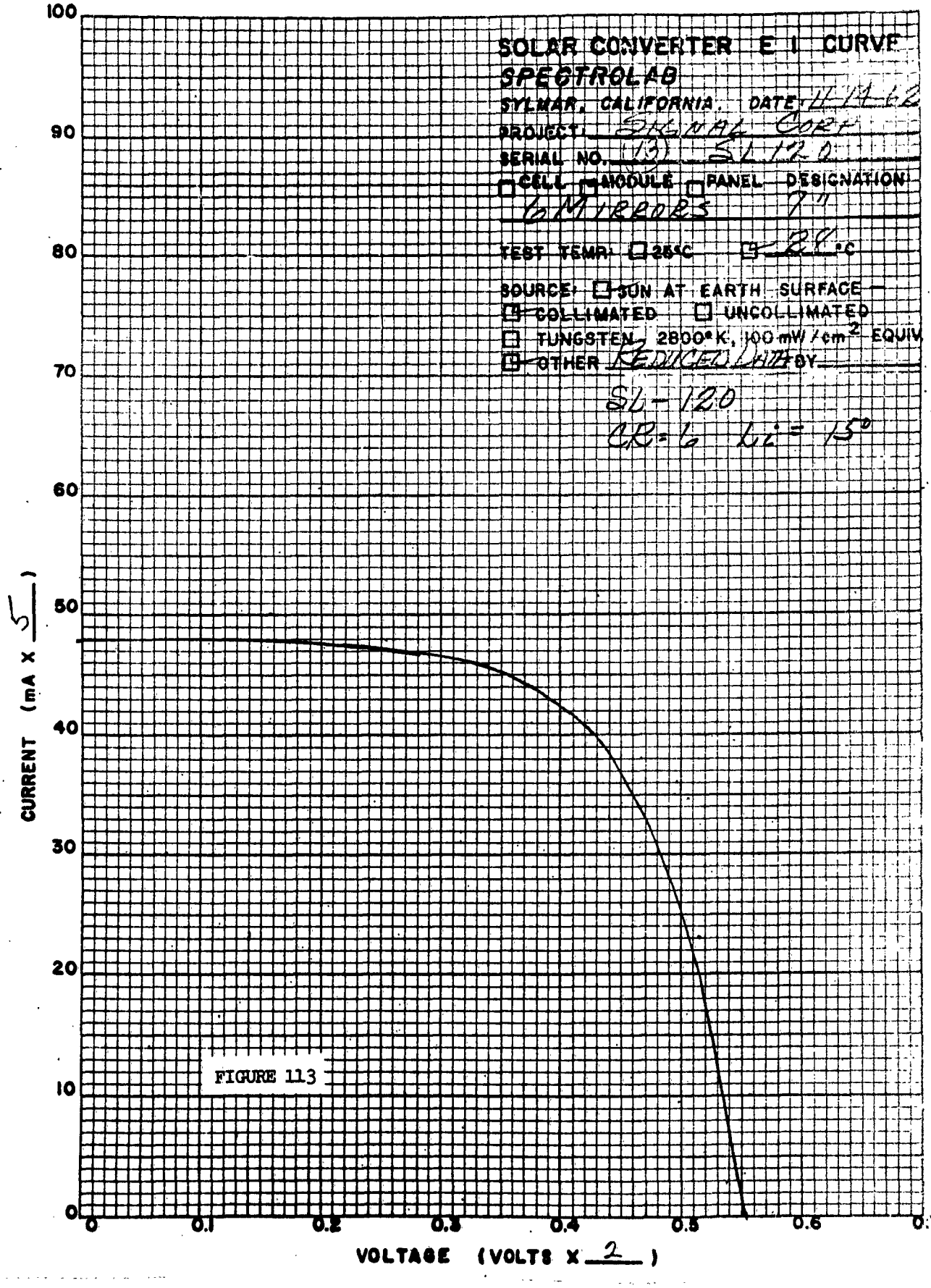

SOLAR CONVERTER E I CURVE
SPECTROLAB
SYLMAR, CALIFORNIA. DATE: 4-11-62
PROJECT: SKYNET COPY
SERIAL NO. 131 SL 120
CELL MODULE PANEL DESIGNATION
6 MIRRORS 9"
TEST TEMP: 25°C 28°C
SOURCE: SUN AT EARTH SURFACE
COLLIMATED UNCOLLIMATED
TUNGSTEN 2800°K, 100 mW/cm² EQUIV
OTHER REDUCED LIGHT BY
SL-120
CR=6 Li=15°
CURRENT (mA X 5)
VOLTAGE (VOLTS X 2)
0
10
20
30
40
50
60
70
80
90
100
0.1
0.2
0.3
0.4
0.5
0.6
0.7

FIGURE 113

APPENDIX A

REFLECTION FILTER SPECIFICATIONS

APPENDIX A

REFLECTION FILTER SPECIFICATIONS

1. Performance.

The idealized filter performance curves are shown in Figures I, II and III. The tolerances within which the actual filters may perform relative to these idealized curves are:

a) The reflectance passband centers shall be within ± 0.01, ± 0.02, ± 0.03 micron of the nominal value for filter types SL 120/83, SL 200/82, and SL 350/80, respectively.

b) The reflectance passband widths shall be within ± 0.01, ± 0.02, ± 0.03 micron of the nominal values for filters SL 120/83, SL 200/82, and SL 350/80, respectively.

c) The mean slope, defined as microns per unit of percent transmittance, of the reflectance passband limit on the short wavelength side shall be greater than -0.0003 and on the long wavelength side, less than 0.0003 in the range of transmittance 10% to 80% for all the filter types.

d) The transmittance in the reflectance passband, in a range 0.06 micron less than the nominal passband width for each filter type, shall not exceed 3%.

e) The mean transmittance on the short wavelength side between 0.35 micron and the short wave limit of the passband shall not be less than 90% for all filter types. The minimum transmittance in this range shall exceed 83% for each filter type.

f) The mean transmittance on the long wavelength side between the long wavelength limit of the passband and 1.6 microns shall exceed 82%, 85% and 87% for filter types SL 120/83, SL 200/82 and SL 359/80, respectively. The minimum transmittance

APPENDIX A

REFLECTION FILTER SPECIFICATIONS

1. Performance.

The idealized filter performance curves are shown in Figures I, II and III. The tolerances within which the actual filters may perform relative to these idealized curves are:

a) The reflectance passband centers shall be within ± 0.01, ± 0.02, ± 0.03 micron of the nominal value for filter types SL 120/83, SL 200/82, and SL 350/80, respectively.

b) The reflectance passband widths shall be within ± 0.01, ± 0.02, ± 0.03 micron of the nominal values for filters SL 120/83, SL 200/82, and SL 350/80, respectively.

c) The mean slope, defined as microns per unit of percent transmittance, of the reflectance passband limit on the short wavelength side shall be greater than -0.0003 and on the long wavelength side, less than 0.0003 in the range of transmittance 10% to 80% for all the filter types.

d) The transmittance in the reflectance passband, in a range 0.06 micron less than the nominal passband width for each filter type, shall not exceed 3%.

e) The mean transmittance on the short wavelength side between 0.35 micron and the short wave limit of the passband shall not be less than 90% for all filter types. The minimum transmittance in this range shall exceed 83% for each filter type.

f) The mean transmittance on the long wavelength side between the long wavelength limit of the passband and 1.6 microns shall exceed 82%, 85% and 87% for filter types SL 120/83, SL 200/82 and SL 350/80, respectively. The minimum transmittance

in this range shall exceed 12% less than the nominal values for each filter type.

g) Maximum variation in filter reflectances and transmittances over the filter face shall be less than ± 3%.

2. Construction

The filters shall consist of a single filter stack on a glass substrate. For substrate dimensions and specification, see Figure IV.

3. Environmental Integrity

1. These filters shall endure use and handling outdoors by trained personnel in all atmospheres, including contaminants encountered within the continental United States of America.

2. The exposed surfaces of the filters shall withstand cleaning by light dry brushing and washing with water and a mild detergent.

3. The standard of comparison with respect to its integrity in its environment and use, shall be an aluminized front surface mirror with silicon monoxide overcoat.

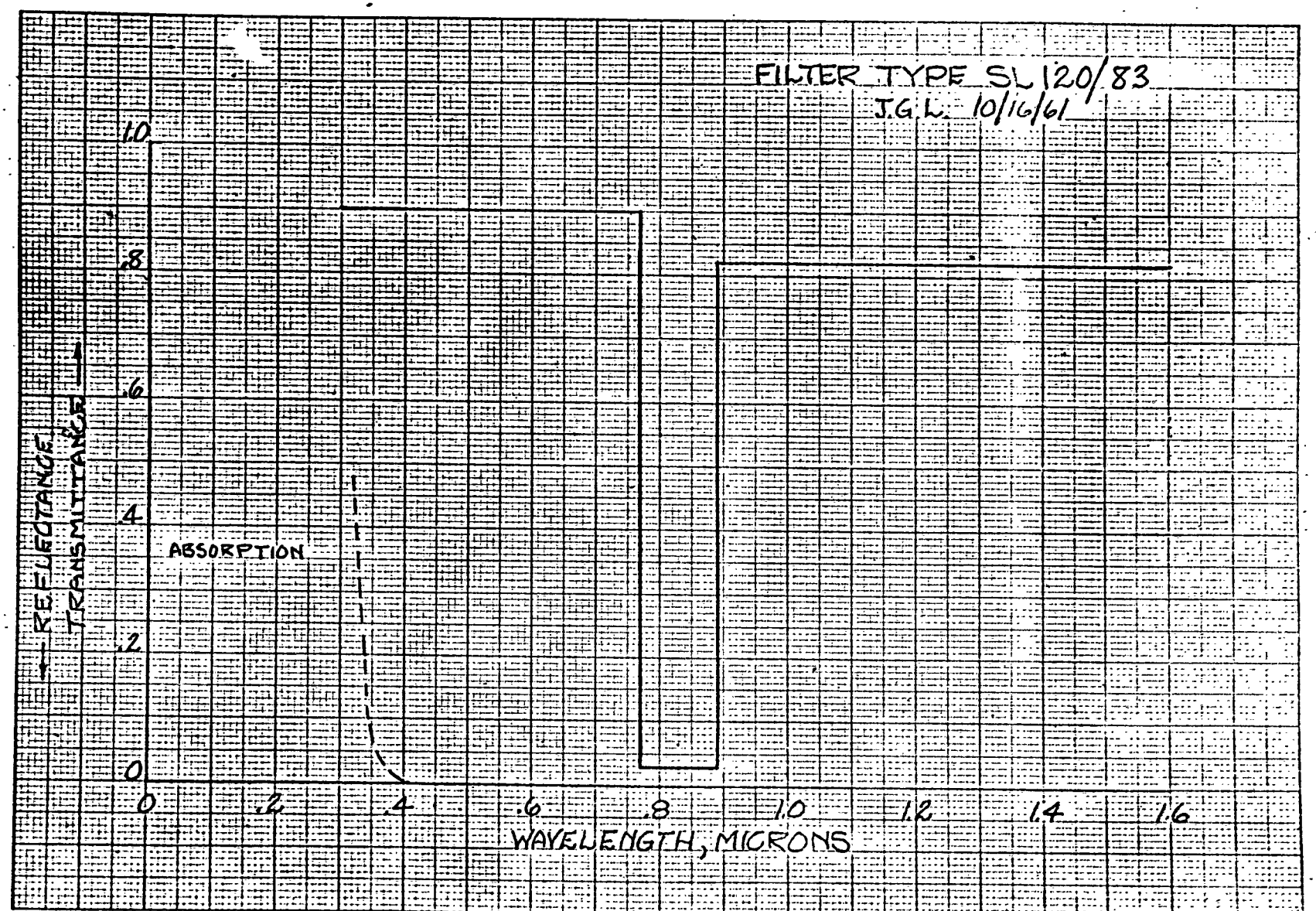


FIGURE I. FILTER SL 120/83 CHARACTERISTICS

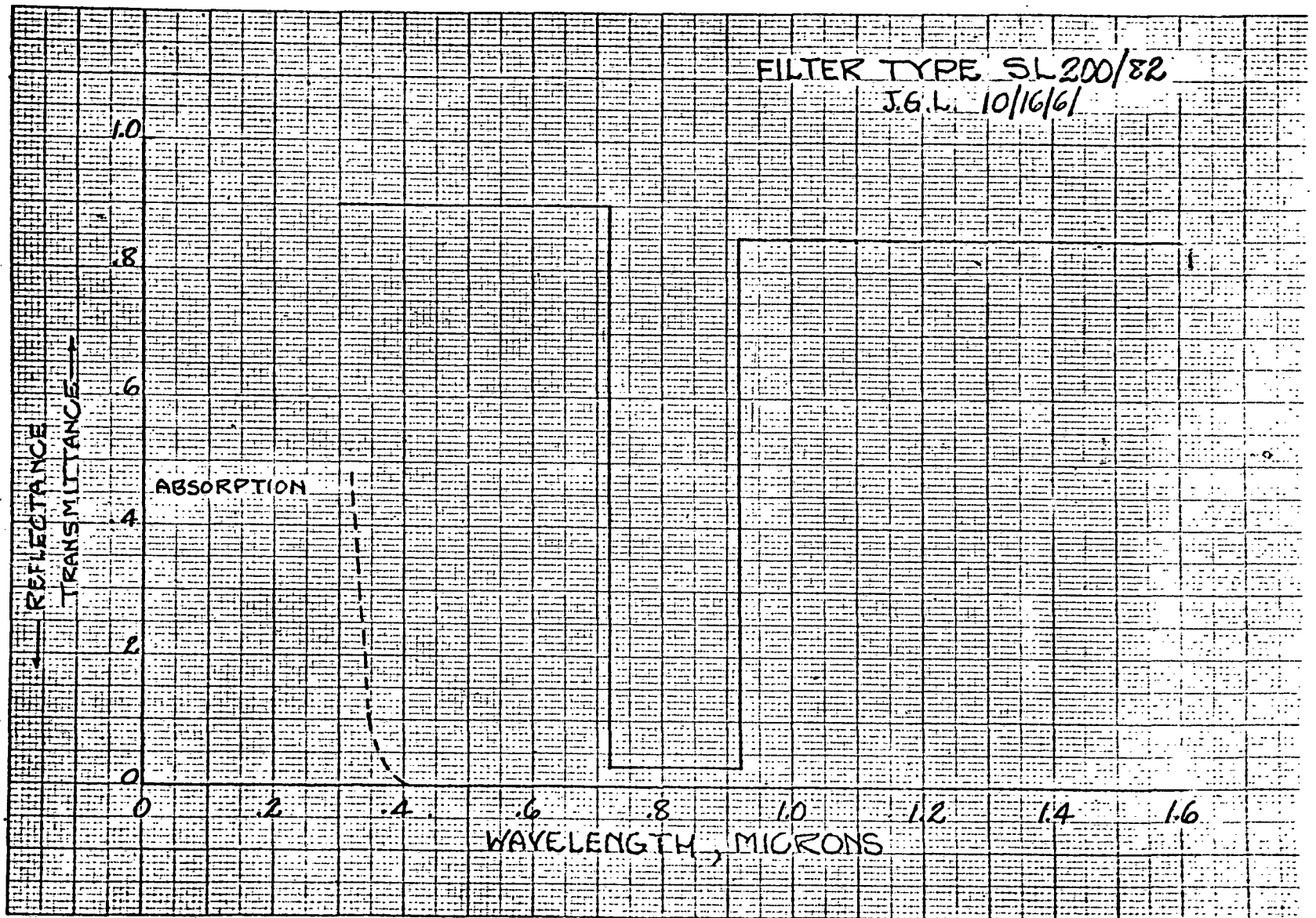


FIGURE II. FILTER SL 200/82 CHARACTERISTICS

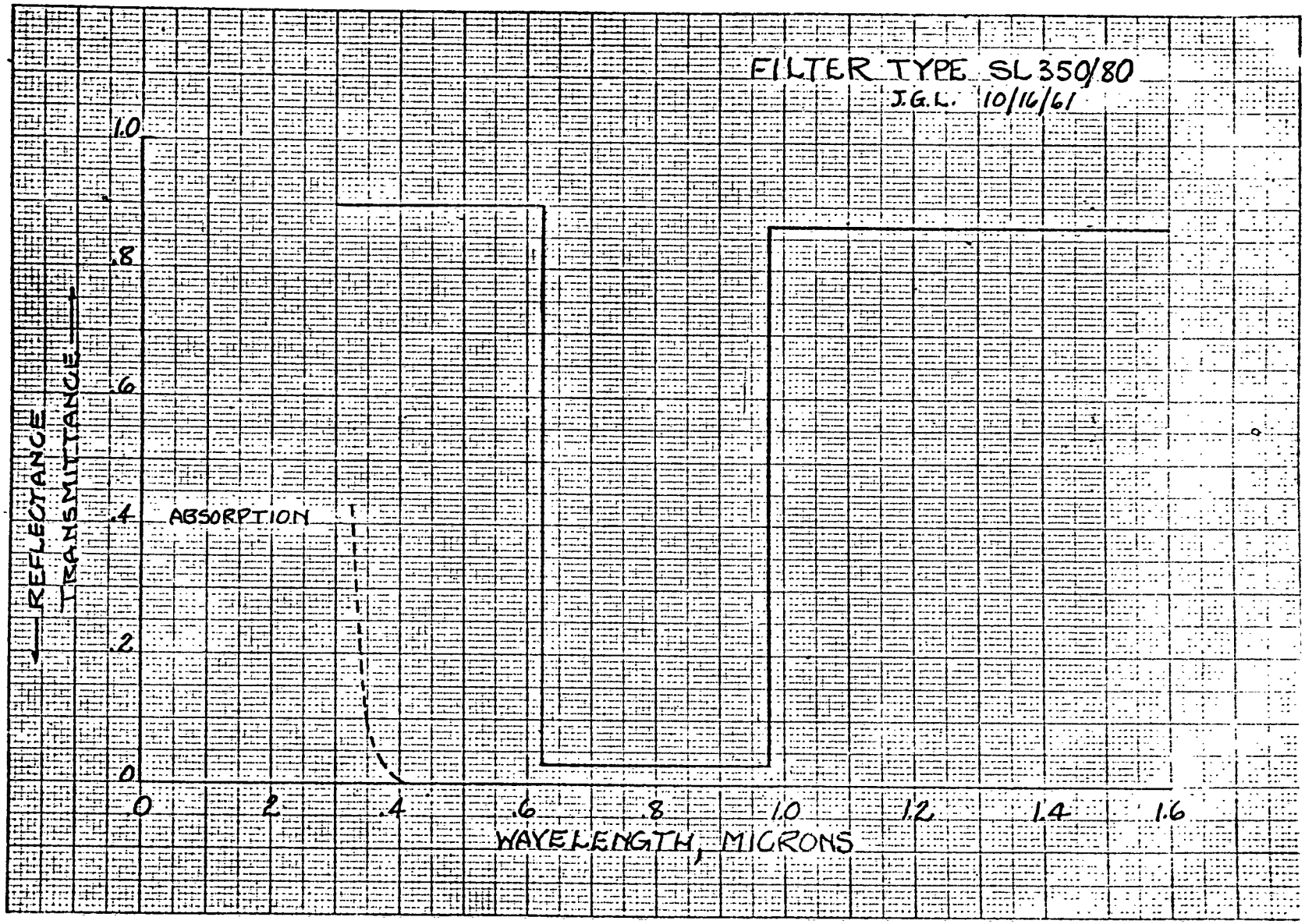
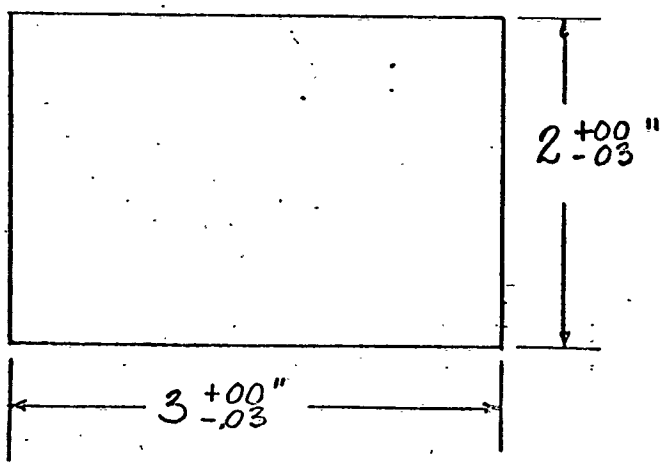


FIGURE III. FILTER 350/80 CHARACTERISTICS



NOTES:

1. Substrate thickness = .236 $^{+00"}_{-03}$
2. All sharp edges shall be broken .010" to .020"
3. Material BSC-2 Type 517645 fine anneal optical glass or equivalent
4. Surface quality 80-50 per MIL-O-13830

Figure IX. SUBSTRATE DIMENSIONS AND SPECIFICATIONS

APPENDIX B

SPECTRAL TRANSMITTANCE CURVES

for

EXPERIMENTAL REFLECTION FILTERS

Appendix B

Spectral Transmittance Curves for Experimental Reflection Filters.

This Appendix consists of 44 spectral transmittance curves for the reflecting filters fabricated by Spectrolab. The curves are photographic reductions of the data recorded by a Cary Model 14 Spectrophotometer using a tungsten light source.

Figures B-1 through B-24 are transmittance curves at 0° angle of incidence for the reflecting filters used in the Table Mountain tests. The first group of six curves (Figures B-1 through B-6) consists of data for the Type SL 350 filters, the second group (Figures B-7 through B-12) for the SL 200-II filters, the third group (Figures B-13 through B-18) for the SL 200-I filters, and the fourth group (Figures B-19 through B-24) for the SL 120 filters.

Figures B-25 through B-44 show the variation in spectral transmittance with angle of incidence for one representative filter of each type. Figures B-25 through B-29 are transmittance curves for an SL 350 filter for $\angle i$ = 0°, 10°, 20°, 30°, and 45°, respectively.

Figures B-30 through B-34 are similar curves for an SL 200-II filter, Figures B-35 through B-39 for an SL 200-I, and Figures B-40 through B-44 for an SL 120.

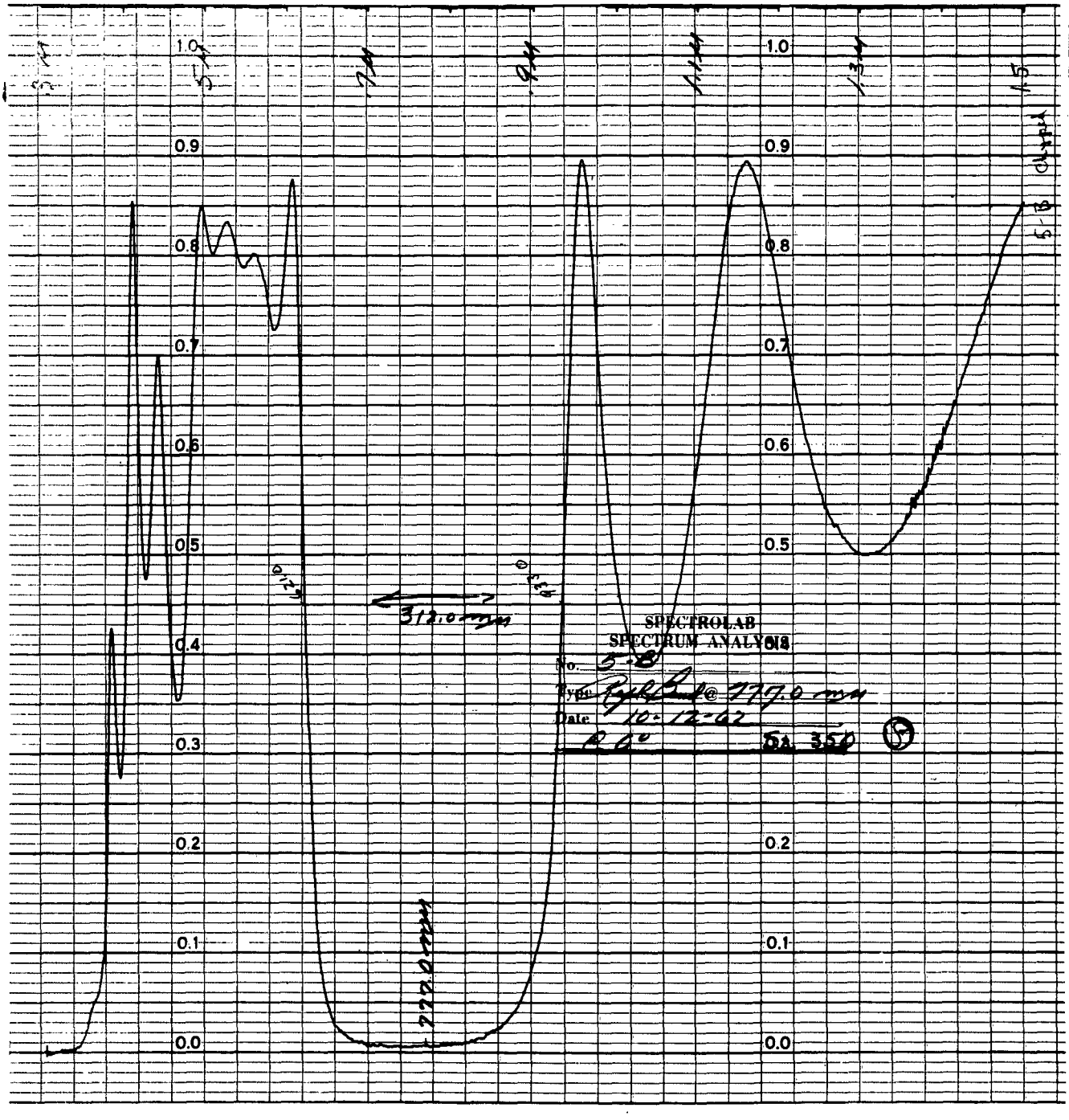

1.0
0.9
0.8
0.7
0.6
0.5
0.4
0.3
0.2
0.1
0.0
SPECTROLAB
SPECTRUM ANALYZER
No. 5-B
Type Ryle @ 777.0 mm
Date 10-12-62
DA. 350

FIGURE B-1

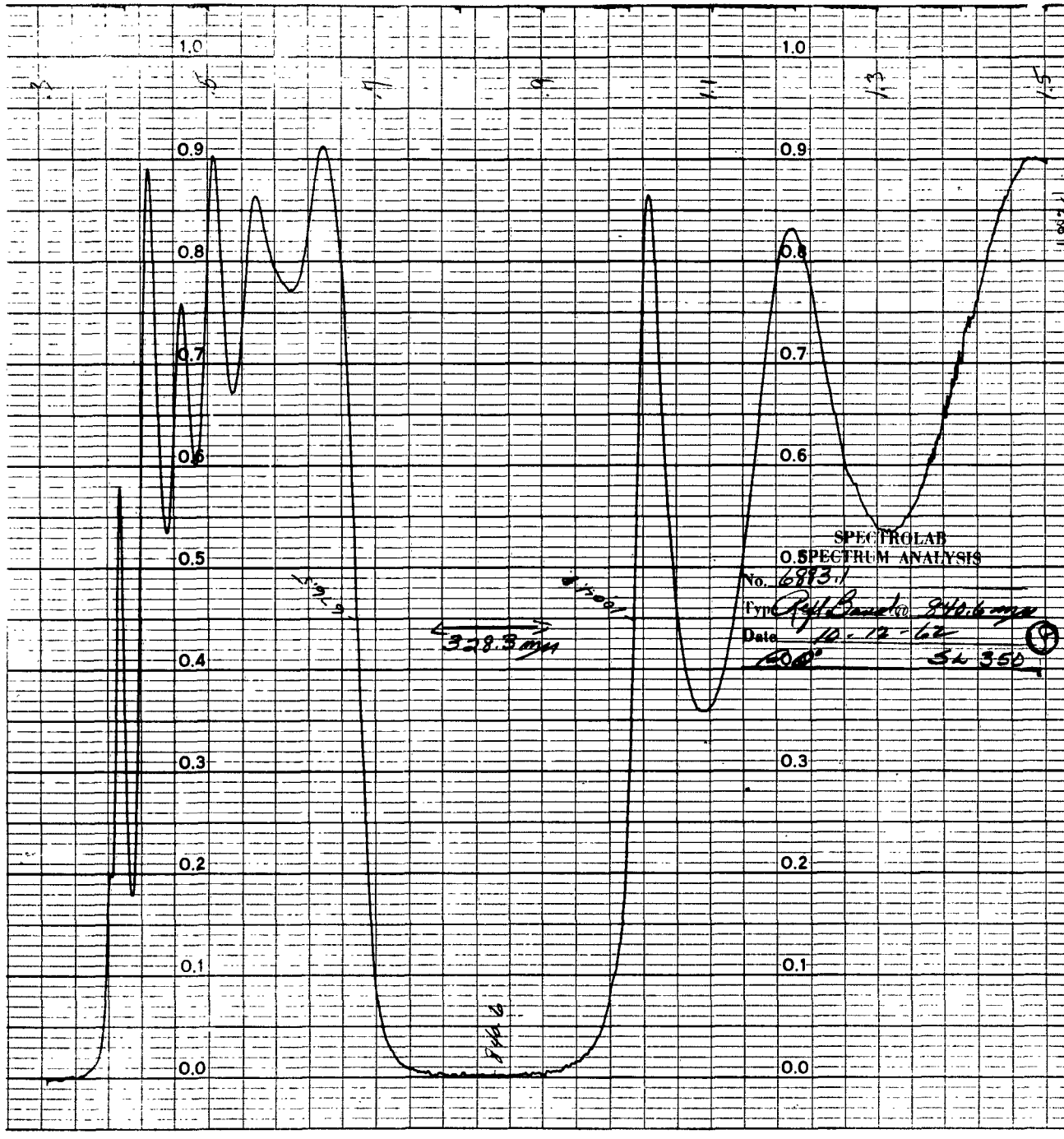

1.0
0.9
0.8
0.7
0.6
0.5
0.4
0.3
0.2
0.1
0.0
SPECTROLAB
SPECTRUM ANALYSIS
No. 6883.1
Date 12-12-62
328.8 mμ

FIGURE B-2

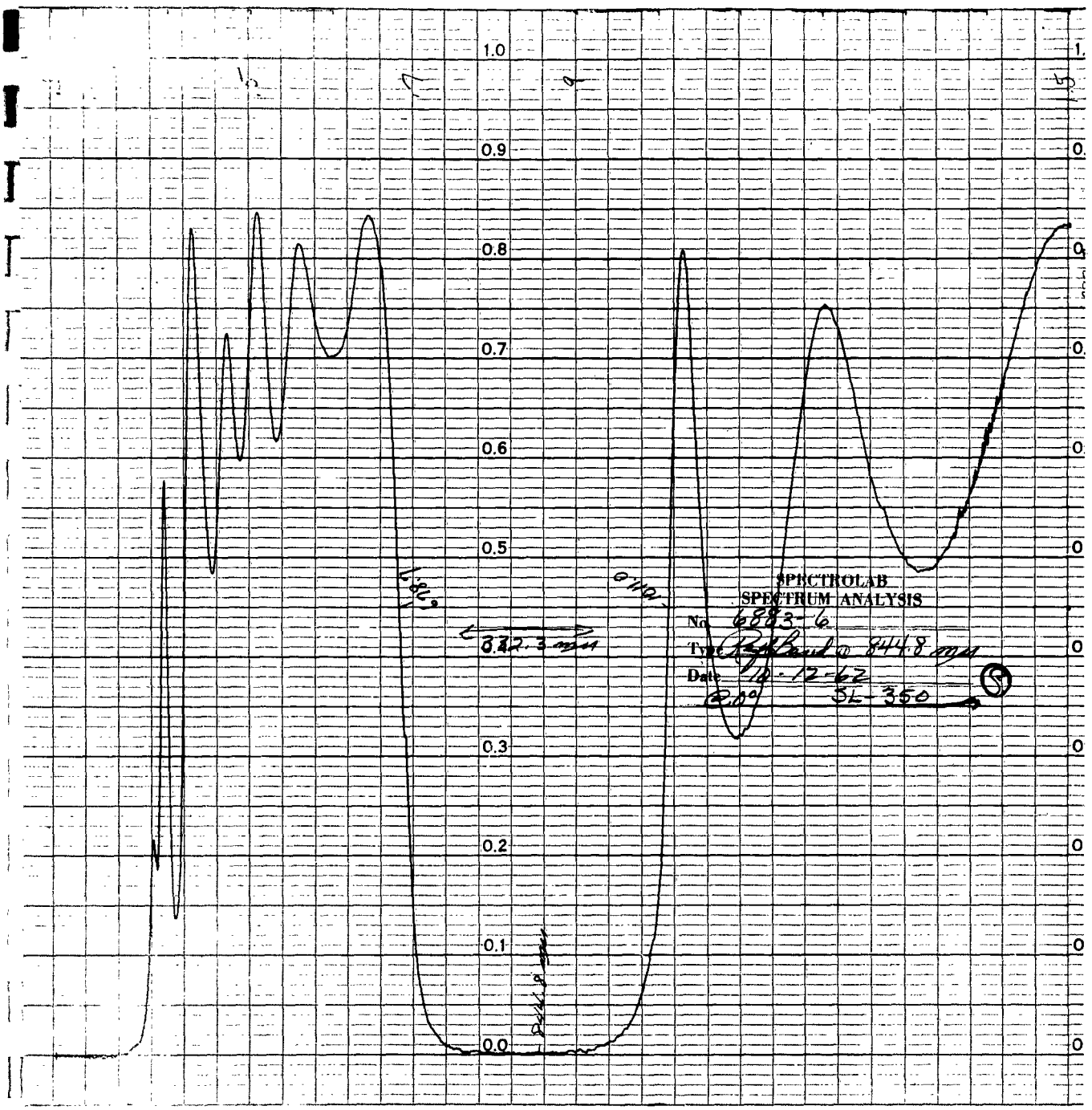

1.0
0.9
0.8
0.7
0.6
0.5
0.3
0.2
0.1
0.0
SPECTROLAB
SPECTRUM ANALYSIS
No. 6883-6
Type
Date 12-12-62
SL-350

FIGURE B-3

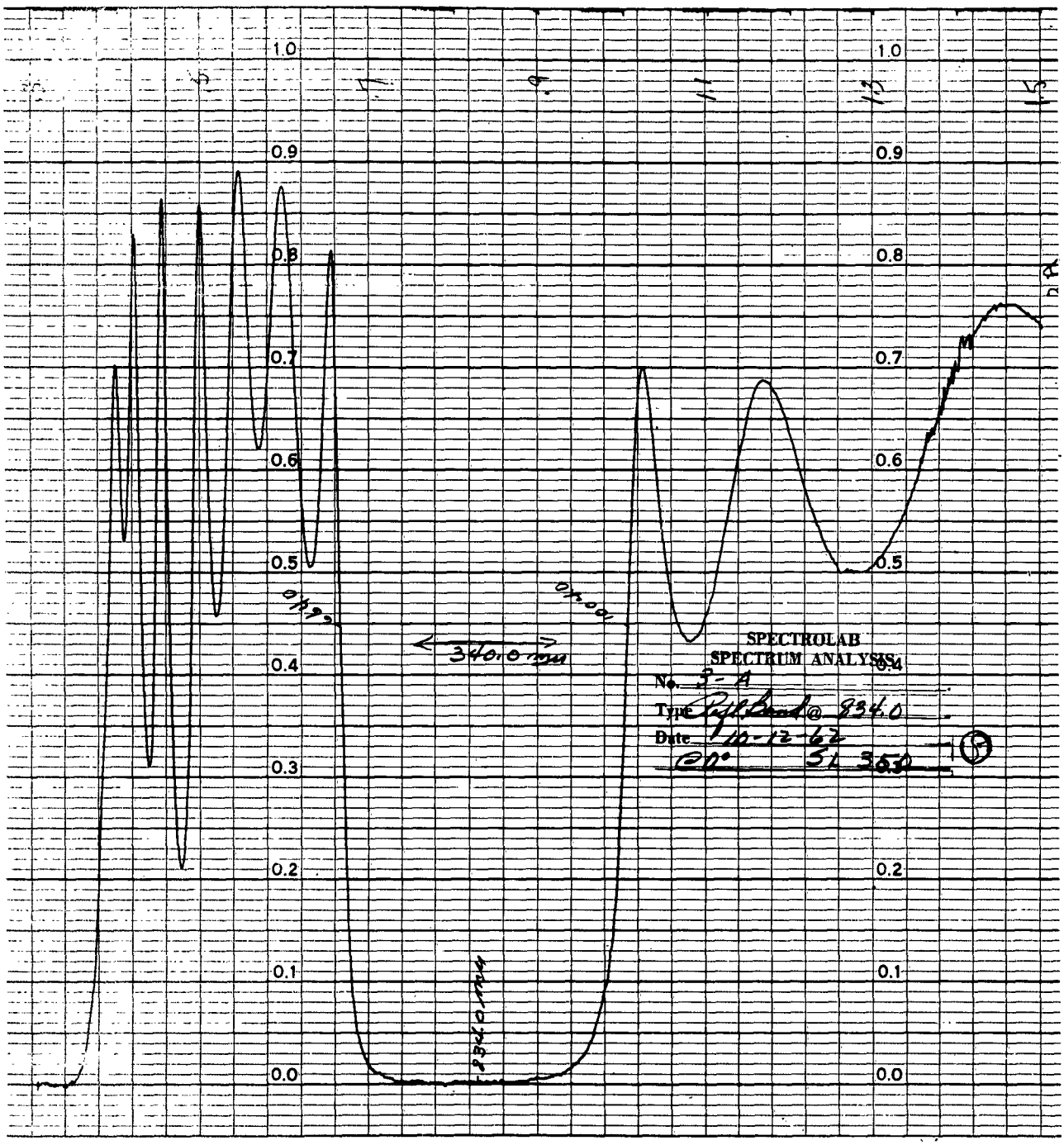

1.0
0.9
0.8
0.7
0.6
0.5
0.4
0.3
0.2
0.1
0.0
340.0 mμ
SPECTROLAB
SPECTRUM ANALYSIS
No. 3-A
Type Pyk. Band @ 934.0
Date 10-12-62
20° SL 350

FIGURE B-4

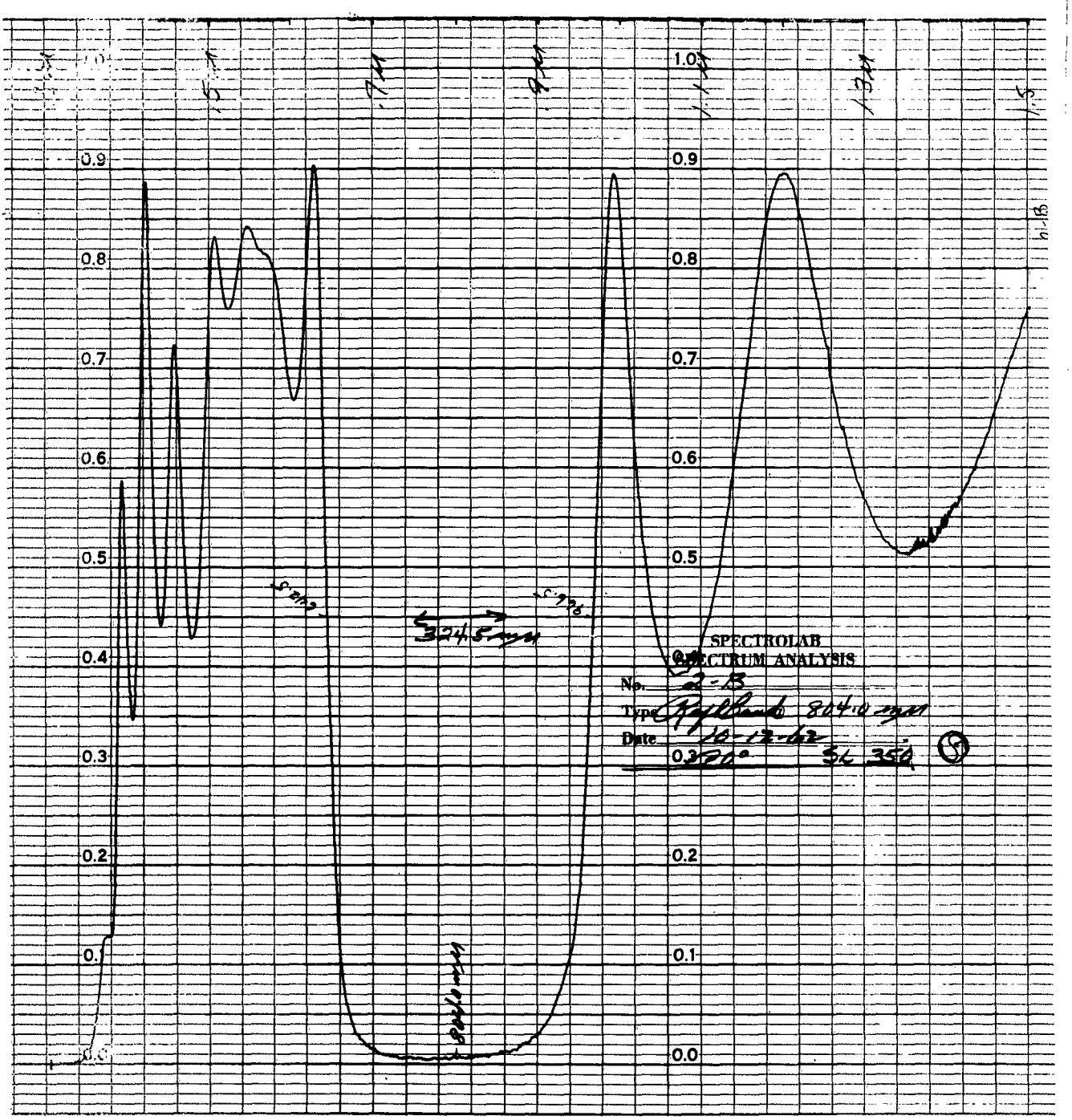

1.0
0.9
0.8
0.7
0.6
0.5
0.4
0.3
0.2
0.1
0.0
SPECTROLAB
SPECTRUM ANALYSIS
No. 2-B
Type Ryllband 804.0 mμ
Date 10-12-62
3720° $L 350

FIGURE B-5

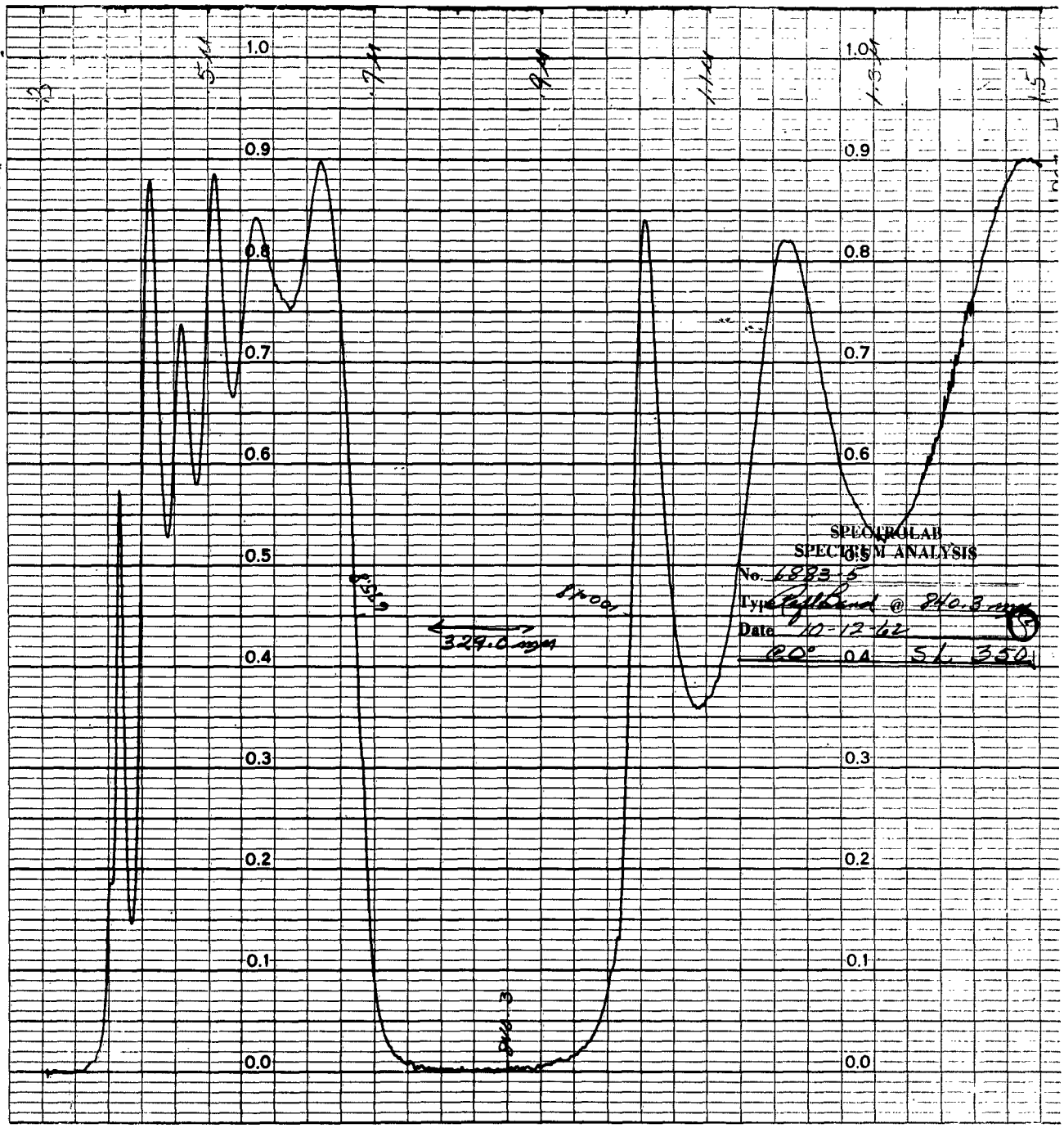

1.0
0.9
0.8
0.7
0.6
0.5
0.4
0.3
0.2
0.1
0.0
329.0 mμ
SPECTROLAB
SPECTRUM ANALYSIS
No. 6883-5
Type Peak Band @ 840.3 mμ
Date 10-12-62
80° 0.4 5 L. 350

FIGURE B-6

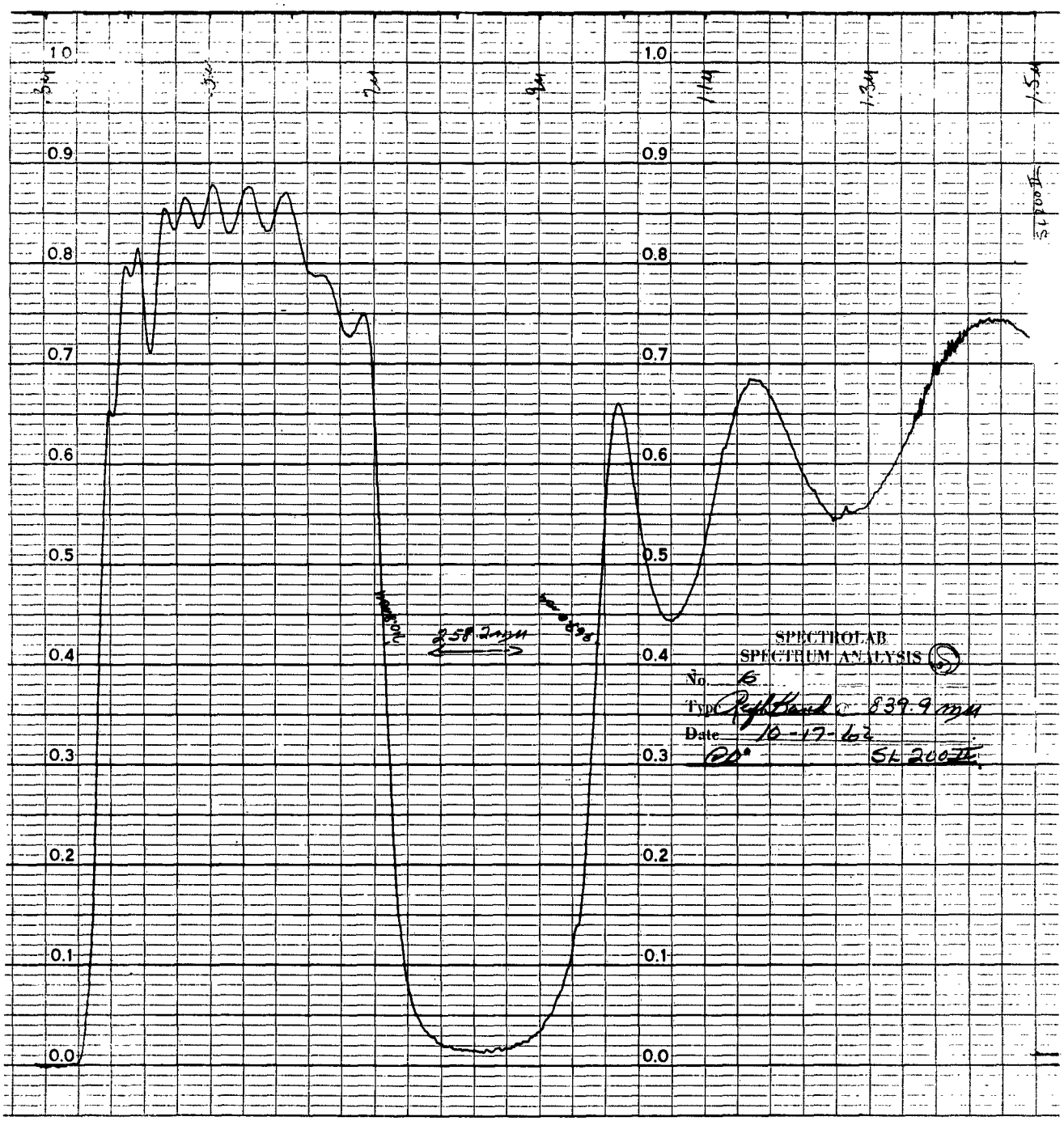

SPECTROLAB
SPECTRUM ANALYSIS
No. 6
Type Right Hand @ 839.9 mμ
Date 10-17-62
0°
5L 200 FL
258 2mμ

FIGURE B-7

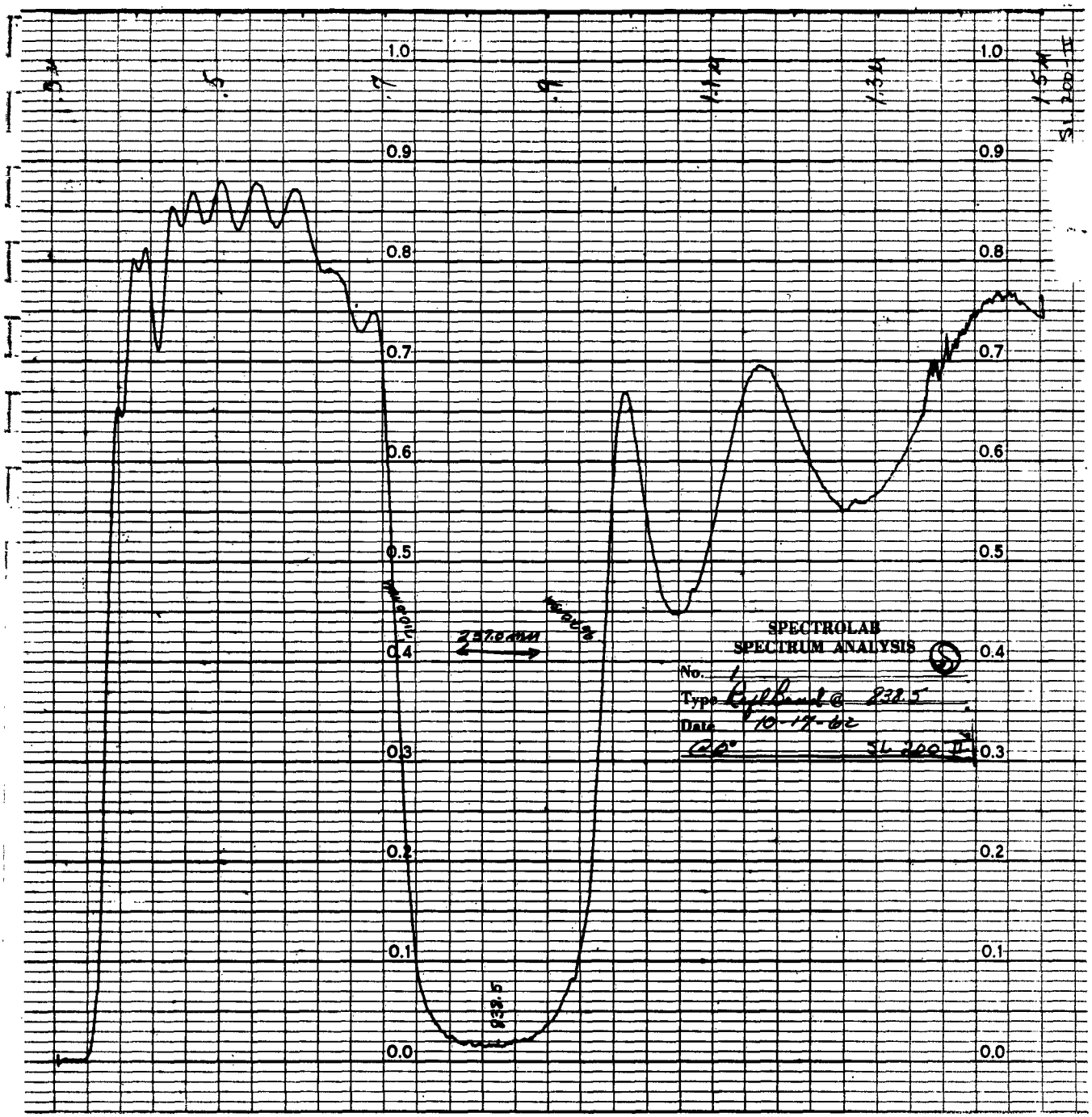

SPECTROLAB
SPECTRUM ANALYSIS
No. 1
Type Cylburn @ 232.5
Date 10-17-62
0°
SL 200 II
1.0
0.9
0.8
0.7
0.6
0.5
0.4
0.3
0.2
0.1
0.0

FIGURE B-8

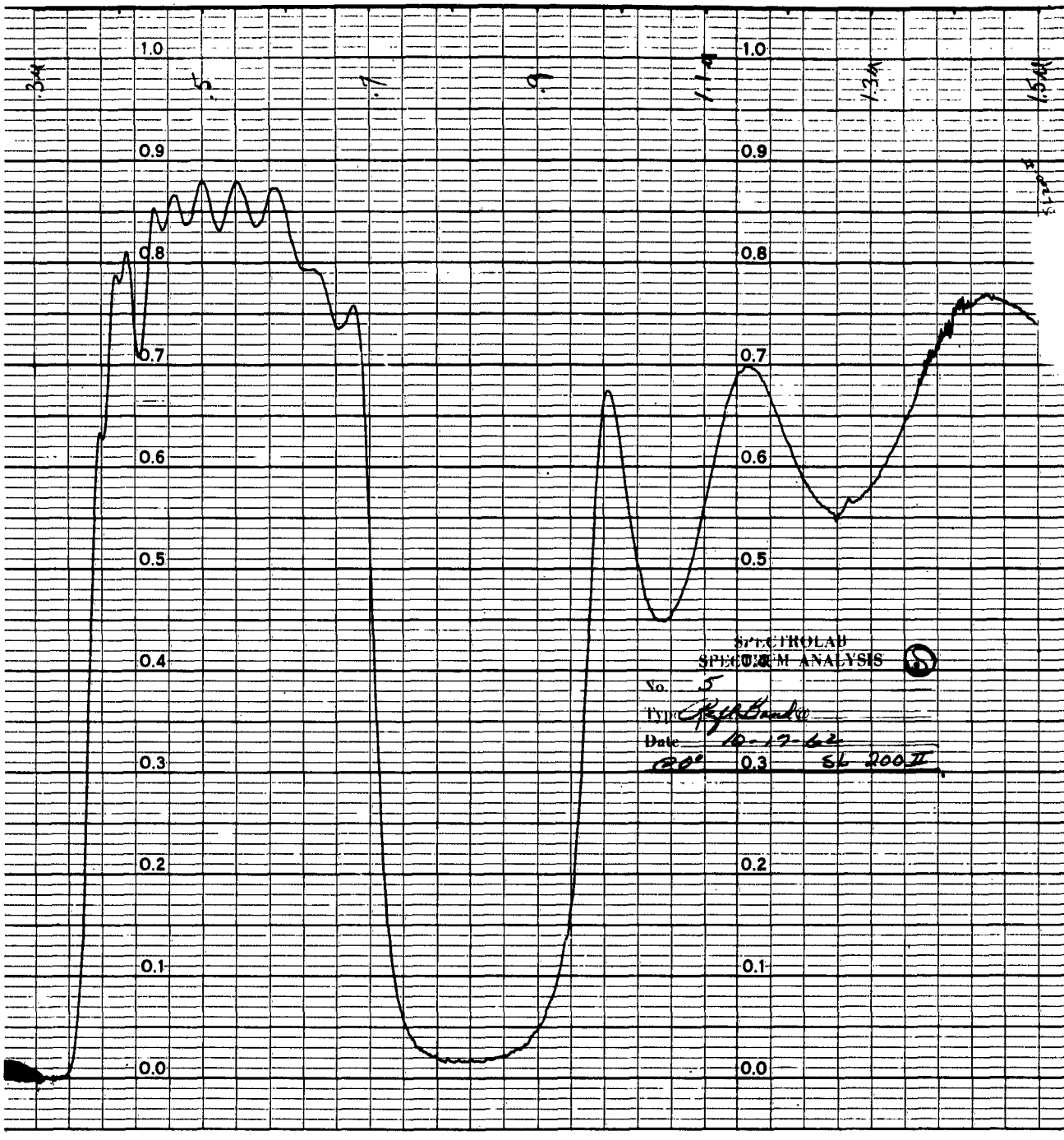

1.0
0.9
0.8
0.7
0.6
0.5
0.4
0.3
0.2
0.1
0.0
SPECTROLAB
SPECTRUM ANALYSIS
No. 5
Type Byk Bond
Date 10-17-62
SL 200 II

FIGURE B-9

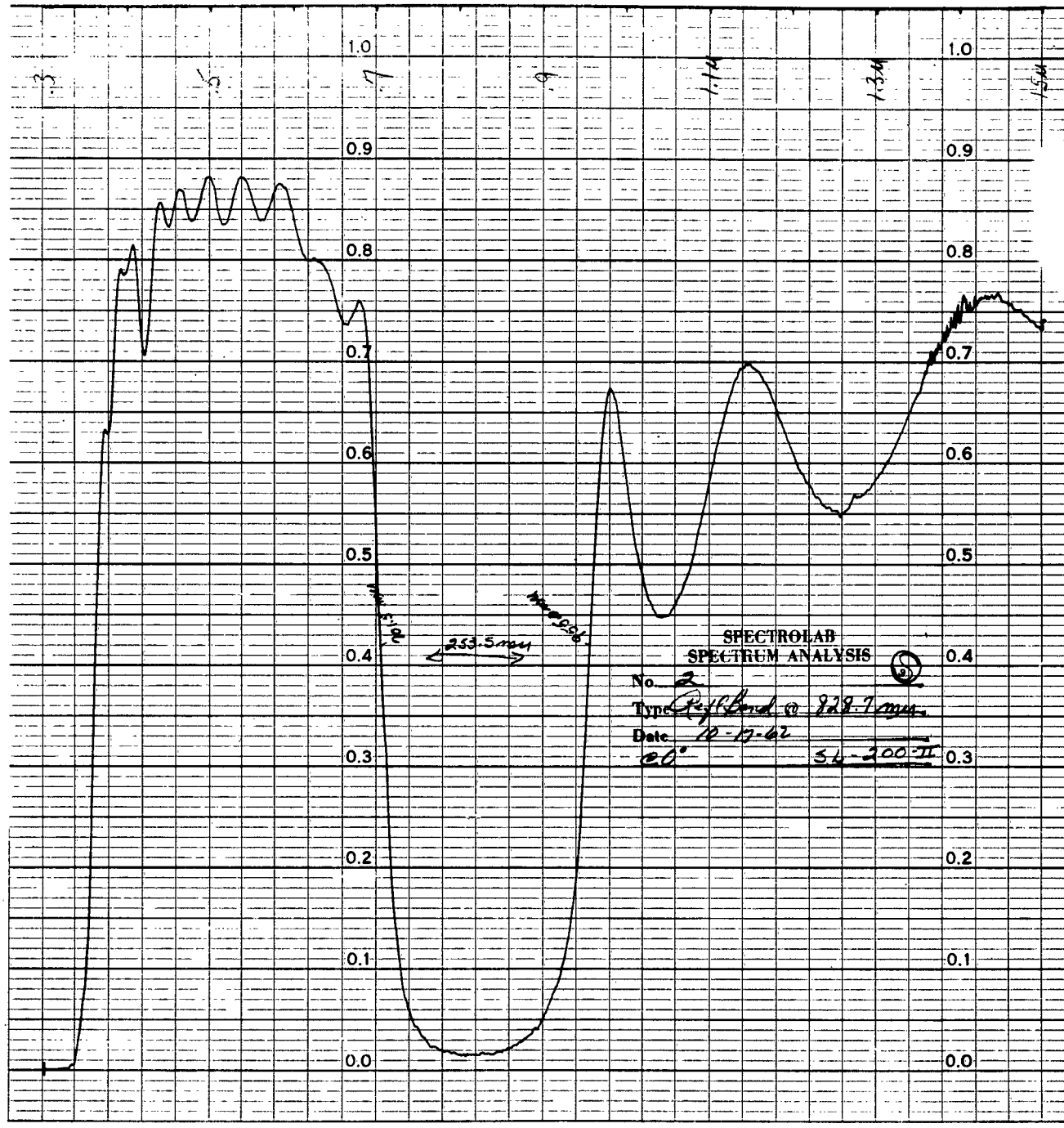

1.0
0.9
0.8
0.7
0.6
0.5
0.4
0.3
0.2
0.1
0.0
253.5 mμ
SPECTROLAB
SPECTRUM ANALYSIS
No. 2
Type Poly Bond @ 828.7 mμ
Date 12-17-62
20°
SL-200-II

FIGURE B-10

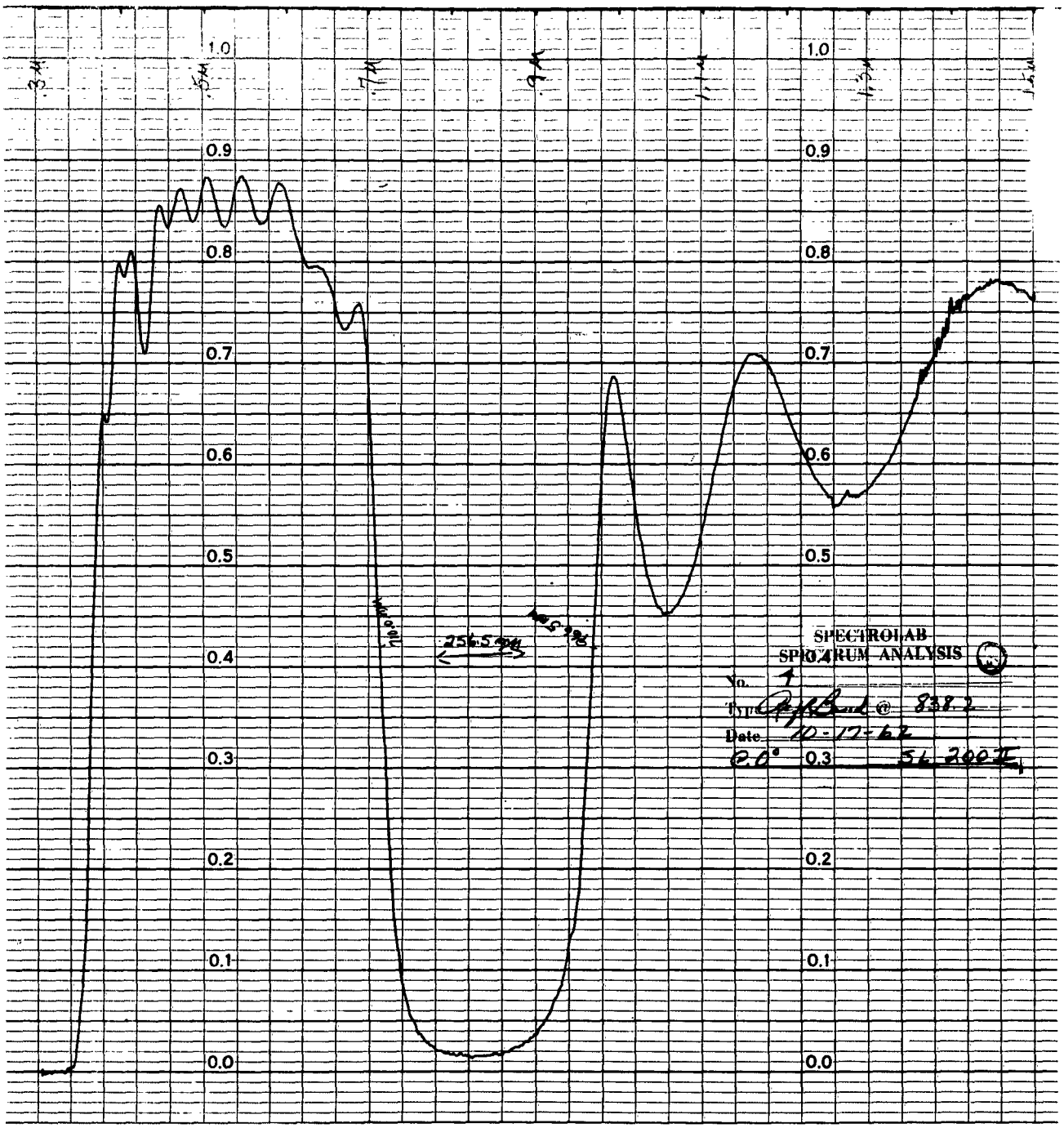

1.0
0.9
0.8
0.7
0.6
0.5
0.4
0.3
0.2
0.1
0.0
SPECTROLAB
SPECTRUM ANALYSIS
No. 1
Date 10-17-62

FIGURE B-11

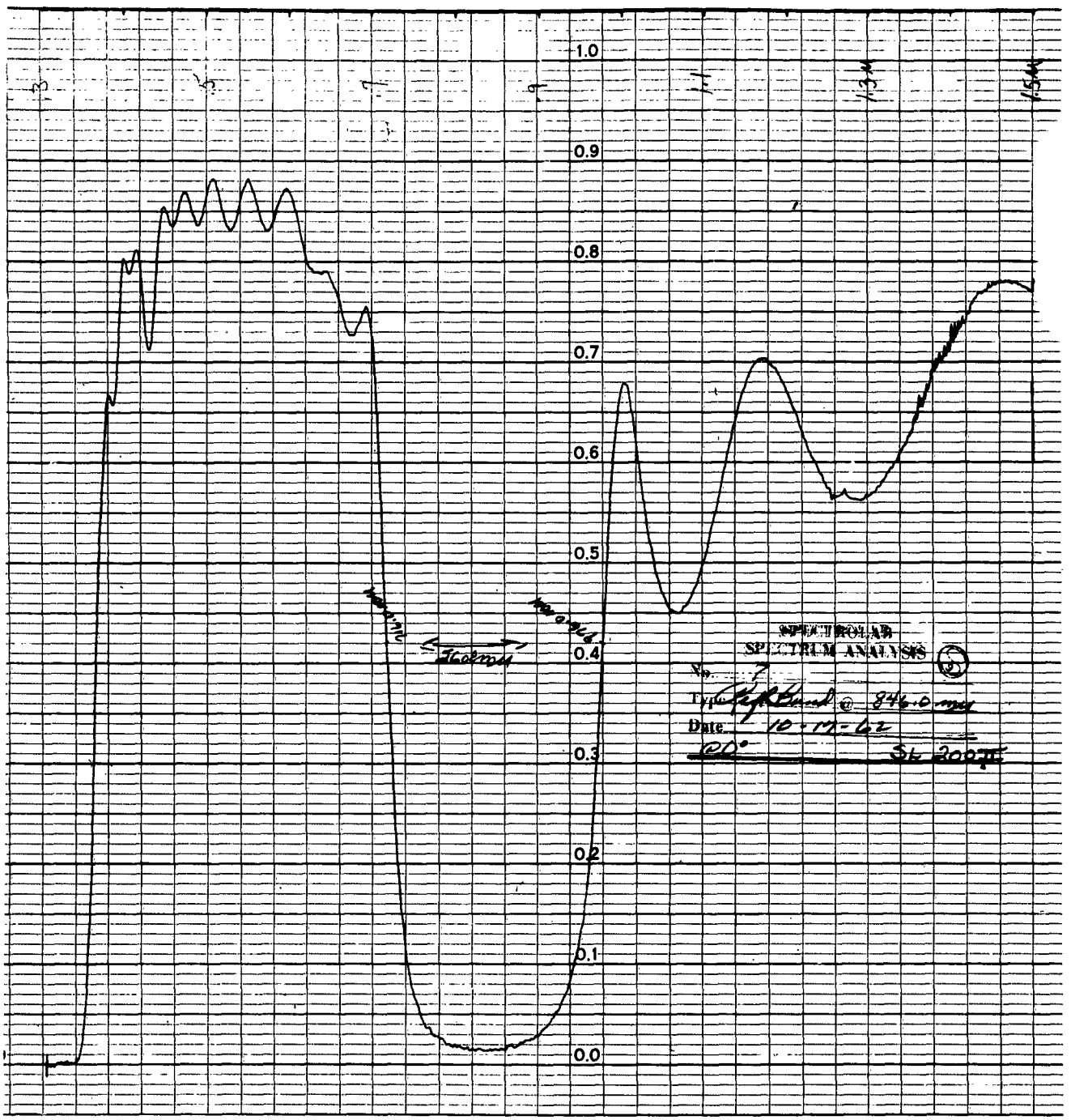

1.0
0.9
0.8
0.7
0.6
0.5
0.4
0.3
0.2
0.1
0.0
SPECTROLAB
SPECTRUM ANALYSIS
No.
Type
Date 10-17-62
20°
$4,200

FIGURE B-12

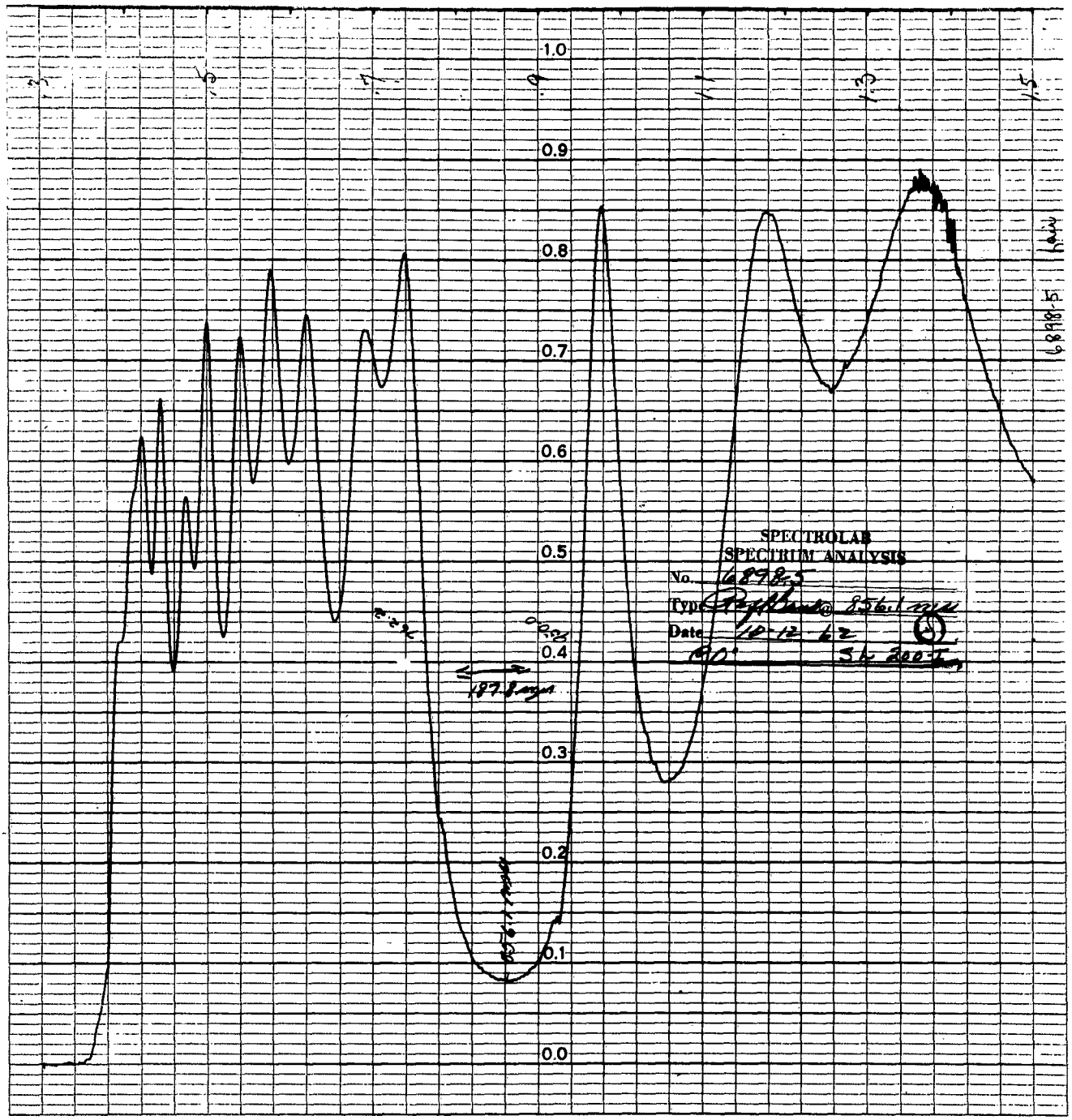

1.0
0.9
0.8
0.7
0.6
0.5
0.4
0.3
0.2
0.1
0.0
SPECTROLAB
SPECTRUM ANALYSIS
No. 6898-5
Type Right Band @ 85db ref
Date 10-12-62
90°
3k 200 Tm
6898-5

FIGURE B-13

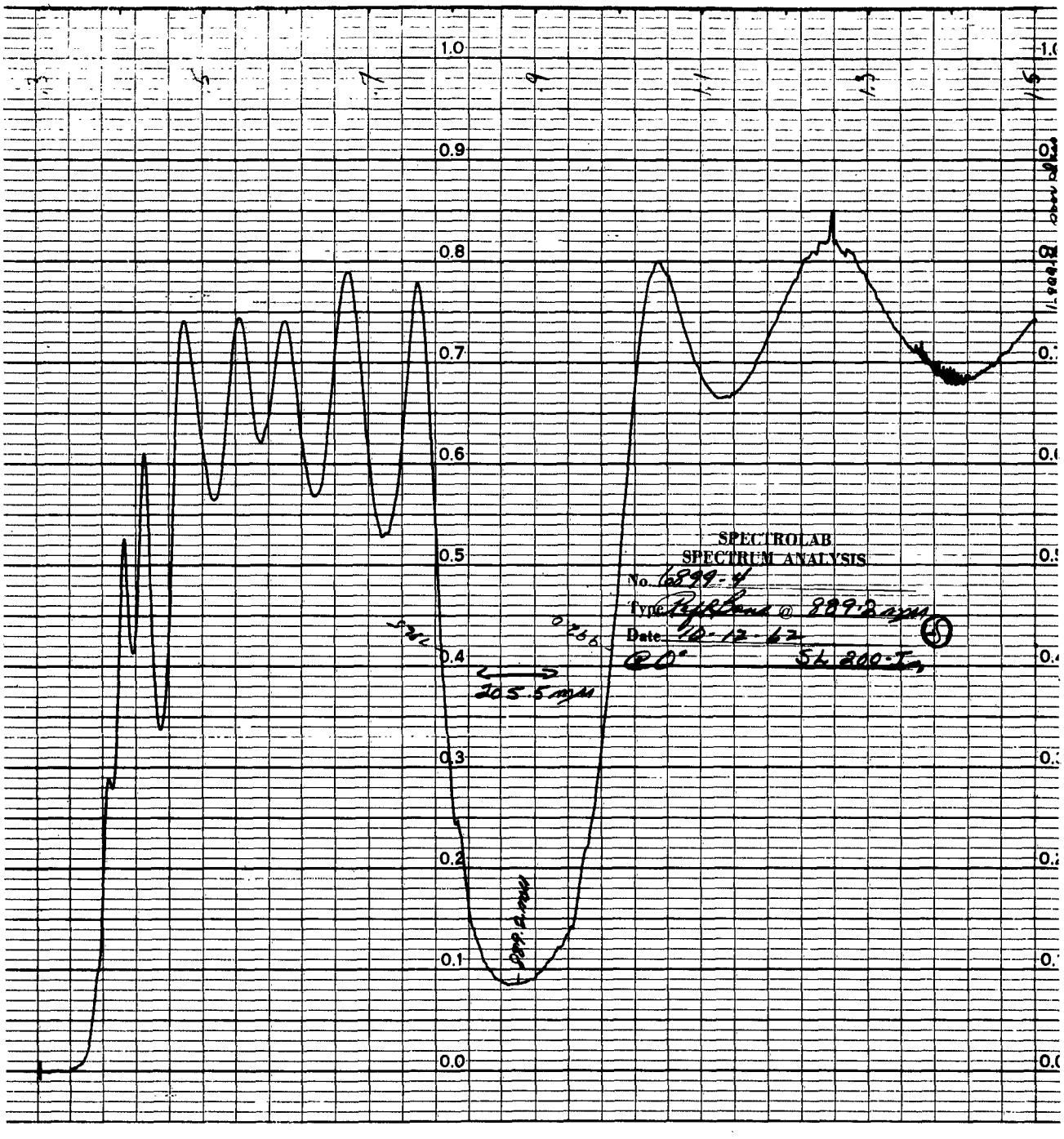

1.0
0.9
0.8
0.7
0.6
0.5
0.4
0.3
0.2
0.1
0.0
SPECTROLAB
SPECTRUM ANALYSIS
No. 6899-4
Type Reflectance @ 889.2 mμ
Date 12-12-67
20°
5% 200-T
205.5 mμ

FIGURE B-14

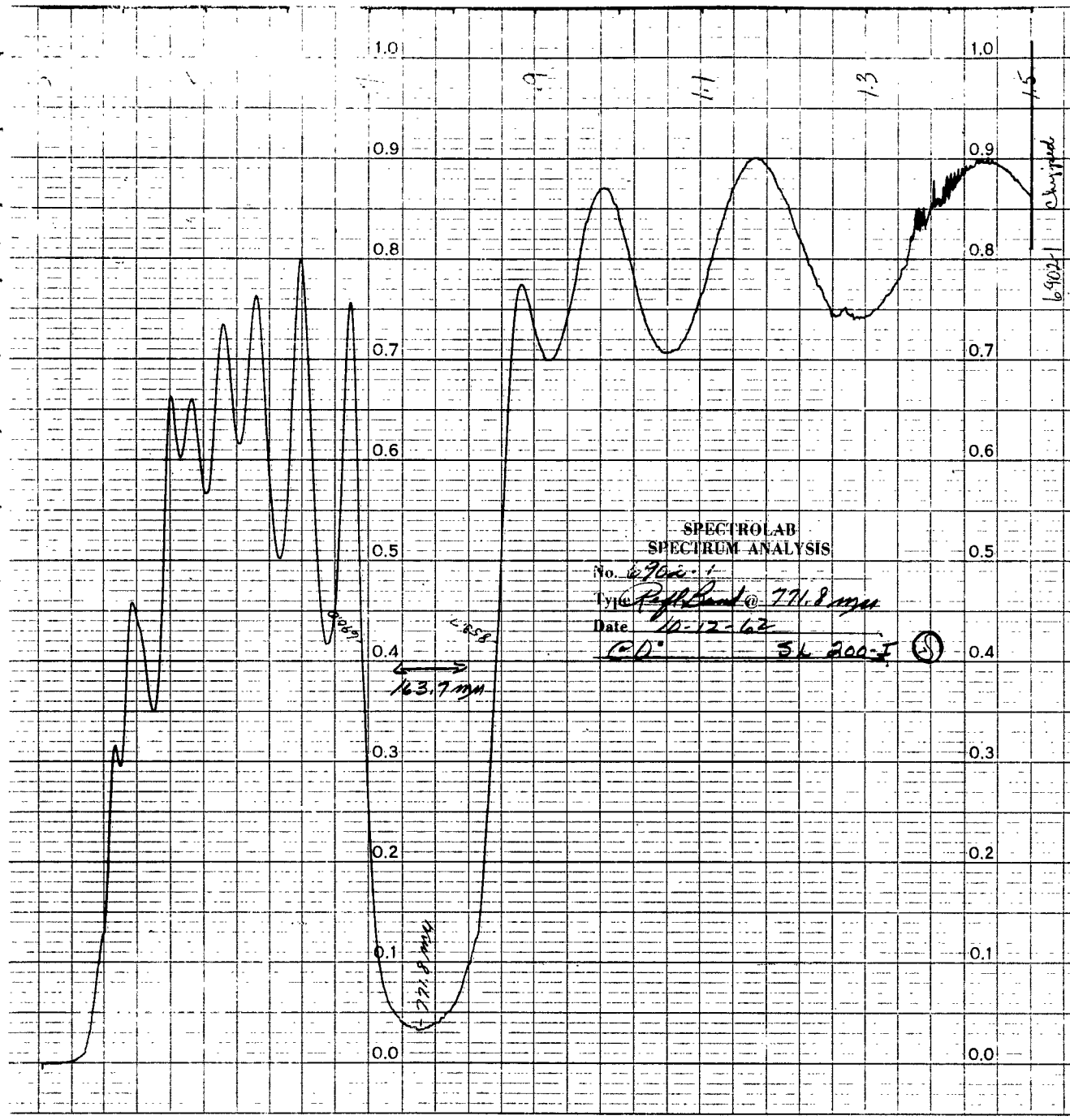

1.0
0.9
0.8
0.7
0.6
0.5
0.4
0.3
0.2
0.1
0.0
SPECTROLAB
SPECTRUM ANALYSIS
No. 690i-1
Type Reflectance @ 771.8 mμ
Date 10-12-62
CD 5L 200-I
163.7 mμ
original

FIGURE B-15

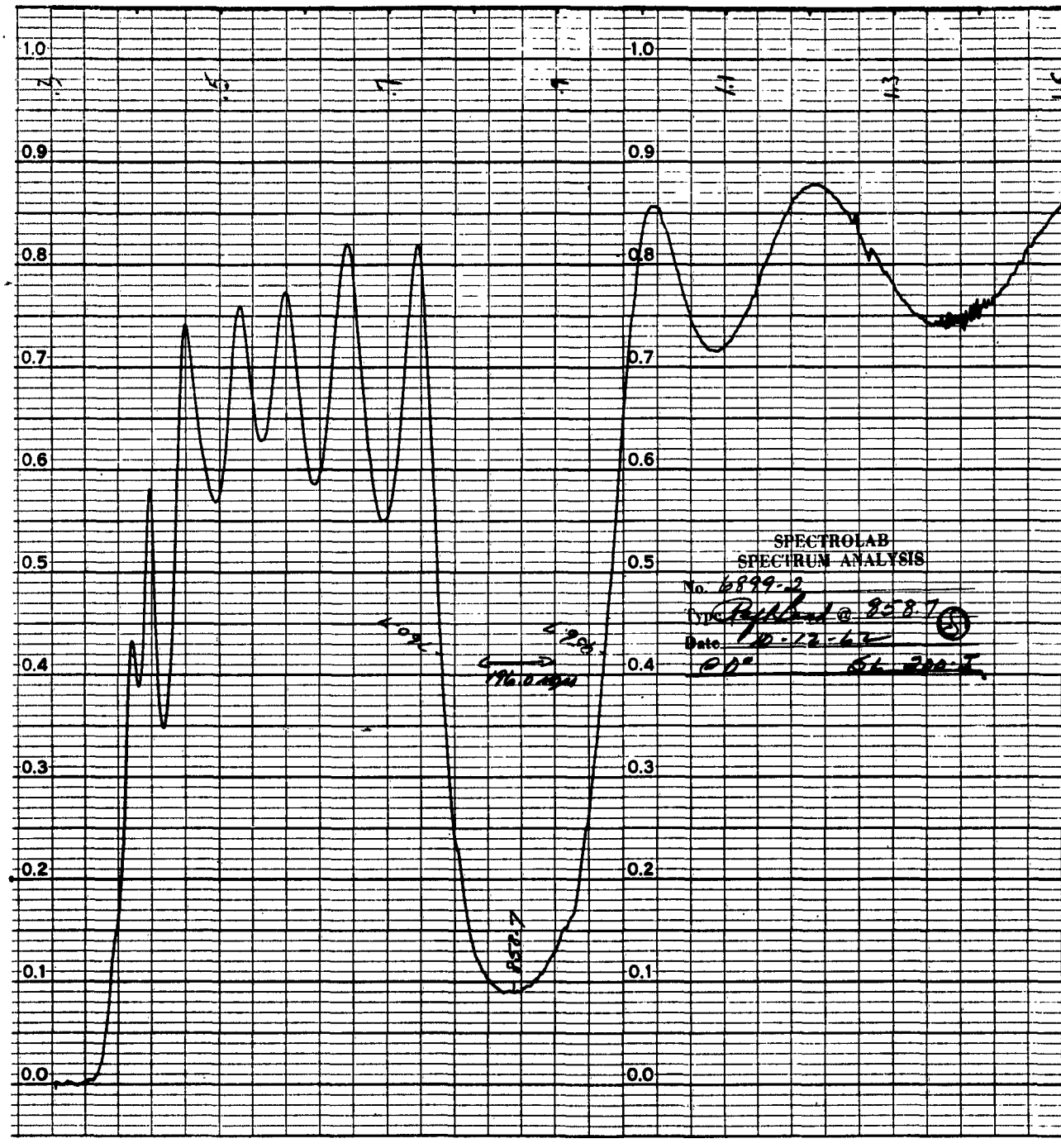

1.0
0.9
0.8
0.7
0.6
0.5
0.4
0.3
0.2
0.1
0.0
SPECTROLAB
SPECTRUM ANALYSIS
No. 6899-2
Date

FIGURE B-16

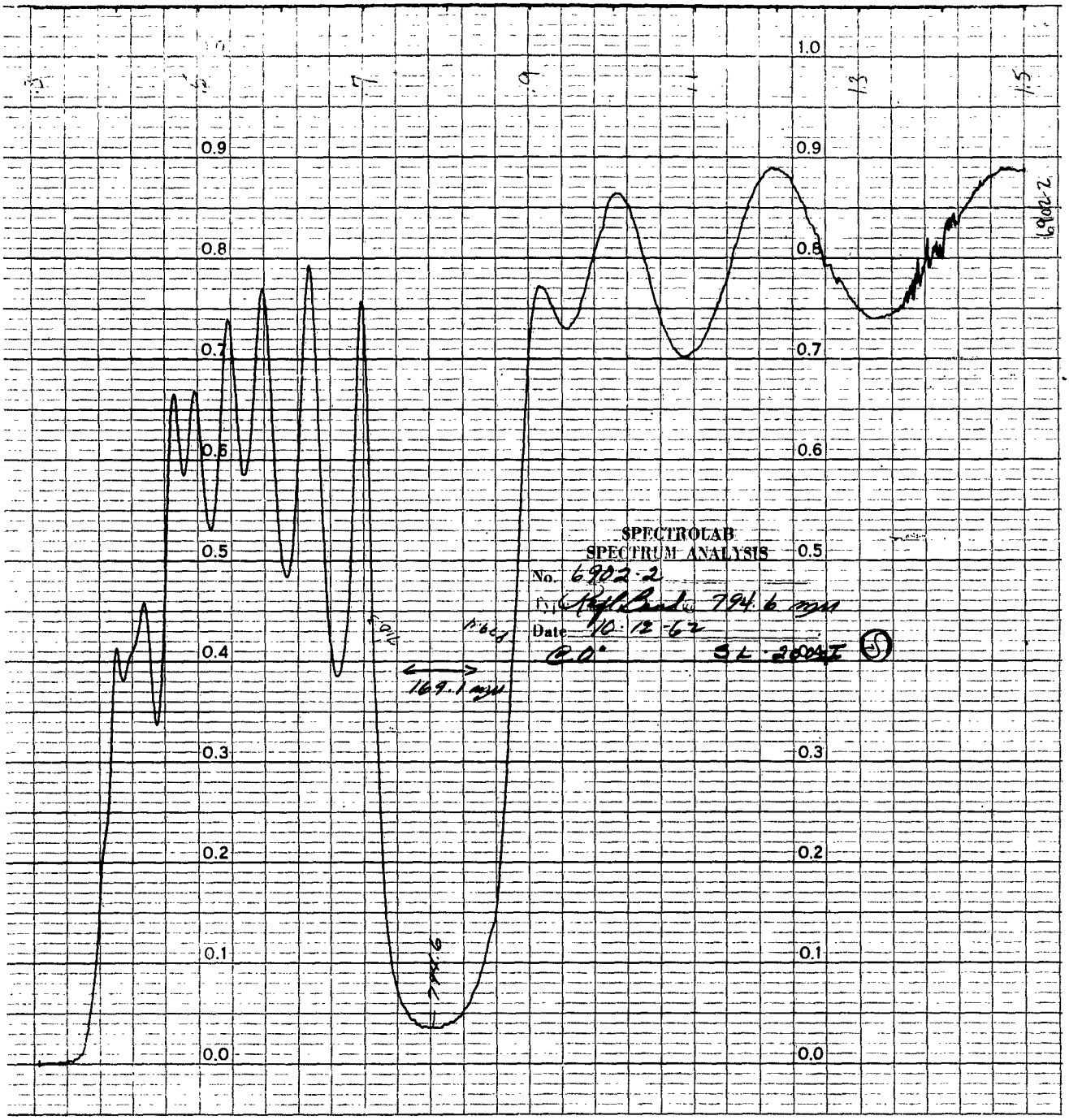

SPECTROLAB
SPECTRUM ANALYSIS
No. 6902-2
Date 10-12-62
169.1 mμ
6902-2

FIGURE B-17

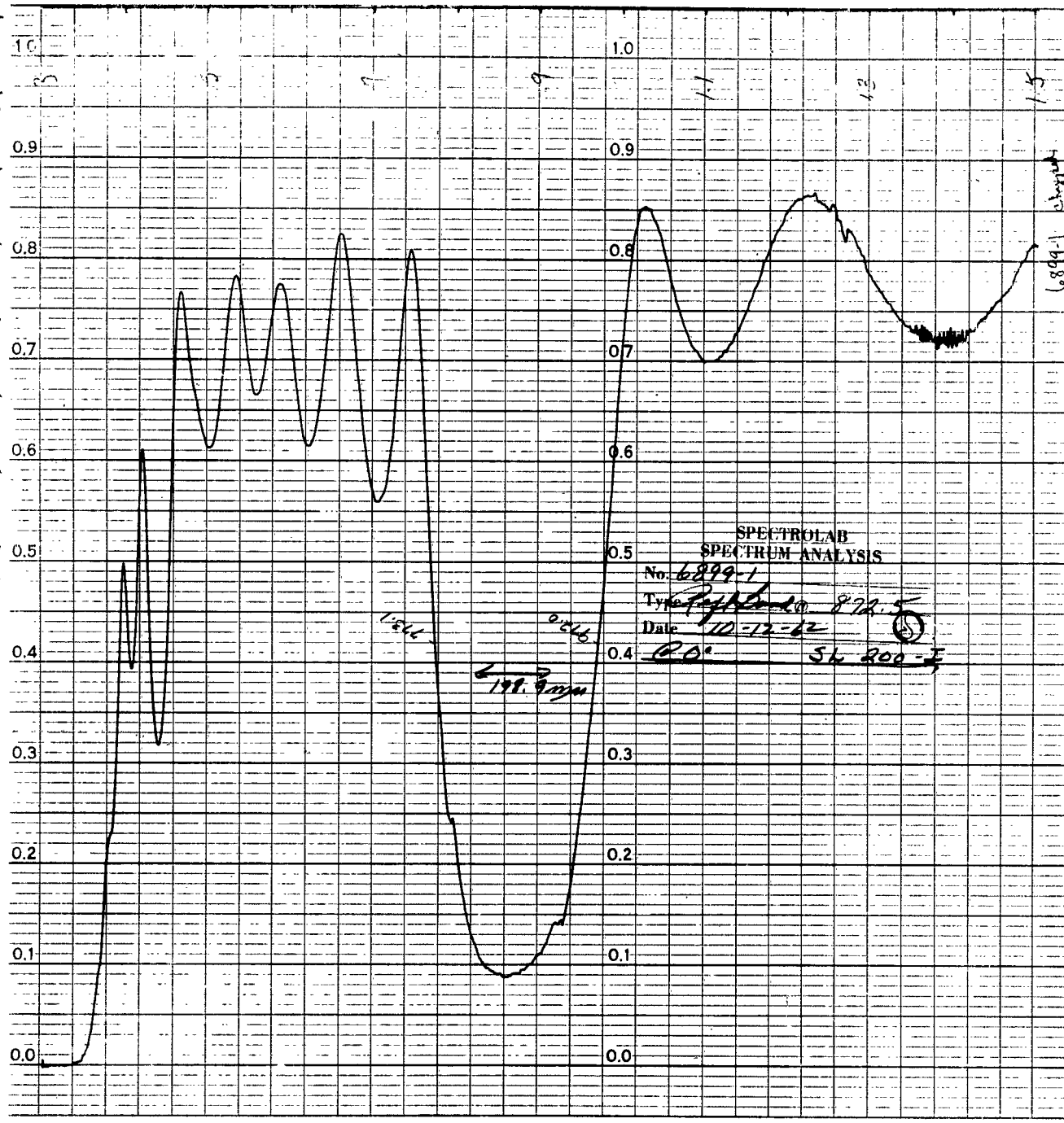

SPECTROLAB
SPECTRUM ANALYSIS
No. 6899-1
Date 10-12-62
60°
SL 200-F
6899-1

FIGURE B-18

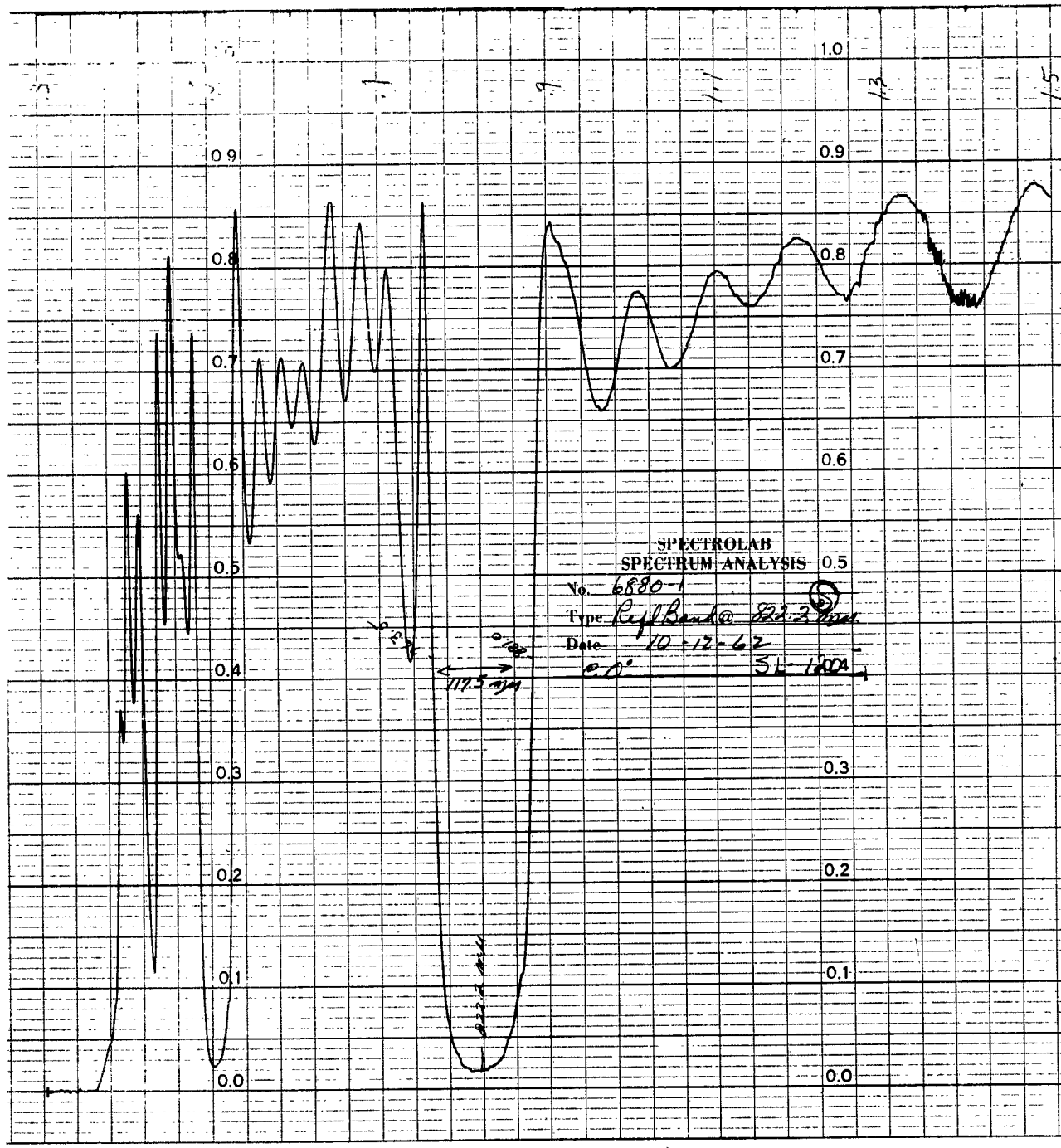

SPECTROLAB
SPECTRUM ANALYSIS
No. 6880-1
Type Refl Band @ 822.2 mμ
Date 10-12-62
0.0
1.0
0.9
0.8
0.7
0.6
0.5
0.4
0.3
0.2
0.1
0.0

FIGURE B-19

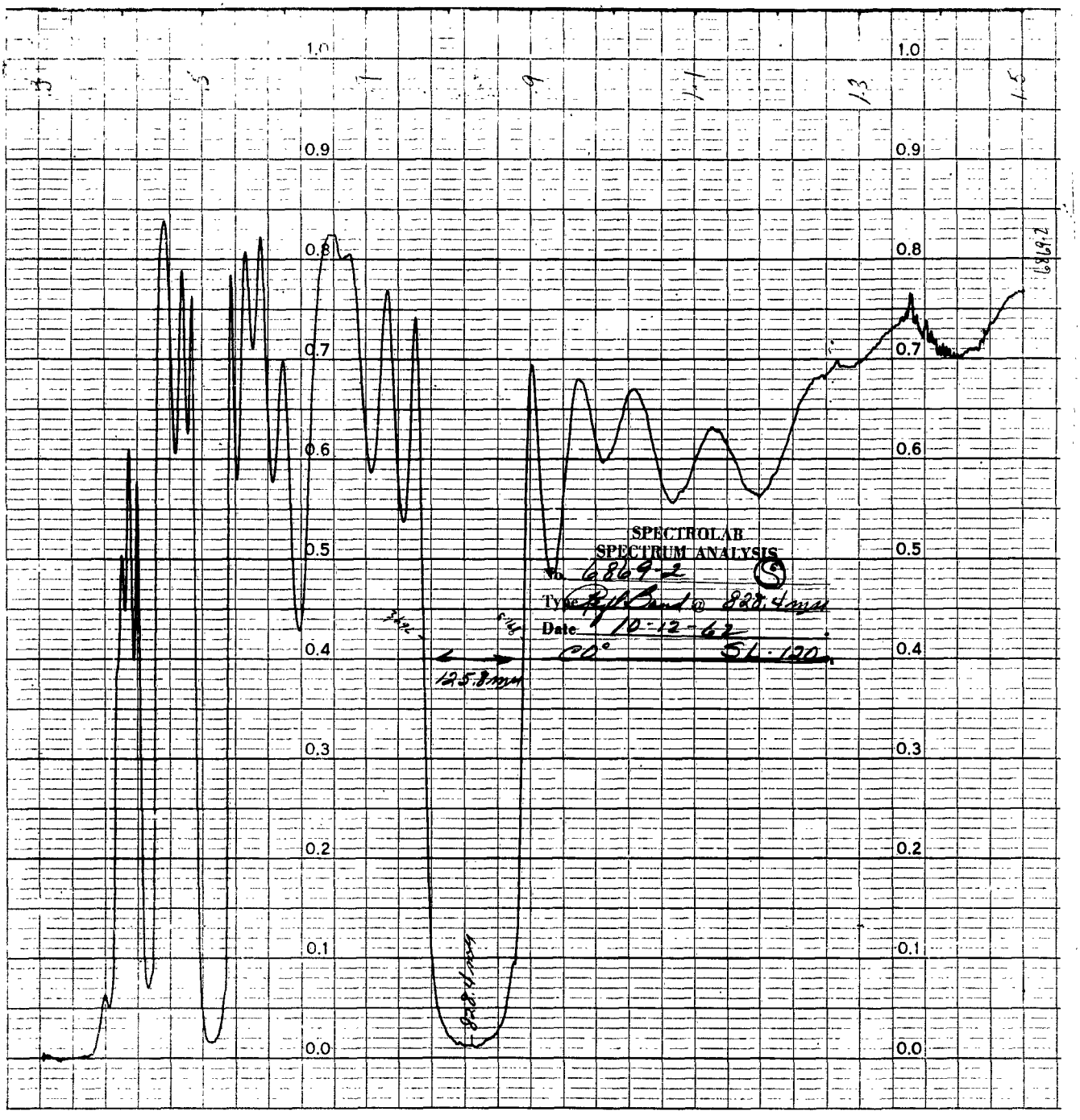

SPECTROLAB
SPECTRUM ANALYSIS
No. 6869-2
Type Ryle Band @ 888.4 cm
Date 10-12-62
CO²
SL-120
125.8 mm
1.0
0.9
0.8
0.7
0.6
0.5
0.4
0.3
0.2
0.1
0.0

FIGURE B-20

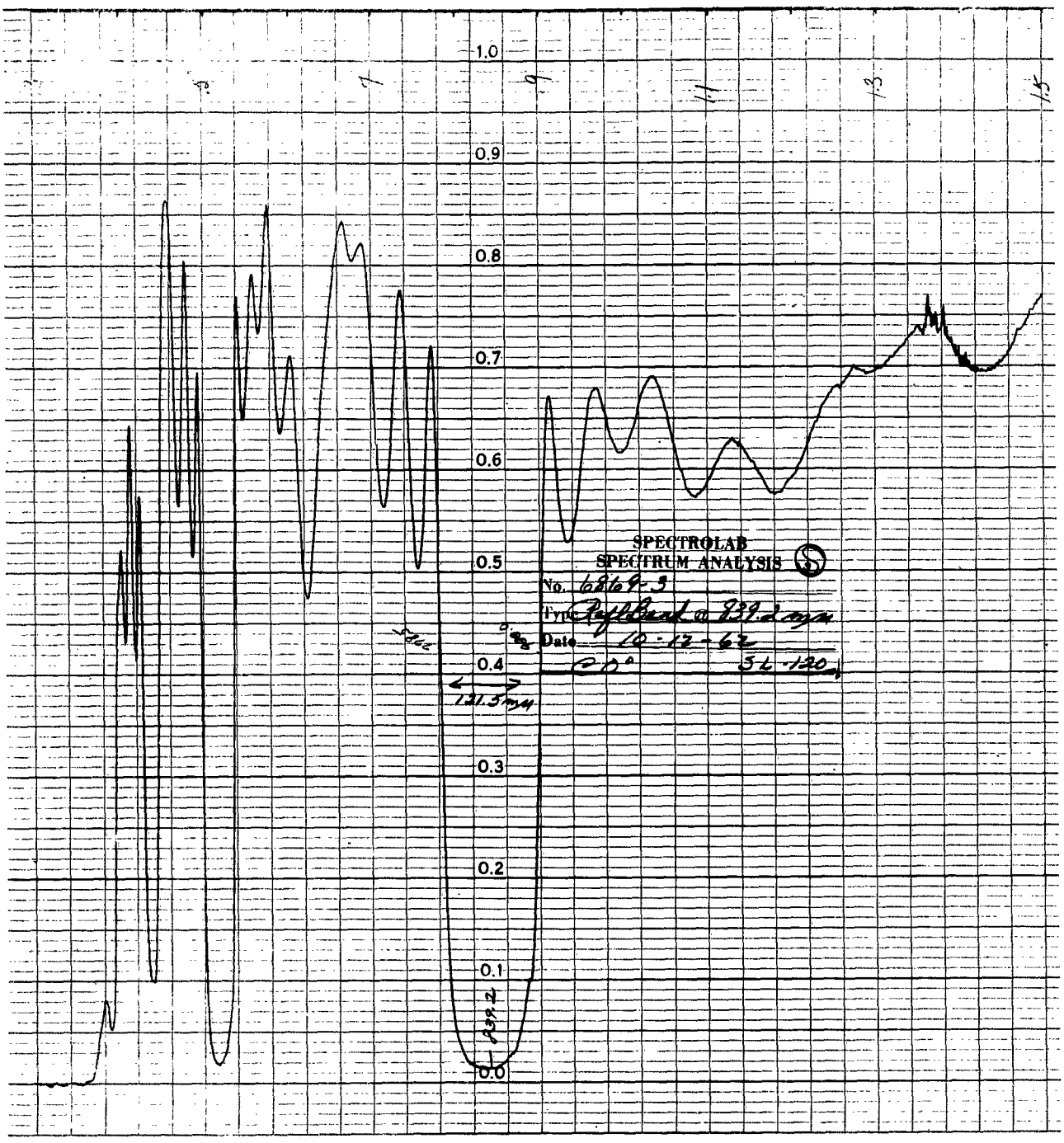

1.0
0.9
0.8
0.7
0.6
0.5
0.4
0.3
0.2
0.1
0.0
SPECTROLAB
SPECTRUM ANALYSIS
No. 6869-3
Type Reflectance
Date 10-12-62
131.3 mμ

FIGURE B-21

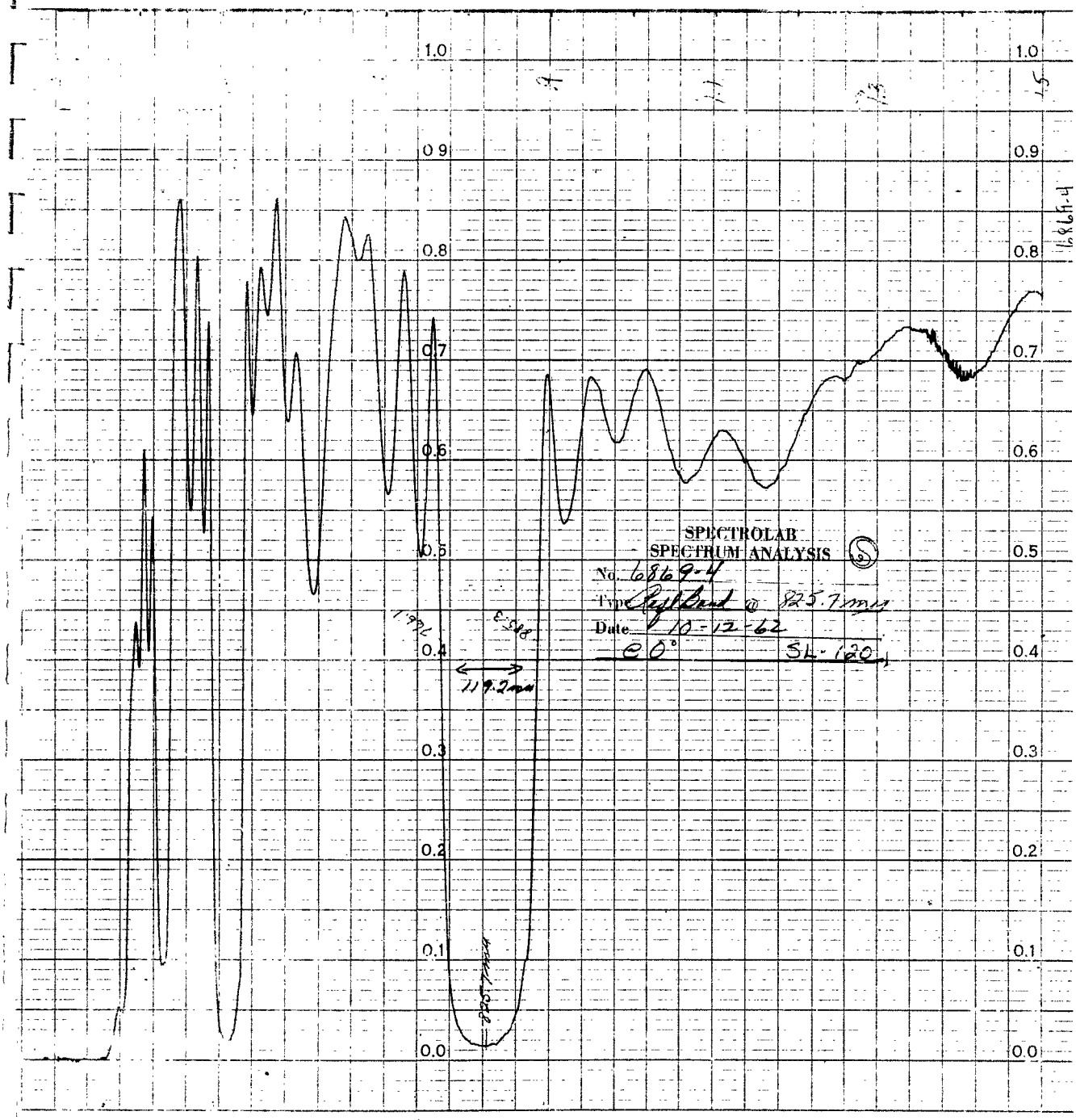

1.0
0.9
0.8
0.7
0.6
0.5
0.4
0.3
0.2
0.1
0.0
SPECTROLAB
SPECTRUM ANALYSIS
No. 6869-4
Type Light Band @ 825.7mμ
Date 10-12-62
0°
SL-120
119.2mm
6869-4

FIGURE B-22

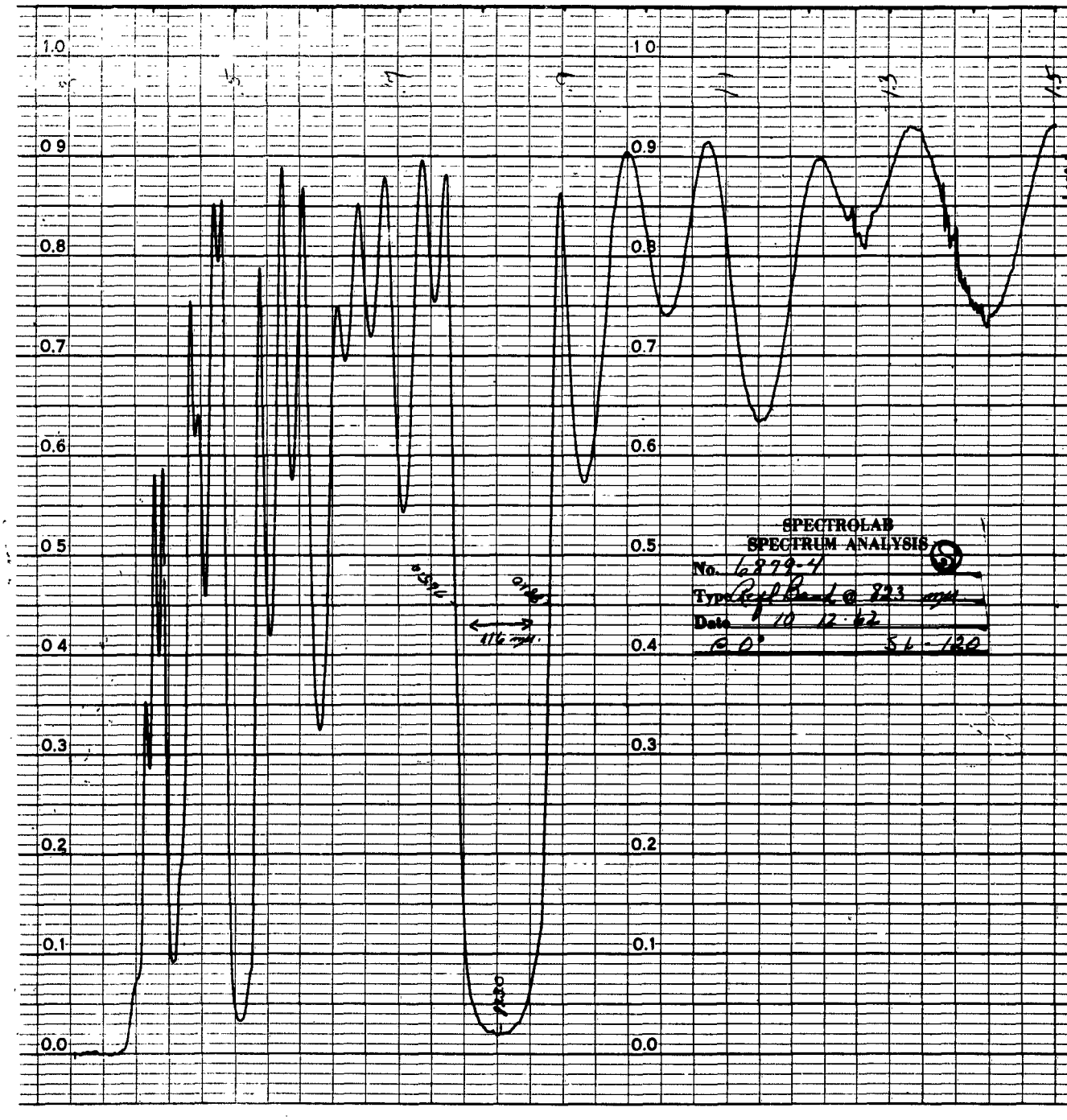

1.0
0.9
0.8
0.7
0.6
0.5
0.4
0.3
0.2
0.1
0.0
SPECTROLAB
SPECTRUM ANALYSIS
No. 6279-4
Type Rigel Bo-L @ 823 mμ
Date 10 12 62
C O' 54-120

FIGURE B-23

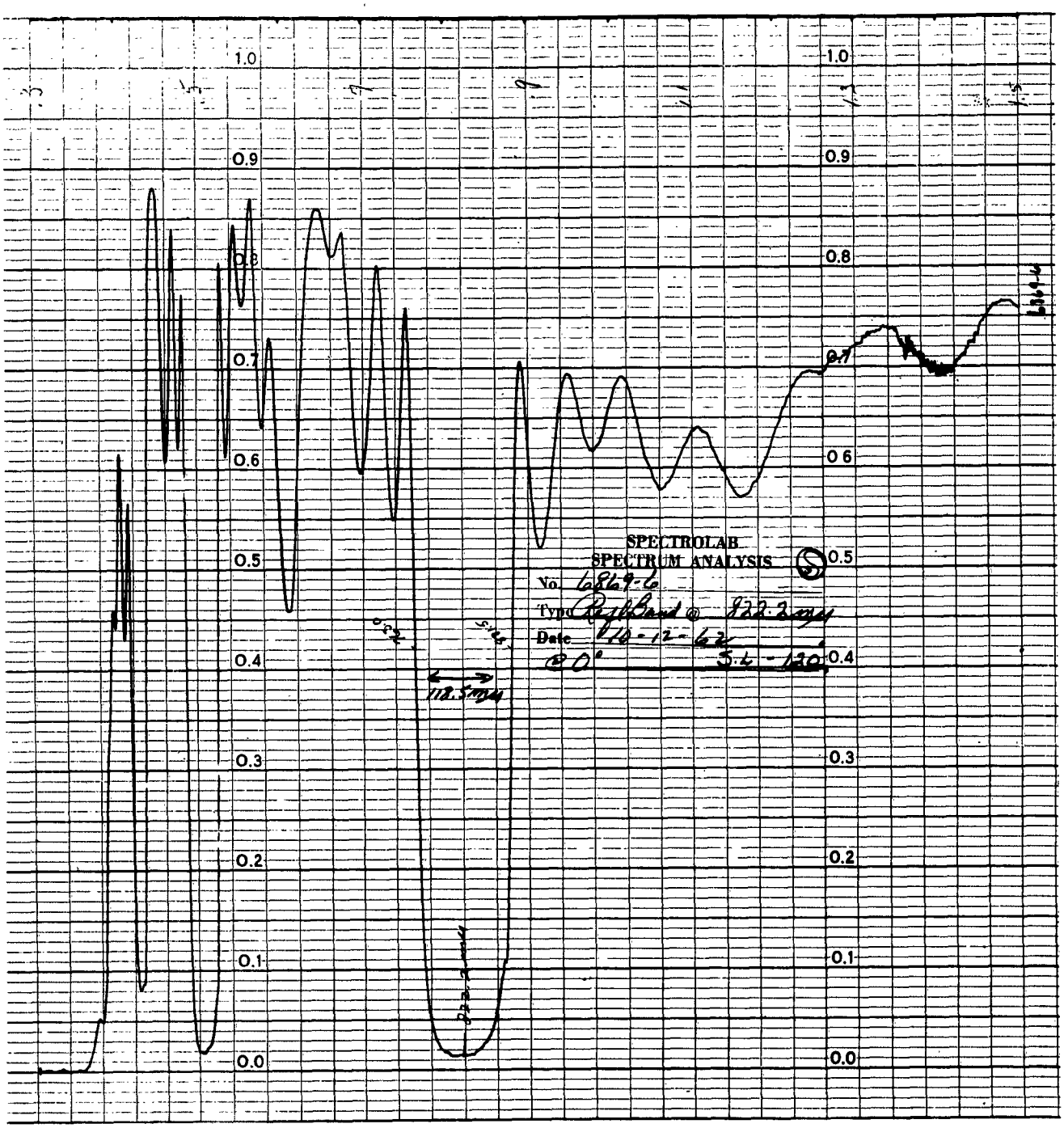

1.0
0.9
0.8
0.7
0.6
0.5
0.4
0.3
0.2
0.1
0.0
SPECTROLAB
SPECTRUM ANALYSIS
No. 6869-6
Type Right Band @ 122.2 cps
Date 10-12-62
@ 0°
5.4 - 130
112.5 cps

FIGURE B-24

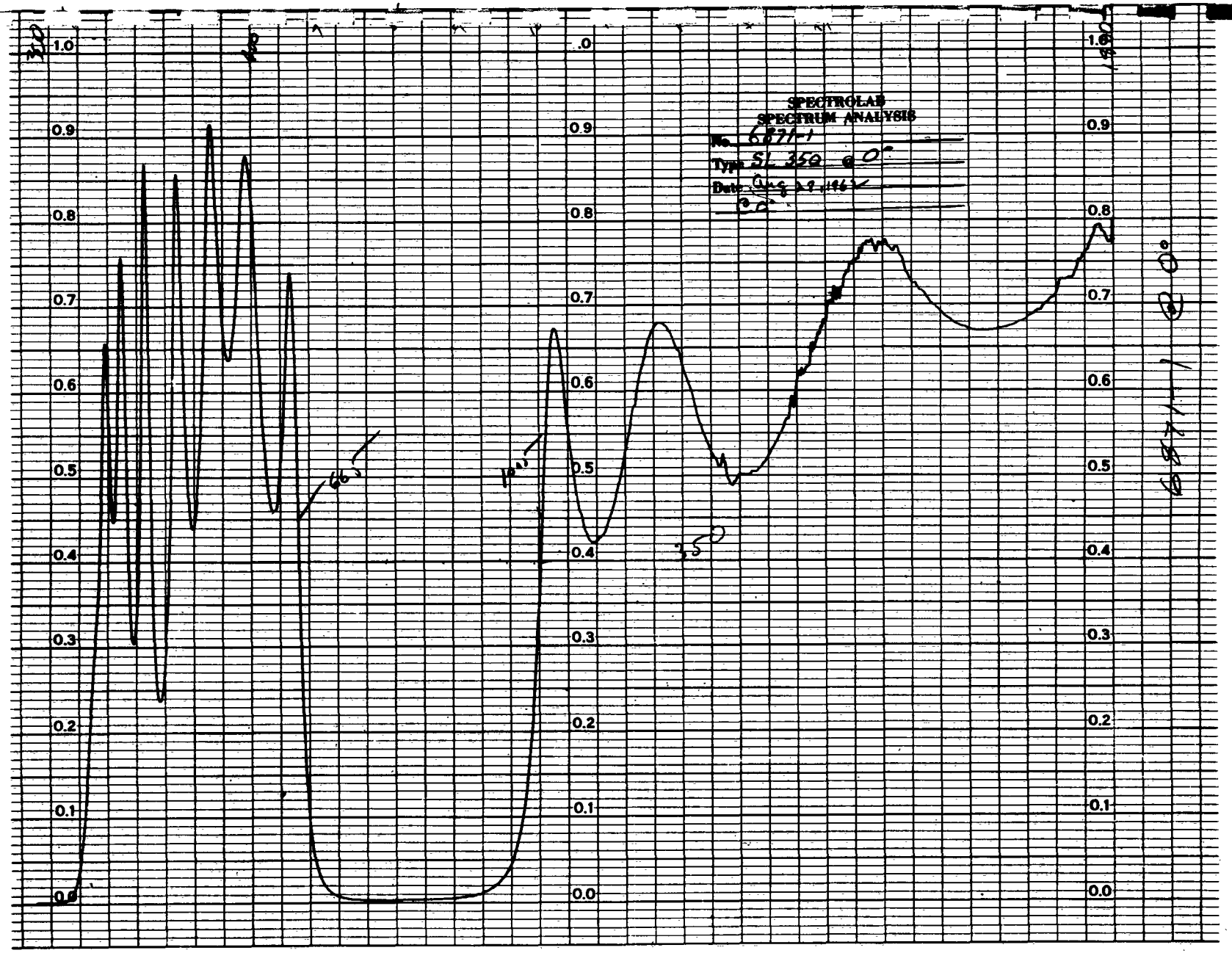

SPECTROLAB
SPECTRUM ANALYSIS
No. 6871-1
Type SL 350 @ 0°
Date 0-6-?-146
1.0
0.9
0.8
0.7
0.6
0.5
0.4
0.3
0.2
0.1
0.0

Figure B-25

SPECTROLAB
SPECTRUM ANALYSIS
No. 6771-1
Type S-1 350 @ 10°
Date 2-2-66
1.0
0.9
0.8
0.7
0.6
0.5
0.4
0.3
0.2
0.1
0.0
6771-1 @ 10°

Figure B-26

SPECTROLAB
SPECTRUM ANALYSIS
No. 6971-1
Type SL-150 @ 20°
Date 8-24-60
1.0
0.9
0.8
0.7
0.6
0.5
0.4
0.3
0.2
0.1
0.0

Figure B-27

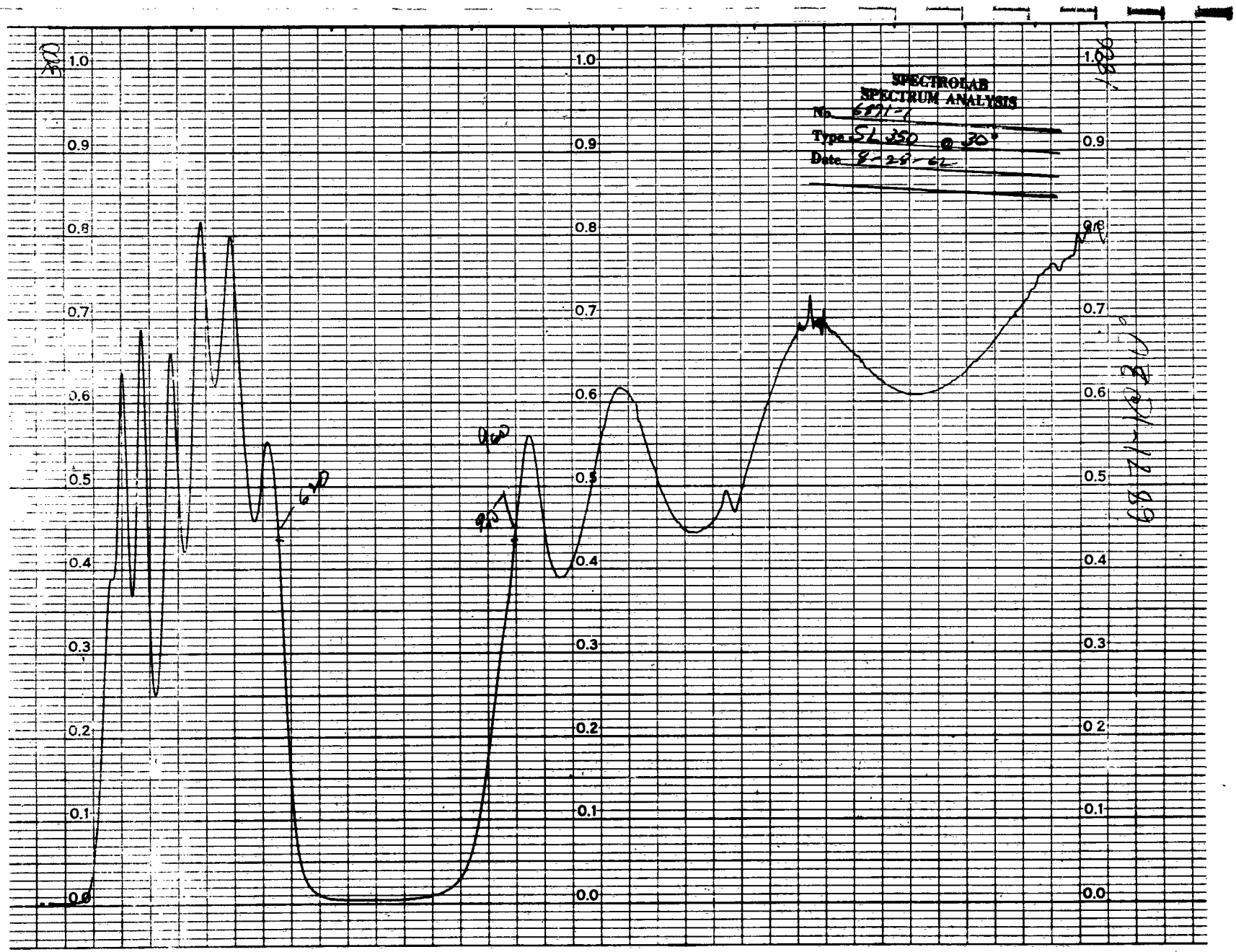

SPECTROLAB
SPECTRUM ANALYSIS
No. 6771-1
Type SL 250 @ 30°
Date 8-29-62
1.0
0.9
0.8
0.7
0.6
0.5
0.4
0.3
0.2
0.1
0.0

Figure B-28

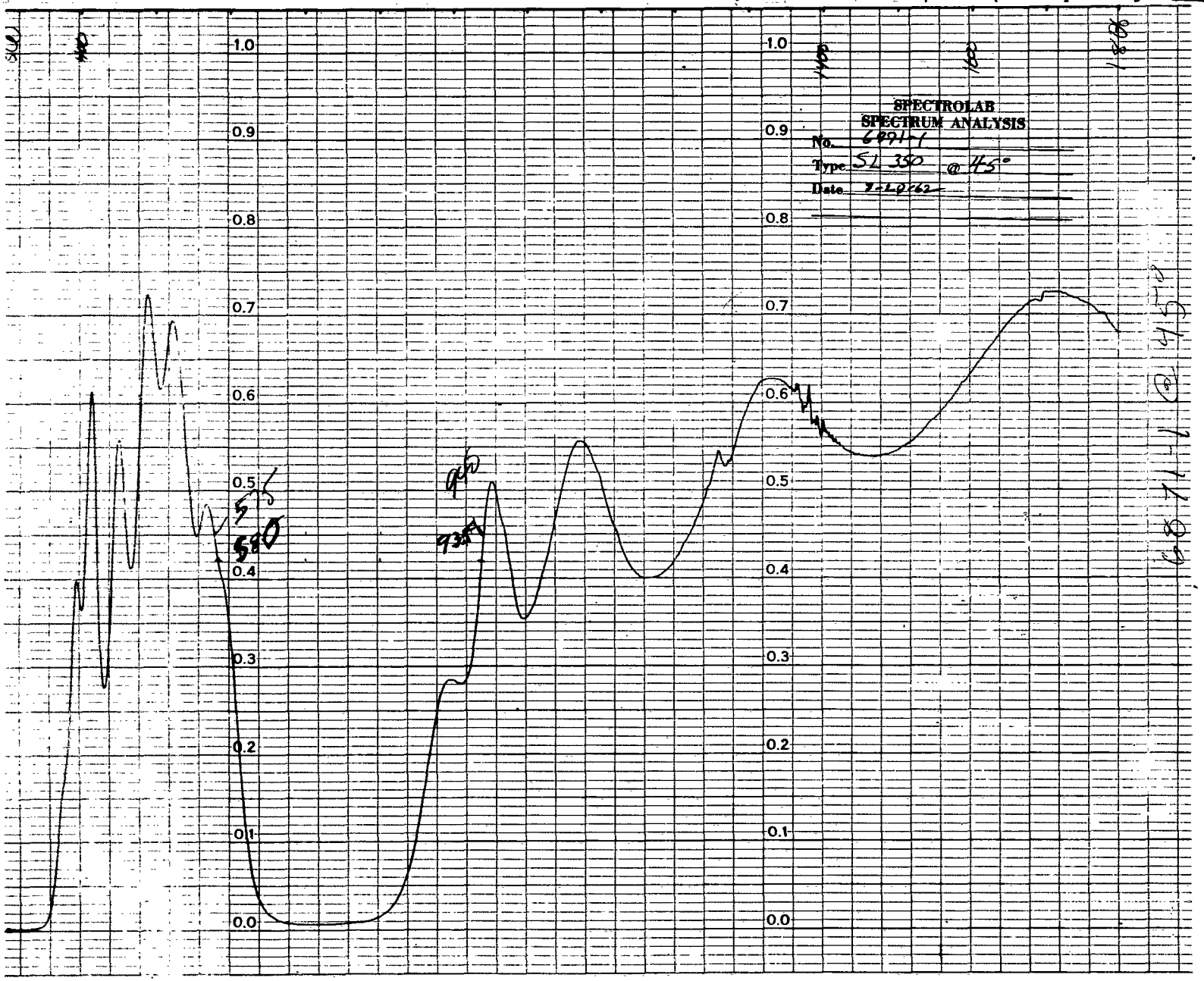

SPECTROLAB
SPECTRUM ANALYSIS
No. 6991-1
Type SL 350 @ 45°
Date 7-20-62
1.0
0.9
0.8
0.7
0.6
0.5
0.4
0.3
0.2
0.1
0.0

Figure B-29

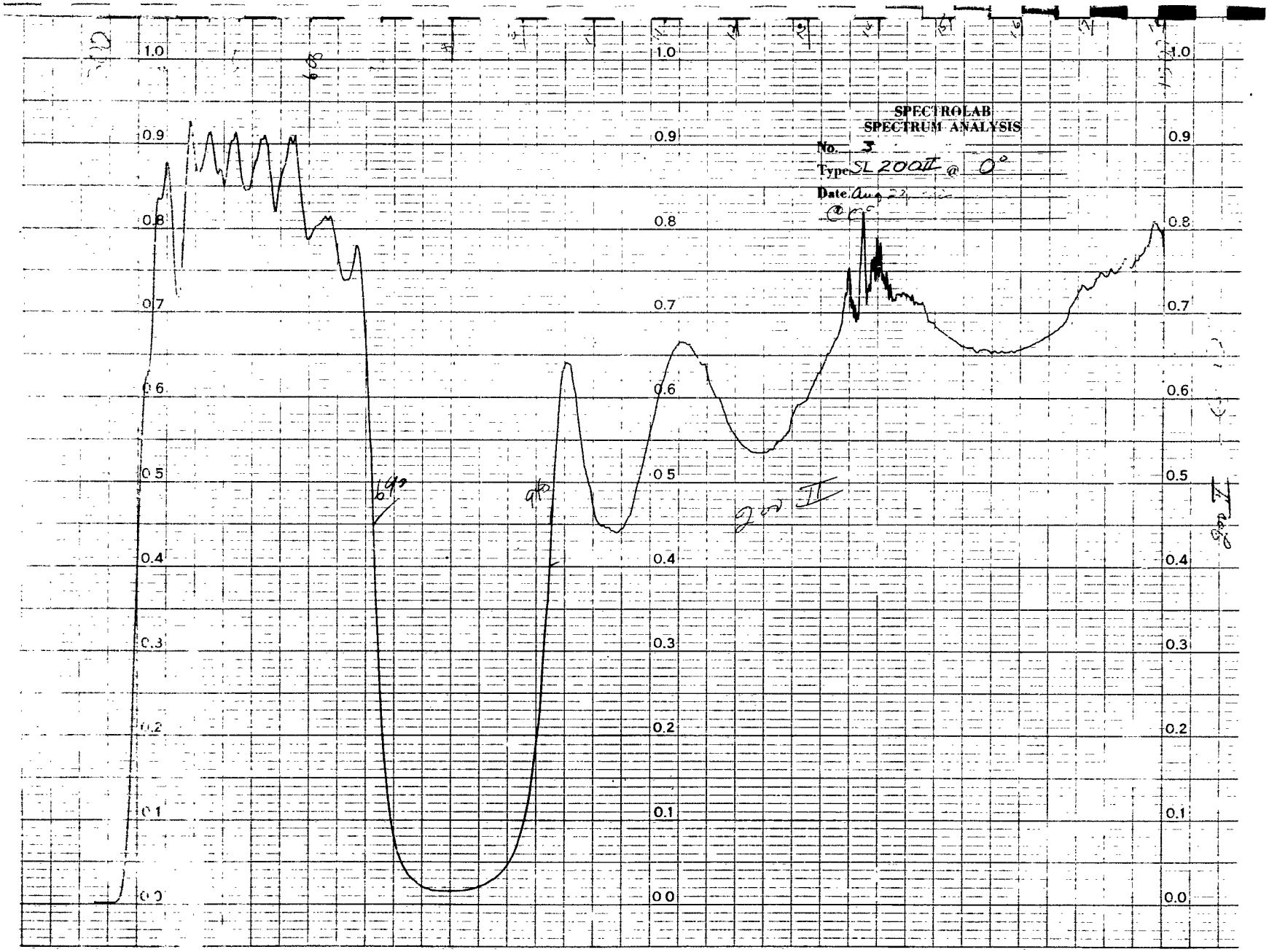
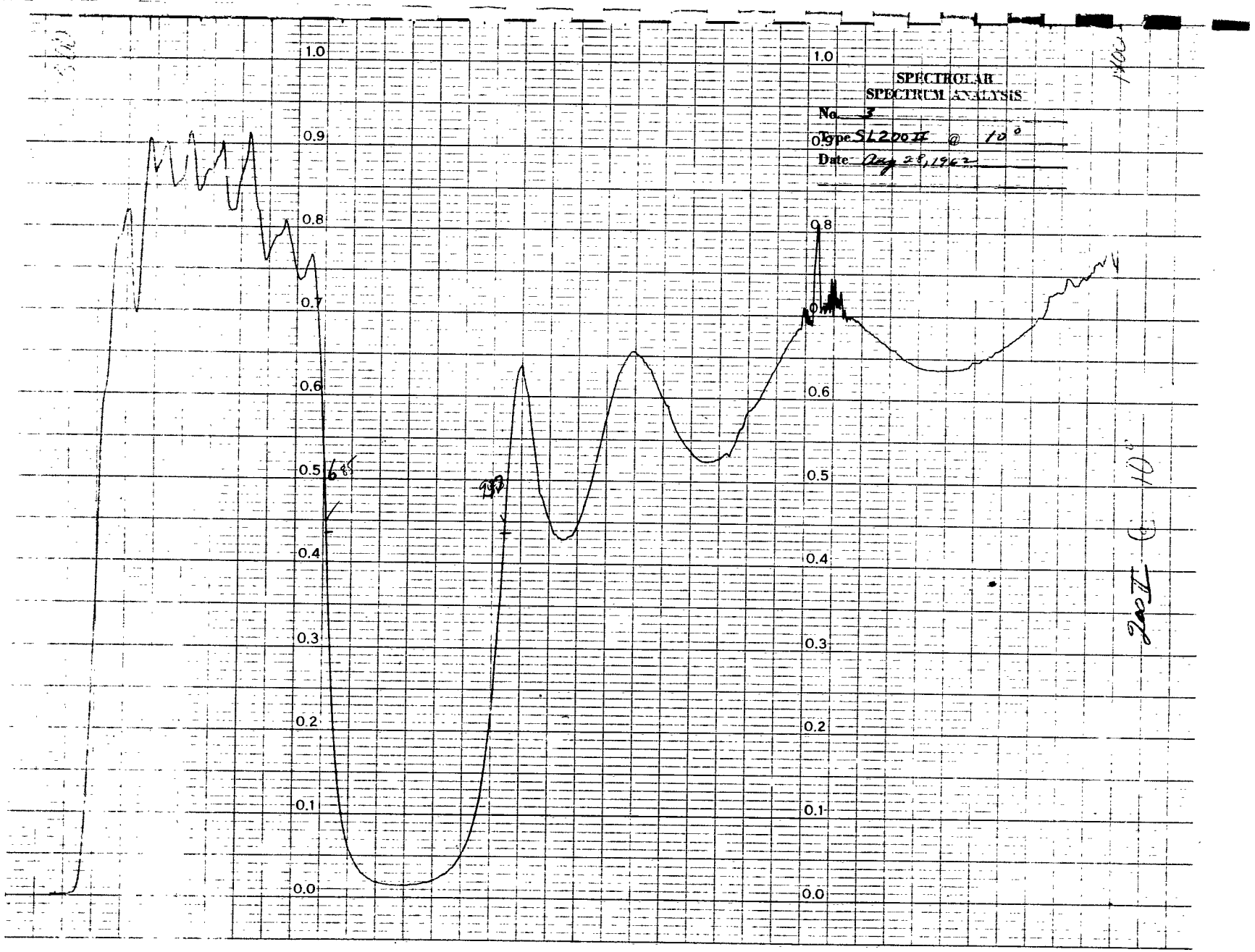

SPECTROLAB
SPECTRUM ANALYSIS
No. 3
Type SL 20 att @ 0°
Date Aug 22
1.0
0.9
0.8
0.7
0.6
0.5
0.4
0.3
0.2
0.1
0.0

Figure B-30


SPECTROLAB
SPECTRUM ANALYSIS
No. 3
Type SL200 II @ 10°
Date Aug 28, 1962
1.0
0.9
0.8
0.7
0.6
0.5
0.4
0.3
0.2
0.1
0.0

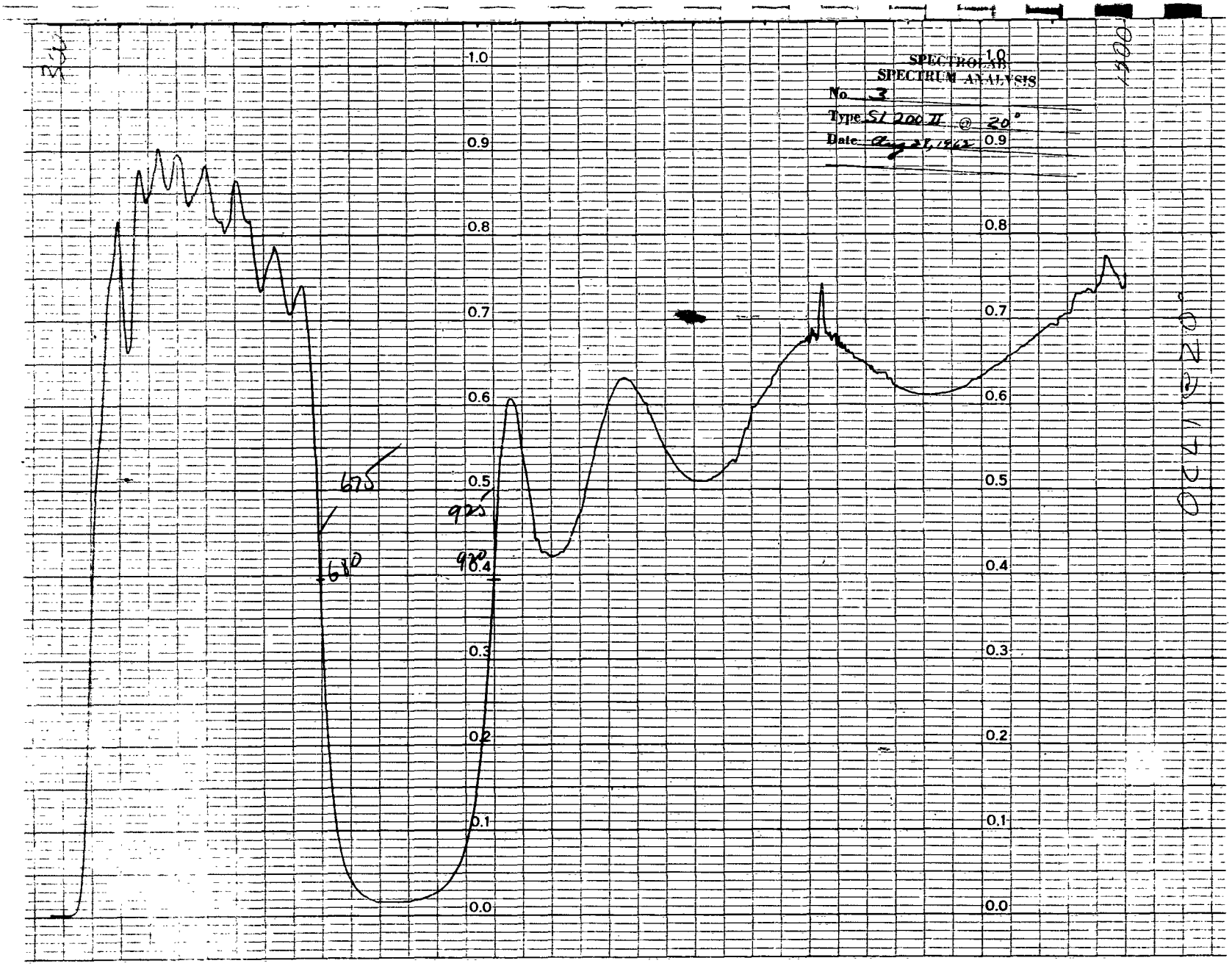

SPECTROLAB
SPECTRUM ANALYSIS
No. 3
Type SL 200 II @ 20°
Date Aug 21, 1962
1.0
0.9
0.8
0.7
0.6
0.5
0.4
0.3
0.2
0.1
0.0
675
925
610
920
1000
0.4 2 4 6 8

Figure B-32

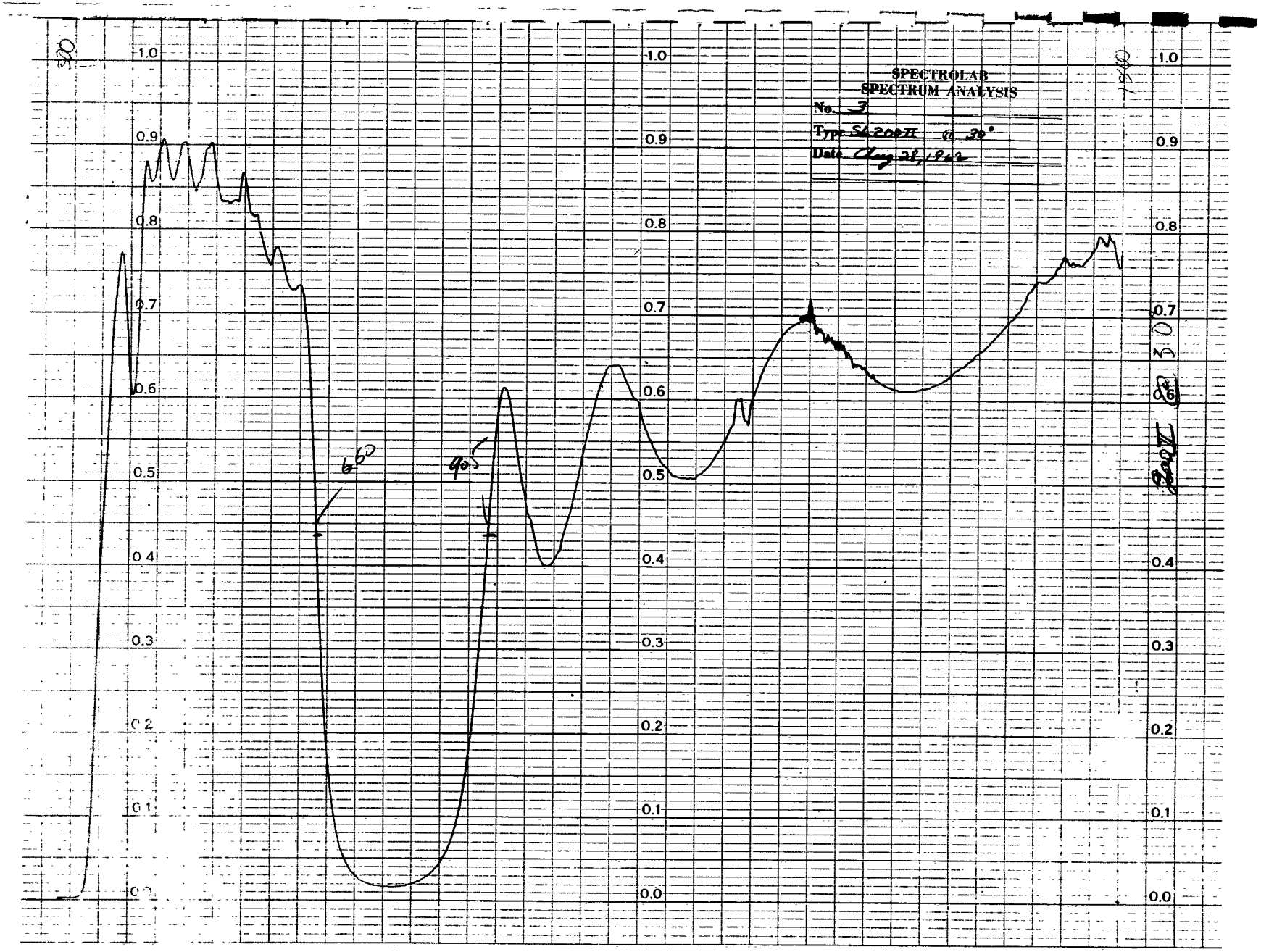
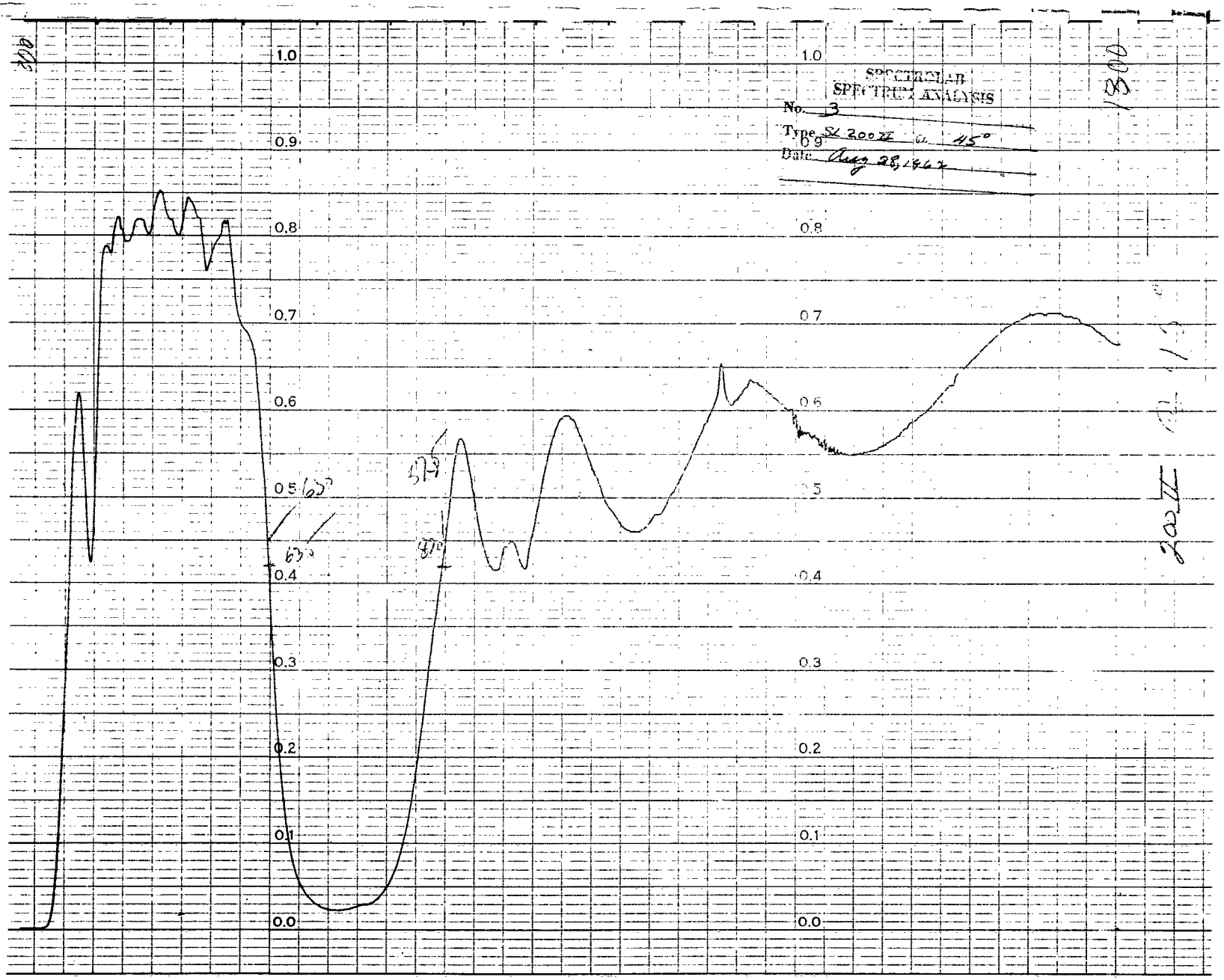
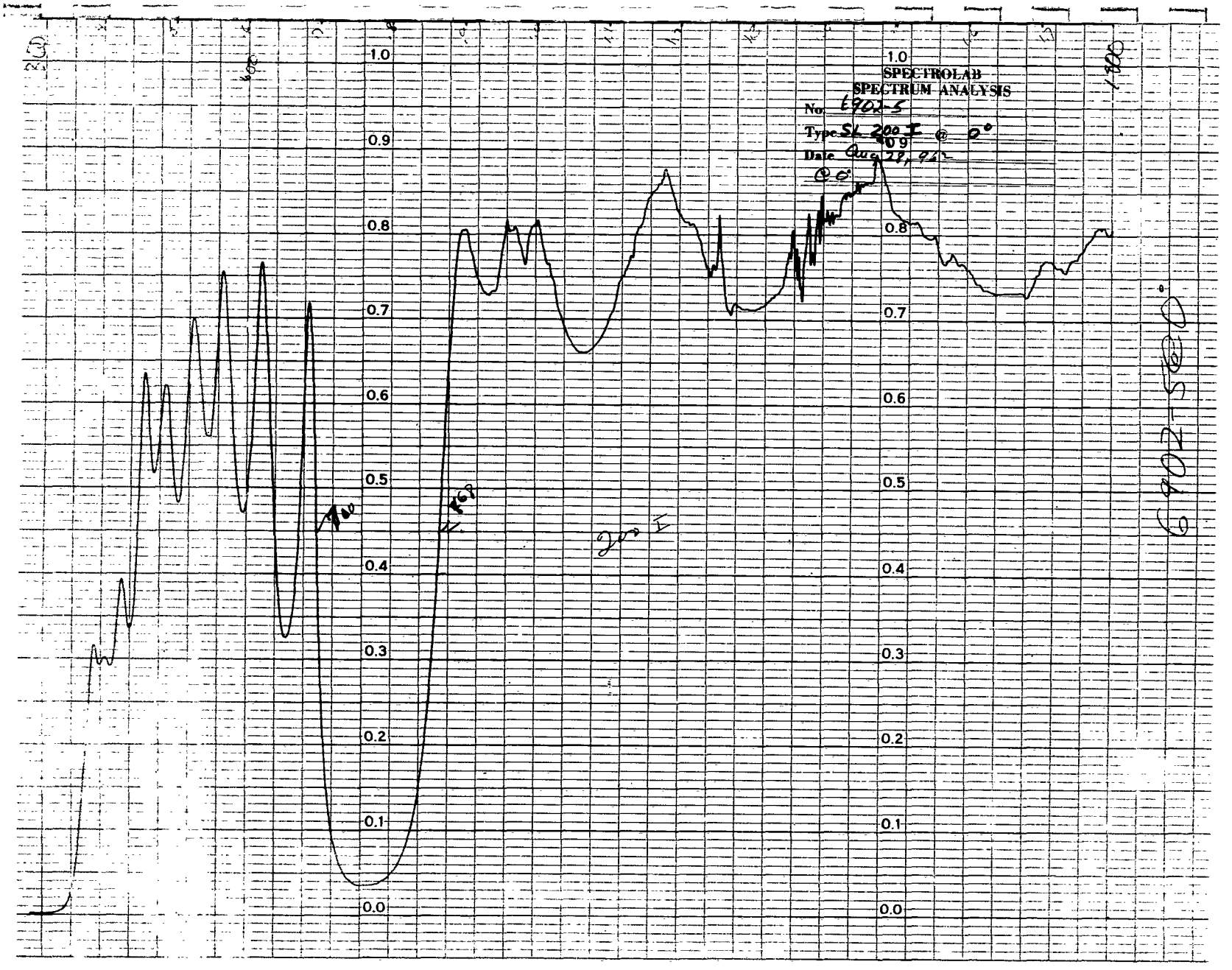

SPECTROLAB
SPECTRUM ANALYSIS
No. 3
Type SA 200 II @ 30°
Date Aug 28, 1962
60°
90°
1.0
0.9
0.8
0.7
0.6
0.5
0.4
0.3
0.2
0.1
0.0

Figure B-33


1.0
0.9
0.8
0.7
0.6
0.5
0.4
0.3
0.2
0.1
0.0
SPECTRUM ANALYSIS
No. 3
Type SL 200 K @ 45°
Date Aug 28, 1962
63°
63°
57°
57°
200
800
2 K


SPECTROLAB
SPECTRUM ANALYSIS
No. 6903-5
Type SL-200 I @ 0°
Date Aug 28, 94
@ 0°
90° V
1.0
0.9
0.8
0.7
0.6
0.5
0.4
0.3
0.2
0.1
0.0

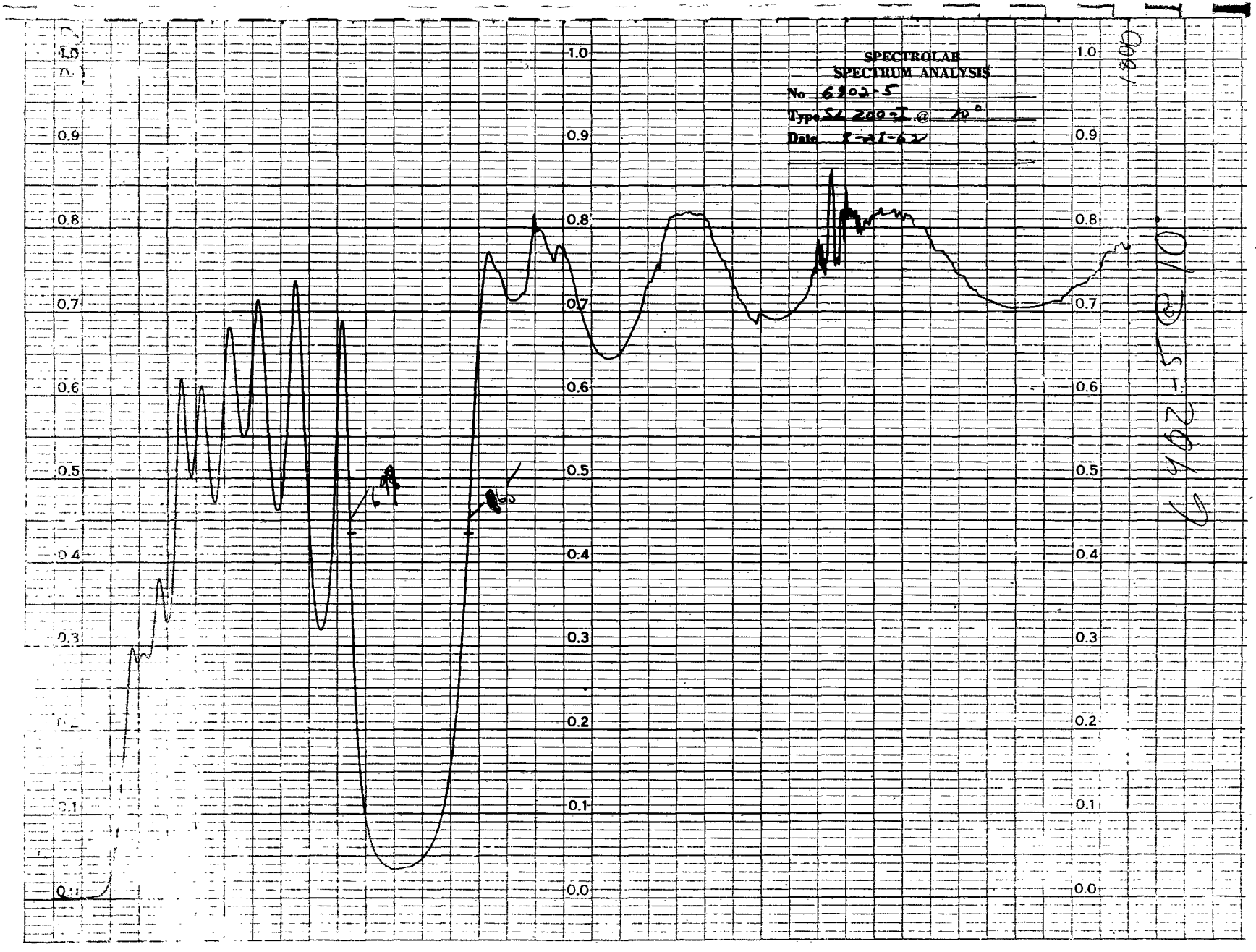

SPECTROLAB
SPECTRUM ANALYSIS
No 6202-5
Type SL 200-2 @ 10°
Date 2-21-62
1.0
0.9
0.8
0.7
0.6
0.5
0.4
0.3
0.2
0.1
0.0

Figure B-36

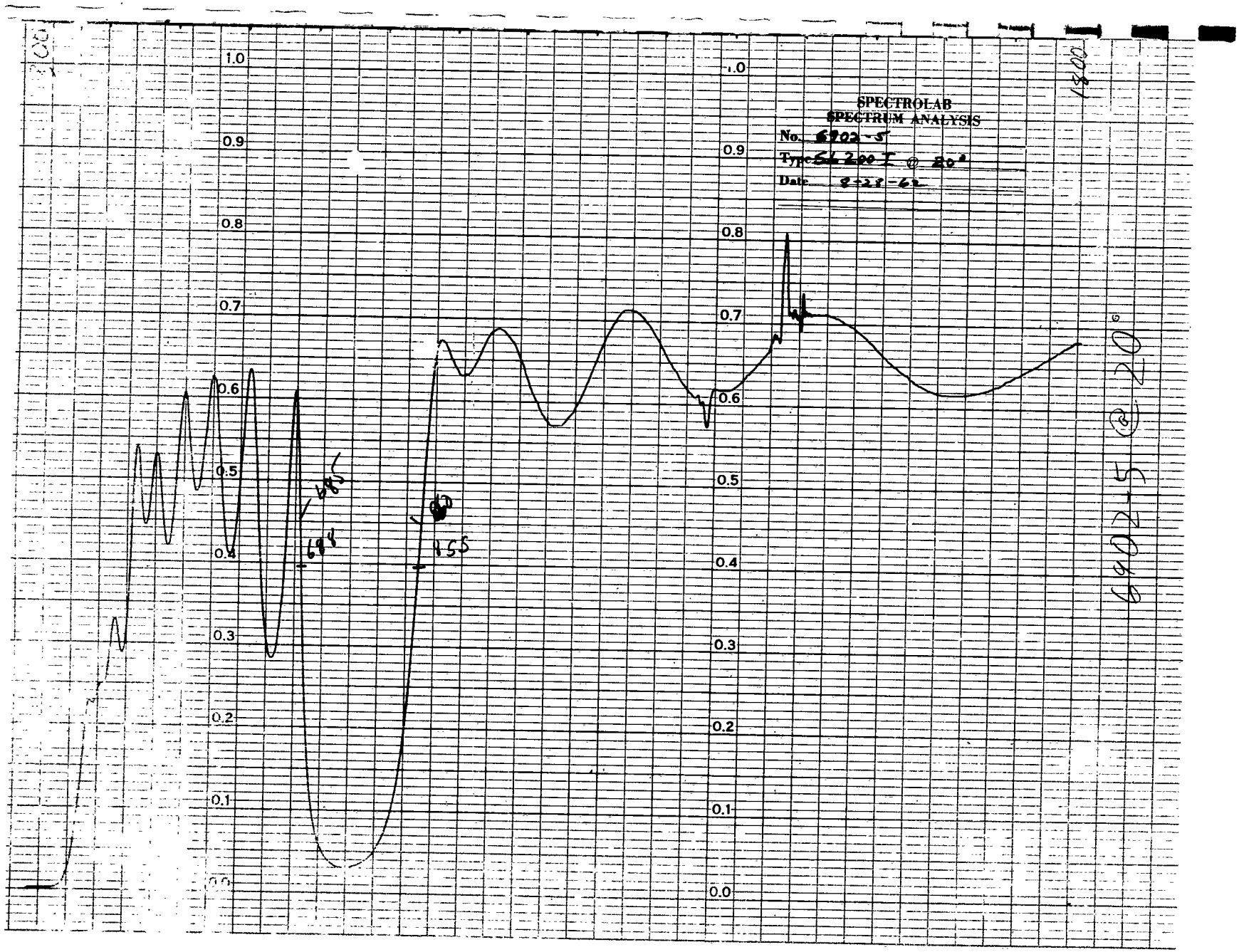

SPECTROLAB
SPECTRUM ANALYSIS
No. 6902-5
Type SL 200 I @ 20°
Date 8-28-62
1.0
0.9
0.8
0.7
0.6
0.5
0.4
0.3
0.2
0.1
0.0
1800
400 2.5 @ 20°
68
155

Figure B-37

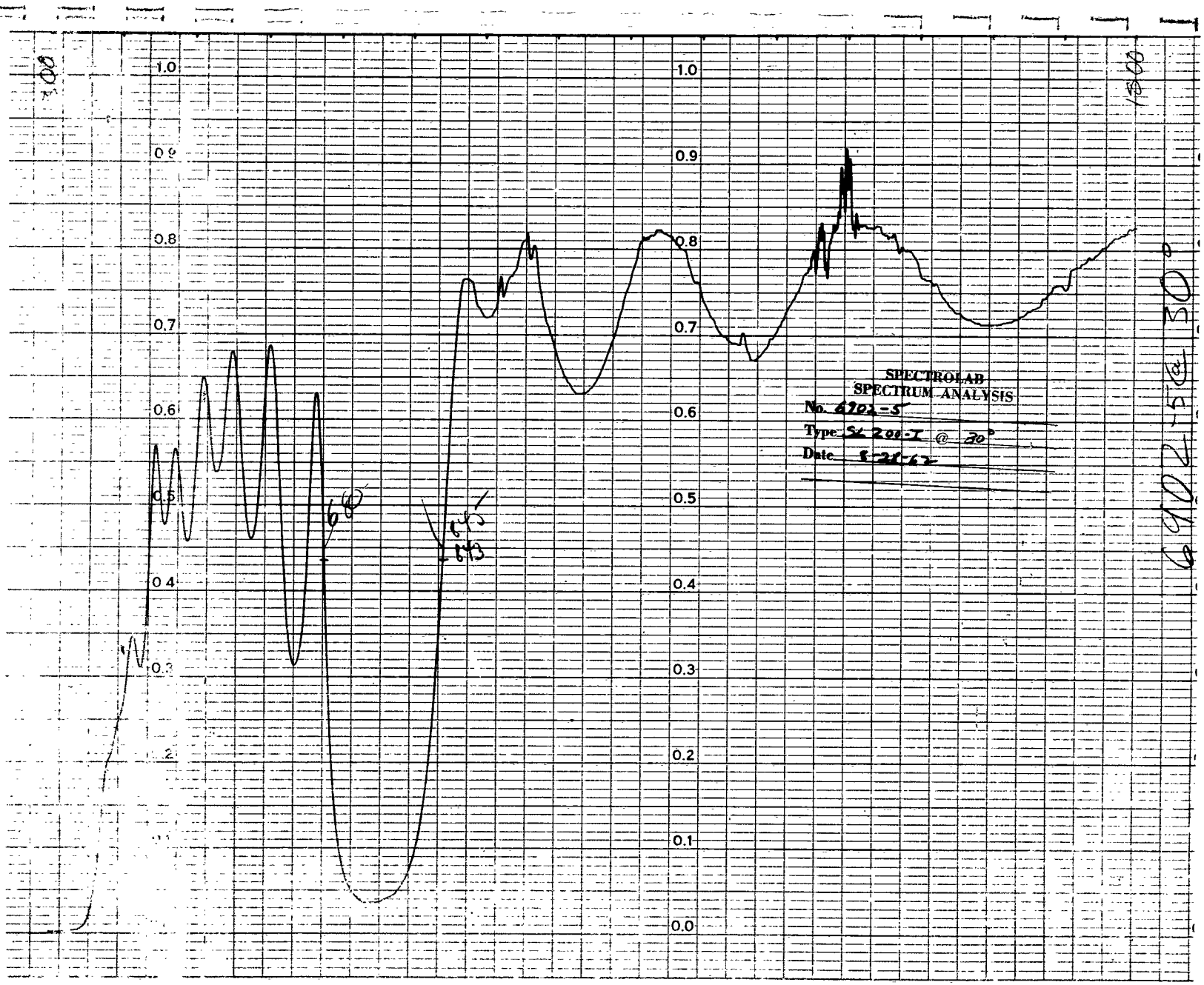
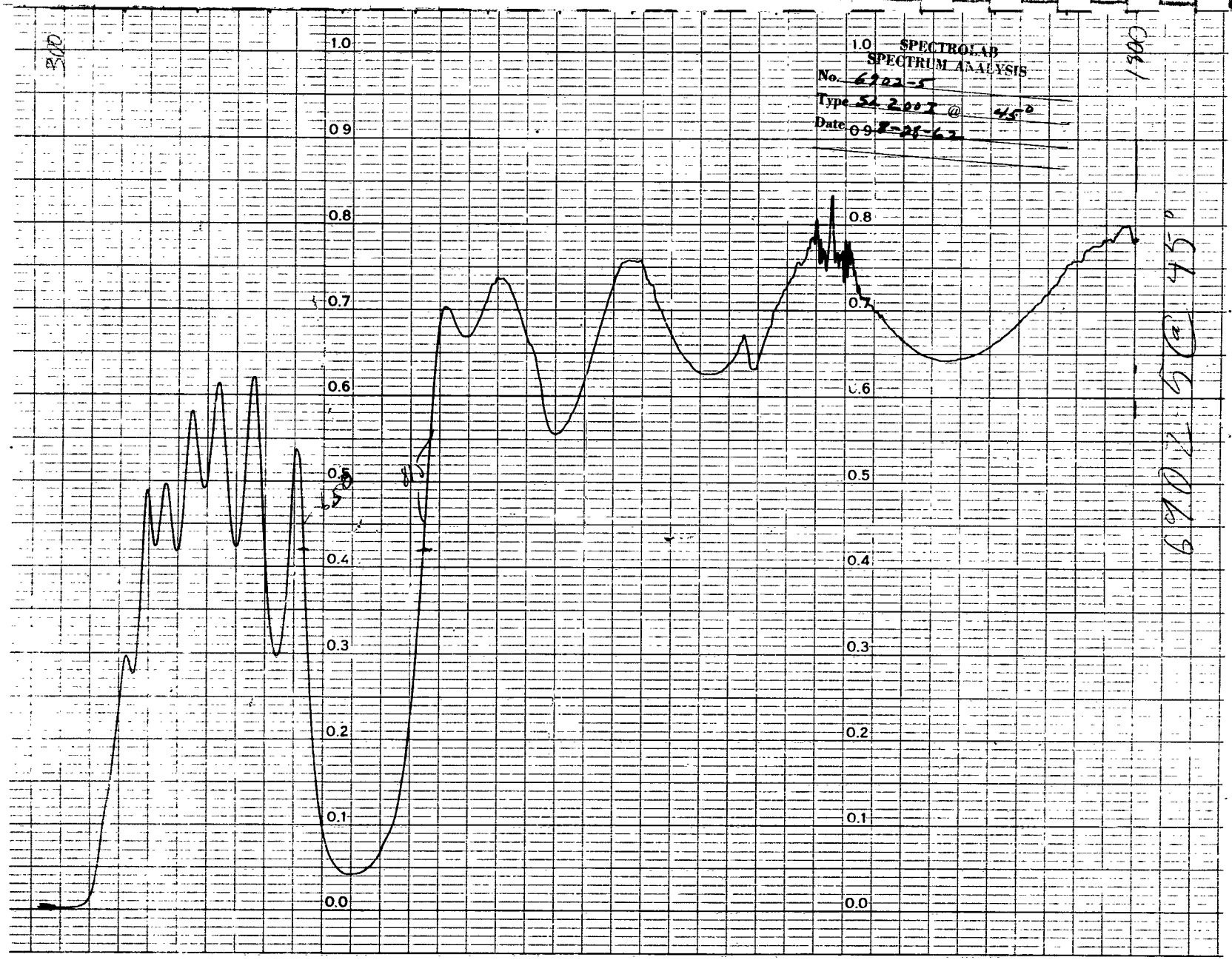

1.0
0.9
0.8
0.7
0.6
0.5
0.4
0.3
0.2
0.1
0.0
SPECTROLAB
SPECTRUM ANALYSIS
No. 4702-5
Type SL 200-T @ 30°
Date 8-21-62
6402-5 @ 30°

Figure B-38


SPECTROLAB
SPECTRUM ANALYSIS
No. 6702-5
Type 54 2007 @ 45°
Date 8-28-62
1.0
0.9
0.8
0.7
0.6
0.5
0.4
0.3
0.2
0.1
0.0
1900
6401 6501 6601 45°

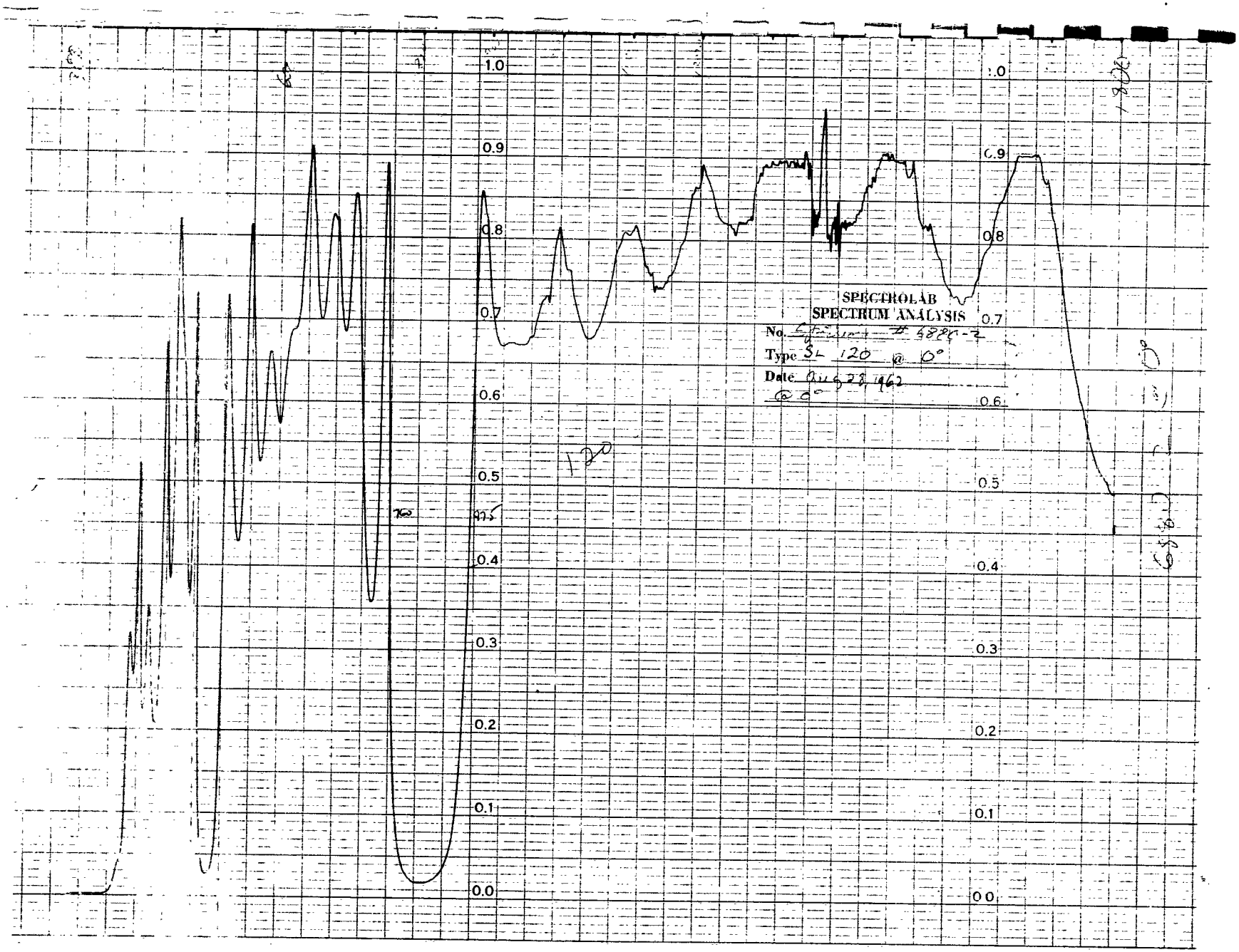

SPECTROLAB
SPECTRUM ANALYSIS
No. [illegible] # 5884-3
Type SL 120 @ 10°
Date Aug 28, 1962
@ 0°
1.0
0.9
0.8
0.7
0.6
0.5
0.4
0.3
0.2
0.1
0.0

Figure P-40

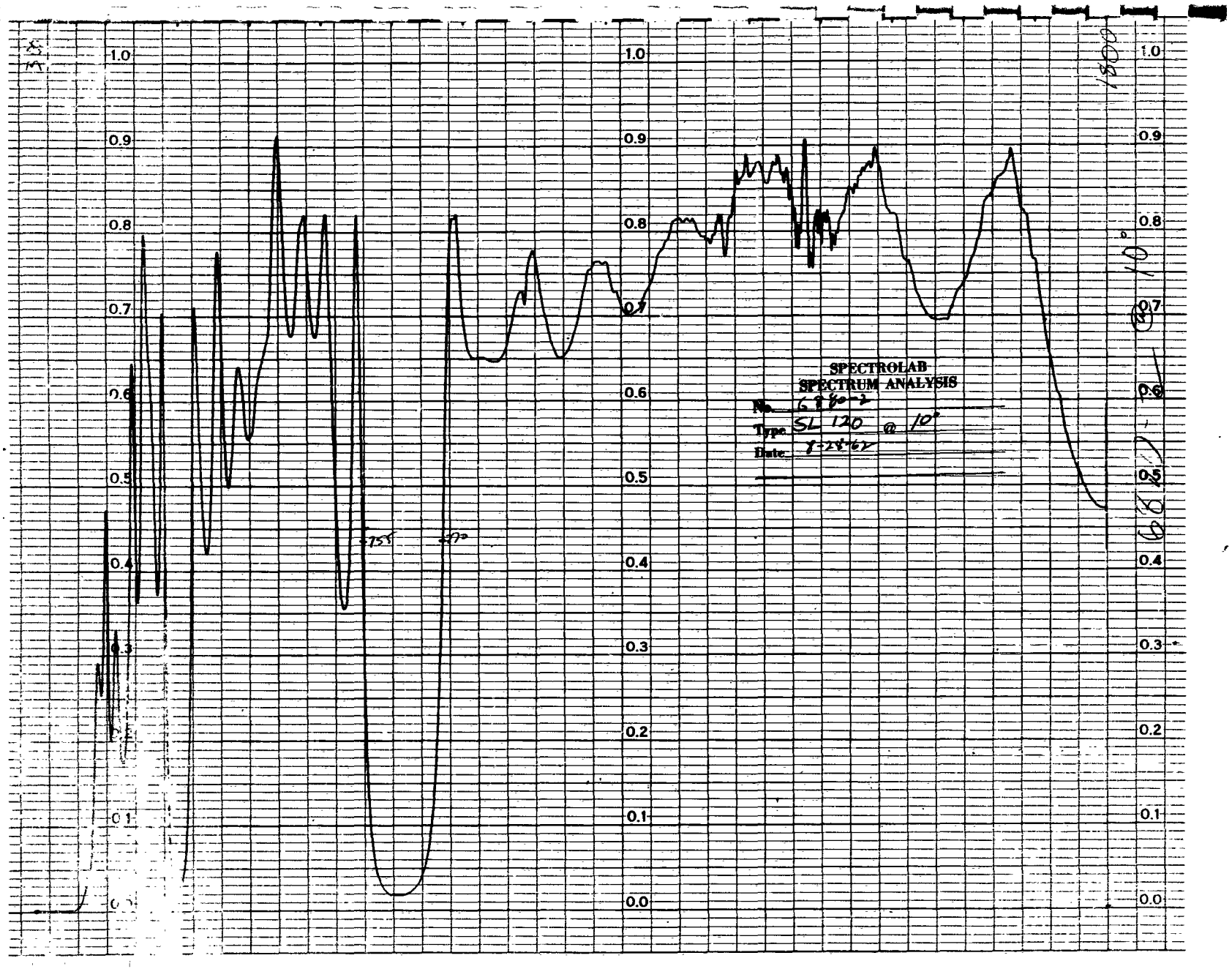
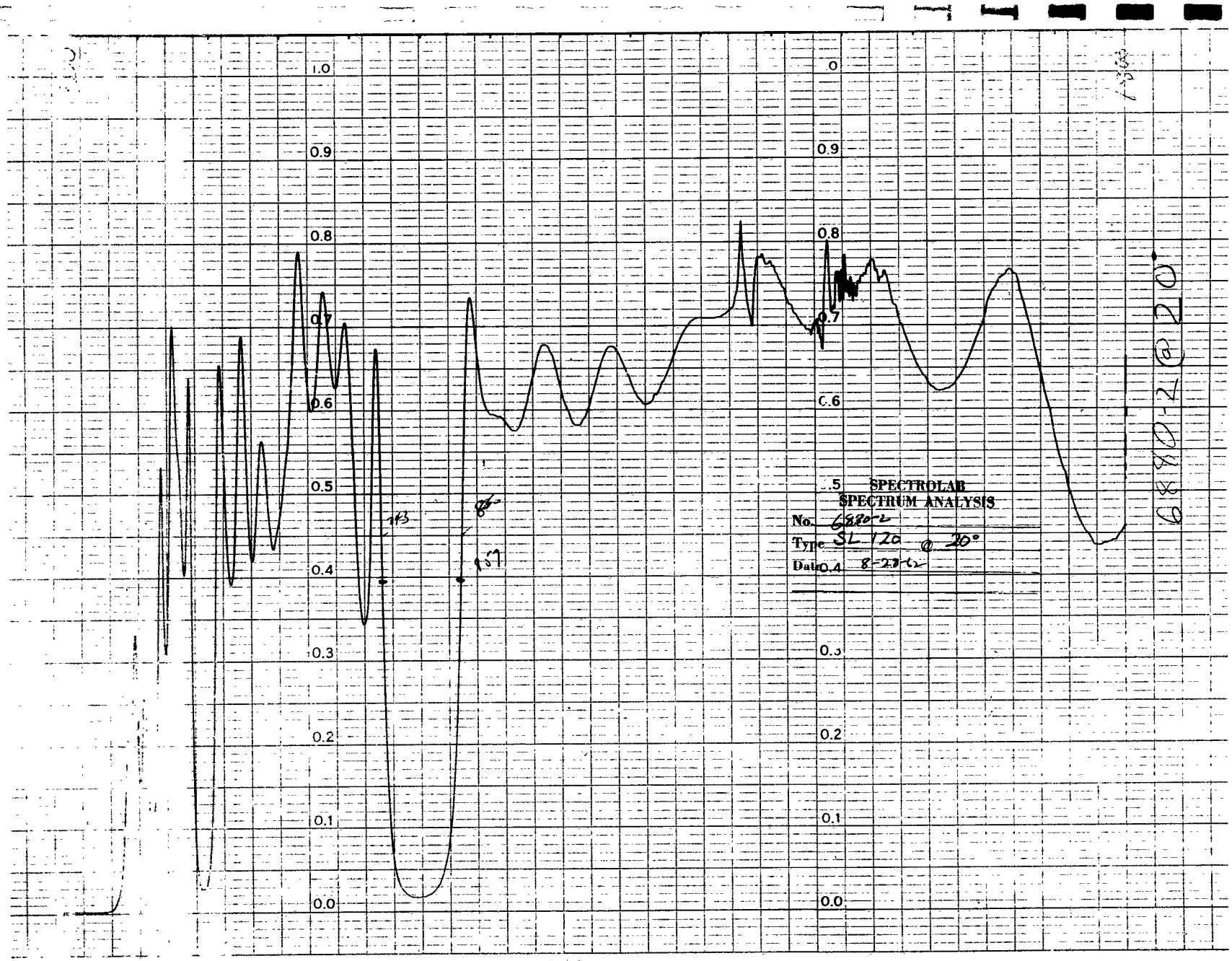
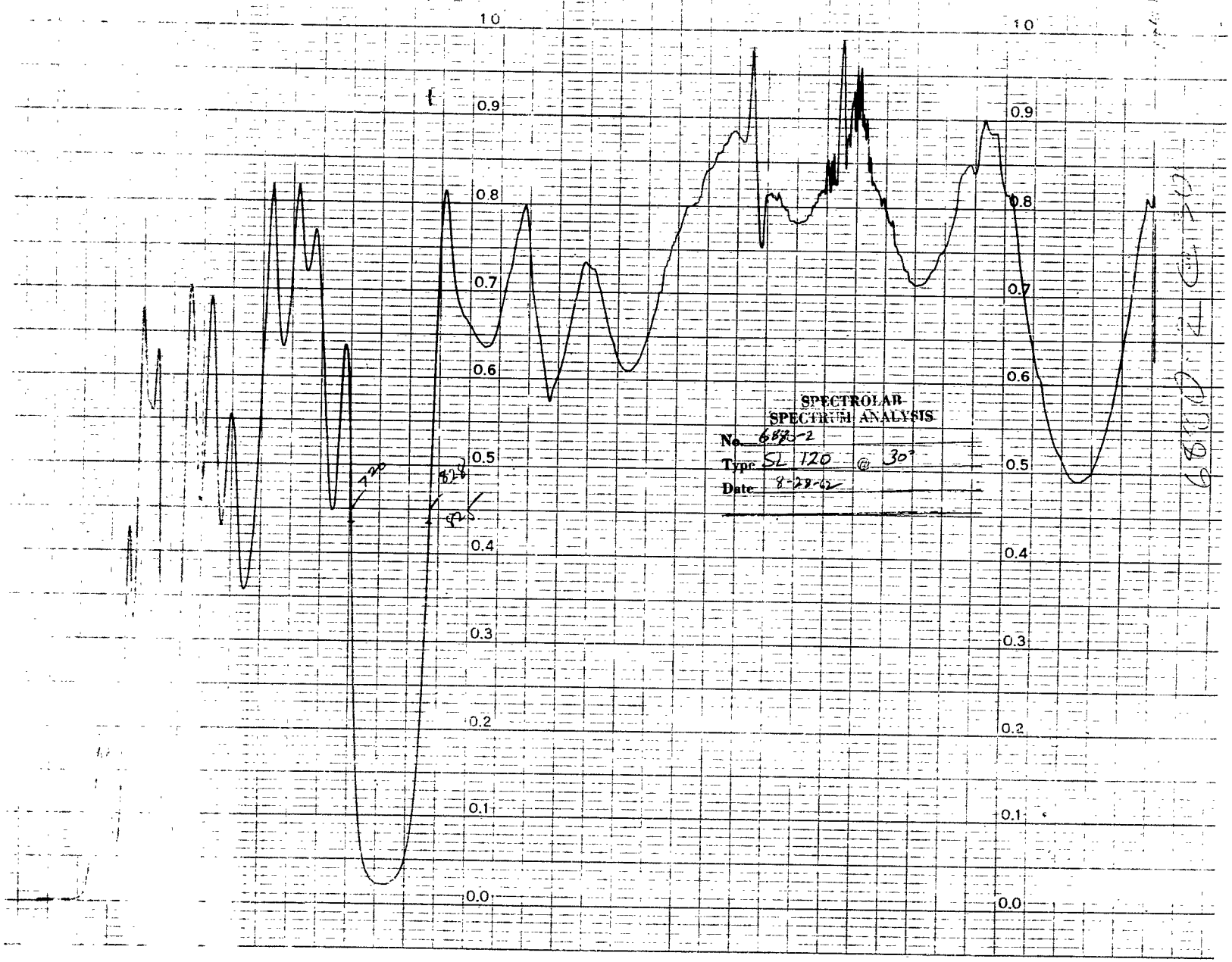

SPECTROLAB
SPECTRUM ANALYSIS
No. 6860-2
Type SL 120 @ 10°
Date 8-28-62
1.0
0.9
0.8
0.7
0.6
0.5
0.4
0.3
0.2
0.1
0.0

Figure Body


1.0
0.9
0.8
0.7
0.6
0.5
0.4
0.3
0.2
0.1
0.0
0
0.9
0.8
0.7
0.6
.5
0.3
0.2
0.1
0.0
SPECTROLAB
SPECTRUM ANALYSIS
No. 6880-2
Type SL 120 @ 20°
Date 8-20-82
6880-2@20°


1.0
0.9
0.8
0.7
0.6
0.5
0.4
0.3
0.2
0.1
0.0
SPECTROLAB
SPECTRUM ANALYSIS
No. 6853-2
Type SL 120 @ 30°
Date 8-29-62
4.0
8.2
18.0

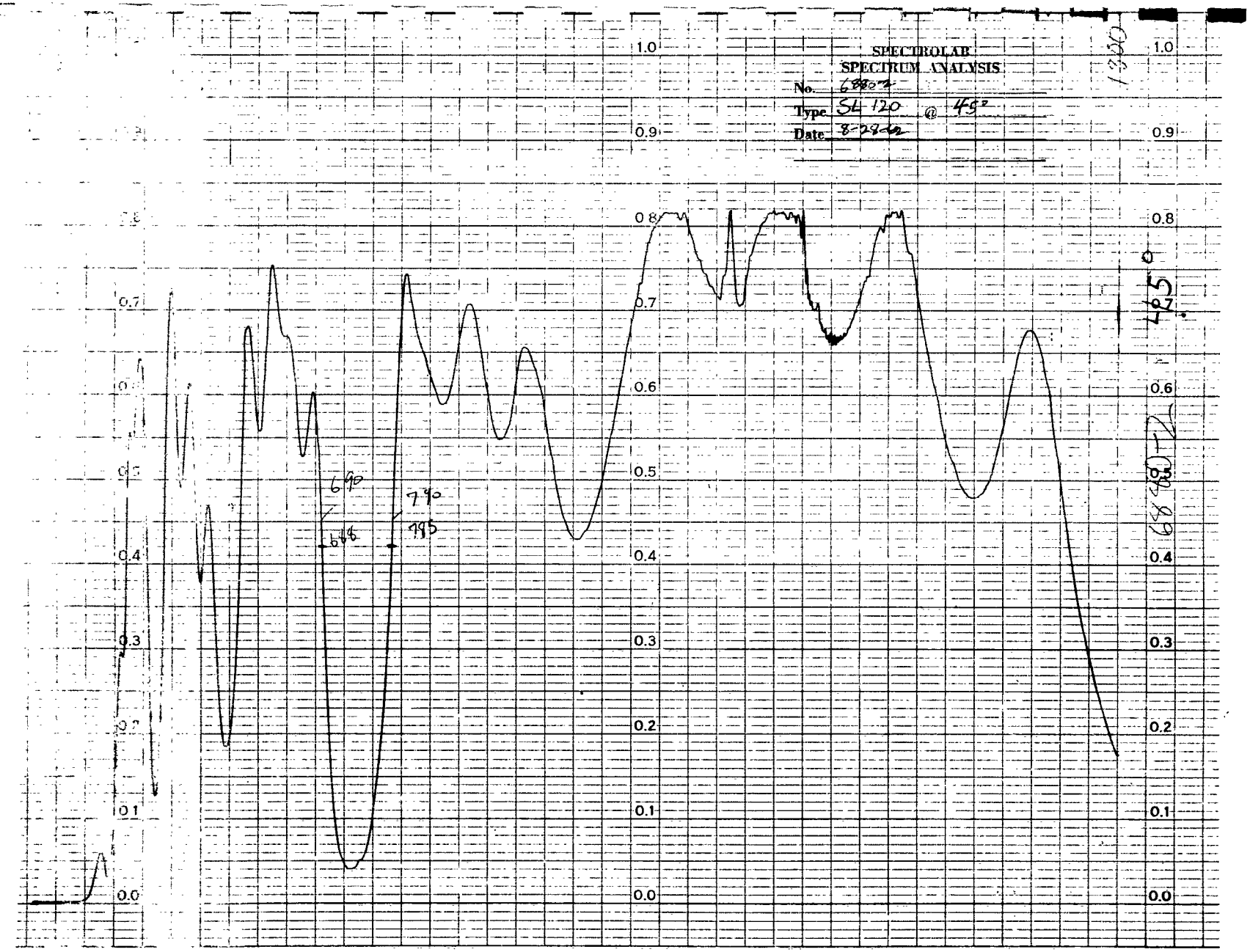

SPECTROLAB
SPECTRUM ANALYSIS
No. 6880-2
Type SL 120 @ 45°
Date 8-28-62
1.0
0.9
0.8
0.7
0.6
0.5
0.4
0.3
0.2
0.1
0.0
690
646
790
795

Figure B-44

Spectrolab, North Hollywood, California INVESTIGATION OF OPTICAL COATINGS FOR SOLAR CELLS, Dr. R.J.Romagnoli September 1962 224 pp.incl.illus. (ARPA Order No. 80-61) Final Report Spectrolab/2004 Contract DA 36-039 SC-87449 Order No. 40647-PM-61-93-93 Unclassified Report (over)	UNCLASSIFIED 1. Power Supplies 2. Solar Energy - Applications I. Romagnoli, Dr.R.J. II. Spectrolab/2004 III. DA-36-039 SC-87449 UNCLASSIFIED	Spectrolab, North Hollywood, California INVESTIGATION OF OPTICAL COATINGS FOR SOLAR CELLS, Dr. R.J.Romagnoli September 1962 224 pp.incl.illus. (ARPA Order No. 80-61) Final Report Spectrolab/2004 Contract DA 36-039 SC-87449 Order No. 40647-PM-61-93-93 Unclassified Report (over)	UNCLASSIFIED 1. Power Supplies 2. Solar Energy - Applications I. Romagnoli, Dr.R.J. II. Spectrolab/2004 III. DA-36-039 SC-87449 UNCLASSIFIED
Performance analyses are made of silicon cell solar power systems using radiation concentration and filtering. The elementary conditions of system design for optimum performance of such systems are established and a plan is outlined for construction of a prototype system. Specifications for suitable mirror filters are formulated. Experimental mirror filters are fabricated and data obtained to evaluate the effect of such filters on solar power system performance. September 1962. 224 pp inc. illus.	UNCLASSIFIED UNCLASSIFIED	Performance analyses are made of silicon cell solar power systems using radiation concentration and filtering. The elementary conditions of system design for optimum performance of such systems are established and a plan is outlined for construction of a prototype system. Specifications for suitable mirror filters are formulated. Experimental mirror filters are fabricated and data obtained to evaluate the effect of such filters on solar power system performance.	UNCLASSIFIED UNCLASSIFIED

Spectrolab, North Hollywood, California INVESTIGATION OF OPTICAL COATINGS FOR SOLAR CELLS, Dr. R.J.Romagnoli September 1962 224 pp incl.illus. (ARPA Order No. 80-61) Final Report Spectrolab/2004 Contract DA 36-039 SC-87449 Order No. 40647-PM-61-93-93 Unclassified Report (over)	UNCLASSIFIED 1. Power Supplies 2. Solar Energy - Applications I. Romagnoli, Dr.R.J. II. Spectrolab/2004 III. DA-36-039 SC-87449 UNCLASSIFIED	Spectrolab, North Hollywood, California INVESTIGATION OF OPTICAL COATINGS FOR SOLAR CELLS, Dr. R.J.Romagnoli September 1962 224 pp.incl.illus. (ARPA Order No. 80-61) Final Report Spectrolab/2004 Contract DA 36-039 SC-87449 Order No. 40647-PM-61-93-93 Unclassified Report (over)	UNCLASSIFIED 1. Power Supplies 2. Solar Energy - Applications I. Romagnoli,Dr.R.J. II. Spectrolab/2004 III. DA-36-039 SC-87449 UNCLASSIFIED
Performance analyses are made of silicon cell solar power systems using radiation concentration and filtering. The elementary conditions of system design for optimum performance of such systems are established and a plan is outlined for construction of a prototype system. Specifications for suitable mirror filters are formulated. Experimental mirror filters are fabricated and data obtained to evaluate the effect of such filters on solar power system performance.	UNCLASSIFIED UNCLASSIFIED	Performance analyses are made of silicon cell solar power systems using radiation concentration and filtering. The elementary conditions of system design for optimum performance of such systems are established and a plan is outlined for construction of a prototype system. Specifications for suitable mirror filters are formulated. Experimental mirror filters are fabricated and data obtained to evaluate the effect of such filters on solar power system performance.	UNCLASSIFIED UNCLASSIFIED

September 1962. 224 pp inc. illus.

Spectrolab, North Hollywood, California INVESTIGATION OF OPTICAL COATINGS FOR SOLAR CELLS, Dr. R.J.Romagnoli September 1962 224 pp.incl.illus. (ARPA Order No. 80-61) Final Report Spectrolab/2004 Contract DA 36-039 SC-87449 Order No. 40647-PM-61-93-93 Unclassified Report (over)	UNCLASSIFIED 1. Power Supplies 2. Solar Energy - Applications I. Romagnoli, Dr.R.J. II. Spectrolab/2004 III. DA-36-039 SC-87449 UNCLASSIFIED	Spectrolab, North Hollywood, California INVESTIGATION OF OPTICAL COATINGS FOR SOLAR CELLS, Dr. R.J.Romagnoli September 1962 224 pp.incl.illus. (ARPA Order No. 80-61) Final Report Spectrolab/2004 Contract DA 36-039 SC-87449 Order No. 40647-PM-61-93-93 Unclassified Report (over)	UNCLASSIFIED 1. Power Supplies 2. Solar Energy - Applications I. Romagnoli,Dr.R.J. II. Spectrolab/2004 III. DA-36-039 SC-87449 UNCLASSIFIED
Performance analyses are made of silicon cell solar power systems using radiation concentration and filtering. The elementary conditions of system design for optimum performance of such systems are established and a plan is outlined for construction of a prototype system. Specifications for suitable mirror filters are formulated. Experimental mirror filters are fabricated and data obtained to evaluate the effect of such filters on solar power system performance.	UNCLASSIFIED UNCLASSIFIED	Performance analyses are made of silicon cell solar power systems using radiation concentration and filtering. The elementary conditions of system design for optimum performance of such systems are established and a plan is outlined for construction of a prototype system. Specifications for suitable mirror filters are formulated. Experimental mirror filters are fabricated and data obtained to evaluate the effect of such filters on solar power system performance.	UNCLASSIFIED UNCLASSIFIED

September 1962. 224 pp inc. illus.

Spectrolab, North Hollywood, California INVESTIGATION OF OPTICAL COATINGS FOR SOLAR CELLS, Dr. R.J.Romagnoli September 1962 224 pp.incl.illus. (ARPA Order No. 80-61) Final Report Spectrolab/2004 Contract DA 36-039 SC-87449 Order No. 40647-PM-61-93-93 Unclassified Report (over)	UNCLASSIFIED 1. Power Supplies 2 Solar Energy - Applications I. Romagnoli, Dr.R.J. II. Spectrolab/2004 III. DA-36-039 SC-87449 UNCLASSIFIED	Spectrolab, North Hollywood, California INVESTIGATION OF OPTICAL COATINGS FOR SOLAR CELLS, Dr. R.J.Romagnoli September 1962 224 pp.incl.illus. (ARPA Order No. 80-61) Final Report Spectrolab/2004 Contract DA 36-039 SC-87449 Order No. 40647-PM-61-93-93 Unclassified Report (over)	UNCLASSIFIED 1. Power Supplies 2. Solar Energy - Applications I. Romagnoli,Dr.R.J. II. Spectrolab/2004 III. DA-36-039 SC-87449 UNCLASSIFIED
Performance analyses are made of silicon cell solar power systems using radiation concentration and filtering. The elementary conditions of system design for optimum performance of such systems are established and a plan is outlined for construction of a prototype system. Specifications for suitable mirror filters are formulated. Experimental mirror filters are fabricated and data obtained to evaluate the effect of such filters on solar power system performance.	UNCLASSIFIED UNCLASSIFIED	Performance analyses are made of silicon cell solar power systems using radiation concentration and filtering. The elementary conditions of system design for optimum performance of such systems are established and a plan is outlined for construction of a prototype system. Specifications for suitable mirror filters are formulated. Experimental mirror filters are fabricated and data obtained to evaluate the effect of such filters on solar power system performance.	UNCLASSIFIED UNCLASSIFIED

September 1962. 224 pp inc. illus.

PSD Dist List B (Steering Group
Members - Mandatory)
January 63

DISTRIBUTION LIST
FINAL REPORT
CONTRACT NO. DA 36-039-SC-87449

Dr. Sidney J. Magram
Physical Sciences Division
Army Research Office
3045 Columbia Pike
Arlington, Va. (1)

Dr. Ralph Roberts
Head, Power Branch
Office of Naval Research (Code 429)
Department of the Navy
Washington 25, D.C. (1)

Mr. Bernard B. Rosenbaum
Bureau of Ships (Code 340)
Department of the Navy
Washington 25, D.C. (1)

Mr. George W. Sherman
Aeronautical Systems Division
ATTN: ASRMFP
Wright-Patterson Air Force Base
Ohio (1)

Dr. John H. Huth
Advanced Research Projects Agency
The Pentagon, Room 3E157
Washington 25, D.C. (1)

Lt. Col. George H. Ogburn, Jr.
Auxiliary Power Branch (SNAP)
Division of Reactor Development
U.S. Atomic Energy Commission
Washington 25, D.C. (1)

Mr. Walter C. Scott
National Aeronautics and Space
Administration
1520 H. Street, N. W.
Washington 25, D.C. (1)

Institute for Defense Analysis
1666 Connecticut Avenue, N.W.
Washington 25, D. C.
ATTN: Dr. George Szego (1)
ATTN: Mr. Robert Hamilton (1)

PSD Dist List A(Mandatory)
January 1963

DISTRIBUTION LIST
FINAL REPORT
CONTRACT NO. DA 36-039-SC-87449

Headquarters
U.S.Army Materiel Command
Research and Development Directorate
ATTN: AMCRD-DE-MO
Washington 25, D.C. (1)

Commanding General
U.S.A. Electronics Command
ATTN: AMSEL-RE-A
Fort Monmouth, N. J. (1)

Commanding General
U.S.A. Combat Developments Command
ATTN: CDCMR-E
Fort Belvoir, Virginia (1)

Commanding Officer
U.S.A. Communications and Electronics
Combat Development Agency
Fort Huachuca, Arizona (1)

Director
Fort Monmouth Office
U.S.A. Communications and Electronics
Combat Development Agency
Fort Monmouth, N. J. (1)

Air Force Systems Command
Scientific/Technical Liaison Office
U.S.Naval Air Development Center
Johnsville, Pennsylvania (1)

Corps of Engineers Liaison Office
U.S.A. Electronics Research and
Development Laboratory
Fort Monmouth, N. J. (1)

Marine Corps Liaison Office
U.S.A. Electronics Research and
Development Laboratory
Fort Monmouth, N. J. (1)

AFSC Scientific/Technical Liaison Office
U.S.A. Electronics Research and
Development Agency
Fort Monmouth, N. J. (1)

Power Information Center
Moore School Building
200 South Thirty-Third Street
Philadelphia 4, Pennsylvania (1)

PSD Dist List A (Mandatory)
January 1963

DISTRIBUTION LIST
FINAL REPORT
CONTRACT NO. DA 36-36-039-SC-87449

Commanding Officer
U.S.A. Electronics Research and Development Laboratory
Fort Monmouth, N. J.
ATTN: Logistics Division (MARKED FOR PROJECT ENGINEER) (7)
ATTN: SELRA/P (1)
ATTN: Dir.of Research/Engineering (1)
ATTN: File Unit #1 (1)
ATTN: Technical Document Center (1)
ATTN: Technical Information Div. (UNCLASSIFIED REPORTS ONLY FOR RETRANSMITTAL TO ACCREDITED BRITISH AND CANADIAN GOVERNMENT REPRESENTATIVES) (3)
ATTN: SELRA/DR, ARPA Coorinator (1)

OASD (R and D), Rm. 3E1065
ATTN: Technical Library
The Pentagon
Washington 25, D.C. (1)

Chief of Research and Development
OCS, Department of the Army
Washington 25, D.C. (1)

Commanding General
U.S.A. Electronics Command
ATTN: AMSEL-AD
Fort Monmouth, N. J. (3)

Director
U.S.Naval Research Laboratory
ATTN: Code 2027
Washington 25, D.C. (1)

Commanding Officer and Director
U.S. Naval Electronics Laboratory
San Diego 52, California (1)

Air Force Cambridge Research Laboratories
ATTN: CRZC
L. G. Hanscom Field
Bedford, Massachusetts (1)

Rome Air Development Center
ATTN: RAALD
Griffiss Air Force Base, N. Y. (1)

Commanding General
U.S.A. Electronics Research and Development Activity
ATTN: Technical Library
Fort Huachuca, Arizona (1)

Commanding Officer
Harry Diamond Laboratories
ATTN: Library, Rm. 211, Bldg. 92
Connecticut Ave. and Van Ness St.N.W.
Washington 25, D.C. (1)

Commanding Officer
U.S.A. Electronics Material Support Agency
ATTN: SELMS-ADJ
Fort Monmouth, N. J. (1)

Deputy President
U.S.A. Security Agency Board
Arlington Hall Station
Arlington 12, Virginia (1)

Commander
Armed Services Technical Information Agency
ATTN: TISIA
Arlington Hall Station
Arlington 12, Virginia (10)

Chief
U.S.A. Security Agency
Arlington Hall Station
Arlington 12, Virginia (2)

Commander
Aeronautical Systems Division
ATTN: ASAPRL
Wright-Patterson Air Force Base
Ohio (1)

Air Force Cambridge Research Laboratories
ATTN: CRXL-R
L. G. Hanscom Field
Bedford, Massachusetts (1)

Director
Advanced Research Projects Agency
Washington 25, D.C. (6)

DISTRIBUTION LIST - Cont'd.

Commanding General
U.S.Army Satellite Communications Agency
Fort Mormouth, N. J.
ATTN: Mr. William Shorr (1)

Mr. Phil Youngblood
Marshall Space Flight Center
ATTN: ORDAB-DCEG
Huntsville, Alabama (1)

Dr. Ralph Zirkind
Bureau of Aeronautics
Department of the Navy
Washington 25, D.C. (1)

Major George W. Austin
Air Force Ballistic Missile Div.
Headquarters ARDC
ATTN: WDZW
Air Force Unit Post Office
Los Angeles 45, California (1)

U.S.Army Research Office
Chemical and Material Branch
Office of Chief of Research and Development
Department of the Army
Washington 25,D.C. (1)

Mr. Rudolph A. Bradbury
Air Force Cambridge Research Center
ATTN: CRRSC
L. G. Hanscom Field
Bedford, Massachusetts (1)

Mr. Joseph M. Hallissy, Jr.
USA Langley Research Center
Langley Air Force Base
Virginia (1)

General Electric Company
Monmouth District Office
43 W. Front Street
Red Bank, New Jersey (1)

Engelhardt Industries
Hanovia Liquid Gold Division
113 Astor Street
Newark 2, N. J.
ATTN: Mr. T. W. Cushing (1)

NASA Manned Space Craft Center-SEDD
Houston 1, Texas
ATTN: Mr. Jerome Grayson (1)

Bell Telephone Laboratories
Murray Hill, N. J. (1)

Mr. R. W. Curran
Boeing Airplane Company
Seattle, Washington (1)

International Rectifier Corp.
233 Kansas Street
El Segundo, California
ATTN: Mr. Dudley (1)

Texas Instrument, Inc.
Semi Conductor Components Div.
P. O. Box 312
Dallas, Texas
ATTN: Pat Brown (1)

California Institute of Technology
4800 Oak Grove Drive
Pasadena 3, California
ATTN: Jet Propulsion Laboratory (1)

Radio Corporation of America
RCA Laboratories
Princeton, N. J.
ATTN: Mr. P. Rappaport (1)

Lockheed Aircraft Corporation
Missiles and Space Division
3251 Hanover Road
Palo Alto, California
ATTN: Dr. W. Kapp (1)

Armour Research Foundation
10 West 35th Street
Chicago 16, Illinois (1)

Transitron Electronic Corp.
168-182 Albion Street
Wakefield, Mass. (1)

Hoffman Electronics Corporation
Semiconductor Division
1001 Arden Drive
El Monte, California (1)

Heliotek Corporation
12500 Gladstone Avenue
Sylmar, California
ATTN: Dr. M. Wolf (1)

Westinghouse Electric Corp.
3 Gateway Center
P.O. Box 2278
Pittsburgh 30, Pa. (1)